INTERNAL FLOW SYSTEMS

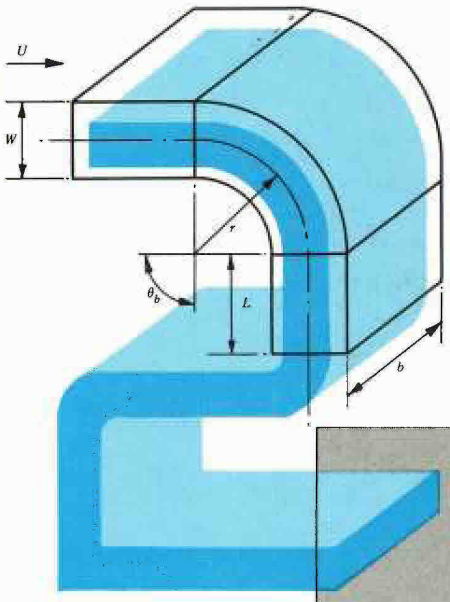

D.S. MILLER

Second Edition

INTERNAL FLOW SYSTEMS

BHRA
THE FLUID ENGINEERING CENTRE

INTERNAL FLOW SYSTEMS

(second edition)

D. S. MILLER

Published by

BHRA (INFORMATION SERVICES)

First edition published in 1978
Reprinted, 1984, 1985, 1986
This second edition published by:

BHRA (Information Services)
The Fluid Engineering Centre,
Cranfield, Bedford MK43 0AJ, UK
Tel. (0234) 750422 Telex: 825059 Fax: (0234) 750074

British Library Cataloguing in Publication Data
Miller, Donald S. (Donald Stuart), *1936-*
Internal flow systems.—2nd ed.
1. Fluids. Steady flow in pipe networks. Measurement
I. Title
532'.052

ISBN 0-947711-77-5

Printed and bound by Unwin Brothers Ltd.,
The Gresham Press, Old Woking, Surrey GU22 9LH
A Member of the Martins Printing Group

CONTENTS

FOREWORD

The first edition of this book has been used in the design of tens of thousands of internal flow systems. In the process the data and procedures it contains have come to be adopted by many organisations as part of their design and analysis methods.

Given the widespread use of the first edition, it would be easy to believe that it met its set objective of being comprehensive and easy to use. In reality, it can serve only a small part of industries' needs for flow system analysis and design. The problem lies in the vast amount of information needed to cover the wide variety of industrial flow systems. Information is distributed in many books, standards and design guides, and in innumerable papers and articles. Approximately 10,000 were considered in some way in the preparation of the first edition but only a small fraction of the information they contained was included in the text.

Producing this edition has reinforced my belief that the priority of R & D organisations, and their funders, should be to make available existing knowledge. This has been a major research topic at BHRA for the past 8 years. One outcome is the first large knowledge bases for fluid engineering applications. Advances in computer technology provide the means for recording, storing and intelligently accessing a mass of information. It is the only means by which the large amounts of data, procedures and calculations for flow systems can be handled. It will enable substantial improvements in the industrial processes that are industrial societies' main energy resources, the largest consumers of energy, the means whereby new materials are converted into products and the major cause of environmental pollution.

Fluid-based processes are serviced by a wide variety of internal flow systems. Often poorly designed, a major cause of plant disasters and pollution, responsible for a high percentage of plant maintenance costs and plant shut-downs, and major users of energy these systems are responsible for up to 40% of plant costs. Aspects of system design greatly influence safety, reliability, operating and maintenance costs and hence plant profitability. Most of the problems associated with these systems are due, not to inadequacies in the state-of-the-art, but to insufficient consideration at the design stage as information is not accessible to design teams. To achieve their full potential, computer-based aids will need to prompt designers to consider all the relevant factors. Hundreds of thousands of ''chunks of knowledge'' about internal flow systems must be made available within knowledge-based software that engineers, designers and operators can access in the workplace.

Relative to the existing body of information on flow system design, little new material is being generated. When the difficulties of accessing information are acknowledged, it is sensible to concentrate on making available the existing information, rather than generating small amounts of new material. Producing computer-based design aids requires a team of engineers and software specialists. Before a team can commence developing computer-based aids, substantial sums of money must be committed.

The first edition has been used to justify raising funding to start the process of developing easy to use, comprehensive and reliable computer based aids. However, much remains to be done for which very considerable investment will be necessary. Despite the clear evidence that computer based aids can improve the design of flow systems with the attendant benefits, the cost of up-front investment, the long development period and the high cost of convincing companies of the benefits of such design aids has limited conventional funding. The mechanism must be established for collaborative projects to develop techniques for effective building of knowledge bases, their modification and extension within companies and the procedures for quality assurance.

A major start has been made on a graphics-based analysis suite of programs that use the data and procedure from this book in its data bases and mathematical models. The suite of programs, called FLOWMASTER, has been financed by Legal & General Assurance Society Limited through its

subsidary, Amazon Computers Limited, and by BHRA. (FLOWMASTER is owned and marketed by Amazon Computers.)

FLOWMASTER is in use in a diverse range of industries and has proven it can meet corporate objectives for consistency of design, enhanced safety and reduced risk, development of in-house capabilities in flow system design. FLOWMASTER modules currently include steady-state network analysis, pipe sizing, flow balancing, transient network analysis, two-phase flow, fluid power systems, heat transfer, component interactions and compressible flow.

Meanwhile, a number of major changes and additions have been made to the text for this edition of "Internal Flow Systems". Sections have been re-written to improve their clarity and errors have been corrected. In revising the text I have tried to take account of the many comments I have received from users around the world.

Chapter 4 on the management of the design of flow systems is an addition. It aims to generate awareness of how to achieve efficient, reliable, safe flow systems which are easy to operate and maintain.

Chapter 7 on compressible flow replaces a chapter on transient flow in the first edition. Transient analysis is so strongly computer-based that a discussion on it needs to sit alongside a transient analysis program, such as the transient module in FLOWMASTER. Compressible flow calculations in Chapter 7 use the data from Part 2 of the text and form a natural extension to the remainder of the text.

Chapter 11 on diffusers has been substantially revised to make better use of available data and to bring out the important factor to be considered in diffuser design. Major additions to Chapter 13 include a new section on T junction-bend interactions. This interaction information fills a serious gap in the accurate prediction of pressure losses in a number of commonly encountered piping arrangements.

In the past I have been made very aware of the problems companies face when revisions are made to loss coefficient data, in particular changes to loss coefficient contour lines on complex figures which users find difficult to identify. I have, therefore, indicated in the text which figures have been significantly modified from the first edition. Comments about the changes are given in an appendix.

Data from the first edition is referenced in computer programs, safety cases, standards, etc. In order to avoid confusion I have retained, as far as possible, the same figure numbers in Part 2 of this edition as the first. This has led to some problems in the figure numbering system as regards new figures, but these are far outweighed by the importance of similarity between the two editions. A note on figure numbering and classification of loss coefficients is given at the start of Part 2.

The performance data from Chapter 6 onwards are classified for accuracy. Since I have had to revise some of the Class 1—definitive data—from the first edition, I clearly made a number of wrong judgements. Hopefully, classifications in this edition are nearer to the truth. Please let me know if you think differently. Your help will be appreciated in identifying errors, lack of clarity and misunderstandings.

I acknowledge with thanks the permission of the Pipeline Research Supervisory Committee (PRC) of the American Gas Association to use the results of the work they funded at BHRA on T-bend interactions. In particular I would like to thank the Compressor Research Supervisory Committee, chaired by Lawrence Williams, for their active support. The American Gas Association plans to publish "An Engineers Design Handbook for Pressure Losses in Compressor Yard Pipework" based on work at BHRA.

Much of my understanding of fluid engineering has come from interacting with my colleagues at BHRA. I thank present and past colleagues for their help and insights into the interesting and challenging technologies we seek to provide to industry.

Donald S. Miller
November 1989

SYMBOLS AND PRESSURE DEFINITIONS

SYMBOLS

The general practice is to define symbols as they occur in each chapter. Only the principal symbols are listed below.

		Units
A	cross-sectional area	m^2
A	constant	
a	pressure wave velocity	m/s
B	constant	
b	width or breadth	m
C	correction factor	
C	constant	
C_p	pressure recovery coefficient	
D	hydraulic diameter ($4A/P_r$)	m
d	pipe diameter	m
f	friction coefficient	
g	gravitational acceleration	m/s^2
H	total head	m
ΔH	total head loss	m
h	head	m
K	loss coefficient	
k	roughness coefficient	m
L	length	m
l	length	m
N	diffuser length	m
P	total pressure	N/m^2 (Pa)
ΔP	total pressure loss	N/m^2 (Pa)
P_r	perimeter (wetted perimeter)	m
p	static pressure	N/m^2 (Pa)
Q	flow rate	m^3/s
R	radius	m
Re	Reynolds number	
r	radius	m
t	time	s
U	mean velocity	m/s
W	width	m
γ	specific weight	N/m^3
θ	angle	degrees
μ	absolute viscosity	$N\,s/m^2$
ν	kinematic viscosity	m^2/s
ρ	density	kg/m^3
σ	cavitation parameter	

PRESSURE DEFINITIONS

Hydraulic engineers often deal with fluids flowing from one level to another, for example, from one reservoir to another. In describing system performance it is appropriate to use differences in levels or heads expressed in metres of fluid. Low speed air and gas flows are usually measured using manometers, which register pressures as a displacement of a fluid column. For these and other reasons it has become common, in certain branches of fluid mechanics, to use the terms total head and velocity head in preference to total pressure and

velocity pressure. This practice is followed here as it reduces the monotonous use of pressure terms and follows the convention adopted with SI units of continuing, where appropriate, to express pressures in terms of "pressure heads". It should always be remembered that, although heads are taken as the height of a liquid column, the units of head are those of pressure, N/m^2 (height of liquid column (m) $\times$ density (kg/m^3) $\times$ gravity (m/s^2)).

static pressure	the pressure acting equally in all directions at a point in a fluid
velocity pressure	given by $1/2\rho U^2$, also called the kinematic pressure
total pressure	the sum of the static and velocity pressures
total pressure loss	the difference in total pressures between two points related to a common datum; as all pressure losses in the text are total pressure losses the words total and pressure are often dropped
gauge pressure	the pressure above or below local atmospheric pressure, if the gauge pressure is less than atmospheric pressure it is also called the vacuum pressure
absolute pressure	the pressure above zero, given by the sum of the local atmospheric pressure and the gauge pressure
atmospheric (barometric) pressure	the local pressure measured with a barometer
standard atmospheric pressure	equal to 101.325 kN/m^2
vapour pressure	the pressure exerted when a liquid is in equilibrium with its own vapour
piezometric or hydraulic head	the head above a datum to which fluid rises in a tube connected to a tapping in a pipe or passage, or the water level in a reservoir
velocity head	given by $U^2/2g$
total head	the sum of the piezometric and velocity head
total head loss	the difference in total head between two points related to a common datum; as all head losses in the text are total head losses, the words total and head are often dropped
pump head	head generated by a pump, given by the piezometric head difference across the pump plus the difference in velocity heads between outlet and inlet
vapour head	the head in fluid exerted when a liquid is in equilibrium with its own vapour

PART 1

1. INTRODUCTION

1.1. TYPES OF FLOW CONSIDERED

Internal flow is concerned with fluids flowing in pipes, passages, ducts, conduits, culverts, tunnels and components such as bends, diffusers and heat exchangers. In the text, "pipe" is used for flow through circular cross-sections and "passage" if the cross-section is non-circular. Confined in pipes and passages, most liquids and gases behave in a similar manner so the general term fluid is appropriate and is used throughout the text.

Except for Chapter 6 on cavitation and Chapter 7 on compressible flow, the present work is restricted to steady flow of a single phase nearly Newtonian fluid. A Newtonian fluid is characterised by shear stress being proportional to strain, with the constant of proportionality being the absolute viscosity. Most gases and many liquids are Newtonian fluids. Generally fully turbulent flows are assumed except in discussions on important aspects of low flow Reynolds numbers. Turbulent single phase internal flows predominate in engineering flow systems but are the exception in nature. For instance, the most common form of pump, the heart, operates cyclically in the laminar to turbulent transition region, pumping a complex fluid with living cells and solids in suspension, whilst the flow of nutrients in plants occurs wholly in the laminar region.

Loss coefficients and calculations of pressure losses in Part 2 are for incompressible flow. This is no restriction as regards liquids which have pressure wave velocities (velocity of sound) of the order of 1000 m/s compared with typical flow velocities of less than 10 m/s — equivalent to a Mach number of 0.01. For gases the performance data can be used directly for flows at Mach number less than 0.2 — equivalent to 70 m/s for air at normal temperature and pressure. Chapter 7 contains procedures for applying incompressible loss coefficients to compressible flows.

1.2. SYSTEMS OF UNITS AND FLUID PROPERTIES

1.2.1. SI UNITS

In SI units mass is measured in kilograms, kg; length in metres, m; and force in newtons, N. One newton is the force required to accelerate 1 kg at a rate of 1 m/s^2:

$$1\ N = 1\ kg \times 1\ m/s^2$$

1.2.2. PRESSURE

The basic pressure unit is the newton per square metre, N/m^2, which is given the name pascal, Pa:

$$1 \text{ Pa} = 1 \text{ N/m}^2$$

When the only acceleration is that due to gravity of 9.81 m/s^2, holding an apple or a small glass of water involves exerting a force of roughly 1 N. If the glass of water is poured over a metre-square tray it would form a layer approximately 0.0001 m deep. The basic unit of N/m^2, is often used. Another pressure unit is the bar, which is equal to 10^5 Pa.

1.2.3. DENSITY

The mass per unit volume is referred to as the fluid density, ρ. Units of density are

$$\text{kg/m}^3$$

At normal temperatures and pressures the density of water is approximately 1000 kg/m^3 and the density of air is approximately 1.2 kg/m^3.

1.2.4. SPECIFIC WEIGHT

The specific weight γ $(=\rho g)$ is the weight of fluid per unit volume and has dimensions of force per unit volume, which are

$$\text{N/m}^3$$

For water with a density of 1000 kg/m^3 and an acceleration due to gravity of 9.81 m/s^2 the specific weight is

$$\gamma_{\text{water}} = 1000 \times 9.81 = 9810 \text{ N/m}^3$$

and for air at normal temperature and pressure the density is approximately 1.2 kg/m^3, so

$$\gamma_{\text{air}} = 1.2 \times 9.81 = 11.8 \text{ N/m}^3$$

1.2.5. ENERGY

The unit of energy is the joule, J, which is the work done when a force of 1 N is displaced through a distance of 1 m in the direction of the force:

$$1 \text{ J} = 1 \text{ N m}$$

1.2.6. VISCOSITY

A Newtonian fluid subjected to shear will deform continuously so long as the shearing force

exists. The magnitude of the force controls the rate of deformation which is opposed by molecular friction — called viscous shear. The relationship between shear stress, τ, and rate of deformation du/dy is

$$\tau = \mu \frac{du}{dy} \tag{1.1}$$

where μ is called the absolute viscosity of the fluid. The units of τ are N/m^2 and the units of the velocity gradient du/dy are s^{-1}, giving units of μ as

$$N\ s/m^2 \quad \text{or} \quad kg/m\ s$$

Absolute viscosity is sometimes quoted in CGS units, poises (P) or centipoises (cP):

$$1\ P = 100\ cP = 0.1\ N\ s/m^2 \qquad (Pa\ s)$$

A more useful relationship for fluid flow is the kinetic viscosity, ν, which is the absolute viscosity divided by the fluid density. The kinematic viscosity has units of m^2/s.

Kinematic viscosity is sometimes quoted in CGS units, stokes (St) or centistokes (cSt):

$$1\ St = 100 cSt = 10^{-4}\ m^2/s$$

1.3. EQUATIONS OF INCOMPRESSIBLE FLUID FLOW

Fluid mechanics is based on the fundamental principles of conservation of mass, energy and momentum, and Newton's laws of motion.

1.3.1. CONSERVATION OF MASS

For incompressible flow the equation of steady flow through a non-branching system is

$$Q = A_1 U_1 = A_2 U_2 \tag{1.2}$$

where A is the cross-sectional area and U is the mean velocity.

When dividing or combining of flow occurs, the equation for a junction or node with n legs is

$$\sum_{i=1}^{i=n} Q_i = 0 \tag{1.3}$$

which is a statement that the flow into a node must equal the flow out.

1.3.2. CONSERVATION OF ENERGY

Energy is not created or destroyed, so the terms pressure loss and energy dissipation in common use in fluid mechanics are not strictly correct. However, some forms of energy are more useful in relation to fluid flow than others — static, potential and velocity energy are useful, whereas internal energy is not.

The energy equation for fluid flow is known as the Bernoulli equation. A fluid may have energy due to elevation, z, above some datum, equal to gz per unit mass, where g is the acceleration due to gravity. It may have energy due to static pressure, p, equal to p/ρ per unit mass and it may have energy due to its motion equal to $\frac{1}{2}U^2$ per unit mass. The sum of these energies is

$$E = gz + \frac{p}{\rho} + \frac{U^2}{2} \tag{1.4}$$

E is the total energy per unit mass and has units of

$$\text{N m/kg} \quad \text{or} \quad \text{J/kg}$$

In internal flow it is often more convenient to express equation (1.4) in terms of energy per unit weight. This is achieved by dividing through equation (1.4) by g. Each term is then expressed in terms of a length, to give a total head, H:

$$H = z + \frac{p}{\rho g} + \frac{U^2}{2g} \tag{1.5a}$$

where z is the height of the pipe centreline above a datum (m), $p/\rho g$ is the pressure head of the fluid within the pipe measured at the pipe centreline (m) and $U^2/2g$ is the velocity head of the fluid (m).

Figure 1.1 illustrates the physical meaning of the terms in equation (1.5a).

In hydraulics the practice is to call the sum $z + p/\rho g$ the piezometric or hydraulic head. Using the piezometric head, h, the total head given by equation (1.5a) becomes

$$H = h + U^2/2g \tag{1.6}$$

The use of head in relation to liquid flows, as shown in Fig. 1.1, is easy to visualise. Low velocity gas flow pressures are usually measured using U-tube manometres, as shown in

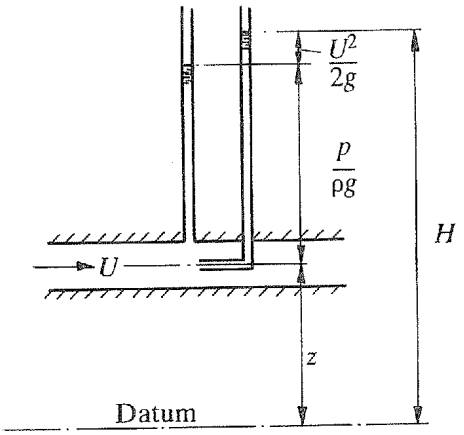

Fig. 1.1. Contributions to total head

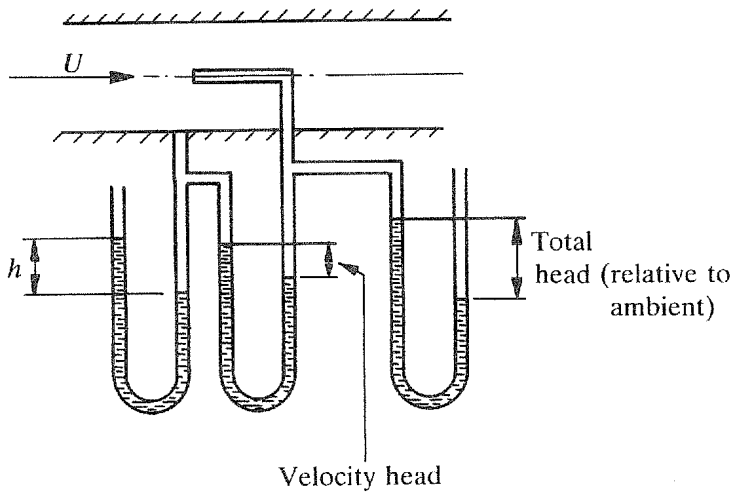

Fig. 1.2. Gas flow measurement

Fig. 1.2. Since the pressure is usually measured as a water column, the practice is to quote pressures in terms of a head in millimetres or metres of water gauge.

In terms of pressure, equation (1.5a) becomes

$$P = \rho g z + p + \rho U^2/2 \tag{1.5b}$$

where P is called the total pressure and p is the static pressure. For example: what is the pressure corresponding to 50 mm of water gauge? ($\rho_{water} = 1000$ kg/m^3)

$$P = \rho g h$$
$$= 1000 \times 9.81 \times (50/1000) = 490 \text{ N/m}^2$$

1.3.3. HEAD AND PRESSURE LOSS EQUATIONS

Throughout the text head loss and pressure loss are abbreviations for the total head loss or the total pressure loss. Between two points in a system the head loss is equal to the difference in the total heads at the two points. For the notation shown in Fig. 1.3 the head loss, ΔH, is given by

$$\Delta H = \left(h_1 + \frac{U_1^2}{2g}\right) - \left(h_2 + \frac{U_2^2}{2g}\right) \tag{1.7a}$$

Similarly, the pressure loss is given by

$$\Delta P = \left(p_1 + \rho\frac{U_1^2}{2}\right) - \left(p_2 + \rho\frac{U_2^2}{2}\right) + \rho g(z_1 - z_2) \tag{1.7b}$$

where $(z_1 - z_2)$ is the difference in level between pressure gauges.

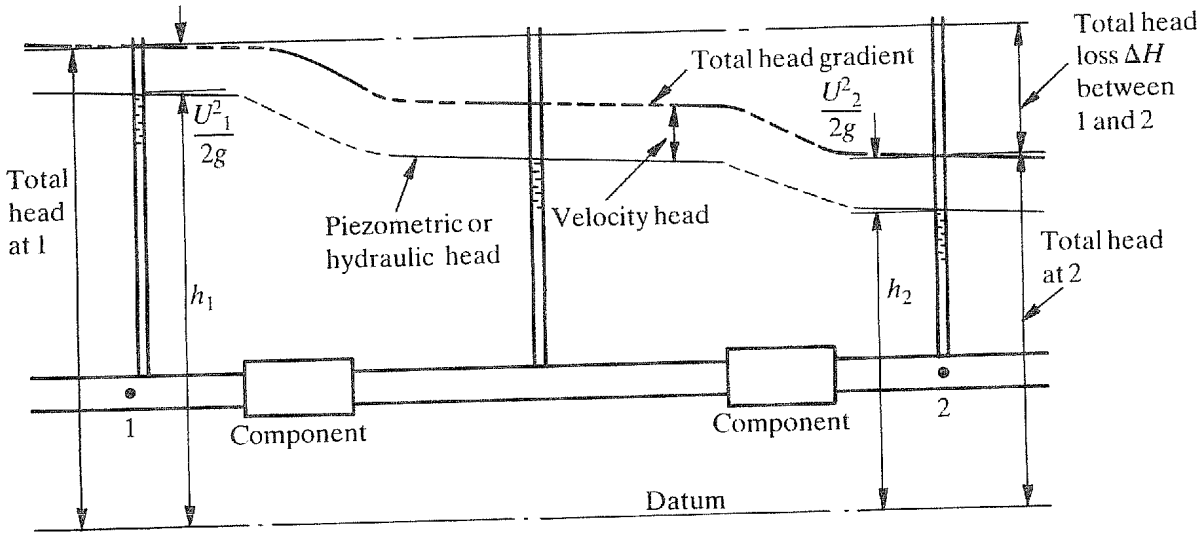

Fig. 1.3. Total head loss

1.3.4. LOSS COEFFICIENTS

Head losses with turbulent flows are approximately proportional to (velocity)^2. A loss coefficient for a pipe, a passage or a component is defined as

$$K = \frac{\Delta H}{U^2/2g} = \frac{\Delta P}{\rho U^2/2} \tag{1.8}$$

1.3.5. SYSTEM POWER REQUIREMENTS

The overall head or pressure loss of a system consisting of n components such as pipes, valves, bends and restrictions is

$$H(\text{overall}) = \sum_{i=1}^{i=n} \Delta H_i \tag{1.9a}$$

and

$$P(\text{overall}) = \sum_{i=1}^{i=n} \Delta P_i = \rho g H(\text{overall}) \tag{1.9b}$$

The head H or pressure P to be generated by a pump or other device is

$$H = H(\text{overall}) + \text{static lift across system} \tag{1.10a}$$

and

$$P = P(\text{overall}) + \text{pressure difference across system} \tag{1.10b}$$

The basic unit of power in the SI system is the watt, W:

$$1\ \text{W} = 1\ \text{J/s} = 1\ \text{N m/s}$$

For a pump or fan of efficiency, η, producing a total head rise of H, the power input is

$$\text{Power (W)} = Q\rho gH/\eta = QP/\eta \tag{1.11}$$

For example, a pump with an efficiency of 80 per cent is required to deliver 0.2 m^3/s of oil of specific gravity (SG) = 0.85 against a total head of 130 m. What is the power input? Take the density of water as 1000 kg/m^3.

$$\text{Power (W)} = \frac{0.85 \times 1000 \times 9.81 \times 0.2 \times 130}{0.80} \quad \left(\frac{\text{kg}}{\text{m}^3} \times \frac{\text{m}}{\text{s}^2} \times \frac{\text{m}^3}{\text{s}} \times \text{m}\right)$$

$$= 271\ \text{kW}$$

As a second example, a fan with an efficiency of 78 per cent is required to deliver 6 m^3/s of atmospheric air of density 1.2 kg/m^3 against a total head of 500 mm of water gauge. What is the motor power? Take the density of water as 1000 kg/m^3.

The head rise in metres of air is

$$H = \frac{1000}{1.2} \times \frac{500}{1000} = 417\ \text{m of air}$$

So

$$\text{Power} = \frac{1.2 \times 9.81 \times 6 \times 417}{0.78}\ (\text{W})$$

$$= 37.8\ \text{kW}$$

1.3.6. REYNOLDS NUMBER

The only criterion to be satisfied for incompressible, non-Newtonian-flow for conditions to be the same in two geometrically similar systems is that the ratio of inertia to viscous forces should be the same in both systems. This ratio of forces is known as the Reynolds number and is given by

$$\text{Re} = UD/v \tag{1.12}$$

where U is the mean velocity, D is the hydraulic diameter (4 × area/perimeter) and v is the kinematic viscosity.

1.4. UNIVERSALITY OF LOSS COEFFICIENTS

A question sometimes asked by engineers, with only an occasional involvement with fluid mechanics, is whether loss coefficients obtained with other fluids can be used for their particular application. As an example of the generality of fluid flow coefficients, the Reynolds number

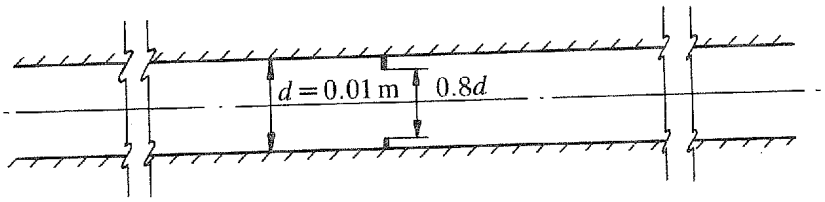

Fig. 1.4. Orifice plate

relationship will be established assuming that an experimental investigation is carried out on an orifice plate of orifice/pipe diameter ratio of 0.8. This arrangement shown in Fig. 1.4 is selected because it illustrates clearly that there is a phenomenon associated only with fluid motion and not with fluid properties or system geometry — this is turbulence, which is discussed in Chapter 2.

For a known flow rate the head differential, with and without the orifice plate in the pipe, is measured. From the difference between the values, the head loss, due solely to the orifice plate, is obtained against pipe velocity. For the fluids given in Table 1.1, the head loss-velocity relationships are plotted in Fig. 1.5.

The most important features of Fig. 1.5 are the similarity of the curves and that, at sufficiently high velocities, the curves are coincident. Once the curves become coincident, losses, in terms of flowing fluid, are identical for all fluids flowing at the same velocity. In practice, depending on the component, the head-velocity curves for different fluids may only tend to be the same value. It is therefore necessary to establish a relationship that correlates the results from different fluids by collapsing all the curves to a single curve.

At higher velocities the curves of Fig. 1.5 indicate that losses are proportional to (velocity)^2. Since the velocity head is given by $U^2/2g$, the head losses can be non-dimensionalised by the velocity head. This non-dimensional ratio is called the loss coefficient. To isolate geometrical and flow factors, geometrically similar models of the orifice and pipe could be tested with a single fluid. Keeping the product of size and velocity constant, it is found that the results fall on a single curve.

Selecting the pipe diameter, D, as the size parameter, Fig. 1.5 can be replotted as Fig. 1.6. Comparing the curves of Fig. 1.6 and the kinetic viscosities in Table 1.1, it is evident that

Table 1.1. Fluid densities and kinematic viscosities

Fluid	Density (kg/m^3)	Kinematic viscosity (m^2/s)
Hydrogen	0.09	1.1×10^{-4}
Air	1.2	1.5×10^{-5}
Crude oil	860	1.0×10^{-5}
Water	1000	1.1×10^{-6}
Mercury	13 600	1.1×10^{-7}

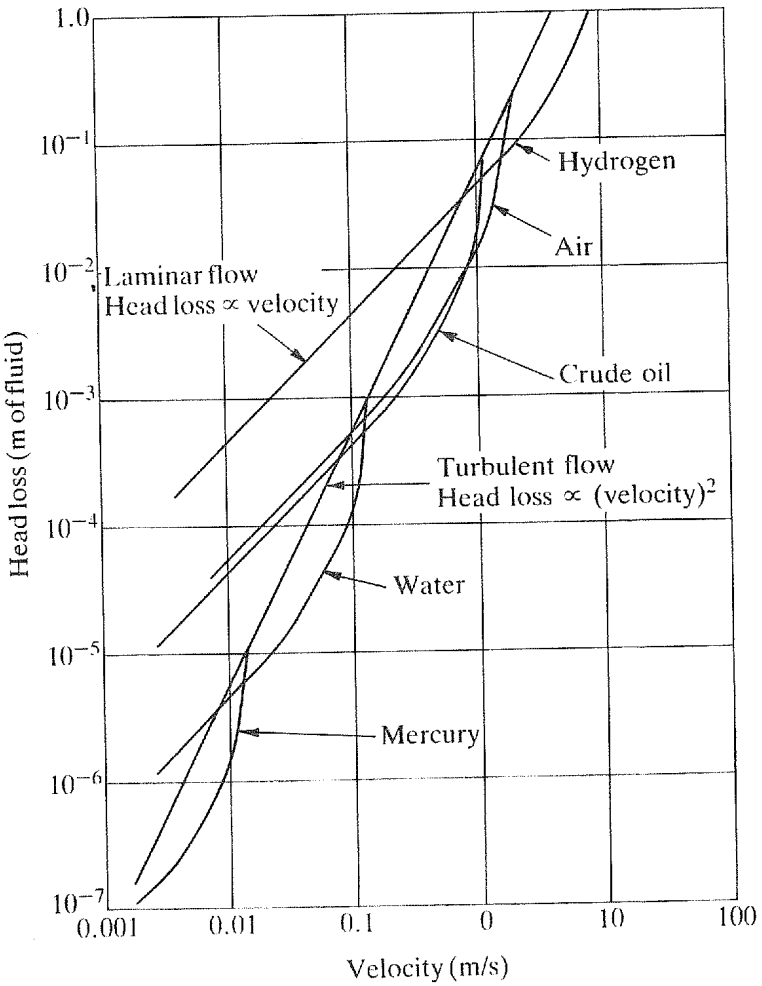

Fig. 1.5. Head loss–velocity relationship

the curves are displaced from one another by the ratio of their kinematic viscosities. Replotting, with UD/ν, the Reynolds number, as the horizontal axis, collapses all the curves to a single curve (Fig. 1.7).

This example indicates how experimental results could be used to show that the Reynolds number is an adequate scaling criterion for a particular arrangement. To date the Reynolds number has been found to be the only scaling criterion for the flow of Newtonian fluids in geometrically similar systems at low Mach numbers.

For the orifice plate configuration considered, an abrupt change in flow conditions takes place at Reynolds number of about 10^3. This is caused by the onset of turbulence, which is evidently a property of fluid motion. Turbulence is remarkable in that it can adjust its characteristics to maintain energy dissipation approximately proportional to (velocity)^2.

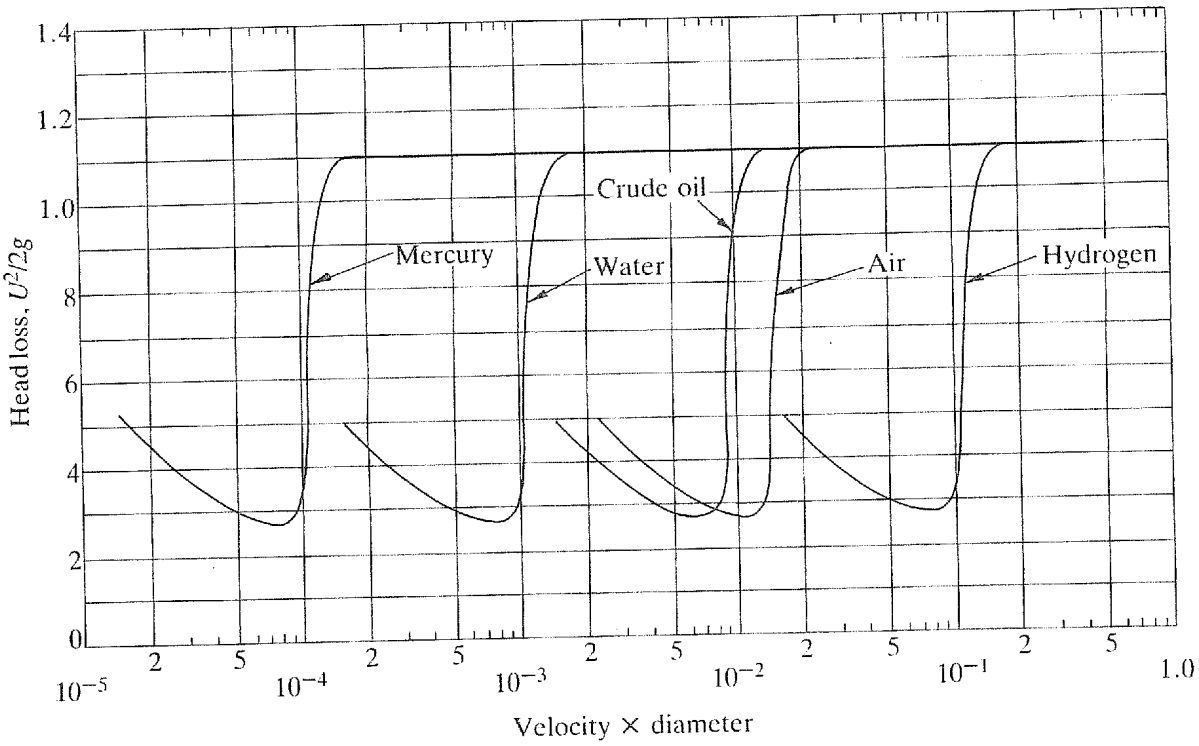

Fig. 1.6. Loss coefficient versus velocity × diameter.

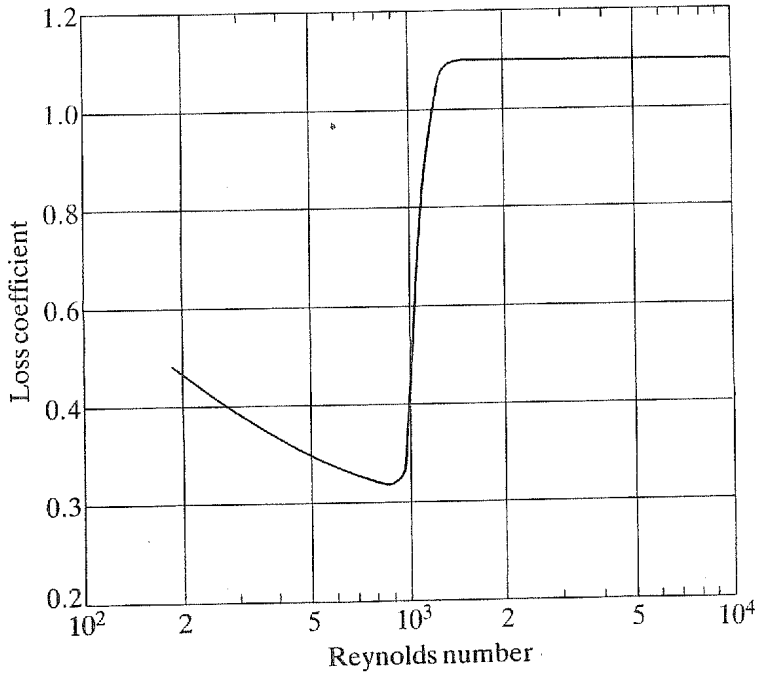

Fig. 1.7. Loss coefficient versus Reynolds number.

1.5. SYSTEM LOSS COEFFICIENTS

1.5.1. INTRODUCTION

The development of particular aspects of internal flow has often hinged upon adopting experimental methods and definitions that were generally accepted. This has been particularly true of system pressure losses, because so many variables are involved. The first step was to reduce the number of variables by fixing or at least limiting the effects of certain parameters. Experimental data could then be accumulated for the reduced parameter situation, allowing basic loss coefficients to be extracted. Once basic loss coefficients are available a broad understanding of a component's performance is possible by systematically varying additional parameters.

For logical reasons, different performance criteria have been adopted for various components; for instance, diffuser development has often been associated with turbomachinery where efficiency or pressure recovery is important, whereas bends are usually encountered in piping systems where the interest is in the pressure loss. Because of the small contribution by components to overall pressure losses in many systems, the practice arose of quoting components as being equal to so many diameters of straight pipe. A bend might be quoted as being equal to 25 pipe diameters and a globe valve to 300 pipe diameters. Although convenient for approximate calculations, the equivalent pipe concept suffers from an inherent defect in that friction and component losses vary differently with the Reynolds number.

There are considerable advantages in adopting one performance parameter, the system loss coefficient, for all system components, irrespective of the component's application. This section is concerned with defining a system loss coefficient.

1.5.2. SYSTEM LOSS COEFFICIENT

A system loss coefficient is defined as the non-dimensional difference in total pressure between the extreme ends of two long straight pipes or passages when there is a zero-loss component between the two pipes or passages and when the real component is installed. In non-dimensionalising the pressure loss the convention is to use the component's inlet velocity pressure, except when the component is an inlet from a large space, when the pipe or passage velocity pressure is used. The long pipe or passage before the component ensures a developed flow at inlet and the long pipe or passage at outlet from the component ensures that losses caused by flow redevelopment after the component are debited to the component. Figure 1.8 illustrates the procedure for establishing a loss coefficient. The inlet and outlet developed friction gradients are projected to the component and the difference between them established. The loss coefficient, K, is given by

$$K = \frac{\Delta H}{U^2/2g} = \frac{\Delta P}{\rho U^2/2} \tag{1.8}$$

where ΔH is the total head loss and ΔP is the total pressure loss.

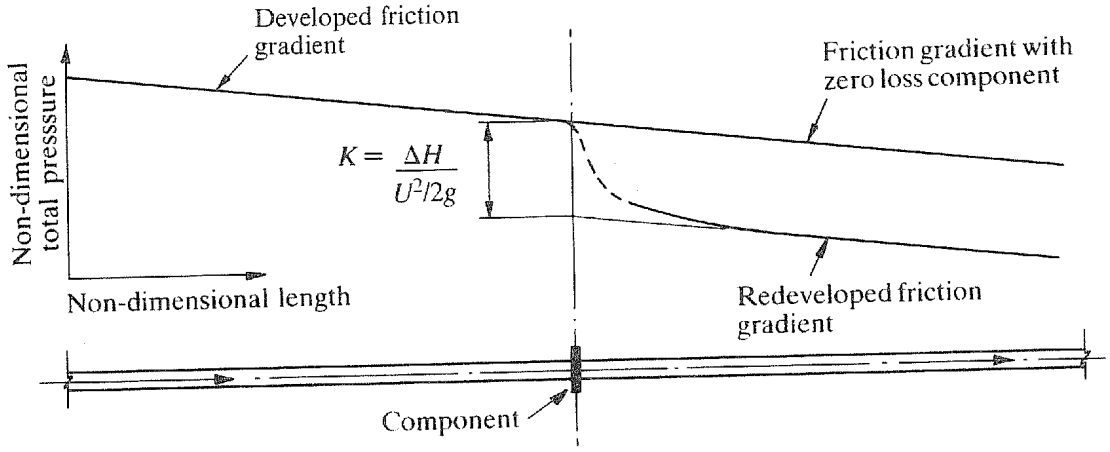

Fig. 1.8. Definition of the system loss coefficient

Obviously, many components do not have inlet or outlet pipes and others have only short inlet or outlet pipes. It is usually evident when the requirement for an inlet and outlet pipe is not applicable; for instance, bellmouth inlets from a large reservoir or diffusers discharging into a large reservoir. In these cases the requirement is only for a pipe after the bellmouth and a pipe before the diffuser. Experience shows that if the inlet and outlet pipes or passages are 30 or more diameters long, loss coefficients typically lie within about 0.02 of their value with much longer pipes or passages. When the inlet and outlet length requirements are not met, corrections have to be applied to system loss coefficients.

An extreme but illustrative example of the need for a standard definition for loss coefficients is provided by considering the flow and static pressure distribution through a 90° mitre bend (Fig. 1.9). Flow separates at the inside edge at the bend to give a peak/mean velocity ratio of about 2 at C. Following C there is a static pressure rise of two mean velocity heads and a loss of one mean velocity head. Based on static pressure measurements for the locations marked in Fig. 1.9, the following loss coefficients are obtained:

$$K_{b_{1C}} = 3.0 \qquad K_{b_{12}} = 1.0 \qquad K_{b_{13}} = 1.1$$

is the system loss coefficient.

1.5.3. BASIC COEFFICIENTS

It is convenient to nominate loss coefficients at a particular Reynolds number as being basic loss coefficients. In selecting a Reynolds number for basic loss coefficients it is necessary to take the following into account.

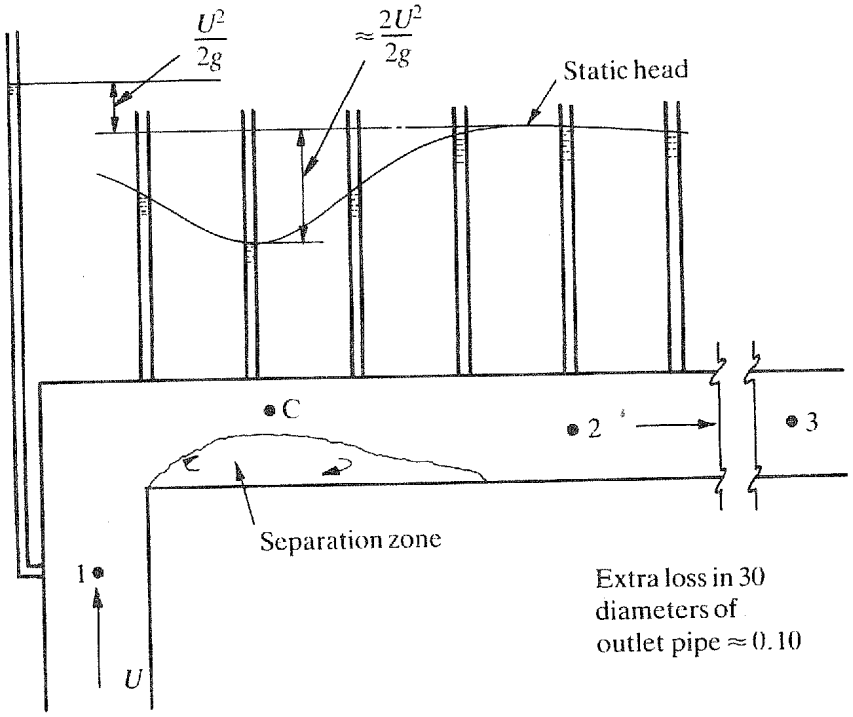

Fig. 1.9. Mitre bend loss coefficients based on static pressures

1. Major industrial flow systems and equipment, involving high energy costs, operate at Reynolds numbers of 10^6–10^8.
2. Above a Reynolds number of about 0.5×10^6 variations in loss coefficients are much smaller than at lower Reynolds numbers.
3. For cost and space reasons a Reynolds number of 10^6 is about the maximum that can be reached in laboratory experiments when a large number of tests is required.

Where possible the basic loss coefficients in Part 2 are for a Reynolds number of 10^6.

The most important aspect of the definition for a system loss coefficient is that it attempts to control the inlet and outlet flow conditions. Unfortunately, inlet conditions cannot be reproduced accurately as flow development is seldom symmetrical along a pipe or passage, even if extreme precautions are taken to have uniform flow at inlet to the pipe or passage. This means that there are no absolute values for loss coefficients. The component whose loss coefficients are influenced most by inlet flow conditions is the diffuser. Chapter 11 on diffusers contains a discussion on inlet effects.

Loss coefficients are only yet known over a limited range of Reynolds numbers. Virtually no information is available for loss coefficients above a Reynolds number of 10^6. Although some loss coefficients appear to become independent of Reynolds number below 10^6, it is unlikely that true Reynolds number independence is ever reached.

1.5.4. STRAIGHT PIPE LOSS COEFFICIENTS

The equation for straight pipe friction losses is

$$\Delta H = f\frac{L}{D}\frac{U^2}{2g} \tag{1.13}$$

or

$$\Delta P = f\frac{L}{D}\rho\frac{U^2}{2}$$

where ΔH is the total head loss (m of fluid), ΔP is the total pressure loss (N/m^2), f is the friction coefficient, L is the pipe length (m), D is the pipe diameter (m) and U is the mean velocity (m/s).

The friction coefficient in equation (1.13) is in effect the ratio of the head loss in a one diameter length of pipe to the mean velocity head, as illustrated in Fig. 1.10. It is convenient when carrying out computer solutions to describe a system in terms of modules and nodes. Modules are system components, including pipes, and nodes are the connection points between modules. To be consistent, straight pipes should have loss coefficients of the same form as for components. A pipe loss coefficient is defined as

$$K_f = fL/D \tag{1.14}$$

In order to define the friction coefficient in equation (1.13) unequivocally, the friction coefficient is the value obtained from measurements over a long section of straight pipe, preceded by a sufficient length of similar pipe, such that the friction coefficient does not change with position along the measuring section. This developed flow friction coefficient is used in all calculations involving straight pipes. Any departure from developed flow friction is accounted for in the loss coefficient of the component causing the non-developed flow.

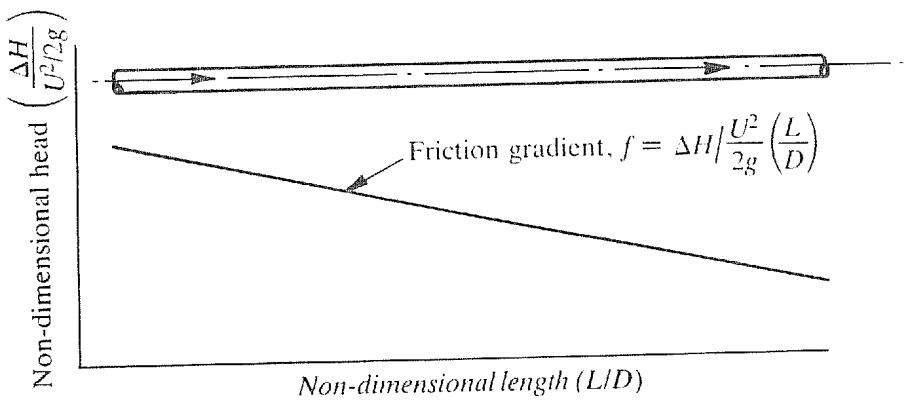

Fig. 1.10. Straight pipe friction gradient

1.6. KINETIC ENERGY DISTRIBUTION

Averaged over a pipe or passage cross-section, developed flow has a higher kinetic energy than an equivalent one-dimensional flow with a velocity equal to the mean velocity of the developed flow. Developed turbulent flow has about 2–4 per cent higher kinetic energy than an equivalent one-dimensional flow. This extra kinetic energy is obtained at the expense of the mean total pressure of the flow and is non-recoverable. Part of the static pressure drop in the initial section of a pipe or passage is associated with the redistribution of flow across the pipe, but for convenience in calculations it is treated as a loss attributed to the upstream component.

Developed laminar flow has a peak/mean velocity ratio of 2 and twice the kinetic energy of an equivalent one-dimensional flow. Laminar flow friction coefficients for pipes are given by 64/Re, so that at Reynolds numbers less than 64 more than one velocity head is lost per diameter length of pipe. At low Reynolds numbers the errors in accounting for the extra kinetic energy of the flow are usually not important, but at a Reynolds number of 2000, close to the laminar to turbulent transition region, one mean velocity head is equal to the loss in 30 diameters of pipe, making it essential to account for the excess kinetic energy. Where loss coefficients are given for laminar flow they are for developed laminar flow at inlet and following the component and, therefore, account fully for flow redevelopment after the component.

1.7. EXAMPLES

Until a calculation for a particular system is required, fluid mechanics is a non-dimensional science. Except for the worked examples, the text is concerned with non-dimensional ratios.

Examples are aimed at demonstrating the application of loss coefficients to particular system configurations. In order not to detract from the main purpose, and to give a feel for the quantities involved, the calculations are usually made with water as the flowing fluid, and pressure losses are expressed in terms of a head of flowing fluid. The use of head, either in metres of fluid for a liquid or in millimetres of water for a gas, is not only conceptually useful, it is also consistent with many modern fluid mechanics textbooks and with quoted performance for fluid machines — pumps, turbines and fans.

1.8. CLASSIFICATION OF LOSS COEFFICIENTS

Sufficient experimental data are available on a particular system components to classify the data as to their adequacy or otherwise for design. Where appropriate, data or a suggested design approach has been put into one of three classes. In broad terms, class 1 are definitive loss coefficients; class 2 loss coefficients are adequate for normal design purposes; class 3 are suggested values for situations where experimental data are not available or are of doubtful origin.

Class 1. Loss coefficients in this class are based on experimental data usually from two or

more sources or from research programmes which have been cross-checked against other work. The loss coefficients are considered definitive. In practice, because of the severe restraints imposed on inlet and outlet conditions, geometric accuracy and the range of Reynolds number over which tests have been made, the loss coefficients in class 1 are usually not directly applicable. Correcting the coefficients to apply to situations different from those under which they were established puts them into class 2 or class 3.

Class 2. Loss coefficients in class 2 are:

1. experimentally derived loss coefficients from isolated research programmes where no detailed cross-checking is possible against other sources;
2. estimated loss coefficients from two or more research programmes whose results do not agree within what could be expected to be the experimental accuracy; and
3. loss coefficients from class 1 converted to apply outside the strict limitations imposed for class 1 coefficients and about which experimental information is available to predict the effects of departing from class 1 conditions.

Class 3. Loss coefficients in class 3 are:

1. experimentally derived values from less reliable sources; and
2. loss coefficients from classes 1 and 2 converted to apply outside their range of application and about which there is little information to predict the effects of departing from the conditions under which they were derived.

2. ORIGINS OF PRESSURE LOSSES

2.1. INTRODUCTION

In this chapter a number of the important characteristics of turbulence and turbulent boundary layers are described. Except for biological systems, flow of viscous liquids, and flow in porous medium and fine clearances, turbulent flow is the normal state for fluids in motion, but it is only in special circumstances that turbulence or its effects are seen or felt. Whirls in water close to a river bank show the rotational motions characteristic of turbulence; buffeting by the wind on a gusty day is an example of the fluctuations associated with turbulent eddies; breathing out on a cold day reveals the turbulent nature of the jet formed by exhaling and the fortunately rapid dispersion that follows.

Turbulent dissipation is at a minimum in a smooth, straight pipe or passage. Deviation from these conditions — by roughening the walls, or turning or diffusing the flow — enhances turbulence. Within components are regions where fluid is accelerated and regions where it is decelerated. During acceleration static pressure is converted to velocity pressure, which is a stable and a low energy dissipation process. In regions where velocities are reduced, intense turbulence is generated as velocity pressure is converted to static pressure. The term "adverse gradient" is used to denote a region where the static pressure rises in the direction of flow.

In internal flow, turbulence is a phenomenon which is considered desirable in some situations and undesirable in others; for instance, it is responsible for the majority of pressure losses but it also makes many heat transfer, mass transfer and combustion processes economically possible. Turbulence presents the greatest puzzle in the physical sciences. In studying the physical world it is usually possible to derive sufficient relationships, in the form of partial differential equations, to determine uniquely the state of a system, given a set of initial conditions for the system and the boundary conditions of the system. This is not the case for most engineering fluid flows, because boundary conditions cannot be defined.

Take the simple situation of flow in a long straight pipe. A physically appropriate boundary condition is that there can be no flow perpendicular to the pipe wall. In reality this is not the case, because above a certain Reynolds number the flow becomes turbulent. An observer moving at the local mean velocity in a turbulent flow would see fluid particles moving in all directions. From this observation it is evident that, in turbulent flow, boundary conditions do not determine the flow uniquely. Instead of being able to describe the state of turbulent flow in a particular system uniquely, the reality is that on a microscopic level and at an instant in time, flow conditions are unique, never being repeated in that particular system or in any other system.

Turbulent eddy sizes in industrial flow systems typically extend down to 10^{-4} m in diameter. Of the order of 10^{12} calculations per second per cubic metre of system volume are required for a realistic simulation using the basic equations of fluid flow. Since interest is in

time-averaged conditions within a flow, it is possible to simplify the computation of turbulent flows by using coefficients derived from experiments. This makes practical the calculation of flows in complex internal flow passages. However, for the foreseeable future the cost and expertise required to carry out such calculations limits the use of computer methods to important flows which cannot be readily simulated using physical model studies.

2.2. TURBULENCE

In pipes and passages, away from smooth contractions, flows are usually turbulent if the Reynolds number exceeds 2000 — equivalent to a water velocity of 0.002 m/s in a 1 m pipe or 2 m/s in a 1 mm pipe. Following a smooth contraction the flow may still be laminar even though the Reynolds number is much greater than 2000. In engineering systems, transition of the wall layer to turbulent flow following a smooth contraction typically takes place before a Reynolds number — based on the longitudinal distance from the inlet — of 10^6 is reached. Close to a boundary is a region known as the laminar or viscous sub-layer. The thickness of this sub-layer is related to the smallest turbulent eddies that can exist without viscosity almost instantly transforming their kinetic energy into heat. In the steep velocity region outside the viscous sub-layer (Fig. 2.1) shear stresses tear the fluid into small energetic eddies. Away from the walls, in the region of low shear stresses, eddies are larger and elongated.

Turbulence consists of three-dimensional irregular eddies with length scales ranging from the dimensions of the flow passage down to eddies whose Reynolds numbers, based on the eddy diameter, are of the order of unity. Even these eddies are very large compared with molecular length scales, so turbulence takes place in a continuum.

Turbulence needs a continual supply of energy or it decays rapidly. This energy is provided by shear forces at the expense of the total energy of the flow. Part of the energy transferred into turbulence is immediately dissipated, particularly in regions close to boundaries and along the edges of discontinuities in velocity associated with wakes and flow separation. The

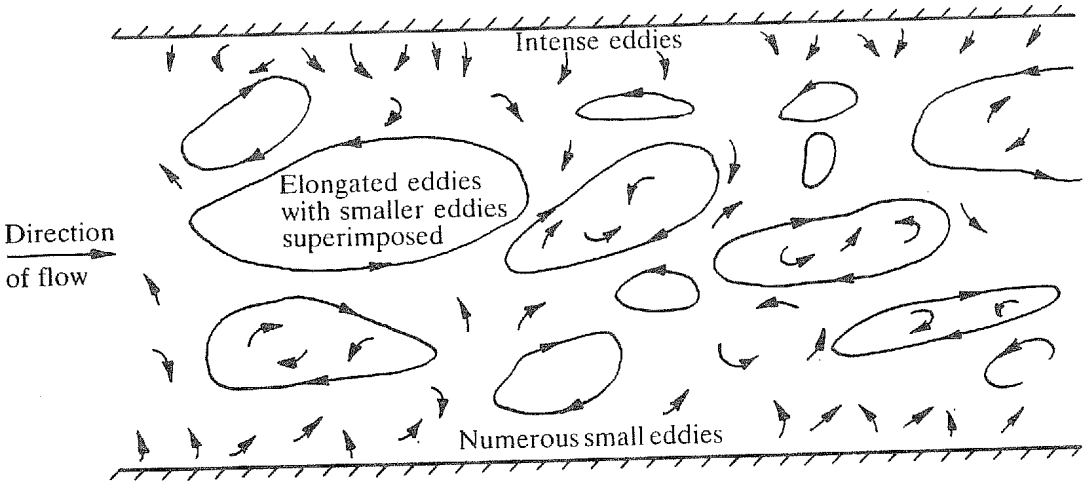

Fig. 2.1. Turbulence in pipes and passages, as seen by an observer moving at the mean flow velocity

remaining energy is transferred to large eddies and cascaded down to smaller and smaller eddies, eventually to be converted into internal energy by viscous shear.

Turbulence increases momentum, heat and mass transfer. In pipes and passages turbulence is mainly swept downstream by the mean flow so that radial transfer across the flow is a relatively slow process. For example, at high Reynolds numbers it takes 30 pipe diameters following a smooth contraction before turbulence reaches a pipe centreline, whereas up to 200 pipe diameters are required before a tracer injected from a point in the wall is reasonably dispersed across the flow. In the case of developing flow following a smooth contraction, the centreline velocity peaks at 30 diameters from the inlet. In trying to reach equilibrium the centreline velocity undershoots at 60 diameters from the inlet and starts to increase again.

In smooth pipes turbulence intensities vary from 10 per cent (r.m.s.) of the local velocity close to the wall to 4 per cent at the centre of the pipe. Along the edges of jets and wakes turbulence levels may exceed 30 per cent (r.m.s.). Close to a boundary, where maximum turbulence generation and dissipation occurs, eddies have short time scales compared with the rest of the flow. Equilibrium conditions are, therefore, rapidly approached close to the wall, making the flow near the wall almost, but never totally, independent of the main flow. Many of the difficulties of uniquely defining component loss coefficients and discharge coefficients for orifice plates and other flowmeters are due to the slow and unstable development of the main flow and its interaction with the near-wall layer. Minor variations in developing boundary layers show up as a distortion of the flow near the centreline tens of diameters later.

Because the non-uniform growth of boundary layers appears to be the norm, absolute reproduction of flow conditions, even in apparently geometrically similar situations, is impossible. Although a mean velocity profile similar to that of developed pipe flow can be generated artificially, the turbulence structure is always out of balance, causing the profile to change rapidly in the downstream direction. This rules out using artificially generated profiles as standard profiles. Following a smooth contraction, friction gradients settle to a steady gradient 15 diameters after the contraction. More than 30 diameters are required before a steady friction gradient is established following components such as bends, diffusers and orifice plates.

2.3. ADVERSE GRADIENTS

Potential and static pressure can be converted to velocity pressure with virtually no energy loss, but the opposite process usually involves significant energy dissipation. The reason for the non-reversibility lies in the non-uniformity of velocity in parallel flow as against the uniformity of the static pressure. Referring to Fig. 2.2, which shows the non-dimensionalised velocity and velocity pressure for developed pipe flow, it can be seen that there is a serious deficiency in energy in the near-wall part of the cross-section. When the energy deficient fluid enters a region of rising static pressure, involving a conversion of velocity pressure to static pressure, it either has to be supplied with energy from the higher energy fluid away from the walls, or it gives up all its velocity energy and comes to rest. If part of the flow is brought to rest the flow is said to have stalled or separated from the boundary. When separation

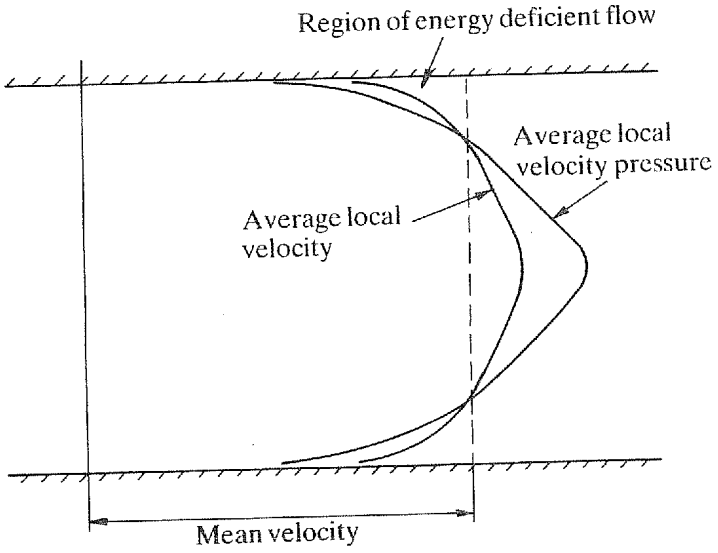

Fig. 2.2. Velocity and velocity pressure distributions for developed pipe flow

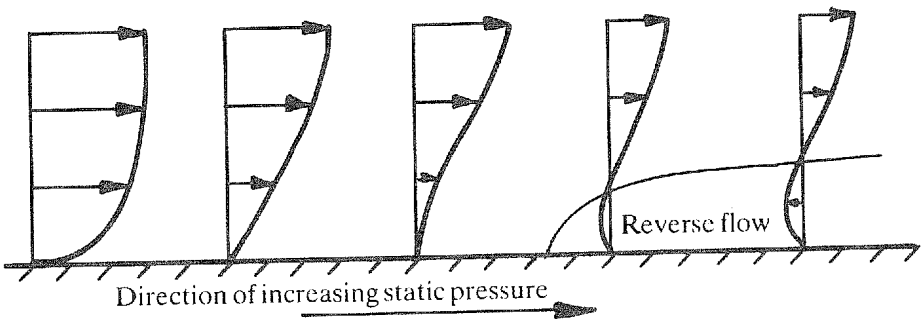

(a) Change in near wall velocity profile in an adverse pressure gradient

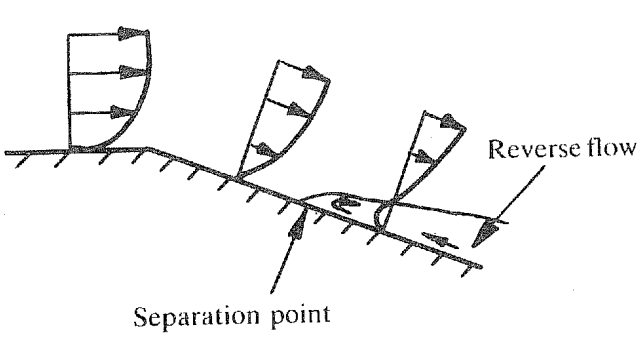

(b) Flow along a diffuser wall

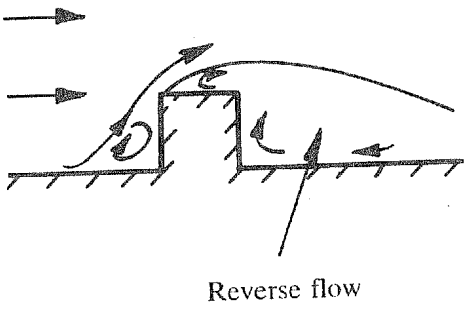

(c) Flow over an obstruction

Fig. 2.3. Flow separation

takes place the main flow usually contracts for some distance downstream of the separation point and an area of reverse flow forms (Fig. 2.3). Following separation large scale mixing spreads through the main flow, evening out the energy distribution at the expense of a drop in total pressure; flow re-attachment follows.

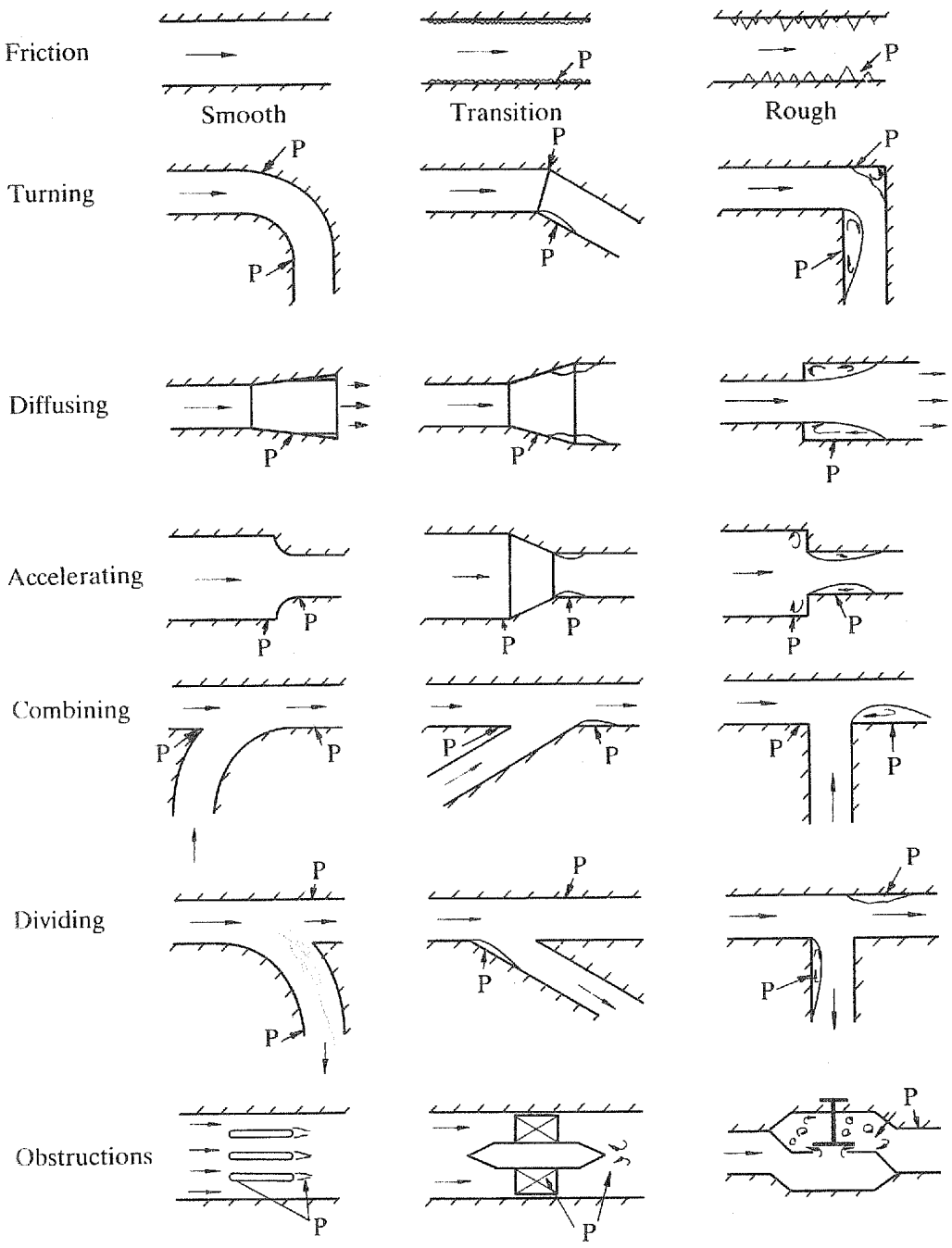

Fig. 2.4. Location of adverse gradients

When the main flow is turned, static pressure gradients are set up across the flow. In this situation the possibility exists for low energy fluid entering a region of high static pressure to escape around the boundaries towards a region of lower static pressure. The result is secondary flows superimposed on the main flow, with additional losses due to mixing in the turning section and in the outlet pipe or passage.

All system components have one or more region where the static pressure rises in the direction of flow. The location of the principal adverse gradients for common system components is shown in Fig. 2.4.

Low loss components in the left-hand column of Fig. 2.4 involve no, or only small, areas of separation. A significant part of the head loss of a component occurs in the redevelopment of the flow after the component.

Components in the middle column of Fig. 2.4 have moderate areas of separation. In the case of pipe flow the individual roughness elements are beginning to project through the laminar sub-layer and cause flow separation and mixing in the wakes from individual elements.

Components in the right-hand column of Fig. 2.4 have large areas of flow separation followed by regions of high energy dissipation.

3. CALCULATION OF SYSTEM PRESSURE, FLOW OR SIZE

3.1. INTRODUCTION

The steps in obtaining an estimate of system head requirements or flow rate or size are the following.

1. Define the geometric parameters of the system and components.
2. Define the flow parameters — velocities and Reynolds numbers.
3. Select appropriate loss coefficients.
4. Calculate individual component losses and correct as necessary for interactions between components.
5. Sum the individual system losses, plus the static lift or the pressure differential across the system, to establish the required pump or fan head.

When geometrical and flow parameters are known, the selection of appropriate loss coefficients is the main task. In situations where the flow or pipe and component size has to be found, the simplest and usually the quickest method is to adopt a trial and approximation procedure, as demonstrated in Examples 2 and 3 in Section 8.6.

3.2. EQUATIONS FOR LOSSES

The following equations from Chapter 1 are sufficient to calculate pressure losses for liquids and also for gases flowing at Mach numbers less than 0.2 — equivalent, in the case of air, to a velocity of 70 m/s at normal temperature and pressure.

For individual pipes, passages and components

$$\Delta H = KU^2/2g \tag{3.1a}$$

$$\Delta P = K\rho U^2/2 \tag{3.1b}$$

where K is the loss coefficient, ΔH is the total head loss (m) and ΔP is the total pressure loss (N/m^2).

Note: For flow in pipes and passages K in equations (3.1) is given by

$$K = fL/D$$

where

$$f = \frac{\text{Head loss in a one hydraulic diameter of pipe or passage}}{U^2/2g}$$

and D is the hydraulic diameter or pipe diameter. For a passage D is given by

$$D = \frac{4 \times \text{Passage cross-sectional area}}{\text{Passage perimeter}}$$

The loss coefficients, K, in equation (3.1) are provided as a function of the Reynolds number. The coefficients can be found from Part 2 or from additional sources.

The overall system head loss, H, or pressure loss, P, is found by summing the head and pressure losses for individual components. For a system with n components

$$H_{\text{overall}} = \sum_{i=1}^{i=n} \Delta H_i \tag{3.2a}$$

$$P_{\text{overall}} = \sum_{i=1}^{i=n} \Delta P_i = \rho g H_{\text{overall}} \tag{3.2b}$$

To obtain the duty of a pump or fan it is necessary to add the static lift or pressure difference across the ends of the system to the values obtained from equations (3.2a) or (3.2b).

3.3. SYSTEM CALCULATION AND PUMP OR FAN SELECTION

The method adopted for carrying out a calculation of overall pressure loss depends on individual preference and the suitability of the method for particular types of system. For instance, if the mean velocity is constant throughout the system, the individual loss coefficients could be summed and multiplied by the velocity head to obtain the overall head loss.

Complexities arise mainly from interaction between closely spaced components involving a departure from simple summing of individual component losses. For systems consisting mainly of straight pipes or passages, interaction effects are seldom important as regards pressure losses. If the distance between components is more than four diameters, neglecting interaction effects will usually result in the loss being slightly overestimated.

As an example of one calculation procedure, consider the simplified system in Fig. 3.1. For calculation purposes the components are best represented connected together at nodes as in Fig. 3.2, pipes being treated in the same manner as components. This type of system representation has advantages when carrying out computer solutions of complex systems and pipe networks.

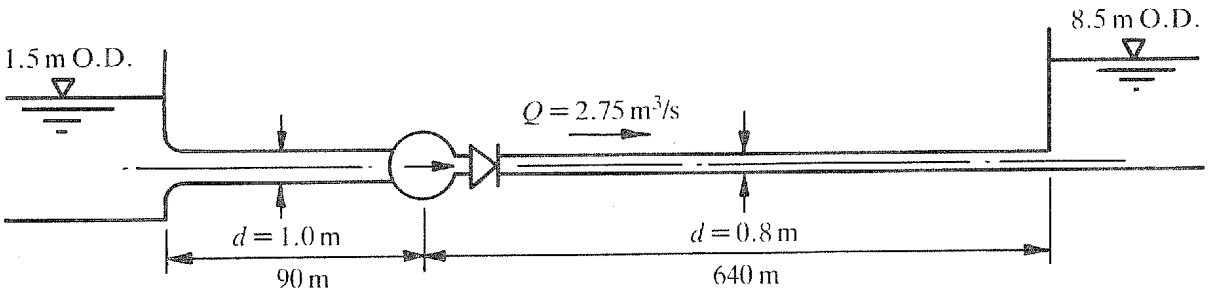

Fig. 3.1. Simple system

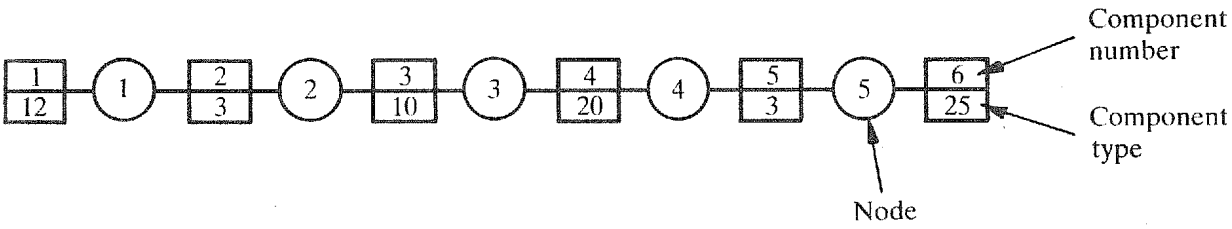

Fig. 3.2. Node and component representation of the system in Fig. 3.1

Table 3.1. Calculation for the system shown in Fig. 3.1

($\rho = 1000$ kg/m^3, $\nu = 1.1 \times 10^{-6}$ m^2/s, friction coefficient taken as 0.015, including an allowance for fouling)

Node	Component No.	Component Type	Diameter (m)	Velocity (m/s)	Reynolds number	$U^2/2g$ (m)	K*	Head loss (m)	Pressure loss (kN/m^2)
1	1	12–reservoir inlet	1.0	3.50	3.2×10^6	0.625	0.1	0.06	0.589
1–2	2	3–pipe	1.0	3.50	3.2×10^6	0.625	1.35	0.84	8.240
2–3	3	10–pump	—	—	—	—	—	—	—
3–4	4	20–reflux valve	0.8	5.47	4.0×10^6	1.53	0.5	0.76	7.456
4–5	5	3–pipe	0.8	5.47	4.0×10^6	1.53	12.0	18.36	180.112
5	6	25–reservoir outlet	0.8	5.47	4.0×10^6	1.53	1.0	1.53	15.000
							Total loss =	21.55	211

*For pipes $K = fL/D$.

From Part 2 the loss coefficients, K, in Table 3.1 are appropriate for the various components of Fig. 3.1. Other relevant data are given in Table 3.1 to which, in some cases, it will be necessary to add details of pipe roughness and of interaction correction factors if components are close together. An example using interaction correction factors is included in Chapter 10.

$$\text{Pump head} = \text{Total head loss} + \text{Static lift}$$
$$= 21.6 \text{ m} + 7 \text{ m}$$
$$= 28.6 \text{ m}$$
$$= 28.6 \times 1000 \times 9.81 = 280 \text{ kN/m}^2 = 2.8 \text{ bar}$$

A pump or fan that most closely meets a design duty will usually be selected from a standard range. The head-flow characteristic of a suitable pump for the system in the example is shown in Fig. 3.3. Also shown in Fig. 3.3 is the system characteristic. For most purposes

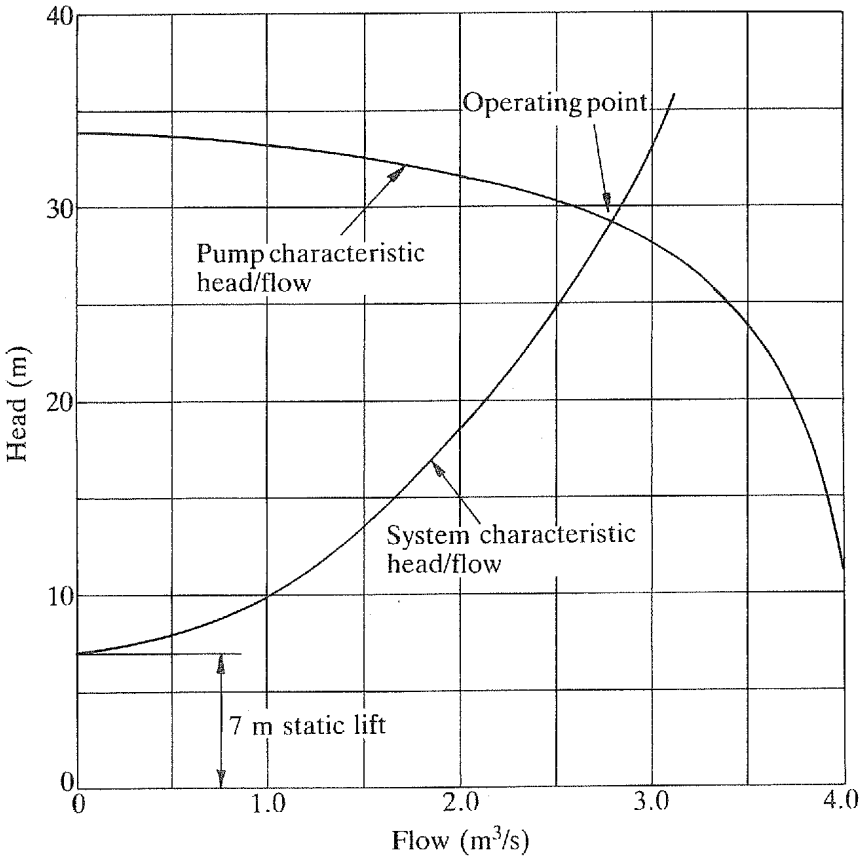

Fig. 3.3. Pump and system characteristics

the system characteristic is obtained by calculating the overall head loss at the design flow and obtaining the head loss at other flows, assuming that it varies as (flow rate)^2.

For security of supply and flexibility in operation two or more pumps or fans may be used. The head-flow characteristics with two 50 per cent duty pumps operating in parallel are shown in Fig. 3.4. Because most of the head loss is due to friction, failure of one pump results in only a 33 per cent reduction in the system flow, as indicated in Fig. 3.4. If most of the head is used in static lift, one pump out of two will only deliver slightly over 50 per cent of the two-pump flow.

In the case of a system where most of the pump or fan head is used in overcoming friction parallel operation is usually not a problem as the head varies markedly with the number of machines operating. When system flows are controlled by throttling, care is necessary to ensure that:

1. the head-flow curves of pumps or fans operating in parallel rise steadily to the shut valve condition, as in Fig. 3.4; and
2. if the head-flow curves of the pumps or fans are different, the maximum system head is below the shut valve head of any of the pumps or fans.

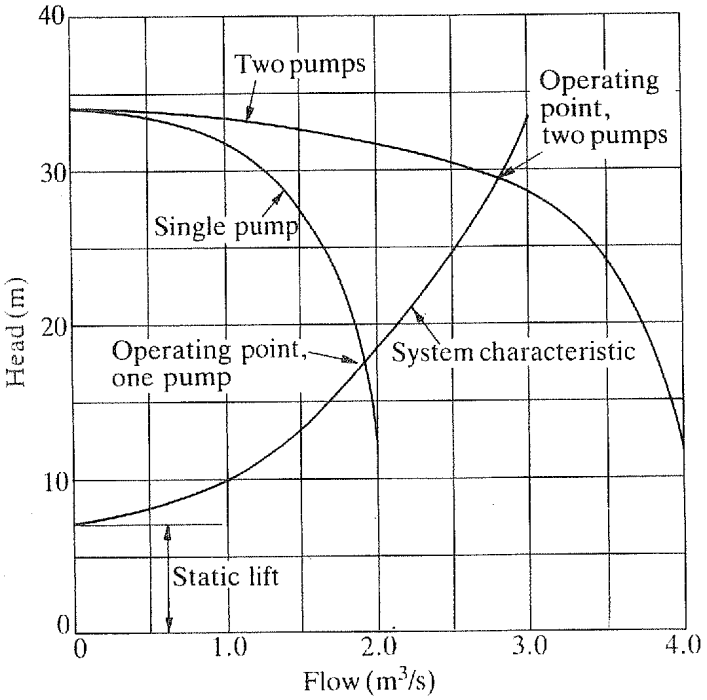

Fig. 3.4. Two 50 per cent pumps in parallel

When variable speed pumps or fans are used it is necessary to include additional lines on the head-flow plot as in Fig. 3.5. For the particular case shown in Fig. 3.5 a pump speed of about 70 per cent is necessary before the pump overcomes the static lift and flow commences. Flow regulation is therefore achieved over a 30 per cent speed range from 70 up to 100 per cent.

3.4. TOLERANCE ON CALCULATED VALUES

One of the most difficult aspects of head requirement calculations is deciding what allowance to add to the calculated value in order to allow for uncertainties in the loss coefficients, departures from nominal dimensions and deterioration in service. Because of the predominance of friction losses in many systems and the fact that deterioration usually affects friction losses more than other losses, the problem usually concerns the value that the friction coefficient should take.

The procedure for obtaining a friction coefficient, outlined in Chapter 8, is to estimate a roughness height and use this along with the pipe diameter and Reynolds number to obtain a friction coefficient. In practice, friction coefficients are often based on experience. For example, the reasoning behind the friction coefficients adopted in designing a large sea-water cooling system for a petrochemical complex might be as follows.

1. The pipes will be steel and lined with mortar after construction to prevent corrosion. The

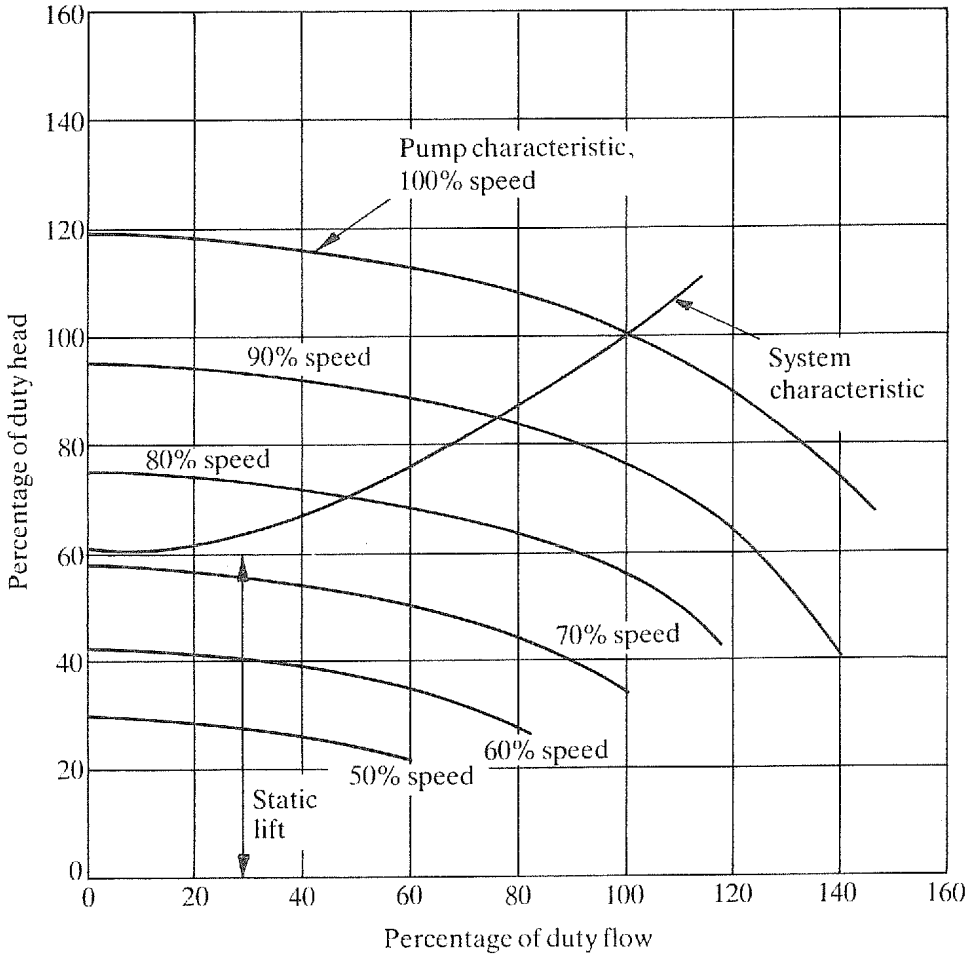

Fig. 3.5. Variable speed pump characteristics

standard of workmanship will be good, corresponding to an initial friction coefficient of about 0.01 at the design Reynolds number of 5×10^6.

2. Chlorination will be used to minimise marine growth and slime formation.
3. A minimum velocity of 2.5 m/s will be used to minimise colonisation by marine animals and to hinder their feeding.
4. For surge calculations a range of friction coefficients between 0.01 and 0.02 are to be used.
5. In calculating head losses when sizing fixed orifices, installed to balance flows through various heat exchangers, a friction coefficient of 0.015 will be used.
6. The pump head to be based on a friction coefficient of 0.02. Either the system will be cleaned if this value is exceeded, or some loss of capacity will be accepted.

Because so many factors are involved in the selection of friction coefficients for systems that deteriorate in service, experience and information about similar systems have to be the main guides.

5. INTERNAL FLOWS

5.1. INTRODUCTION

The aim of this chapter is to provide an insight into flows within system components and the relationship between flow patterns and the performance of a component. Straight pipes and passages are considered first since they provide the inlet conditions for components as well as being important in their own right. Discussion of component flows starts with straight wall diffusers which have a single adverse pressure gradient. Flows involving two or more adverse gradients, some with additional complications of secondary flows, are treated in the following sections.

To illustrate various aspects of component behaviour, simplified versions of component performance charts from Part 2 are included. It is not intended that the performance charts in this section be used for design. The main discussion of flow in pipes, passages and components is for Reynolds numbers greater than 10^5, where component performance is only weakly dependent on the Reynolds number. Comments are made on the effects of operating with lower Reynolds numbers in the turbulent flow regime. Laminar flows are considered in the final section.

5.2. STRAIGHT PIPES AND PASSAGES

5.2.1. INTRODUCTION

Viscosity causes fluid particles immediately adjacent to a rigid surface to be brought to rest. With increasing distance from a surface, fluid particles are less and less influenced by the surface, so the velocity increases up to a maximum which is usually at the pipe or passage centreline. The term "boundary layer", used to describe the area of low energy fluid that forms along a surface in external flows, such as an aeroplane wing (Fig. 5.1), is also applied to internal flows. In pipes and passages the flow is confined, so that events in the boundary layer on one part of the perimeter are communicated indirectly to all the flow. For instance, if, because of a change in roughness on one wall of a passage, the flow slows down close to that wall, velocities over the rest of the cross-section must increase. Turbulence generated locally may not immediately affect conditions across the whole cross-section, but as the flow proceeds downstream the turbulence spreads across the flow. Secondary flows, which modify boundary layers, are present in all non-circular cross-sections and are encountered in circular cross-sections after components such as bends. These and other factors make internal flow boundary layers extremely complex which, combined with the low accuracy of boundary layer measurements, makes for poor predictions of boundary layers and of their effects on component performance.

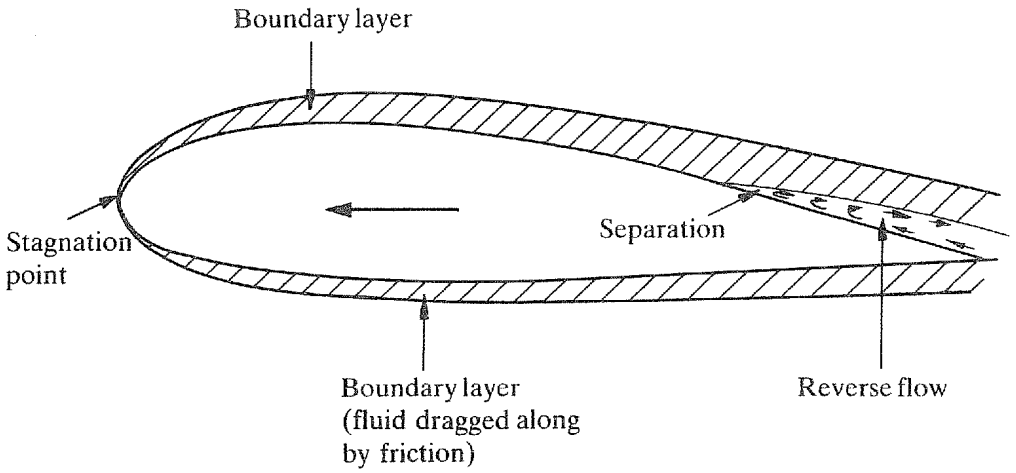

Fig. 5.1. External flow boundary layer

5.2.2. FLOW DEVELOPMENT

The various stages of flow development in a straight pipe, preceded by a well designed contraction, are shown in Fig. 5.2. In region 1, close to the inlet, the velocity profile is virtually one-dimensional with a thin boundary layer. If the flow is laminar leaving the contraction it will become turbulent in this region. Region 2 extends to the point where the boundary layers merge at the centre of the pipe. At a Reynolds number of 10^6 the boundary layers merge 30 diameters from the inlet. As flow on the centreline has not been affected by turbulence, its total energy at the junction of regions 2 and 3 is nearly the same as at inlet to the pipe. Assuming a static pressure drop of 0.35 of the mean velocity head over the first 30 diameters, the velocity at the centreline will be roughly $\sqrt{1.35}$ or 1.16 times the mean velocity. Over region 3 the centreline velocity decreases, reaching a minimum after a further 30 diameters. The variation of the centreline/mean velocity ratio with distance from the inlet is shown in Fig. 5.3.

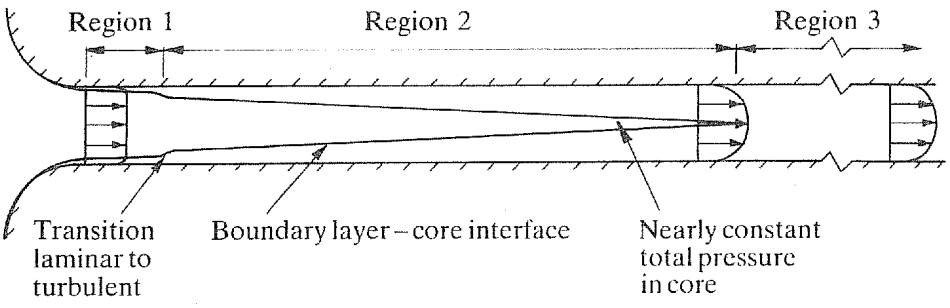

Fig. 5.2. Boundary layer development after a smooth contraction

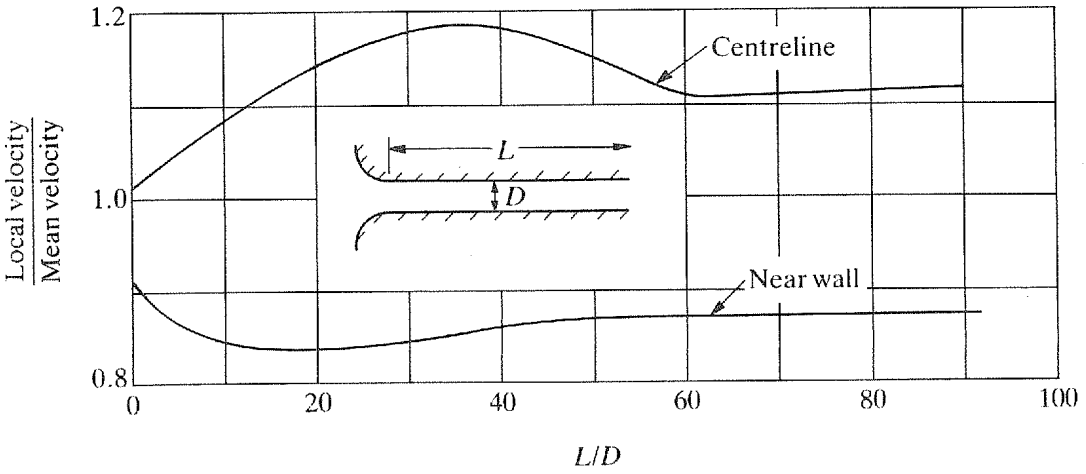

Fig. 5.3. Centreline/mean velocity ratio and near-wall/mean velocity ratio ($Re \approx 10^6$)

Also shown in Fig. 5.3 is a curve of local to mean velocity ratio along a pipe at 0.08 of the pipe radius from the wall. This curve may be significantly different between stations around the wall of a pipe and between measurements made in geometrically similar pipes operating at the same Reynolds number. The fact that the local/mean velocity ratios vary so much causes great difficulties in establishing "definitive" loss coefficients. This is particularly so for diffusers whose performance depends strongly on the energy in the near wall flow.

The laminar to turbulent transition location shown in Fig. 5.2 is not a clearly defined region. It extends over a section of surface whose distance from the inlet will vary around a pipe. Through the transition region, intermittent spots of turbulence, surrounded by laminar flow, become more frequent, until they engulf the complete pipe surface. After full transition to a turbulent boundary layer the flow at the walls is still intermittent. High energy bursts of turbulence penetrate to the wall, causing spots of low energy fluid to be ejected from the wall. It is usual to refer to turbulent flows as having a laminar or viscous sub-layer close to a wall or surface. In reality, although the mean velocity profile close to a wall may be laminar in form, there are marked local fluctuations in velocities.

5.2.3 CIRCULAR CROSS-SECTIONS

The simplest flows occur in pipes where axial symmetry results in every part of the pipe perimeter influencing the flow in the same way. Referring to Fig. 5.4, the shear force, τ, applied to the flow in a pipe of diameter d and length L, acting over the surface area πdL, can be equated to the pressure drop, ΔP, acting on the cross-sectional area, A:

$$\Delta P\, A = \tau \pi d L$$

For calculation purposes a friction coefficient, defined as the head loss in a one diameter

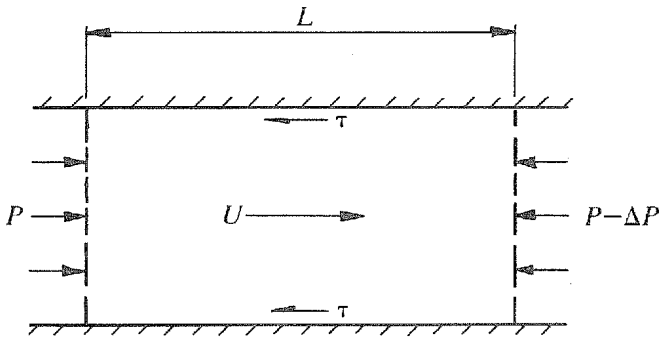

Fig. 5.4. Forces acting on a fluid in a pipe

length of pipe non-dimensionalised by the mean velocity head, is used in preference to the wall shear stress. The friction coefficient is given by

$$f = \frac{\Delta H}{U^2/2g}\frac{d}{L}$$

where $\Delta H = \Delta P/\rho g$, so

$$\tau = \frac{f}{4}\rho\frac{U^2}{2} = \frac{f}{4}(\text{velocity pressure})$$

5.2.4. NON-CIRCULAR CROSS-SECTIONS

In non-circular cross-sections, such as the square passage of Fig. 5.5, the interaction between the walls and the flow varies with position. The result is non-uniform wall shear stresses, as indicated in Fig. 5.5. Since the static pressure change along a passage is the same for all of the flow, a mechanism must be present which compensates for the varying wall shear stresses. This mechanism takes the form of secondary flows which move fluid from low to high shear stress regions, evening out the shear stress distribution and causing an exchange between static and velocity pressures as flow is displaced between high and low velocity regions. Figure 5.6 illustrates the secondary flow paths in a square section. Secondary flow velocities reach a maximum of 1–2 per cent of the axial velocity.

For many non-circular cross-sections a satisfactory procedure for calculating head losses is to replace the pipe diameter in the friction and Reynolds number equations by the hydraulic diameter. The hydraulic diameter, D, is given by

$$D = \frac{4 \times \text{Area}}{\text{Perimeter}} = \frac{4 \times A}{P_r}$$

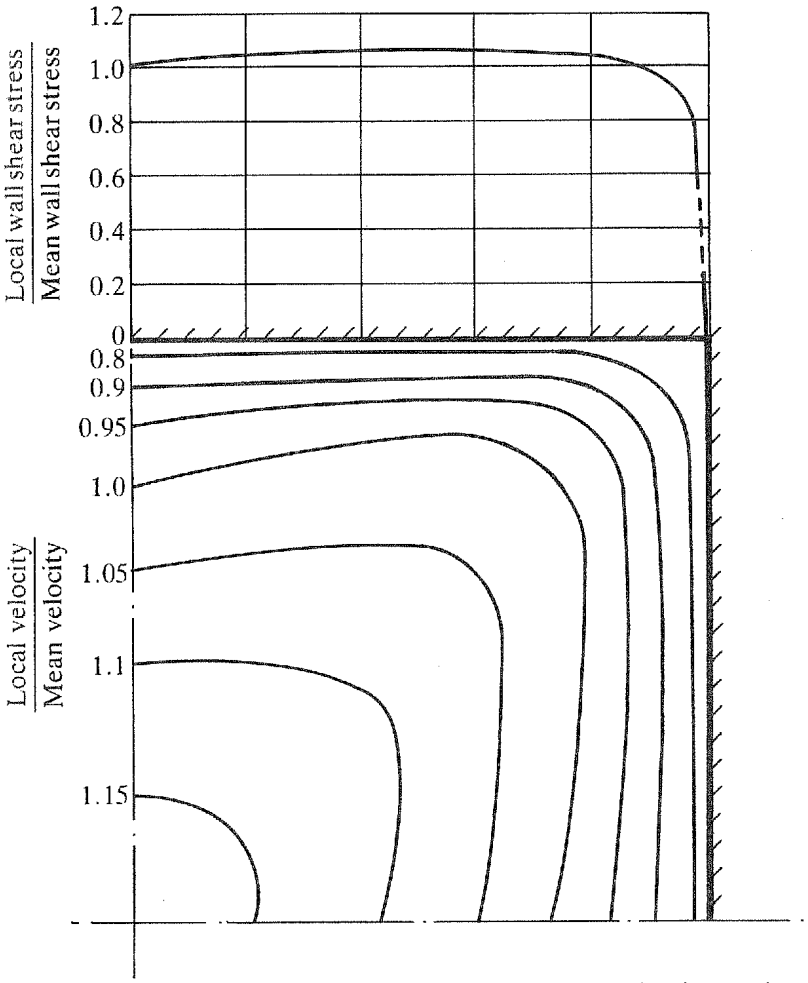

Fig. 5.5. Typical velocity contours and wall shear stress distribution for a quarter of a square passage

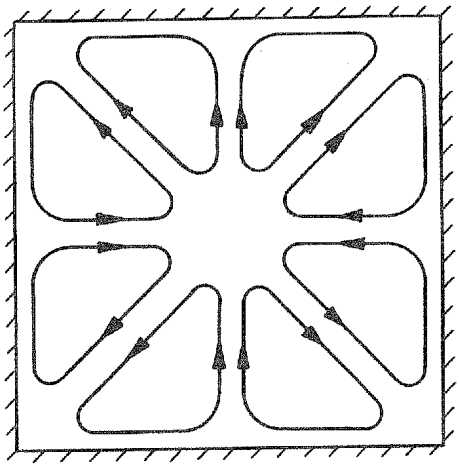

Fig. 5.6. Secondary flow paths in a square cross-section

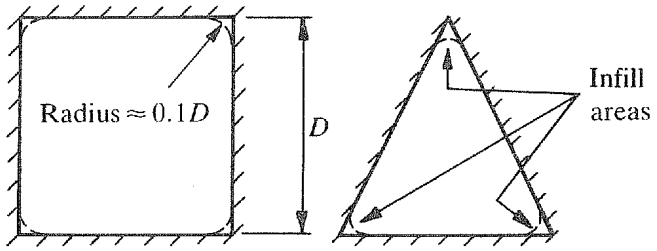

Fig. 5.7. Areas filled in to reduce P_r/A^3

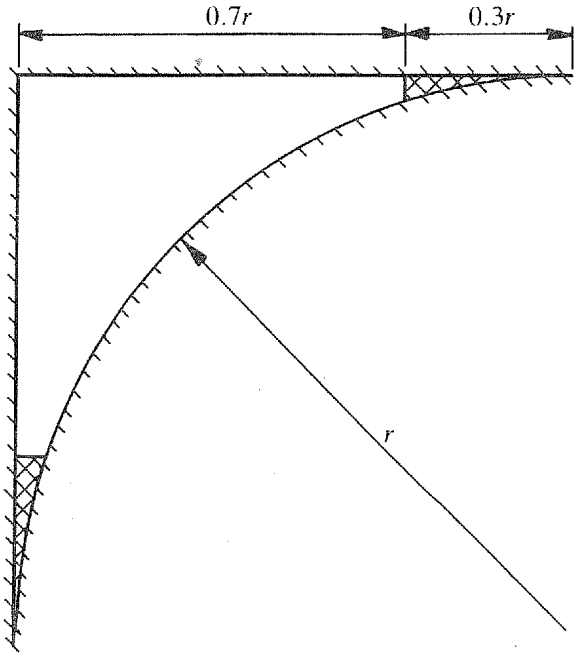

Fig. 5.8. Cross-section with large perimeter for its area

Substituting $U = Q/A$ and the hydraulic diameter into the friction coefficient equation and rearranging gives

$$H = fL\frac{Q^2}{8g}\frac{P_r}{A^3}$$

The hydraulic diameter concept is adequate provided that the P_r/A^3 of the cross-section is not significantly greater than that of any other cross-section than can be drawn inside it.

By rounding the corners of the cross-sections in Fig. 5.7 it is possible to reduce P_r/A^3 by only 1 per cent, so the hydraulic diameter concept is adequate. Cross-sections with small areas influenced by a disproportionate amount of perimeter, as in the cross-section of Fig. 5.8, have P_r/A^3 ratios larger than that of another cross-section that can be fitted within their perimeters. In the case of the cross-section shown in Fig. 5.8, the minimum P_r/A^3 would

exclude the hatched areas. The hatched areas of Fig. 5.8 are filled with slowly moving fluid, contributing very little to the total flow. In calculating pressure losses the minimum P_r/A^3 is found and its associated perimeter and area used in calculating the Reynolds number, the mean velocity and the pressure loss.

5.2.5. SURFACE ROUGHNESS

Provided the height of roughness elements on a pipe wall is less than the thickness of the viscous sub-layer which is present at the wall (Fig. 5.9), then the pipe is said to be hydraulically smooth. A unique relationship exists between the friction coefficient and the Reynolds number for flow in hydraulically smooth pipes. At the other extreme, when most of the roughness elements project through the viscous sub-layer (Fig. 5.10), the friction coefficient is almost totally dependent on the ratio of roughness height to pipe diameter and on the geometric arrangement of the roughness elements. This region, where the Reynolds number is not important, is known as the hydraulically rough region. Between the smooth and rough regions is a transition zone in which the friction coefficient is dependent on both the Reynolds number and the roughness.

To determine the roughness of a pipe it is necessary to establish the relationship between the friction coefficient and the Reynolds numbers and then compare it with experimental values that have been obtained with a known roughness. The standard roughness is closely packed sand grains of a given mean size. Figure 5.11 shows the conventional presentation

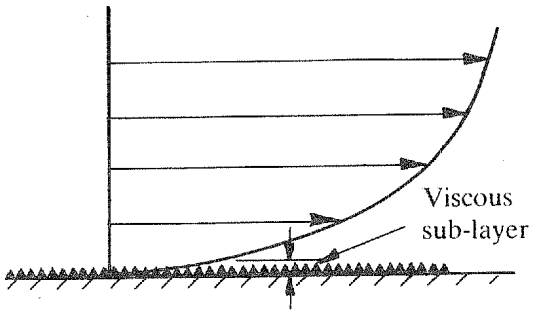

Fig. 5.9. Flow along a hydraulically smooth wall

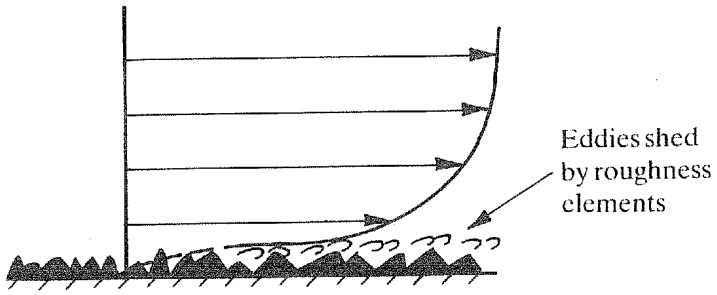

Fig. 5.10. Rough pipe flow

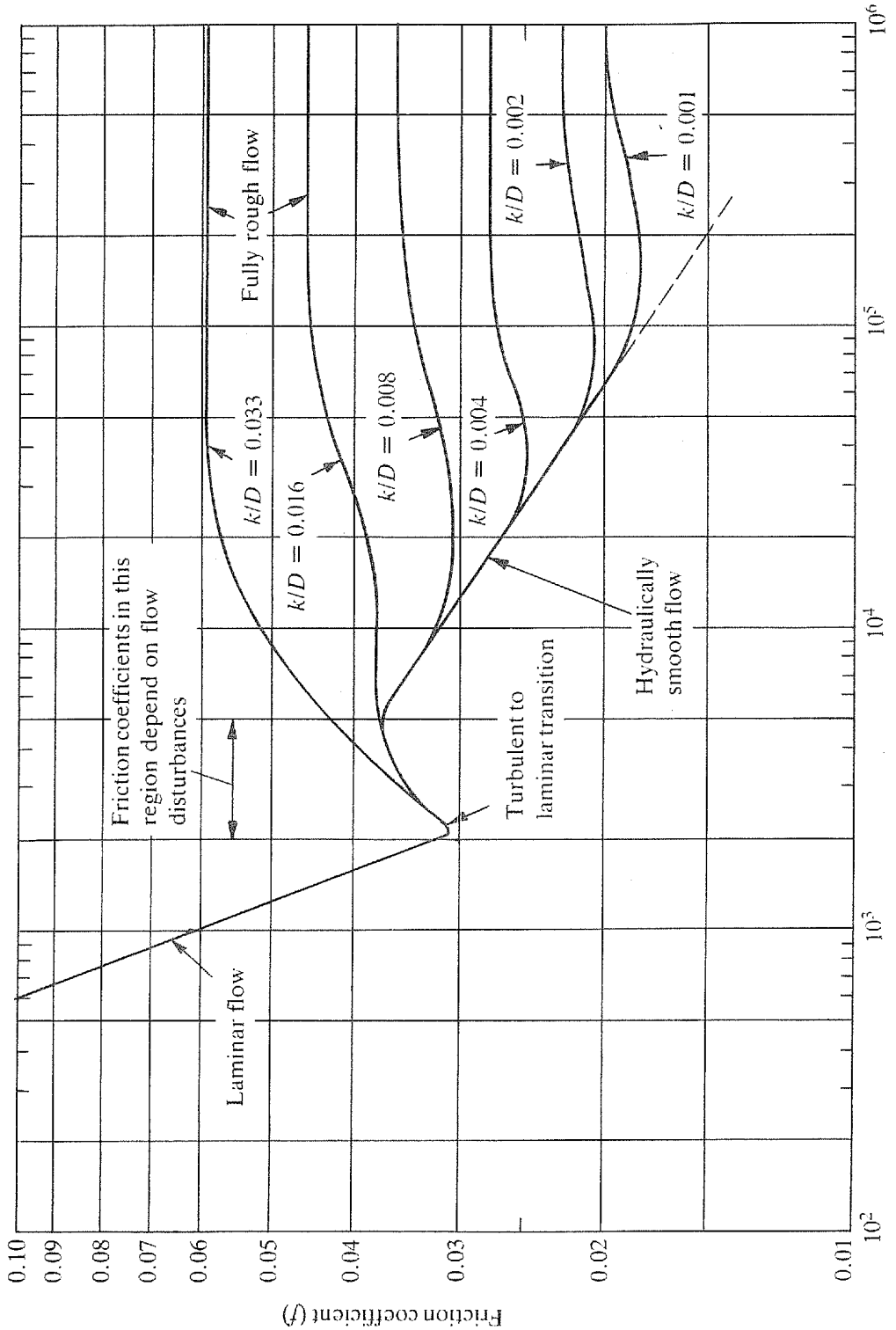

Fig. 5.11. Effect of sand roughness on friction coefficients (k = mean roughness height)

of experimentally measured friction coefficients. Without experimental results for a given pipe surface the adoption of a particular roughness value relies very much on previous experience.

Experimental sand roughness data are available only for pipes. The indications are that errors in applying circular cross-section roughness values to passages, using the hydraulic diameter instead of the pipe diameter, are not large when compared with the unknowns as regards roughness values for commercial pipes.

So far it has been assumed that roughness elements are randomly distributed over the surface of the pipe or passage. When the surface has regular features the ratio of distance between surface features and their height becomes important. Since the effect of regular surface features is markedly different from that of normal roughness, the term effective roughness is used. Figure 5.12 shows two types of surfaces; one is representative of corrugated plastic pipe and the other of a machined surface. As the crest to height ratio increases from 1 to 5 the friction coefficient is doubled. There is evidence that when dissolved minerals form deposits, as occurs in boiler tubes when the fluid becomes saturated, it is in such a manner as to maximise the energy dissipation. There is usually a certain amount of visual regularity about the deposits formed under these conditions. The postulated mechanism for the high energy dissipation, as the crest to height spacing increases, is a change from stable vortices trapped in the trough formed by the roughness to unstable vortices which interact with the turbulent structure of the main flow.

5.3. STRAIGHT WALL DIFFUSERS

5.3.1. DEFINITIONS

Diffusers are devices used for converting velocity pressure to static pressure and for reducing velocities. They are the subject of many thousands of experimental and theoretical papers. The reason for so much interest is that, without efficient diffusers, rotodynamic machinery, such as pumps, compressors and jet engines, would be impractical and industrial society would be very different. The number of diffusers in piping systems is small compared with the number of other components, and they therefore tend to be neglected. This all too often

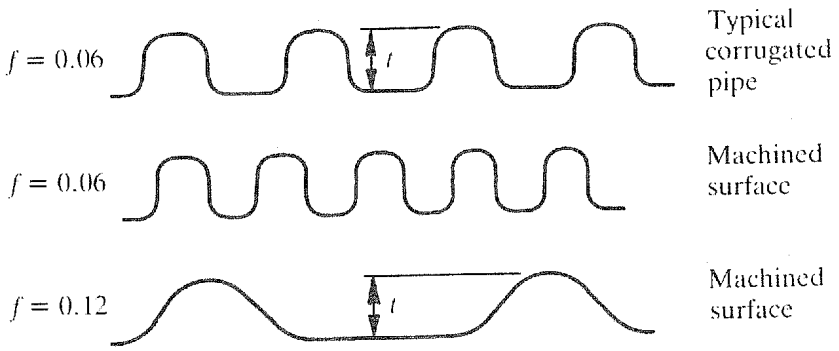

Fig. 5.12. Regular surface roughness ($t/d = 0.06$, $Re = 10^6$, $d = 0.1$ m)

causes problems because a downstream process requires a uniform, low velocity flow for satisfactory performance. Poor diffuser design or the absence of a diffuser is one of the most common causes of flow problems in large flow systems.

Because straight wall diffusers have only one main adverse pressure gradient, an understanding of their performance is desirable before considering components with more than one adverse pressure gradient.

Historically, diffuser performance is interrelated with that of turbo-machinery, leading to the use of efficiency, η, as a performance parameter. Efficiency is defined as

$$\eta = \frac{\text{Actual static pressure recovery}}{\text{Ideal static pressure recovery}}$$

$$\eta = \frac{C_p}{1-(A_1/A_2)^2}$$

where C_p is the static pressure recovery coefficient, given by

$$C_p = \frac{\text{Static pressure recovery}}{\rho U_1^2/2}$$

and A_1/A_2 is the diffuser area ratio.

In general system design the loss coefficient, K_d, is a more appropriate performance parameter, although the static pressure recovery coefficient, C_p, is useful in describing diffuser performance. The loss coefficient, K_d, is related to the recovery coefficient, C_p, by

diffuser with a free discharge (Fig. 5.13)

$$K_d = 1 - C_p$$

diffuser with a constant area section at outlet (Fig. 5.14)

$$K_d = C_{pi} - C_p$$

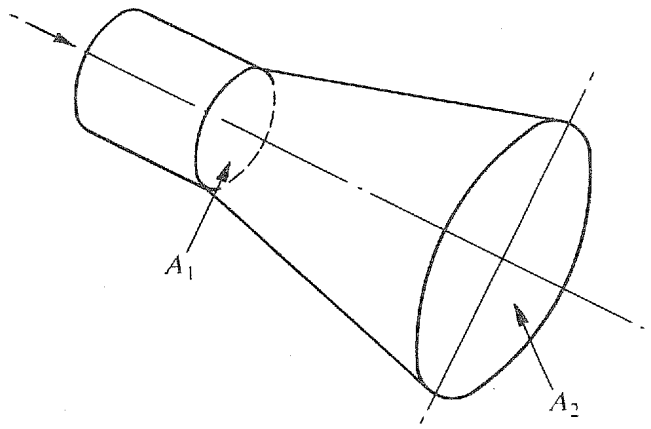

Fig. 5.13. Conical diffuser with a free discharge

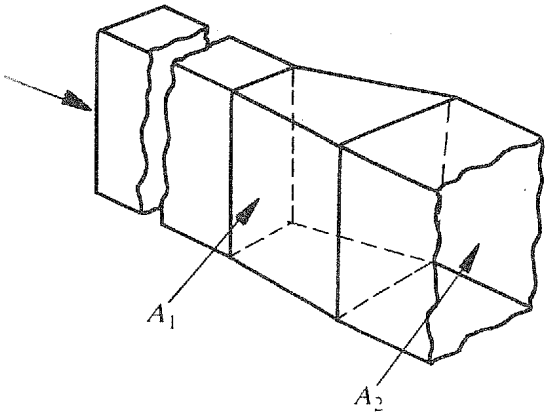

Fig. 5.14. Rectangular diffuser with outlet section

where C_{pi} is the ideal recovery coefficient, given by

$$C_{pi} = 1 - (A_1/A_2)^2$$

5.3.2. FLOW CHARACTERISTICS

Pressure recovery over a diffuser is dependent on the inlet flow distribution — refer to Fig. 5.15(a), which shows a diffuser with an idealised, uniform inlet flow and the location along the diffuser where 60 per cent of the incoming velocity head is converted to static head. To achieve a 60 per cent recovery the velocity decreases from U_1 to $0.63U_1$.

Figure 5.15(b) shows the same diffuser as Fig. 5.15(a), but with an idealised, non-uniform flow. Part of the flow is moving at 1.2 times the mean inlet velocity with the rest at 0.8 of the mean inlet velocity. It can be seen from Fig. 5.15(b) that to recover 60 per cent of the mean inlet velocity head requires a much larger area ratio than for a uniform inlet flow. The reason is the rapid fall off in the velocity of the more slowly moving fluid which fills up the diffuser. For the inlet flow shown, the maximum theoretical head rise is 0.64 of the mean inlet velocity head, and that would require a ratio diffuser of infinite area.

The conclusion to be drawn from the idealised flow of Figs 5.15(a) and (b) is that non-uniformities in the inlet flow reduce the head recovery that can be achieved. In real flows the velocity falls to zero at the wall. Flow near the wall can only move through a diffuser as a result of a transfer of energy from more energetic flow away from the walls.

In the initial section of a diffuser the rapid decrease in velocity of the near-wall flow results in high shear stresses which move inwards as the flow passes through the diffuser. The turbulence generated by the high shear stresses enhances the interchange of energy. Diffusers in most engineering applications have area ratios of less than 3 and they are designed for maximum pressure recovery in a given length. At the oulet from these diffusers the core flow is virtually unaffected by energy dissipation within the diffuser, with the result that the total pressure in the core remains virtually constant. Figure 5.16 illustrates this, along with the

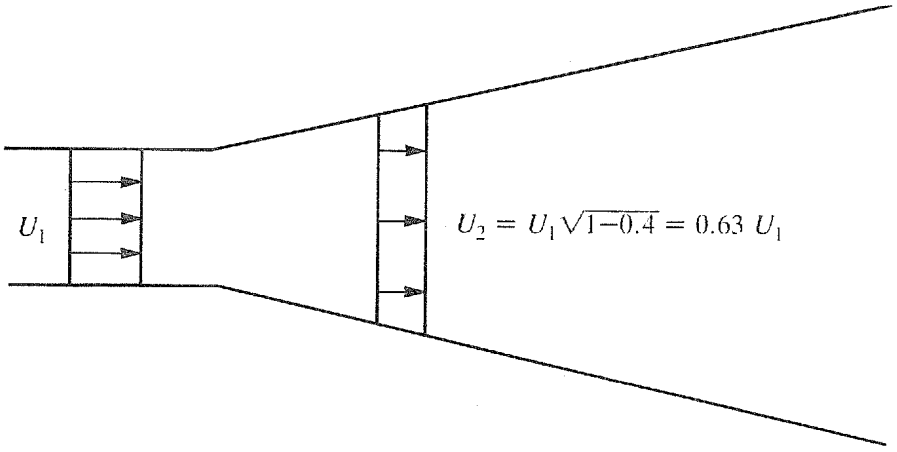

(a) Uniform flow

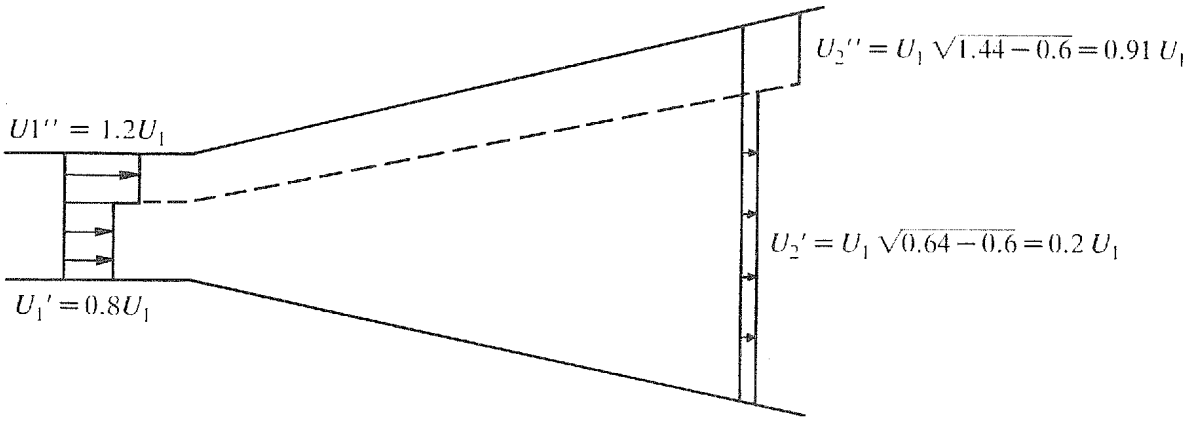

(b) Non-uniform flow

Fig. 5.15. Idealised flow in a diffuser

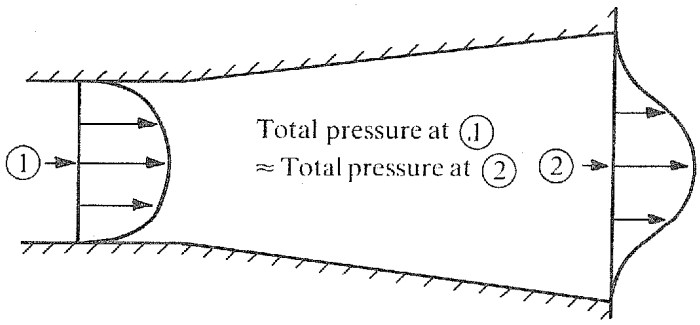

Fig. 5.16. Velocity profile change

poor outlet velocity distribution associated with practical diffusers. It can be concluded that insufficient diffusion, rather than energy dissipation, is the main cause of poor diffuser performance.

5.3.3. STALL AND OUTLET CONDITIONS

If the divergence of a diffuser is too rapid (Fig. 5.17), large scale separation or stall occurs. Re-attachment following separation does not take place unless the divergence is reduced. Pressure recovery in a diffuser with extensive stall is low and the outlet flow is very distorted, with areas of reverse flow. Space restrictions invariably dictate that diffusers operate with areas of stall. The amount of flow separation ranges from numerous, very local areas of stall, which are continually being formed and swept out of the diffuser, to large cells of separation that slowly build up, causing extensive areas of reverse flow, which are then suddenly swept out. The cycle of growth and sweep out is called transitory stall. Large changes in pressure recovery and outlet velocity distribution occur when diffusers operate with transitory stall.

When a section of constant area is added to the outlet of a diffuser, as in Fig. 5.18, part

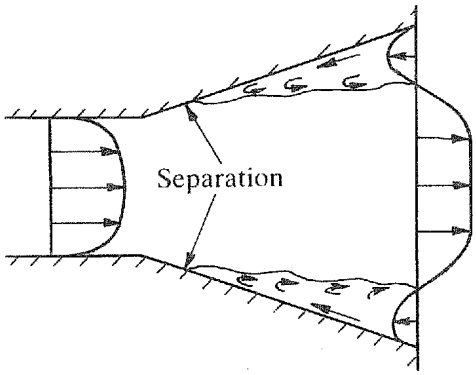

Fig. 5.17. Wide angle diffuser

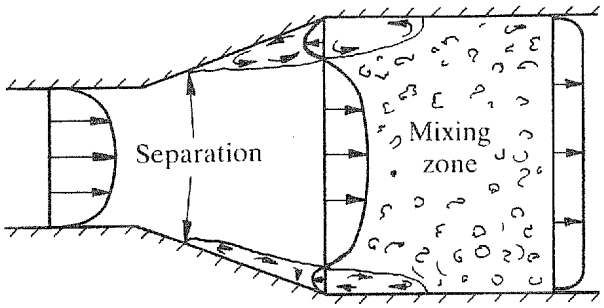

Fig. 5.18. Diffuser with outlet section

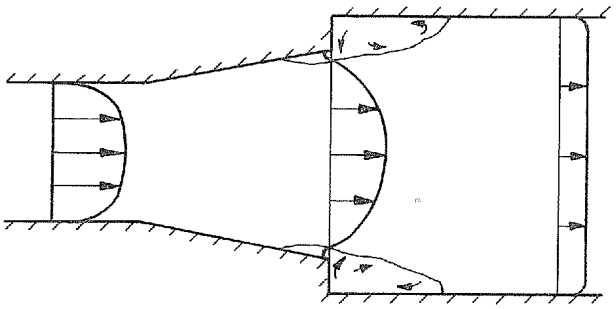

Fig. 5.19. Cropped diffuser

of the excess velocity pressure is converted to static pressure by large scale mixing. Mixing, as a means of converting velocity pressure to static pressure, is an inefficient process compared with diffusion. Where possible, maximum diffusion should be achieved before large scale mixing. An example of efficient diffusion followed by mixing is the cropped diffuser of Fig. 5.19. In the restricted length available for the diffuser, the diffuser area ratio is chosen so as to give the maximum pressure recovery by diffusion within the diffuser. A further recovery, due to mixing, is achieved following the abrupt expansion into the outlet section.

5.3.4. INLET CONDITIONS

The performance of a diffuser depends on the energy distribution at its inlet. If the inlet conditions are the result of boundary layers developing along a length of pipe or passage following a contraction, the poorest performance occurs with an inlet length of about seven diameters. At this location the near-wall flow is deficient in energy (see Fig. 5.3) and the boundary layer structure is not sufficiently developed to feed energy from the core flow towards the wall.

At Reynolds numbers greater than 10^5 the diffuser performance improves slowly with Reynolds number, except in the region of maximum pressure recovery for a given diffuser length, where the improvement is more marked. At Reynolds numbers of less than 10^5 reasonable performance is maintained only if the inlet boundary layer is thin and turbulent.

Rapid diffusion may not be possible if the energy distribution varies around the perimeter at inlet to a diffuser. Depending on the energy distribution, one of several approaches for achieving maximum performance can be followed. If a diffuser is located directly after another component and the kinetic energy of the profile at entry to the proposed diffuser is greater than 1.2 times that based upon the mean flow, it is desirable to allow the profile to decay before diffusing (Fig. 5.20). If the profile is biased to one side of the pipe or passage and there are strong secondary flows, then it is usually better to delay diffusion to allow the secondary flows to reduce profile distortion (Fig. 5.21). When the profile is known to be biased to one side and secondary flows are absent or weak, it is better to concentrate divergence on the higher energy side (Fig. 5.22).

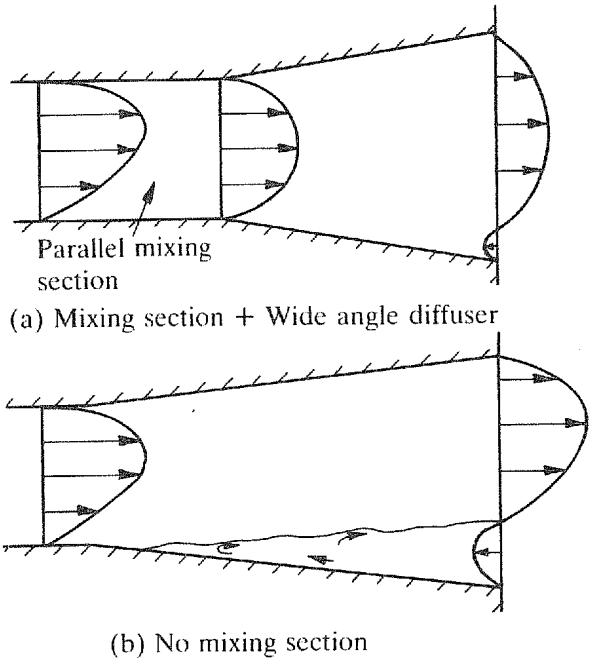

Fig. 5.20. Advantage of mixing section with distorted inlet flow

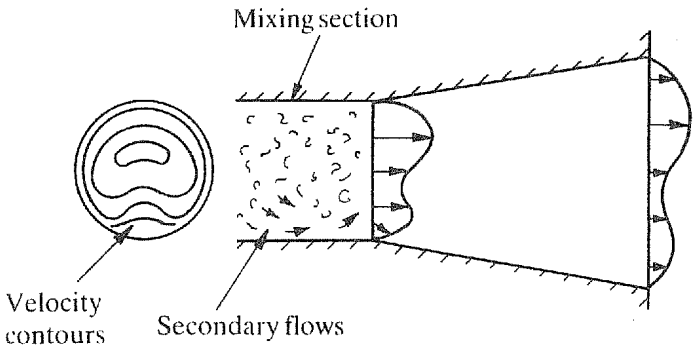

Fig. 5.21. Delayed diffusion followed by rapid diffusion

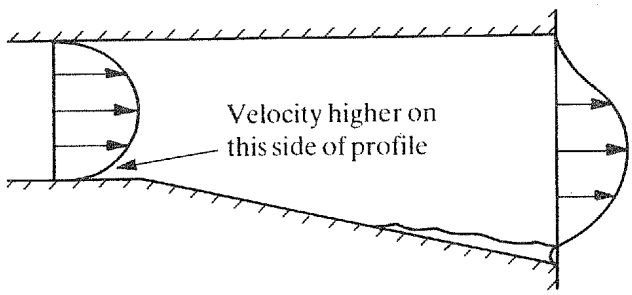

Fig. 5.22. Concentration of diffusion in-line with higher energy flow

5.3.5. CROSS-SECTIONAL SHAPE

Using the appropriate geometric ratios, diffusers of different cross-sectional shape have similar loss coefficients, except for diffusers with low aspect ratio. In low aspect ratio diffusers, such as that shown in Fig. 5.23, friction losses are important, particularly if the Reynolds number is less than 10^5.

5.3.6. METHODS OF IMPROVING PERFORMANCE

Diffuser performance can be improved by the four methods shown in Figs 5.24 and 5.25. Removing low energy near-wall flow by suction or re-energising the near-wall flow by blowing are very effective methods of improving performance, but are practical only in special circumstances, such as wind tunnel diffusers or where fluid has to be bled-off for secondary purposes. Vortex generators placed upstream of a diffuser bring high energy fluid down towards the wall to re-energise the near-wall flow. Since the near-wall flow distribution usually varies around the inlet, the location of vortex generators or other inlet flow redistribution devices must be determined experimentally for each application. Installing vanes within a wide angle diffuser is normally the only practical method of improving static pressure recovery,

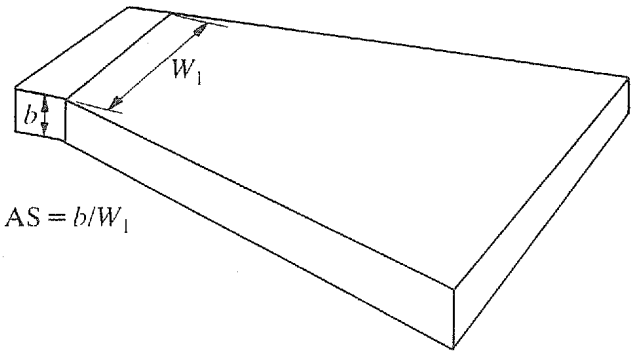

Fig. 5.23. Low aspect ratio diffuser

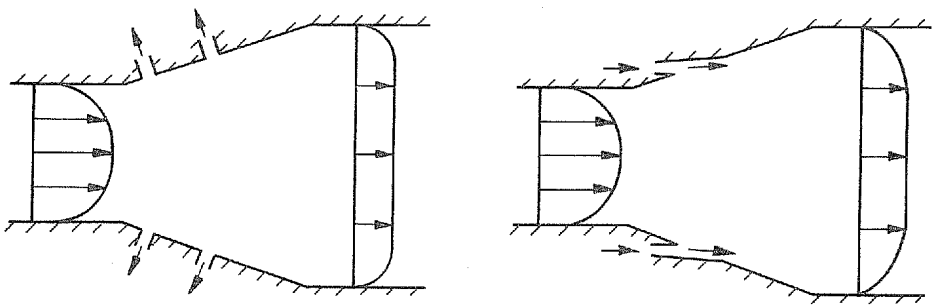

Fig. 5.24. Removal of low energy fluid and re-energising near-wall flow

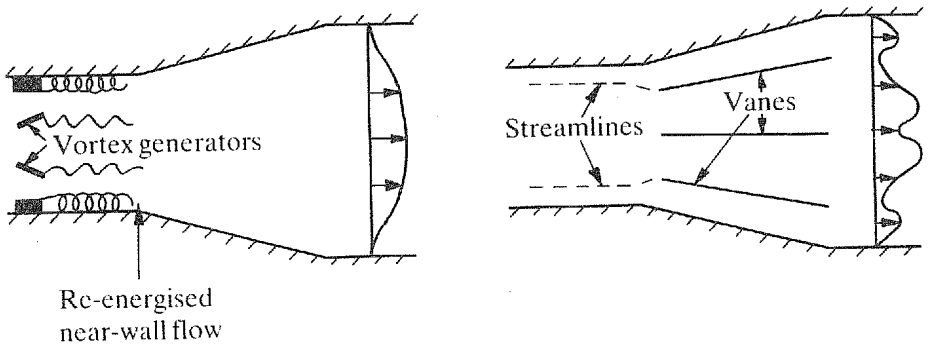

Fig. 5.25. Use of vortex generator and vanes within diffusers

stability and outlet flow distribution. With vanes it is not possible to achieve a static pressure recovery above that of a plain diffuser of the same length but with an area ratio corresponding to that for maximum static pressure recovery.

If geometrical constraints dictate that a wide angle diffuser be used or if the performance of an existing wide angle diffuser installation has to be improved, then a number of approaches are possible. The approach adopted will depend on whether pressure recovery, flow distribution or flow stability is the important criterion. If the performance of a diffuser is critical for the satisfactory operation of equipment or processes, it is advisable to carry out model studies. Model studies are particularly valuable if the inlet conditions are disturbed by a bend or other component.

To improve pressure recovery:

1. Vanes can be installed as in Fig. 5.25.
2. The area ratio of the diffuser can be reduced to that of a diffuser giving maximum pressure recovery for the available diffuser length. Since more than 50 per cent of the possible pressure recovery can be achieved in an area ratio of 1.6, getting the first part of the diffusion process right is critical.
3. A cone or other device can be installed to convert a circular or rectangular diffuser into an annular type of diffuser. The performance of such a diffuser can be estimated from annular diffuser performance data (see Chapter 11).

To improve flow distribution:

1. Appropriately placed vanes can greatly improve the outlet velocity profile.
2. Obstructions placed part way into a diffuser can be used to spread the flow positively.
3. Resistance screens can be located at the diffuser outlet.
4. A combination of items 2 and 3 can be used, with obstructions within the diffuser spreading the flow and increasing turbulence ahead of the screens.

To improve flow stability:

1. A vane or vanes can be installed. Often a single vane will prevent the most serious instability which involves the whole flow switching from one area of a diffuser to another.
2. Appropriately located obstructions or vortex generators can be used to stabilise the flow.

5.3.7. PRESENTATION OF DIFFUSER PERFORMANCE

By adopting the geometric ratios shown in Fig. 5.26, the performance of various diffuser cross-sections can be compared. A compact and informative presentation of diffuser pressure recovery and loss coefficients is the performance chart shown in Fig. 5.27. The axes are the area ratio and the diffuser length, and the contours are lines of constant pressure recovery and loss coefficients.

Figure 5.27 shows a line marked '1' that defines the area ratios producing the minimum total pressure loss from the system in a specified non-dimensional length and a line marked '2' that defines the non-dimensional length producing the minimum total pressure loss in a specified area ratio.

In the region to the right of the line for minimum pressure loss in a specified area ratio, where the contours are almost horizontal, the flow is stable and performance is dependent on the area ratio. Diffusers lying to the right of the line are not of practical importance since they are excessively long for their pressure recovery. Over the region between the lines, where the contours change rapidly from nearly horizontal to vertical, the outlet flow distribution becomes very non-uniform with areas of stall accompanied by pressure fluctuations: most practical diffusers have geometries in this region. Above the line for minimum pressure loss in a specified non-dimensional length steady state stall develops with its associated poor outlet flow distribution and poor performance.

Static pressure recovery contours for diffusers with a constant area section at outlet (Fig. 5.28) differ from the free discharge contours at low non-dimensional lengths. Mixing in the constant area section results in a static pressure rise after short diffusers, which, for an area ratio of 2, amounts to 50 per cent of the mean inlet velocity pressure for a diffuser of zero length (sudden expansion).

The outlet pipe or passage length to obtain maximum static pressure recovery varies with the area ratio and diffuser angle, but is typically of the order of four diameters. After the point of maximum static pressure the friction gradient remains above that for developed flow for 20–50 diameters. Over this length there is an additional loss, above the normal friction, of about 0.1 of the mean velocity pressure in the outlet pipe or passage.

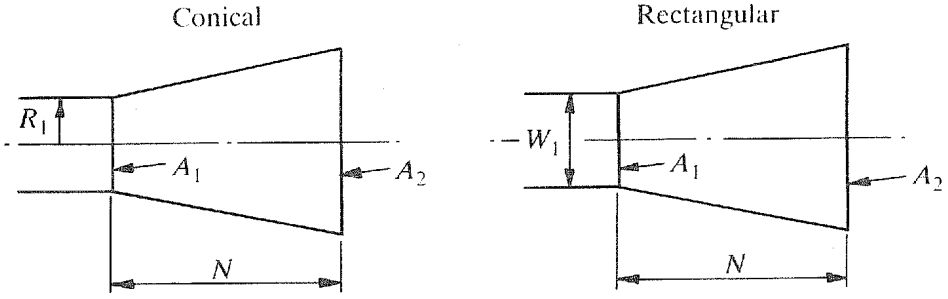

Non-dimensional length $= N/R_1$ Non-dimensional length $= N/W_1$

Non-dimensional area ratio $= A_2/A_1$ Non-dimensional area ratio $= A_2/A_1$

Fig. 5.26. Diffuser geometrical ratios

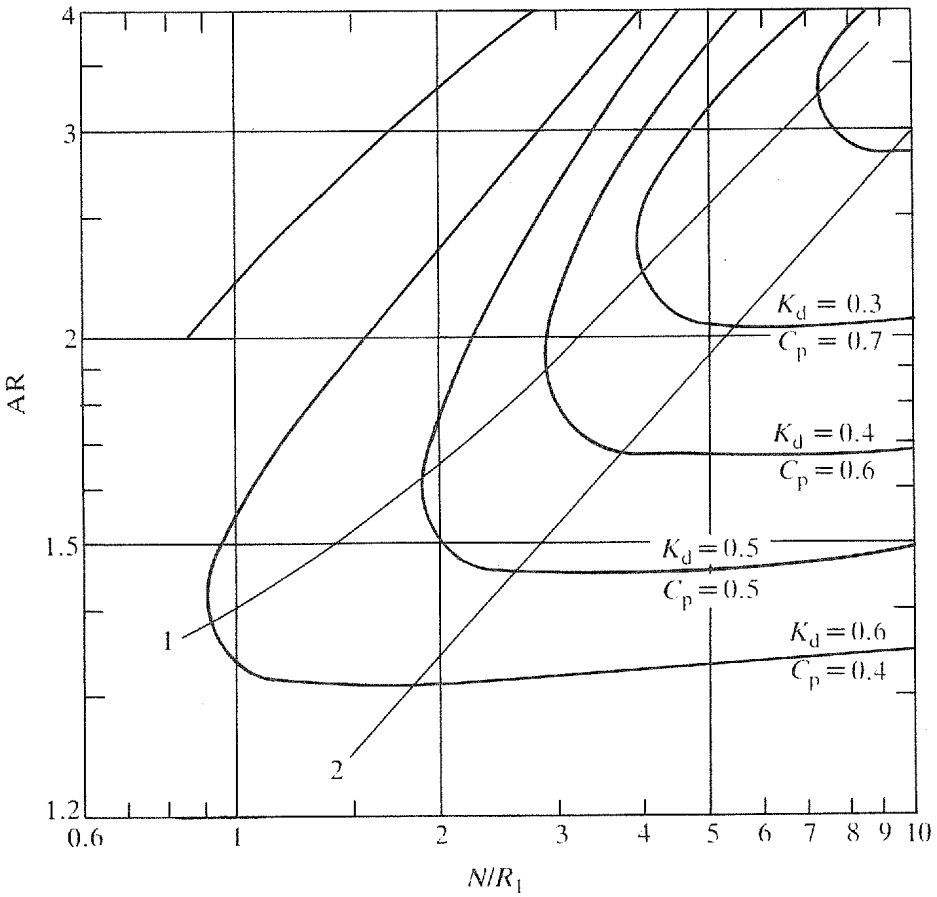

Fig. 5.27. Diffuser performance chart — free discharge

5.3.8. FLOW STABILITY

Flow stability within a diffuser can be extremely important, but is difficult to quantify. The severest pressure fluctuations occur when a diffuser follows a component with which it interacts unfavourably, or when the inlet boundary layer is thin and the divergence is too great.

An appropriate time period, Δt, for quantifying the frequency of pressure fluctuations is the time taken for flow to traverse a distance of one pipe diameter at the diffuser inlet velocity. Referring to Fig. 5.29, lines 1–5 indicate roughly the following regions.

Line 1. To the right of this line the flow is steady.
Line 2. Onset of small areas of flow separation with small amplitude fluctuations with a period of about 20 Δt.
Line 3. Flow very unsteady with areas of stall moving around the diffuser and penetrating far into the flow. The period of pressure fluctuation is about 100 Δt.
Line 4. Extremely unstable flow conditions, large eddies or stall moving violently in the

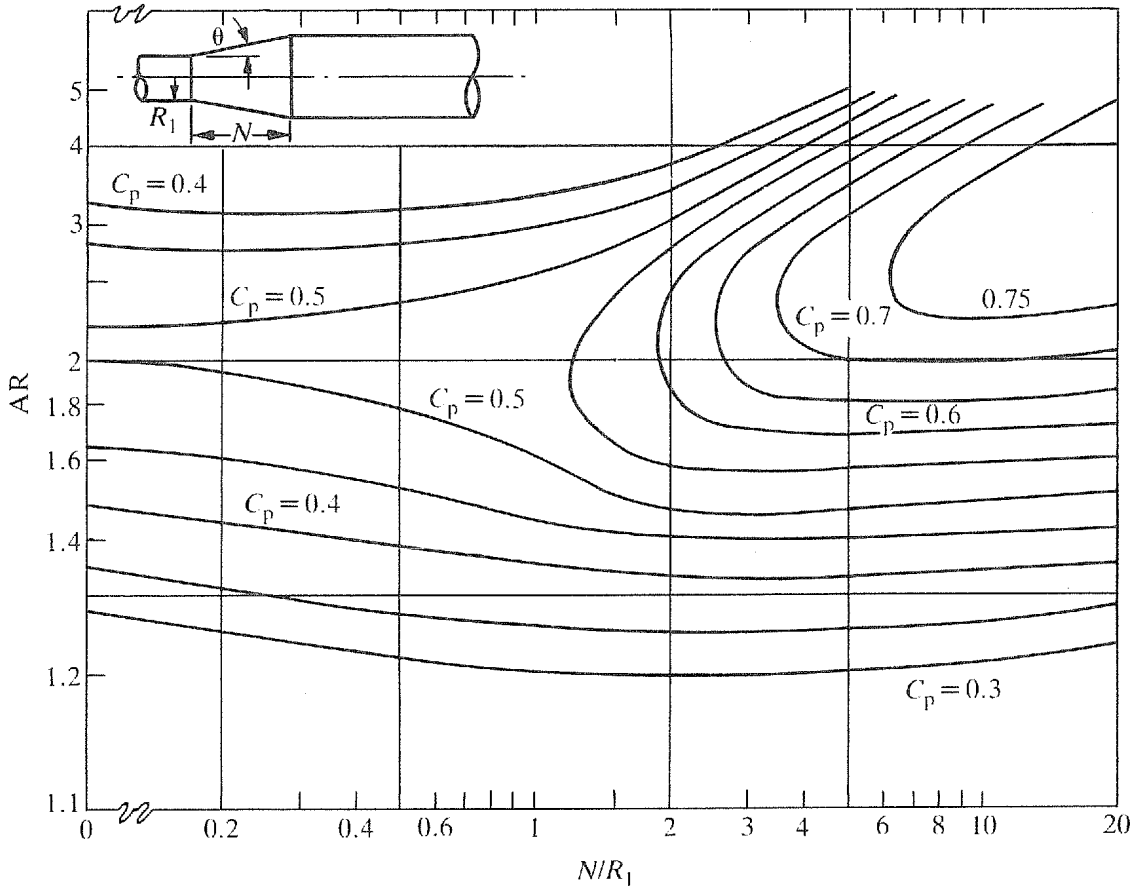

Fig. 5.28. Diffuser performance chart — outlet section

diffuser. The period of pressure fluctuation is 200 Δt with amplitudes in excess of 10 per cent of the inlet velocity pressure.

Line 5. Very unstable flow with low frequency, large amplitude movements of the whole flow. The period of fluctuation is about 2000 Δt.

The crowding together of the contours on Fig. 5.29 provides information on the type of flow expected. Minor changes in the effective length or area ratio of the diffuser, due to a change in flow pattern, cause a large change in static pressure recovery. In regions where the contours crowd together they represent only mean values.

The performance chart in Fig. 5.29 is for conical diffusers with thin inlet boundary layers. Part of the reason for extremely unstable flow in diffusers with a thin, symmetrical inlet boundary layer is the lack of a defined separation region. A developed inlet profile is seldom symmetrical, so part of the inlet perimeter of a diffuser has a lower energy region which stabilises flow separation. Pressure fluctuations in diffusers with development flow at inlet do not reach the extremes observed with thin inlet boundary layers. Maximum achievable pressure recovery is, however, much reduced with developed inlet flow. Figure 5.30 illustrates the changing conditions within a diffuser operating with large scale transitory stall.

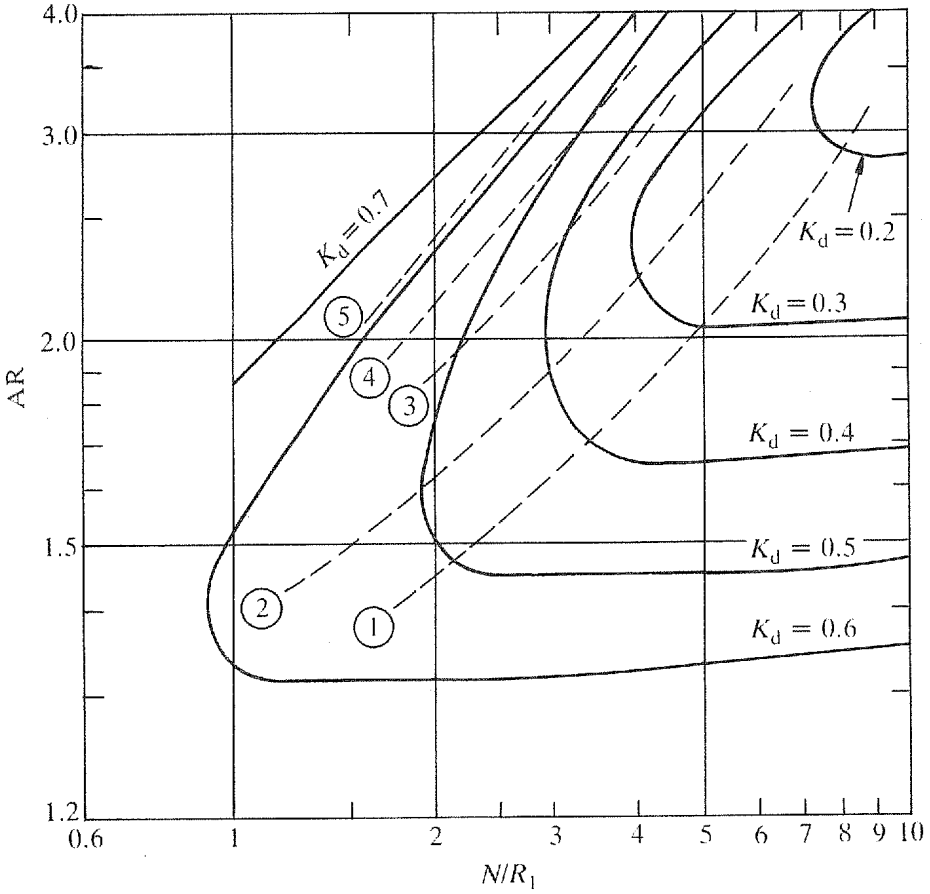

Fig. 5.29. Flow regimes — conical diffuser with a free discharge and nearly uniform inlet flow

5.4. TURNING FLOW

5.4.1. INTRODUCTION

When flow is turned, static pressure and velocity distributions change, at least two adverse gradients are involved, secondary flows are generated and curvature affects the turbulence structure of the flow.

5.4.2 SECONDARY FLOWS

Consider an ideal fluid with a uniform energy distribution passing through a bend (Fig. 5.31). Within the bend the static pressure increases with the radius in order to balance the centrifugal force, and since the sum of velocity and static pressure is the same everywhere, velocities decrease from the inside to the outside of the bend.

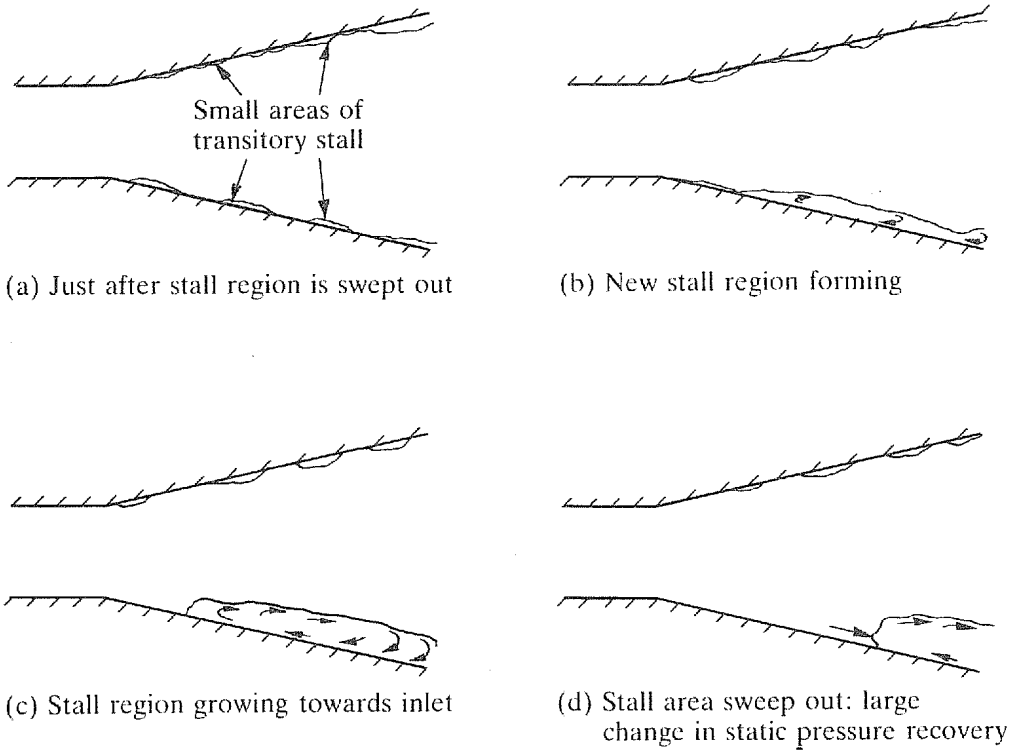

Fig. 5.30. Large scale transitory stall

Because velocities vary from zero at the walls to a maximum in the core, actual flows through bends involve non-uniform energy distributions. Centrifugal and pressure forces acting on the more quickly moving core flow cause the core to be deflected towards the outside of the bend. Fluid approaching the outside of the bend "sees" the adverse pressure gradient shown in Fig. 5.31. Energy deficient near-wall fluid approaching the outer wall cannot pass through the adverse pressure gradient; instead it moves round the walls towards the low static pressure region on the inside of the bend. The movement of low energy fluid towards the inside of the bend, combined with the deflection of the high velocity core region towards the outside of the bend, sets up two cells of secondary flow, as indicated in Fig. 5.32.

In the normal engineering range of bend centreline radius to pipe diameter ratios of 1–3, the secondary flows have angles of 45° or more to the mean flow. Although velocities through a bend are markedly different from those of ideal flow, pressure differentials between the inside and outside of a bend are often similar to those predicted for ideal flow.

There is a limit to the displacement of core region fluid towards the outside and low energy fluid towards the inside of a bend, before centrifugal and pressure forces begin to reduce and ultimately stop or reverse the secondary flows. In engineering situations, secondary flows diminish in strength after about 80° and are very weak at 130°.

Low energy fluid collected on the inside of a bend by the secondary flows has to negotiate the adverse gradient at outlet from the bend. Figure 5.33 shows velocity contours at outlet from

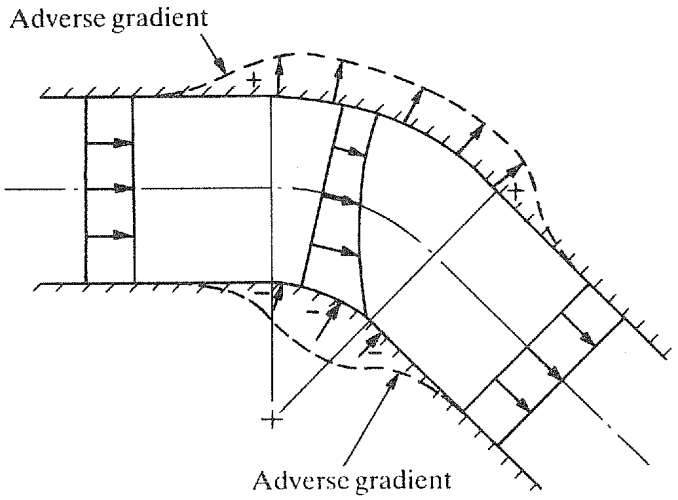

Fig. 5.31. Ideal flow through a bend

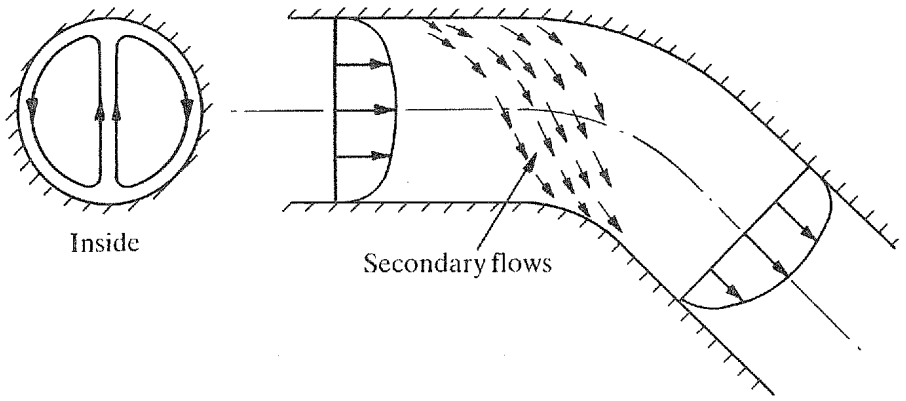

Fig. 5.32. Secondary flows

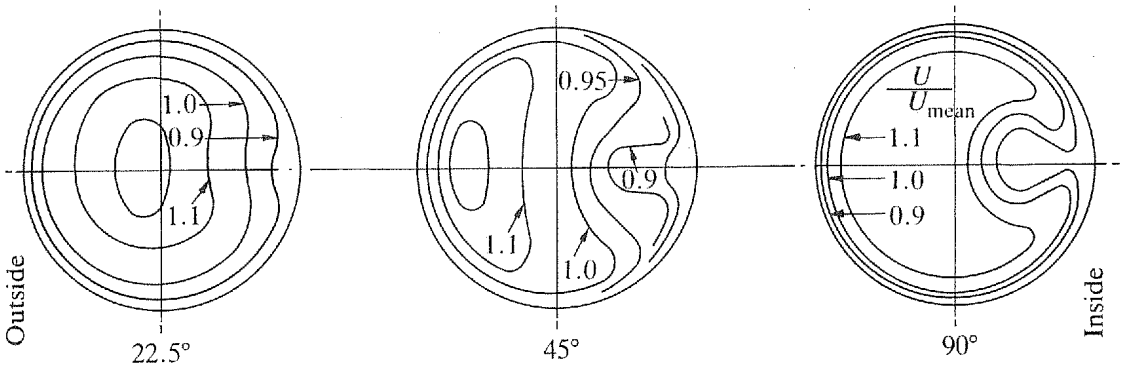

Fig. 5.33. Bend outlet velocity contours (local/mean velocity ratios)

bends of 22.5°, 45° and 90°. The worst condition, as regards low energy flow on the inside wall, is for a bend angle of 45°. Flow separation may occur at outlet from a 45° bend but not at outlet from a 90° bend of the same radius ratio.

5.4.3. CURVATURE EFFECTS ON TURBULENCE

Curvature causes the flow on convex surfaces to be stabilised with a reduction in turbulent shear stresses and to be destabilised on concave surfaces with an increase in turbulent shear stress (Fig. 5.34).

Referring to Fig. 5.35, a particle of fluid near the outer bend wall, displaced towards the wall, has a higher momentum (radius × velocity) than its new neighbours. Because it has a higher velocity than its neighbours, the centrifugal force on the particle acts to displace it further towards the wall. Turbulent energy transfer towards the wall is enhanced, energy dissipation is increased and the velocity gradient close to the wall is steep, enabling near-wall flow to withstand adverse pressure gradients. The opposite situation exists at the inner wall (Fig. 5.36). Energetic particles tend to be displaced away from the inner wall, so low energy fluid accumulates near the wall. Energy transfer is reduced, the velocity gradient away

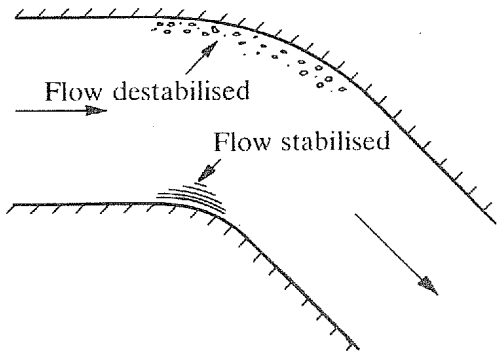

Fig. 5.34. Curvature effect on turbulence structure

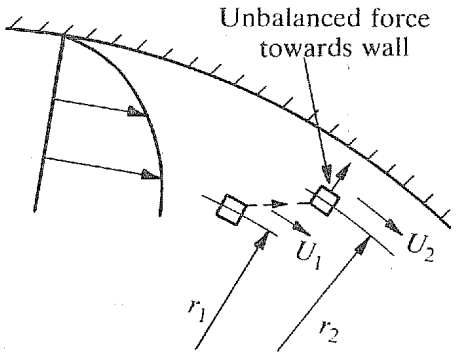

Fig. 5.35. Displacement of high energy fluid particles towards a concave wall

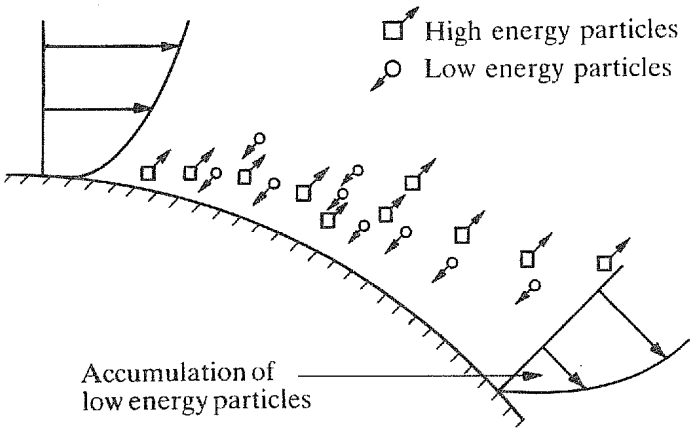

Fig. 5.36. Loss of high energy fluid particles from a convex wall

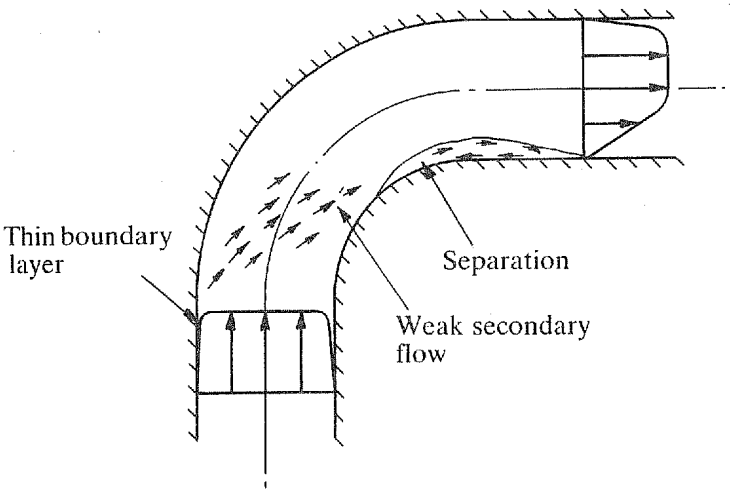

Fig. 5.37. Flow separation when secondary flows are weak

from the wall becomes shallow, energy dissipation is reduced and the near-wall flow is unable to withstand adverse pressure gradients.

Fortunately, the effect of the secondary flows is to re-energise the inner wall regions. A situation where the secondary flows may be too weak to prevent flow separation is when the inlet flow is nearly one-dimensional (Fig. 5.37). For the particular bend radius ratio shown in Fig. 5.37, extensive flow separation occurs because of the adverse pressure gradient on the inner wall at outlet from the bend. In the same bend, but with a developed flow at inlet, strong secondary flows prevent flow separation.

5.4.4. DISTRIBUTION OF LOSSES BETWEEN A BEND AND ITS OUTLET

Bend outlet velocity and turbulence distributions differ substantially from those of developed pipe or passage flows. Additional losses, above normal pipe friction, are involved in establishing developed flow conditions after a bend. Typical non-dimensional static pressures upstream and downstream of a bend are shown in Fig. 5.38. Some 30 diameters from the bend a steady state pressure gradient is re-established. Although the static pressure gradient becomes constant after 30 diameters, weak secondary flows are usually present and continue to be detectable 50–100 diameters after the bend. It is evident from Fig. 5.38 that under some circumstances nearly all of the pressure loss is associated with re-establishing developed flow after a bend.

Considering 90° bends of circular cross-section, the main experimental observations of the distribution of losses between the bend and the outlet pipe are as follows.

1. In bends of centreline radius/diameter ratio of less than 0.8, serious flow separation can be expected. Most of the loss is the result of the separated flow expanding immediately after the bend. Intense turbulence generated by the expanding flow tends to destroy secondary flows.
2. For bends of centreline radius/diameter ratio between 0.8 and 1.5, about 80 per cent of all losses occur in the bend and the first two pipe diameters after the bend. If the flow is nearly one-dimensional at inlet to the bend, large scale separation takes place but secondary flows are weak with very little additional loss after flow re-attachment.
3. About 40 per cent of the loss occurs downstream of bends with centreline radius/diameter ratios of 1.5–3.

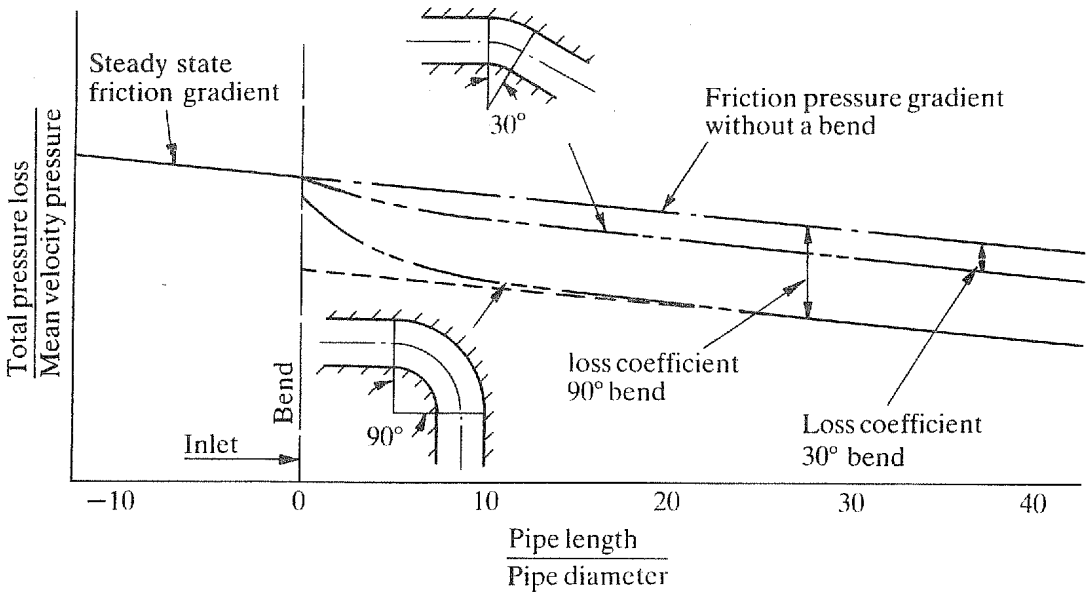

Fig. 5.38. Pressure gradients after a bend

Table 5.1. Distribution of losses for $r/d = 2$ bends of circular cross-section ($Re = 10^6$)

Deflection angle	Total loss coefficient	Loss in bend	Loss in downstream pipe
45°	0.09	0.04	0.05
90°	0.16	0.08	0.08
180°	0.18	0.15	0.03

4. The increasing contribution of wall friction in bends of radius ratio greater than 3 reduces the percentage contribution of the downstream loss to the total loss.

As the deflection angle is reduced below 90° an increasing percentage of the total loss occurs in the downstream pipe. For bends of centreline radius/diameter ratio of less than 3 and angles of less than 40°, more than 50 per cent of the loss is associated with the redistribution of flow in the downstream pipe.

Approximate distribution of losses between bends and their downstream pipes are given in Table 5.1. The remarkable drop in the downstream loss between bend angles of 90° and 180° is associated with the reduction in the strength of the secondary flows.

5.4.5. SHORT OUTLET PIPES OR PASSAGES

Pressure fields set up within a bend with an outlet pipe or passage extend for about one diameter after the bend. When a bend discharges directly into a large space the static pressure at the outlet is the same at the inner and outer radii. The effect, illustrated in Fig. 5.39, is to steepen the adverse gradient on the inner wall. Separation is normally present if the bend centreline/diameter ratio is less than 2. The mean velocity of the separated flow is much

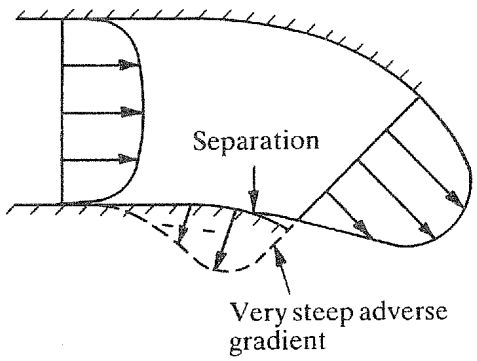

Fig. 5.39. Effect of no outlet section

higher than that of attached flow. Bends with centreline/diameter ratios less than 1.2 have loss coefficients three times those of a bend with a one diameter or more parallel section at outlet. If the bend discharges to a large space there is the additional loss of one mean velocity head from the system.

When the outlet is longer than two and shorter than 30 diameters, part of the loss associated with flow redevelopment in the outlet, included in the basic bend loss coefficient, does not apply.

5.4.6. CROSS-SECTIONAL SHAPE

Velocity distributions at outlet from 90° bends of circular and rectangular cross-section are shown in Fig. 5.40. The rectangular cross-section bends have aspect ratios of 0.5 and 2.

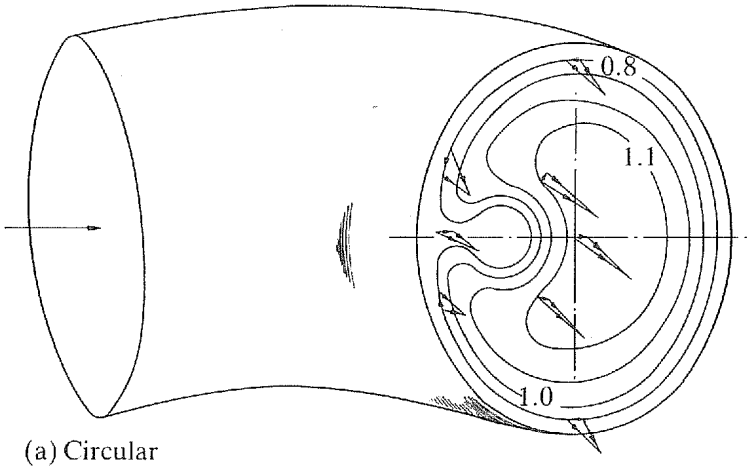

(a) Circular

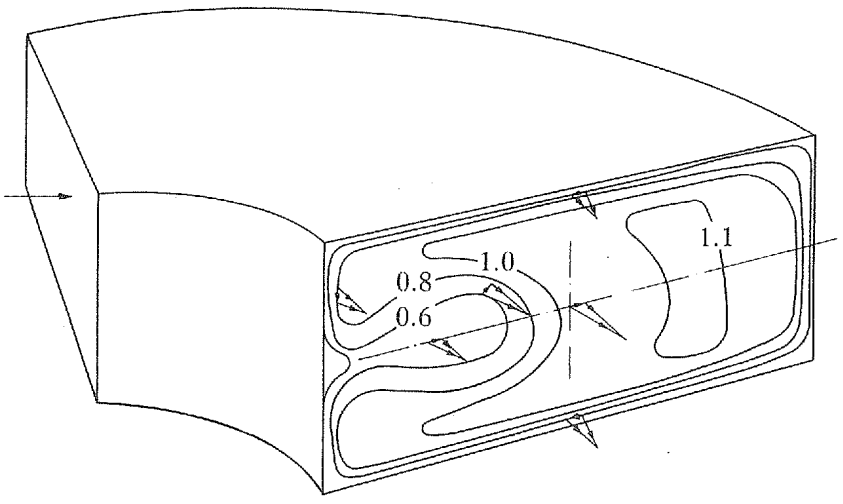

(b) Rectangular, aspect ratio 0.5

Fig. 5.40. Effect of cross-sectional shape on velocity distributions (contours of local/mean velocity)

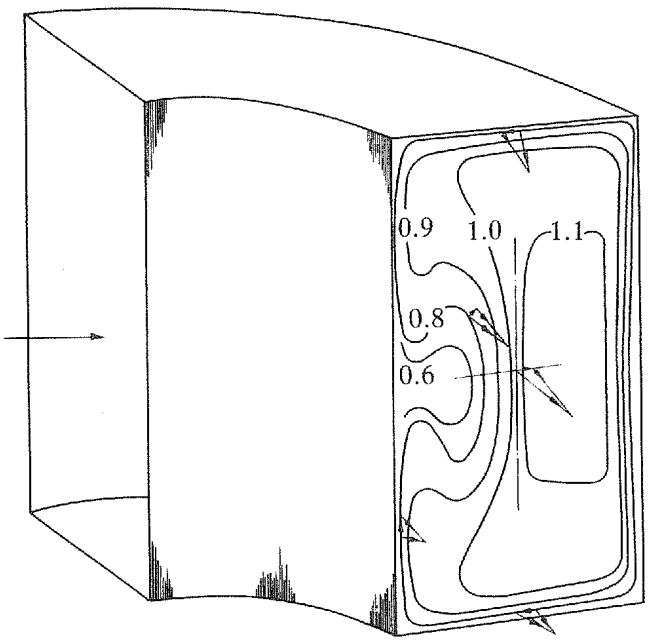

(c) Rectangular, aspect ratio 2

Fig. 5.40. *cont*

Although the rectangular bend of aspect ratio 0.5 has a larger total area of low velocity flow, the amount of low energy fluid on the inner wall is less than in the bend of aspect ratio 2. Separation is therefore more likely at outlet from the bend of aspect ratio 2. Bends of low aspect ratio have more surface area and hence greater friction losses than circular and high aspect ratio bends, but because of their lower flow redevelopment losses there is little difference in performance between bends of different cross-sections. The bend cross-sectional shape can be important when a component is located within two diameters of the outlet of a bend. Secondary flows take longer to redistribute low energy fluid after high aspect ratio bends.

5.4.7. BEND PERFORMANCE CHARTS AND REYNOLDS NUMBER EFFECTS

A compact presentation of bend loss coefficients is provided by the performance chart shown in Fig. 5.41. The axes are deflection angle and the radius ratio, and the contours are lines of constant loss coefficient. It can be seen that as the angle increases, the radius ratio for minimum bend loss rises and then decreases. However, if account is taken of the reduction in the length of the inlet and outlet pipes with a bend of larger radius ratio, minimum overall system loss occurs with the bend of largest radius, assuming that the pipe centrelines are in the same location.

The nearly vertical contours for bends of more than 100° and radius ratios less than 3, in Fig. 5.41, are associated with the diminishing strength of the secondary flows at large angles.

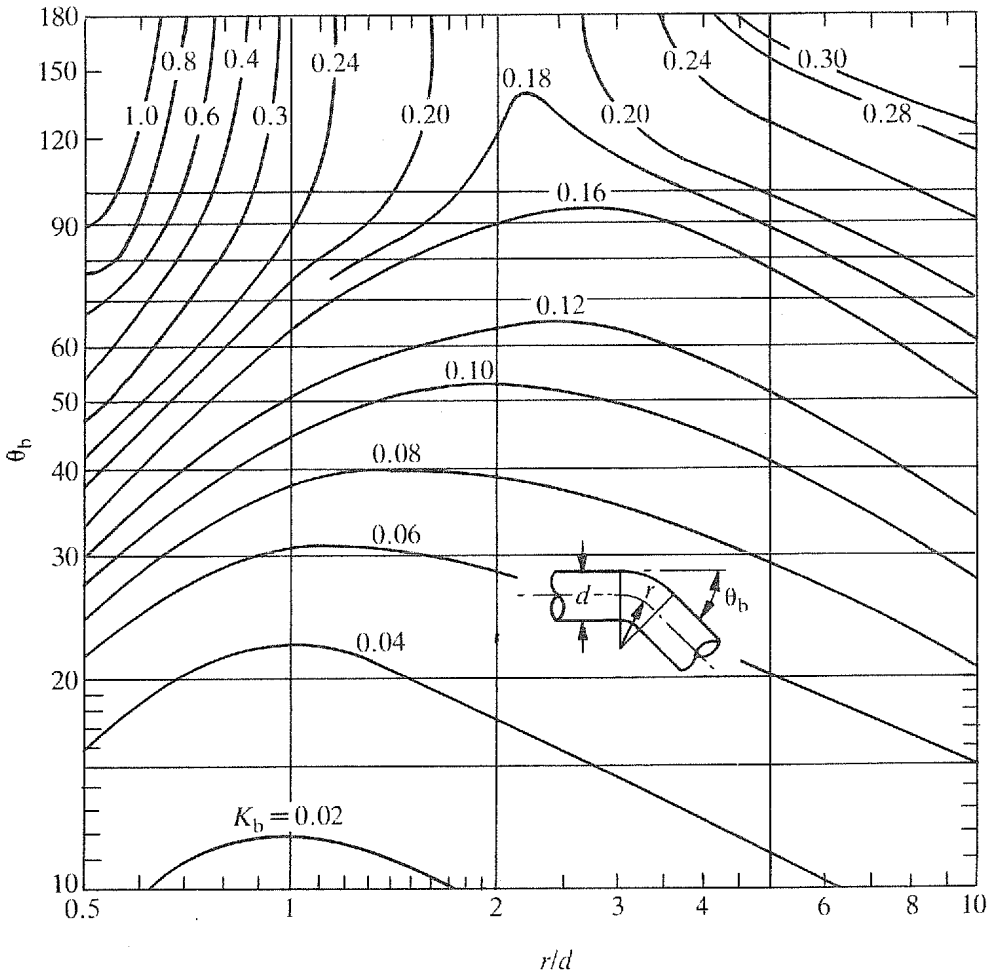

Fig. 5.41. Bend performance chart — circular cross-section ($Re = 10^6$)

Bend loss coefficients vary markedly with Reynolds number, as the curves for 90° bends in Fig. 5.42 show. In order to allow for Reynolds number effects, loss coefficients from performance charts, such as Fig. 5.41, are modified by the application of a Reynolds number correction factor.

5.5. INTERACTIONS BETWEEN BENDS

The term interaction covers the direct interference between pressure and flow distributions when bends are less than two pipe diameters apart, and indirect effects on bend loss coefficients caused by a change in inlet and in outlet flow conditions, compared with an isolated bend.

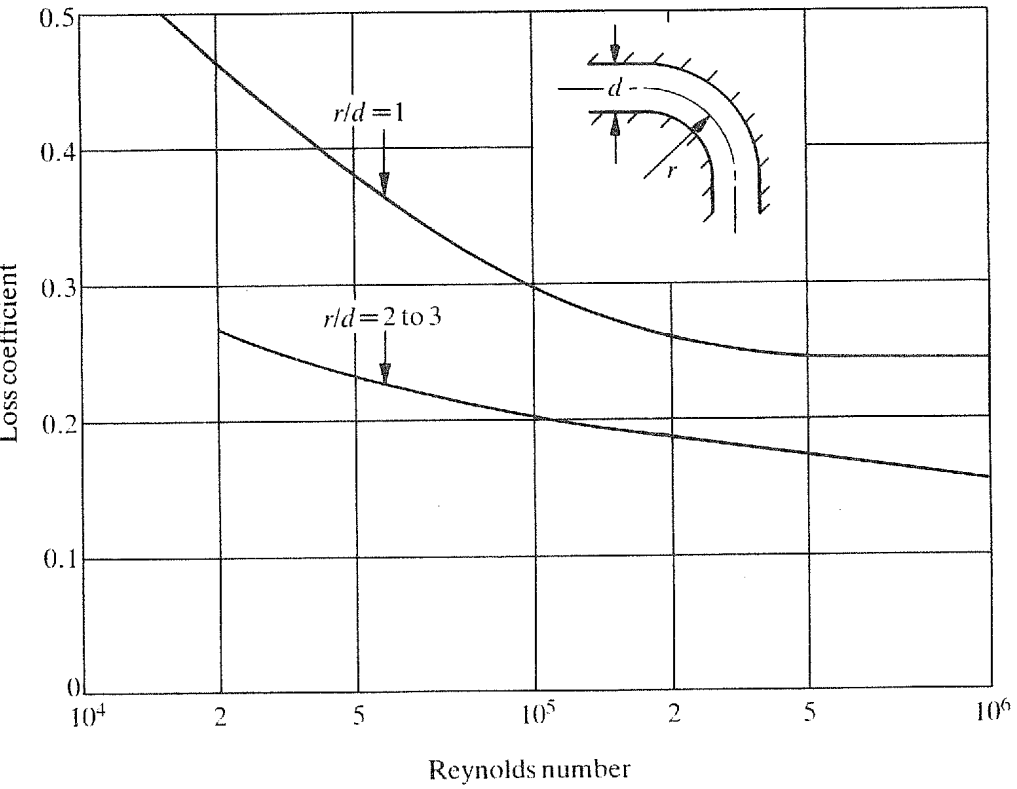

Fig. 5.42. Effect of Reynolds number on 90° bend loss coefficients

Interaction between bends occur for the following reasons.

1. Part of the loss attributed to a bend is due to flow redevelopment after the bend. If another bend is located in the flow redevelopment region, then part of the loss normally associated with the first bend no longer occurs. If the spacer length between bends is more than four diameters, then neglecting interactions between bends overestimates the pressure losses.
2. In the flow redevelopment section after the first bend the velocity profile differs from that used in determining loss coefficients of isolated bends. As this profile is the input to the second bend there is an effect on the second bend.
3. The spacer between bends is so short that their static pressure distributions interact and modify the flow patterns. Direct interactions between bends can both increase and decrease the pressure loss compared with that of two isolated bends.

The most commonly met interactions are between two 90° bends. Figure 5.43 shows the definitions adopted for combinations of two 90° bends. Except for bends of centreline radius/diameter ratio less than 1, losses due to combining two 90° bends are less than the sum of their isolated individual losses. The main problem associated with combinations of bends is the persistent swirl that can be generated over a range of combination angles. Figure 5.44 shows the two 90° bends in a 60° combination angle, which is a combination angle that

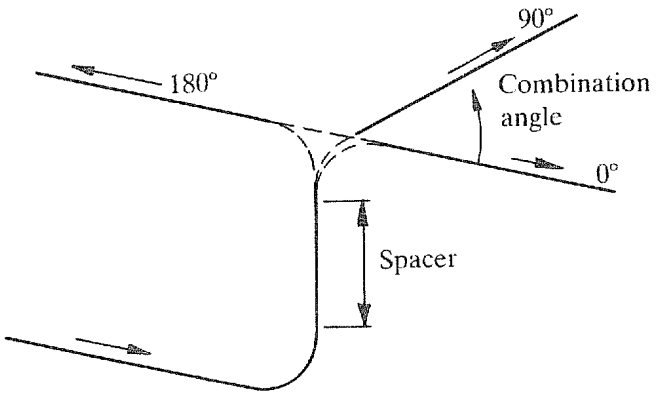

Fig. 5.43. Combination of two 90° bends

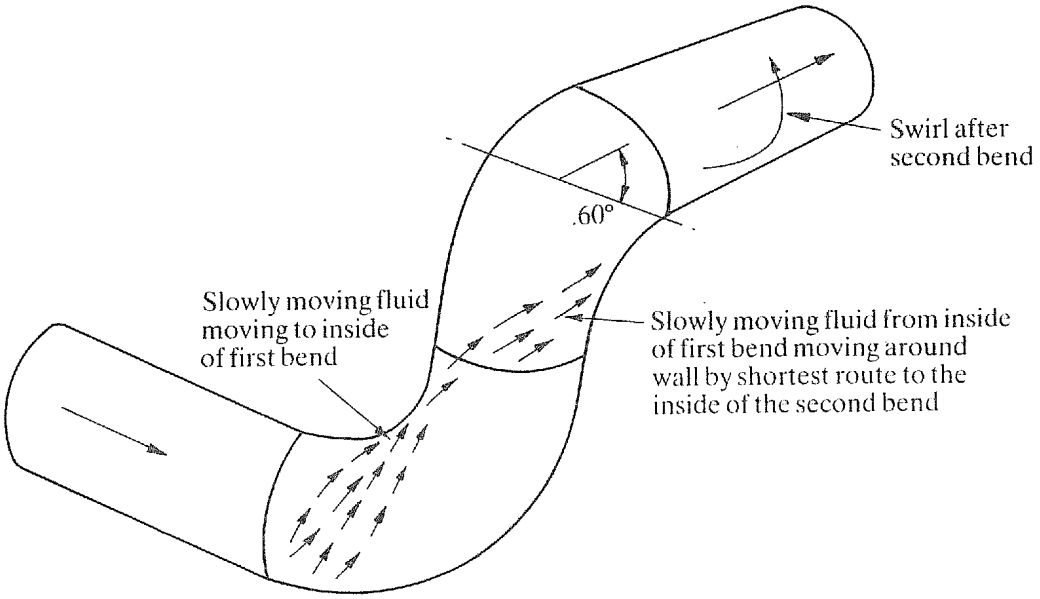

Fig. 5.44. Combination generating strong swirl

creates strong swirl. The mechanism of swirl generation is the flow of low energy fluid from the inside of the first bend to the inside of the second bend. As the combination angle is varied from zero the displacement of low energy fluid takes place preferentially along the shortest route. At combination angles between 30° and 90° nearly all low energy fluid follows the same path, setting up a single secondary flow or swirl, instead of the usual twin cells of secondary flow generated by an isolated bend. Swirl generated by bend combinations can persist for more than 100 pipe diameters.

5.6. COMBINED TURNING AND DIFFUSING FLOW

In combined turning and diffusing passages all of the flow phenomena present in bends and straight diffusers occur, but in more extreme forms. Conversion of velocity pressure to static pressure is much more difficult in curved diffusers than in straight diffusers.

Pressure distributions on the inner and outer walls of a curved diffuser with ideal flow are shown in Fig. 5.45. Adverse pressure gradients, along the outer wall at entry and towards the outlet along the inner wall, are steeper than for turning flow alone. On the inner wall the static pressure remains almost constant until well through the diffuser.

If a bend is added to a straight wall diffuser (Fig. 5.46), the adverse gradient within the diffuser, for fluid moving towards the outer radius of the bend, is increased. If flow separation

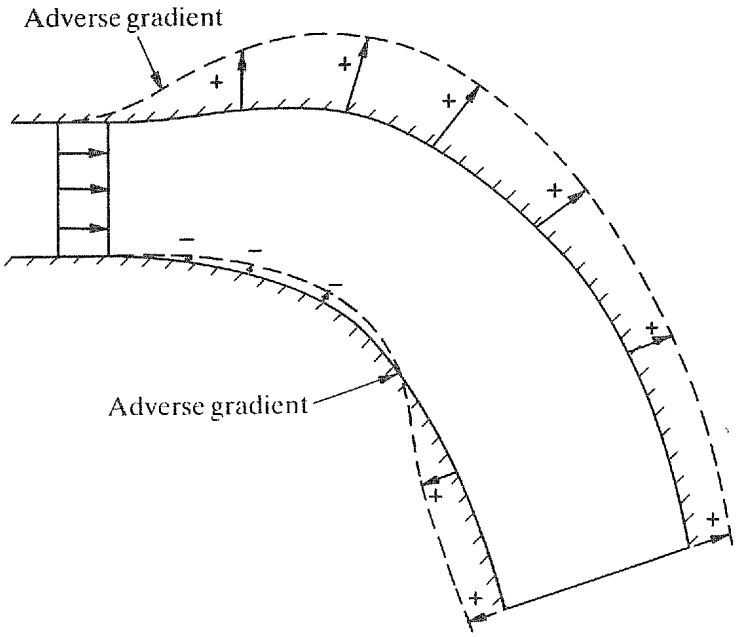

Fig. 5.45. Pressure distribution with ideal flow

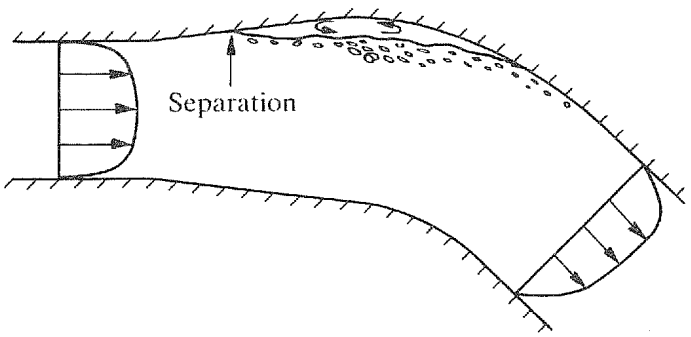

Fig. 5.46. Diffuser followed by a bend

is induced on the outer wall, the resulting intense mixing can, due to the effects of curvature on turbulence, extract considerable energy from the main flow and yet not re-energise fluid on the inner wall. When a diffuser is located directly before a bend, diffusion should be concentrated towards the inside of the bend, as illustrated in Fig. 5.47.

Adding a diffuser to a bend (Fig. 5.48) steepens the inner wall adverse gradient and makes separation inevitable. If a diffuser has to be located immediately after a bend, diffusion should be concentrated away from the outer radius, preferably with a short spacer, as in Fig. 5.49.

Because turbulence is suppressed at the inner wall, continuous turning and diffusing is ineffective. Referring to Fig. 5.50, low energy fluid continues to accumulate on the inner wall until the diffuser outlet. Mixing between the separated region and the main flows is suppressed, so losses within the diffuser are mainly confined to friction at the outer wall, which is not very great if there is no outer wall separation. As little energy dissipation takes place within the curved diffuser, most of the kinetic energy remains at outlet. If the area ratio is less than 1.5 and there is a parallel section after a diffuser of the type shown in Fig. 5.50, then the static pressure recovery in the outlet, combined with recovery in the diffuser, can exceed that

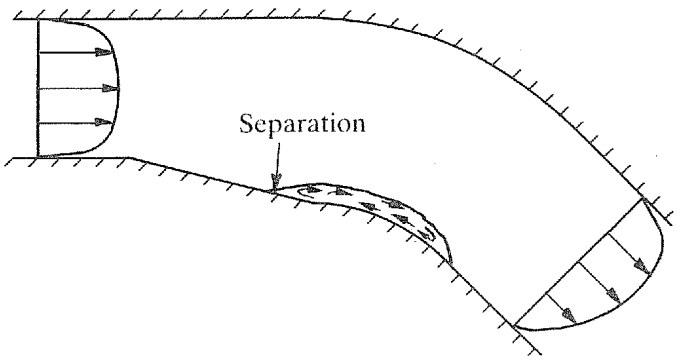

Fig. 5.47. Diffusion towards the inside of a bend

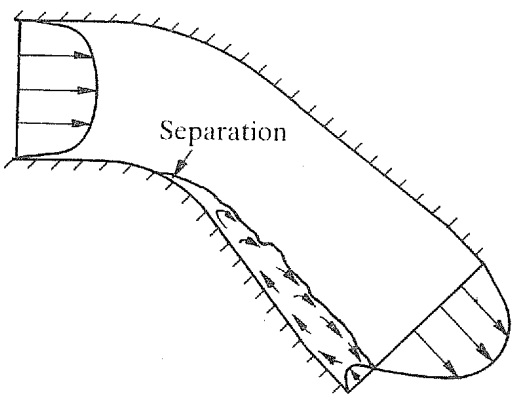

Fig. 5.48. Bend followed by a diffuser

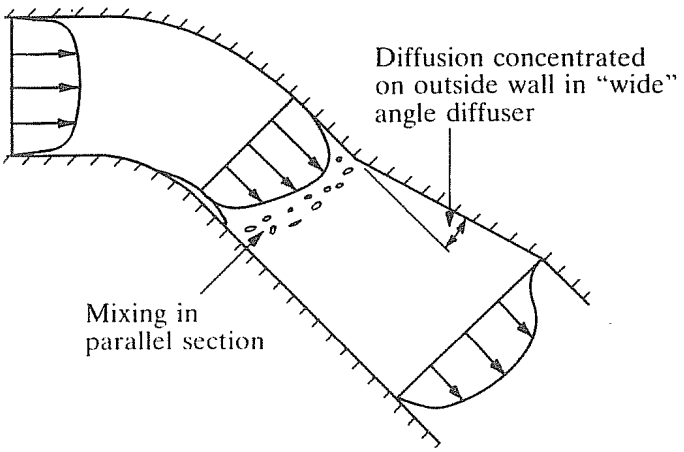

Fig. 5.49. Diffusion away from the outside of a bend

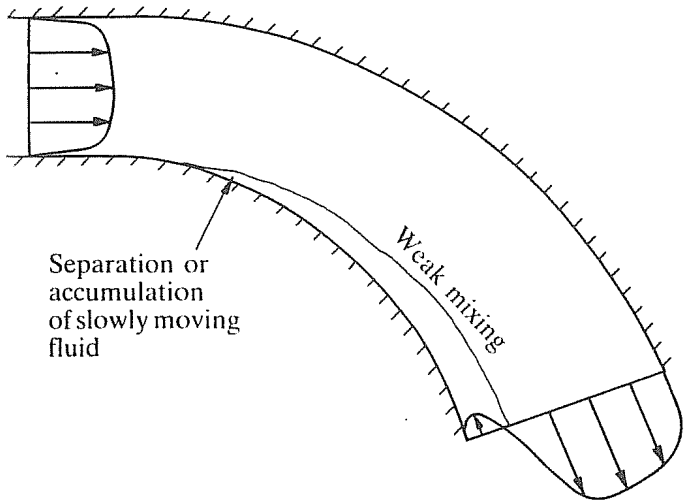

Fig. 5.50. Continuous diffusion

of any other design of curved wall diffuser. However, when allowance is made for the length of parallel section, this arrangement occupies too much space.

With developed flow at inlet, efficient curved wall diffusers have to be designed to use diffusion, secondary flows and mixing in order to achieve a compact arrangement (Fig. 5.51). The aim is to turn and diffuse the flow as rapidly as possible without causing separation on the outer wall. Secondary flows and turbulence can then redistribute the flow with a static pressure rise in the outlet parallel section. If, however, the inlet velocity profile is nearly uniform, rapid diffusion followed by turning is more effective. This is because secondary flows are much weaker, resulting in the inner wall separation region extending further into the outlet parallel section.

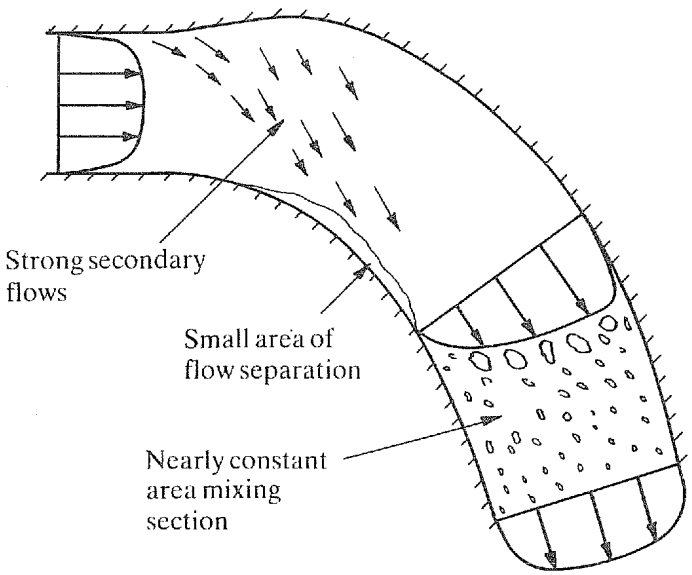

Fig. 5.51. High performance curved diffuser

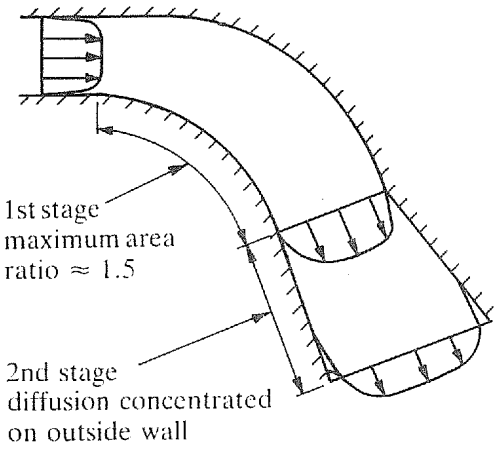

Fig. 5.52. Area ratio greater than 1.5 curved wall diffuser

The arduous conditions imposed by simultaneous turning and diffusing places a limit on the diffuser area ratio before losses become excessive. With developed inlet flow an area ratio of about 1.5 is the maximum that should be used. If a larger area ratio is required, diffusion should be carried out in two stages, with the arrangement shown in Fig. 5.52. Flow at outlet from the first stage of the diffuser in Fig. 5.52 is conditioned so as to achieve almost ideal diffusion in the second stage.

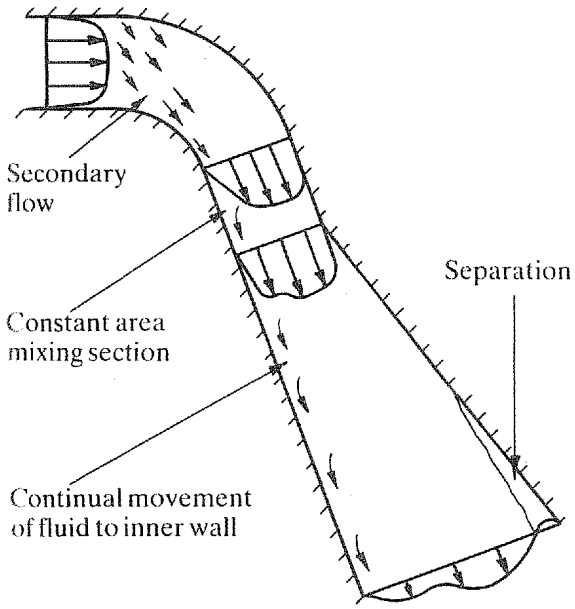

Fig. 5.53. Bend–spacer–diffuser combination

When the area ratio exceeds 2.5 there is little difference in performance between an arrangement based on Fig. 5.52 and a bend–spacer combination (Fig. 5.53). Following a bend, secondary flows redistribute low energy fluid in such a manner that efficient diffusion is possible in a diffuser with a relatively high rate of diffusion.

5.7. COMBINING AND DIVIDING FLOW

5.7.1. INTRODUCTION

Combining and dividing junctions involve additional geometrical parameters compared with components with a single flow path. There is also the need for a flow parameter to account for the distribution of flow between the junction legs. Major energy losses due to combining and dividing flows arise from flow separation and subsequent turbulent mixing. Energy losses associated with separation and re-attachment are discussed in Section 5.8. The main concern in this section is the variation of loss coefficients with geometric and flow parameters. Comments are confined to T junctions but can be interpreted to apply to Y junctions.

As a variety of junction leg numbering systems are in use, it is essential to understand to which flow path a particular loss coefficient relates. The convention adopted in this work is to call the leg carrying the total flow leg 3. This applies to both T and Y junctions (Fig. 5.54). Symmetrical Y junction legs 1 and 2 are interchangeable as regards calculating pressure losses.

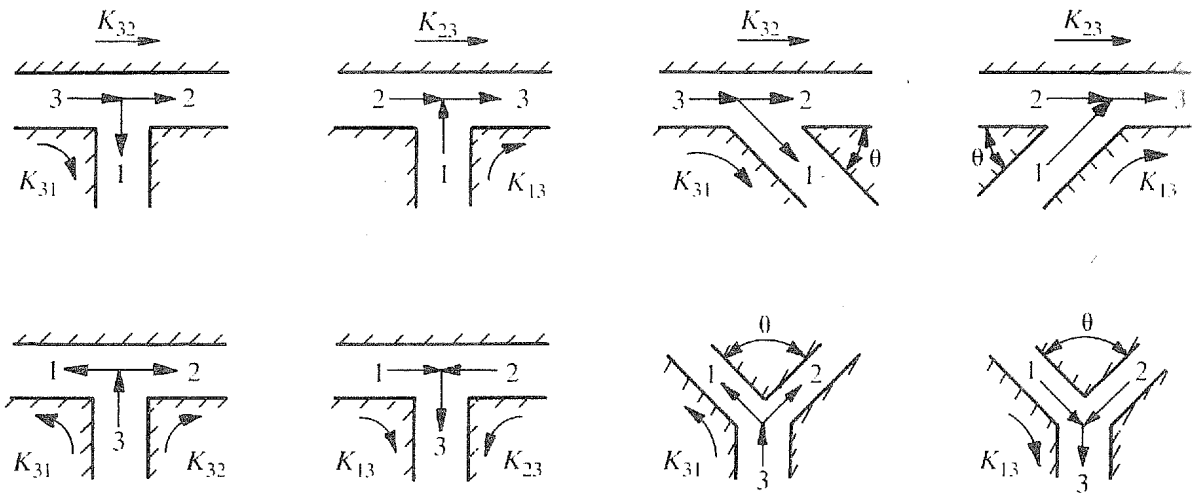

Fig. 5.54. T and Y junctions

The loss coefficients K_{ij} shown in Fig. 5.54 are defined as

$$K_{ij} = \frac{\text{Total pressure in leg } i - \text{Total pressure in leg } j}{\text{Mean velocity pressure in leg 3}}$$

The flow ratio is always expressed as Q_1/Q_3.

T junctions are often the highest loss components in a piping system, particularly if it is a high pressure system where stress requirements favour the use of 90° junctions. In large systems or systems involving high velocities, an economic assessment should be made of whether the initial capital expense of low loss junctions can be justified on the basis of reduced operating costs. On major compressor and pumping installations, 10 per cent of the power input can be dissipated in junctions if large numbers of cross connections are involved.

The high losses in junctions are the result of flow separation. In cases where regions of flow separation are not stabilised, such as in symmetrical dividing junctions, very unstable flows can occur. The potential for damaging instabilities should be considered in the design of large systems, systems operating at high velocities and systems that are flexibly mounted.

5.7.2. COMBINING T JUNCTIONS

Variation in the loss coefficients of sharp-edged 90° combining Ts with branch and main of the same area are considered first (Fig. 5.55). Having fixed the angle at 90° and the area ratio A_1/A_3 at 1, only the branch to main flow ratio Q_1/Q_3 is a variable.

Consider first the flow entering from the branch leg 1 into leg 3. For zero branch flow ($Q_1/Q_3 = 0$) the pressure in the branch is essentially the static pressure of the through flow. If the pressure in the branch is raised slightly, a small flow will leave the branch and be accelerated up to the velocity in leg 3. There is a transfer of energy from the through flow

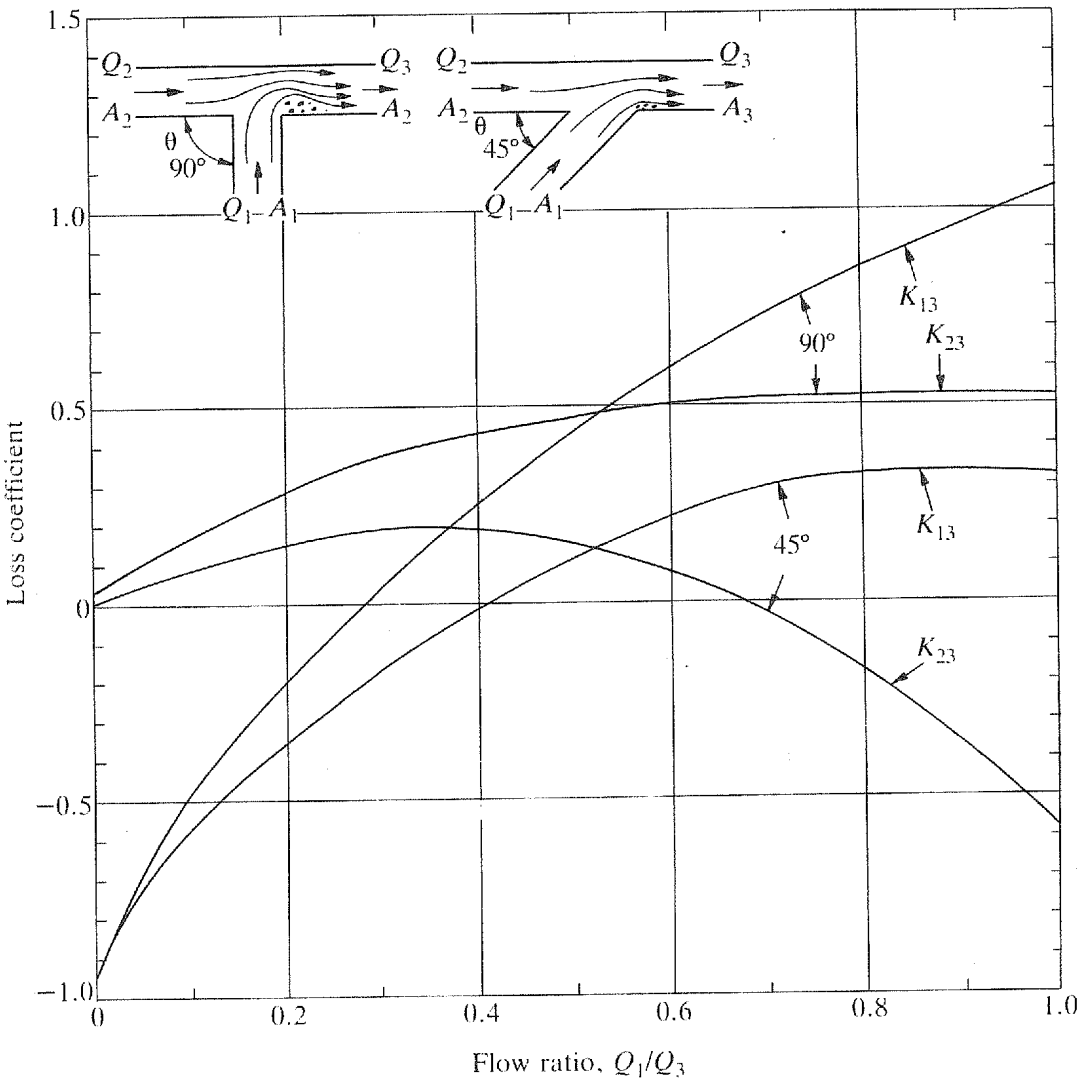

Fig. 5.55. Loss coefficients for sharp-edged 45° and 90° combining Ts

(leg 2) to the flow from the branch, so the loss coefficient for the branch is negative. When the flow ratio Q_1/Q_3 is close to zero the branch loss coefficient K_{13} is about -1.0. The corresponding through flow coefficient K_{23} is positive at about 0.05.

As the flow ratio Q_1/Q_3 increases, the branch loss coefficient K_{13} becomes positive at a flow ratio of 0.3, reaching a maximum of about 1.1 when all of the flow is from the branch. The corresponding through flow coefficient K_{23} increases steadily from nearly zero to a maximum of about 0.55 when all flow is entering from the branch.

If the branch area is less than the through flow area ($A_1/A_3 > 1$) the velocity pressure in the branch, for a given Q_1/Q_3, is greater and the branch loss coefficients are higher. For

instance, when all of the flow is from the branch, the branch loss coefficient will be greater than the coefficient with equal area by roughly the inverse of the (area ratio)^2. Variation in the area ratio has a small effect on the through flow coefficient K_{23}.

If the branch angle is reduced to 45°, with a T junction having $A_1/A_3 = 1$, then the coefficient K_{13} for small branch flows is still negative at about -1.0, it becomes positive at a Q_1/Q_3 of about 0.4 and reaches a maximum of about 0.35 when all of the flow is from the branch. The through flow coefficient K_{23} is approximately zero when there is no flow from the branch, and increases to a maximum of 0.2 at $Q_1/Q_3 = 0.4$. It then falls, becoming negative at $Q_1/Q_3 = 0.7$ and reduces to -0.6 when all flow is from the branch. The negative through flow coefficients K_{23} are the result of energy transfer from the high velocity fluid entering from the branch to the slower through flow. Obviously, if the velocity in the branch is increased by reducing its area, the through flow loss coefficients K_{23} may become more negative and the branch coefficient will increase.

A radius or chamfer at the junction of legs 1 and 3 (Fig. 5.56) has an effect on both the branch and through flow loss coefficients. For 90° Ts with $A_1/A_3 = 1$, a radius or chamfer has most effect when the ratio of branch to main flow Q_1/Q_3 is >0.2. As the area of the branch is reduced, the advantage of having a radius is felt at smaller flow ratios for the branch coefficient, whereas, the through flow coefficient K_{23} is affected only slightly. A chamfer or radius of about 0.1 of the branch diameter is sufficient to obtain about 70 per cent of the possible reduction.

A problem that occurs when Q_1/Q_3 is high and A_1/A_3 is low is the generation of swirl. Swirl may be generated whether the branch is offset or not (Fig. 5.57). A symmetrically located

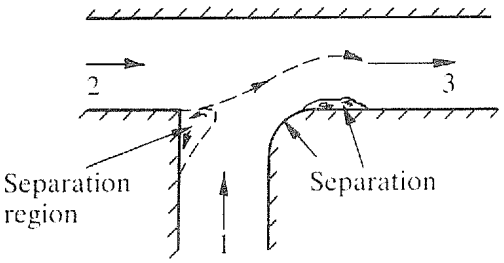

Fig. 5.56. Improved flow with a radius between legs 1 and 2

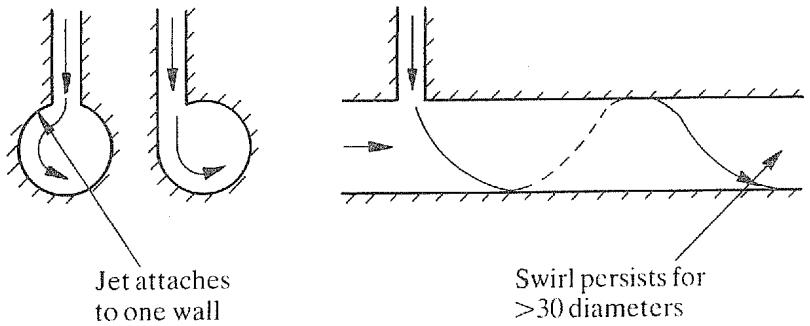

Fig. 5.57. Swirl generated by branch flow

branch is no guarantee that swirl will not develop, because inevitably the flow attaches to one side wall or the other.

5.7.3. DIVIDING T JUNCTIONS

Consider flow entering the branch of a 90° sharp-edged T junction (Fig. 5.58) with $A_1/A_3 = 1$. For very small flows into the branch the static pressure in the branch is essentially the static pressure in leg 3, and the velocity pressure in the branch is virtually zero. Since the energy level in the branch is lower by the velocity pressure in leg 3, the branch loss coefficient is positive at about $K_{31} = 1$. At the other extreme, when all of the flow is into the branch ($Q_1/Q_3 = 1$) the loss is similar to that of a mitre bend at about $K_{31} = 1.1$. Between the two extremes the coefficient K_{31} drops to a minimum of about 0.85 at $Q_1/Q_3 = 0.4$.

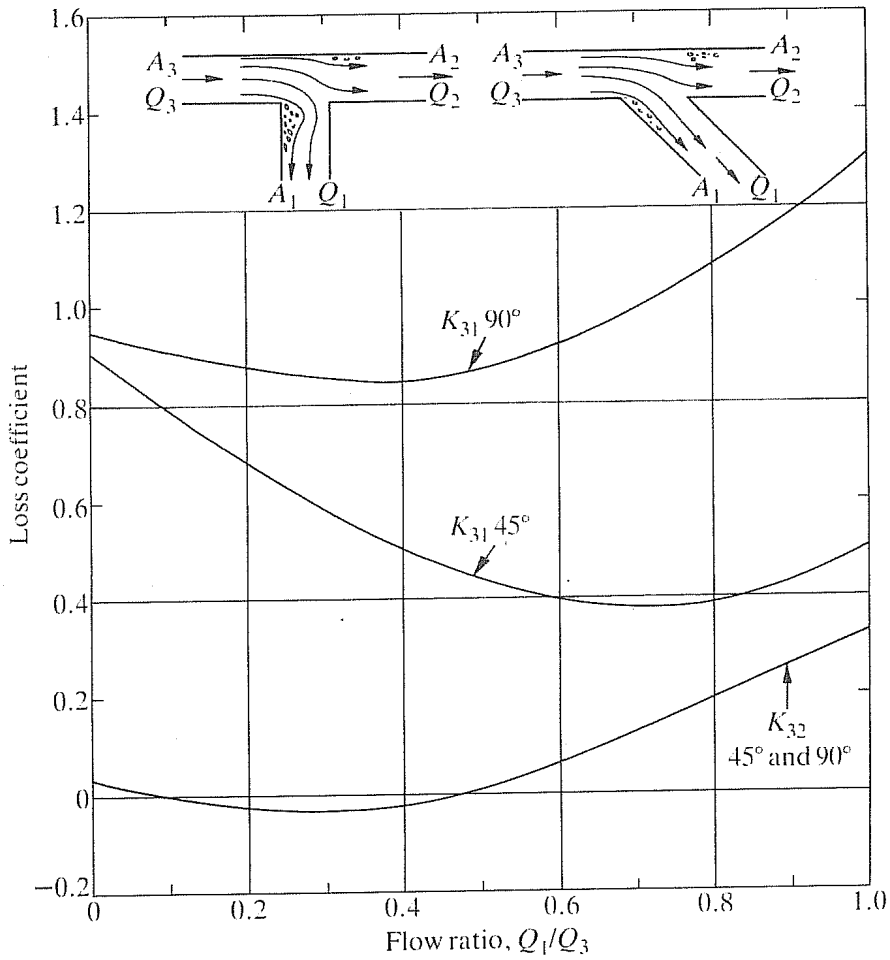

Fig. 5.58. Loss coefficients for sharp-edged 45° and 90° dividing Ts

The loss coefficient for the through flow K_{32} is virtually zero until $Q_1/Q_3 = 0.5$; for low Q_1/Q_3 the fluid drawn off by the branch consists of the slowly moving fluid close to the walls, so the energy per unit mass of the fluid in the through flow may increase slightly. This increase in energy per unit mass is to some extent balanced by the diffusion loss as the through flow slows down at the T junction. Above $Q_1/Q_3 = 0.5$ the through flow coefficient K_{32} increases steadily up to 0.35 when all of the flow is into the branch. The through flow loss coefficient is not affected greatly by changes in branch angle or in area ratio A_1/A_3.

Although reducing the area ratio A_1/A_3 increases the branch loss coefficient, the pressure loss in a branch is a smaller fraction of the branch velocity pressure. Angling the branch at 45° has the effect of halving the branch loss coefficients at $Q_1/Q_3 > 0.5$ for all area ratios.

The through flow coefficient K_{32} is practically unaffected by having a radius or chamfer at the junction of legs 3 and 1 (Fig. 5.59). When flow separation occurs at high Q_1/Q_3 it takes place on the wall opposite the branch and is therefore not affected by the shape of the junction. For the 90° branch the loss coefficient K_{31} falls rapidly as the leading edge is radiused or chamfered, at least up to values equal to the branch diameter, with the reduction in the loss coefficient being greatest for large branch flows and small branch areas.

5.7.4. MANIFOLDS

When manifold branches are more than three manifold diameters apart, or four branch diameters apart if the branch flow is less than 10 per cent of the total flow, loss coefficients for isolated dividing and combining junctions can be used to predict the flow distribution and pressure loss of a manifold. As flow is bled off from a constant area dividing manifold (Fig. 5.60), the velocity of the remaining fluid decreases with a rise in static pressure. In a short dividing manifold the increase in static pressure towards the end of the manifold results in a higher flow rate out of the end branches. The opposite occurs in a combining manifold (Fig. 5.61), where static pressure decreases with the distance from the end of the manifold.

The distribution of flow between branches depends on the length of the manifold, and hence on friction losses, and on either the ratio of the inlet velocity pressure of the manifold to the losses in the branches or the ratio of total branch area to manifold area. When the

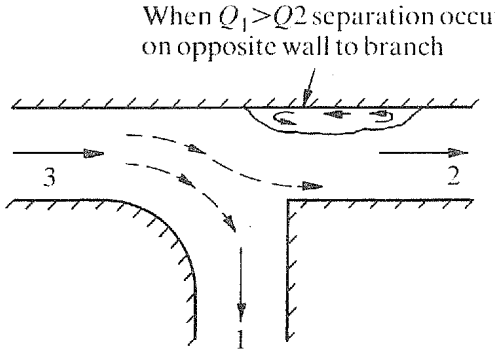

Fig. 5.59. Separation of through flow

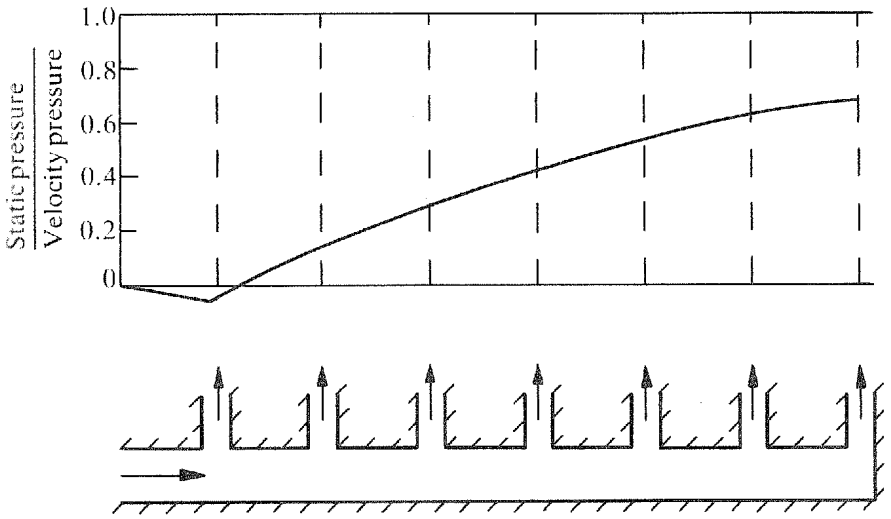

Fig. 5.60. Static pressure within a dividing manifold

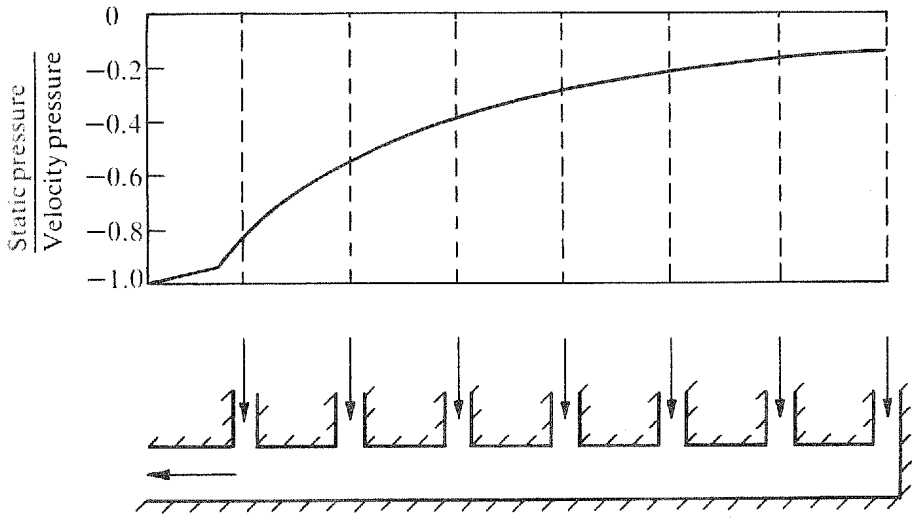

Fig. 5.61. Static pressure along a combining manifold

latter two ratios are greater than unity the flow distribution will usually be very poor. Trends in flow distribution for dividing manifolds are shown in Fig. 5.62 and for combining manifolds in Fig. 5.63.

The flow distributions in Figs 5.62 and 5.63 assume equal branch areas or branch loss coefficients, and constant manifold area and cross-section. By varying the branch and manifold areas, modifying the branch junctions and adjusting branch loss coefficients, it is possible to obtain any required flow distribution, provided the resultant pressure losses are acceptable.

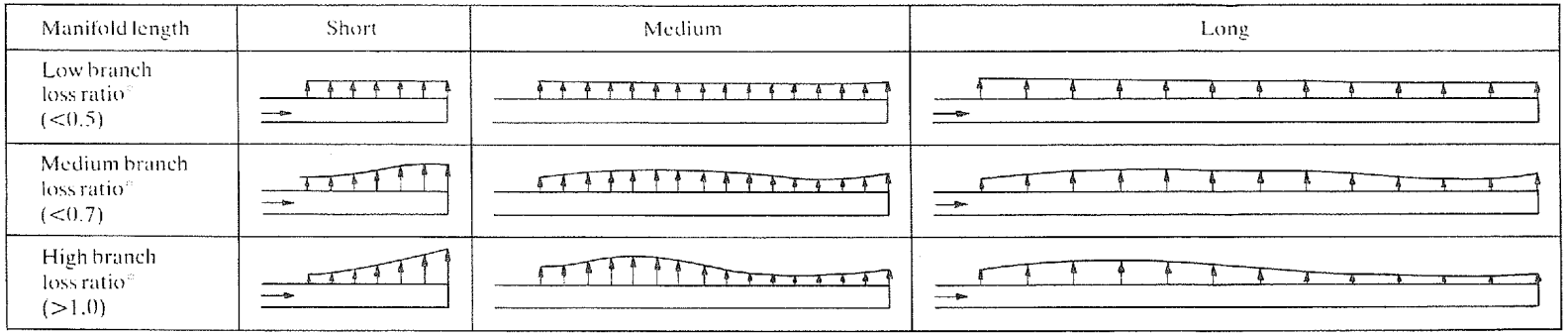

Fig. 5.62. Flow distribution for dividing manifold

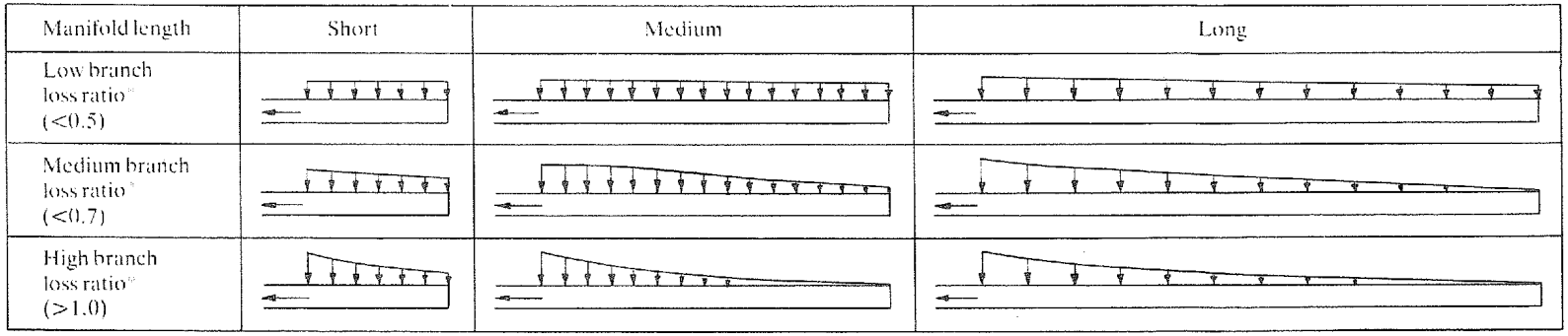

Fig. 5.63. Flow distribution for combining manifold

$$*\text{Loss ratio} = \left(\frac{\text{Velocity pressure}}{\text{Pressure losses in branches}}\right) \quad \text{or} \quad \left(\frac{\text{Total branch cross sectional area}}{\text{Manifold cross-sectional area}}\right)^2$$

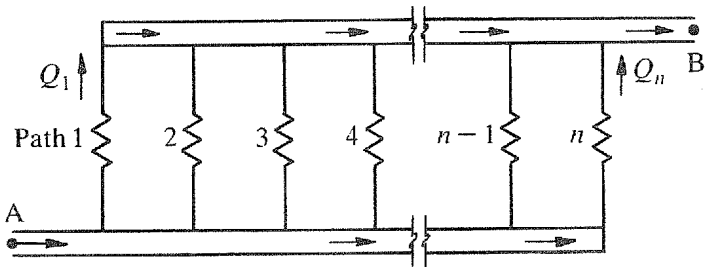

Fig. 5.64. Combined manifold system

When flow divides and recombines, as in Fig. 5.64, the continuity and energy equations, along with estimates for junction loss coefficients, allow the flow distribution and pressure loss to be calculated. Continuity equation:

$$Q_A = Q_B = Q_1 + Q_2 + \cdots + Q_{n-1} + Q_n$$

Energy equation:

Total pressure loss A→B along path 1 = Total pressure loss A→B along path 2
= Total pressure loss A→B along path n

In order to find the pressure loss and flow distribution an iterative procedure is followed. An estimate is made of the flow distribution and the pressure loss calculated for each flow path. Based on the results, new estimates of flow are made and the process repeated.

5.8. ABRUPT CHANGES IN AREA AND DIRECTION

Following flow separation, due to too steep an adverse pressure gradient or an abrupt change in area ratio, large scale turbulence spreads through the flow. The effect of the turbulence is to even out the energy distribution and, aided by fluid turning back to provide entrainment flow, to induce flow re-attachment. Following re-attachment the large scale turbulence decays rapidly. The various processes involved following an abrupt expansion are illustrated in Fig. 5.65.

Energy losses due to an abrupt expansion in area can be calculated approximately from the one-dimensional continuity, momentum and energy equations. A sudden expansion loss is given by

$$K_s = [1 - (A_1/A_2)]^2$$

For an area ratio of 2 the loss coefficient of an abrupt expansion is 0.25, the downstream velocity pressure is 0.25 of the inlet velocity pressure and the static pressure rise is 0.5 of the inlet velocity pressure.

Figure 5.66 shows the loss coefficients and static pressure recovery coefficients C_p for abrupt

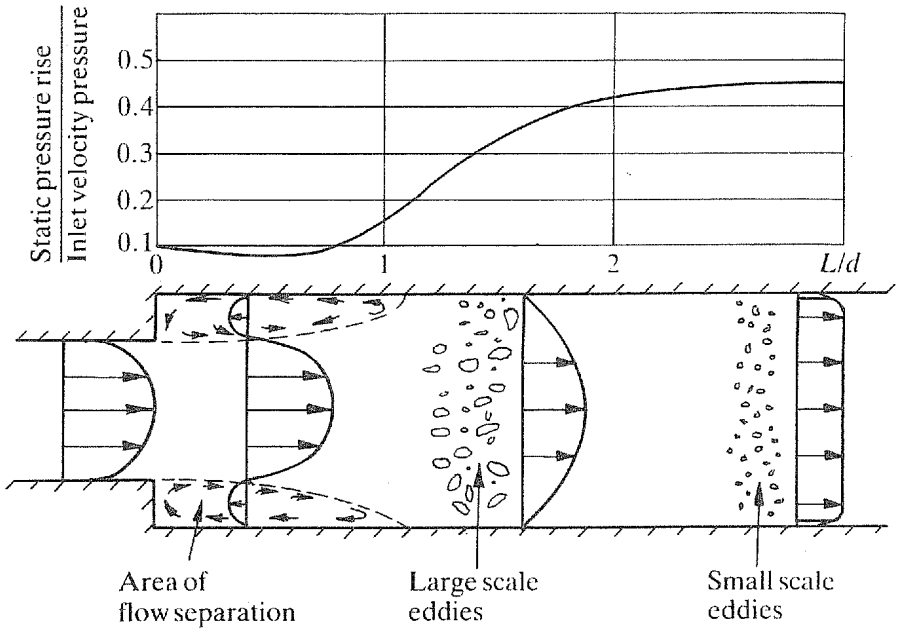

Fig. 5.65. Sudden expansion

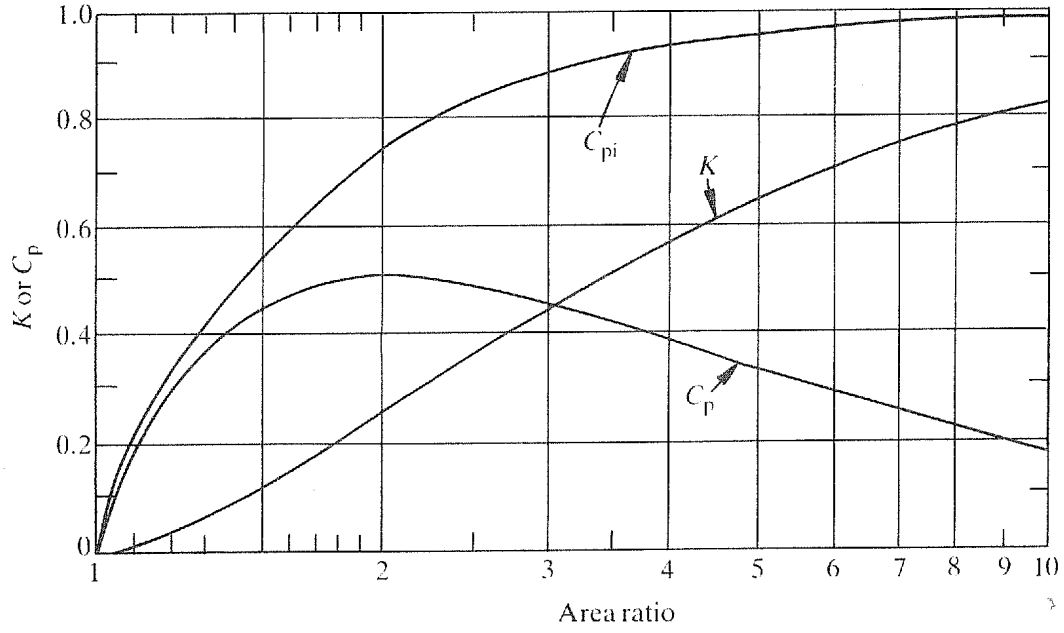

Fig. 5.66. Sudden expansion loss and pressure recovery coefficients

expansions. Also shown on Fig. 5.66 is the ideal static pressure recovery coefficient C_{pi} for lossless expansion. The curves shown on Fig. 5.67 give the number of downstream pipe diameters necessary for mixing to produce the maximum static pressure recovery or a percentage of the maximum recovery.

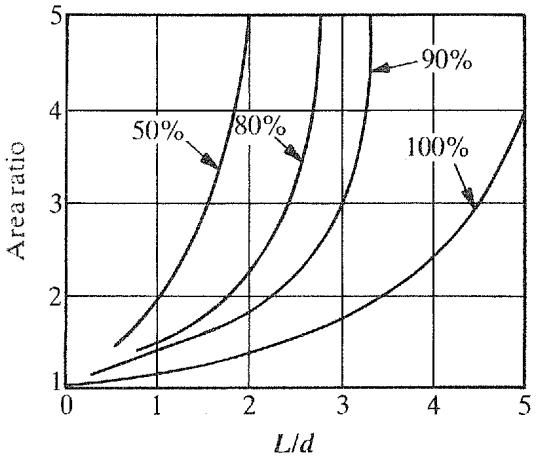

Fig. 5.67. Downstream length required for static pressure recovery (percentage of maximum)

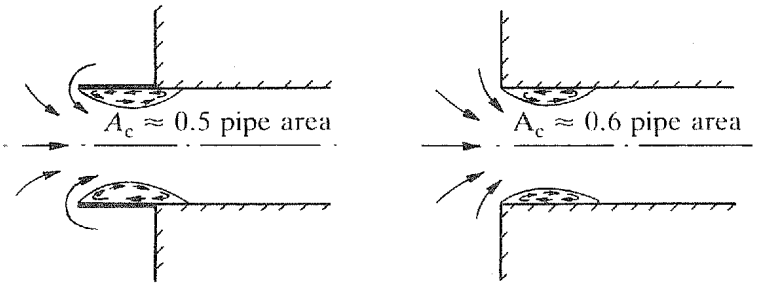

Fig. 5.68. Flow contraction followed by expansion

Many abrupt expansions are preceded by abrupt contractions in flow area. Even though flow is rapidly accelerated in an abrupt contraction, pressure losses are small because the process of converting static pressure to velocity pressure is stable. This means that where a contraction is followed by an expansion, only the losses in the expansion are important. Two examples of flow contraction followed by expansion are shown in Fig. 5.68. Fluid enters the re-entrant inlet from the rear and sides, with the result that the flow contracts to half the pipe area. In expanding to the full pipe area, 0.25 of the velocity pressure at the vena contracta is lost and, since the velocity pressure in the vena contracta is four times that based on the pipe area, the loss coefficient, based on the pipe velocity, is 1.0. Additional losses as the flow develops in about the first 30 pipe diameters adds about 0.1 to the loss coefficient. With no flow from the rear, the flush intake contraction is less at 0.6 of the pipe area. The sudden expansion loss coefficient is 0.16 which, corrected to the mean pipe velocity, is a loss coefficient of 0.45, to which has to be added the loss attributable to flow development after the inlet.

A situation where an abrupt change in flow direction causes a loss equivalent to that of the re-entrant inlet is in a 90° mitre bend (Fig. 5.69). The flow contracts to about half the pipe area and then expands with a loss equivalent to the mean velocity pressure.

It is of interest to consider what the upper limits are on loss coefficients in internal flow. The 90° mitre bend and the re-entrant inlet involve the largest flow contractions encountered in internal flow for a single change in area or direction. In both cases the loss coefficient is about unity based on the pipe velocity, but only 0.25 based on the velocity in the vena contracta. If the outlet pipes are removed from the 90° mitre bend, the re-entrant inlet and the orifice (Fig. 5.70), then their loss coefficients, based on the minimum geometrical area, are 4.0 for the mitre bend and re-entrant inlet and 2.8 for the orifice. A loss coefficient of 4, based on the minimum geometrical flow area, is the maximum that can be achieved with a single change in area or direction. To achieve higher loss coefficients it is necessary to contract the flow by a change in area or direction and then to deflect the flow in such a manner that it contracts further. Energy dissipation then takes place at velocities several times that of the mean velocity. Figure 5.71 shows a flow arrangement that is particularly effective, for the space it occupies, in dissipating energy.

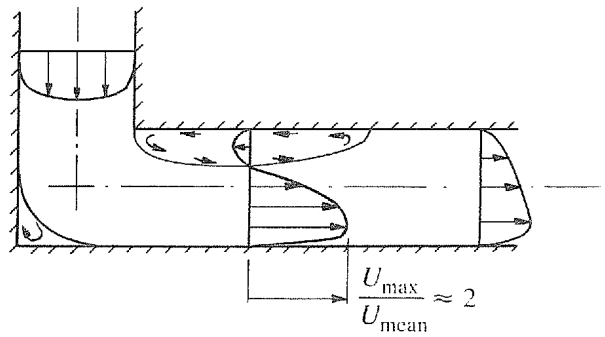

Fig. 5.69. Flow contraction in a mitre bend

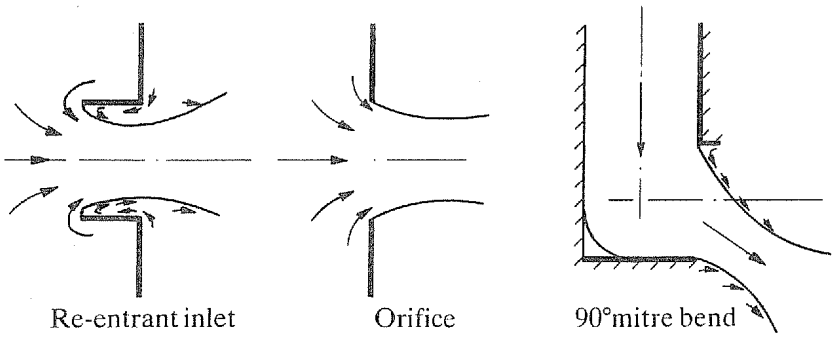

Fig. 5.70. Contraction with no outlet pipes

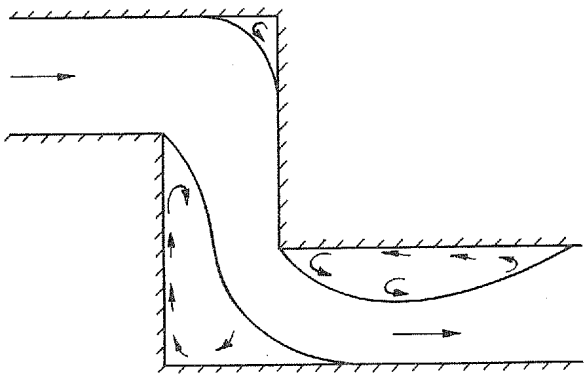

Fig. 5.71. Combination of 90° mitre bends giving high losses ($K_b \approx 4.5$)

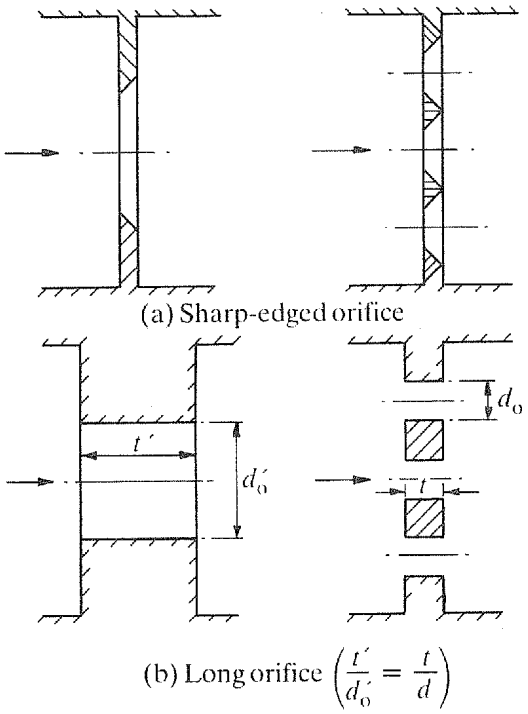

Fig. 5.72. Similarity conditions for orifices

Provided flow separation and re-attachment are duplicated, a number of geometrical parameters are not important in comparing performance. Loss coefficients for orifice plates and perforated plates (Fig. 5.72) are similar if their ratios of total orifice area to pipe area are the same. For the same ratio of total orifice/pipe area the total vena contracta area is similar whether there are single or multiple orifices. In the case of a single orifice the length of the outlet pipe required for full static pressure recovery is considerably greater than with multiple orifices.

With orifices of length/diameter ratio of up to 2, the effect of varying the length/diameter ratio of the orifice is to alter the flow patterns and energy losses. Figure 5.73 shows the flow patterns for various length/diameter ratios. At one extreme is the thin plate with a single expansion from the vena contracta up to the pipe area. At the other extreme is full re-attachment in the orifice, with the flow expanding initially through an area ratio of 0.6 and then from the orifice area up to the pipe area. The latter two-stage expansion is a lower loss process than that for the thin orifice plate. For the same orifice size and flow rate, an orifice arrangement with a length/diameter ratio of 2 has only 0.6 times the loss of a thin orifice plate.

At an abrupt contraction the effect of rounding the edges is to reduce the flow contraction and the subsequent expansion losses. A radius of 10 per cent of the pipe diameter usually keeps the inlet loss coefficient, including an allowance for flow development after the inlet, to less than 0.10.

Losses due to steps at joints and misalignment of components can be calculated approximately by applying data for orifices. The geometrical parameters to use for steps are shown in Fig. 5.74. The losses due to a step can be minimised by rounding the upstream edge or by having a step length of about five times the step height (Fig. 5.75). When the step

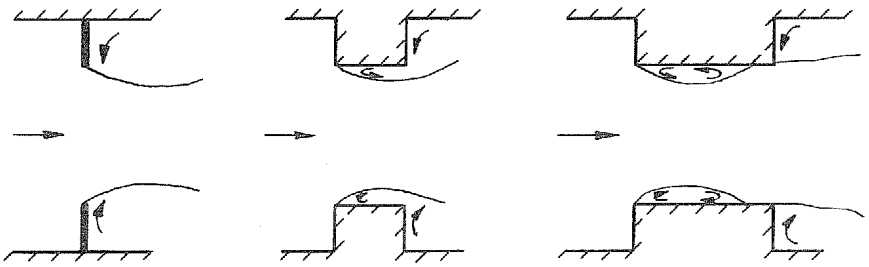

Fig. 5.73. Effect of orifice length

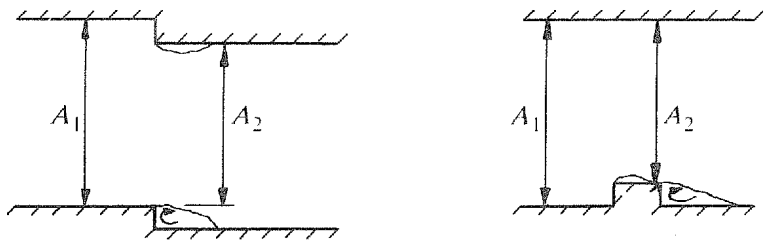

Fig. 5.74. Areas to use in calculating head losses

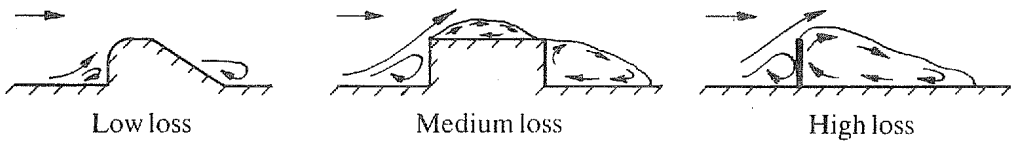

Fig. 5.75. Flow over steps

length is between about two and four times the step height, unstable flow re-attachment may occur, inducing fluctuating pressures.

Losses due to cavities are influenced by the upstream and downstream edge shape and the cavity depth/length ratio (Fig. 5.76). Radiusing the upstream edge increases the flow into the cavity and the energy dissipation. A radius on the downstream edge reduces the energy dissipation. A single, stable vortex, which results in low losses, forms in cavities of depth/length ratios close to unity. Between depth/length ratios of 0.2 and 0.8, circulation within a cavity is unstable, with periodic disturbances influencing the main flow. Loss coefficients for sharp-edged cavities have a maximum of about 0.07 with depth/length ratios of 0.5.

The near-wall velocity distribution has a strong influence on the losses due to steps and cavities, losses being higher after contractions where the boundary layer is thin. Due to periodic eddy formation, steps and cavities can generate considerable narrow band hydrodynamic and aerodynamic noise.

Valves contain one or more flow restrictions. Although there are numerous valve geometries, they can, for performance purposes, be put into one of two categories, depending on the ratio of the maximum static pressure difference to the total pressure loss.

Valves with a high ratio of maximum static pressure difference to total pressure loss are usually of the through flow type (Fig. 5.77). A typical static pressure distribution downstream of one of these valves is shown in Fig. 5.78. Because of the static pressure recovery after the vena contracta, high velocities and hence low pressures are necessary to dissipate a relatively small amount of energy. This type of valve is unsuitable for throttling liquid flows, unless the backpressure is sufficiently high to prevent cavitation. There may also be problems with erosion at moderate pressure differentials due to high velocities along the valve and pipe walls. The advantages of some of the valves shown in Fig. 5.78 are their low losses in the fully open position, their low torque characteristics and their low cost.

Valves with a ratio of maximum static pressure difference to total pressure loss close to unity are shown in Fig. 5.79. Flow through these valves is subject to one or more abrupt change in direction and flow out of constrictions is allowed to expand into a large volume, thereby preventing conversion of velocity pressure to static pressure. When large pressure drops are required multi-stages can be used to reduce maximum velocities, and noise and cavitation.

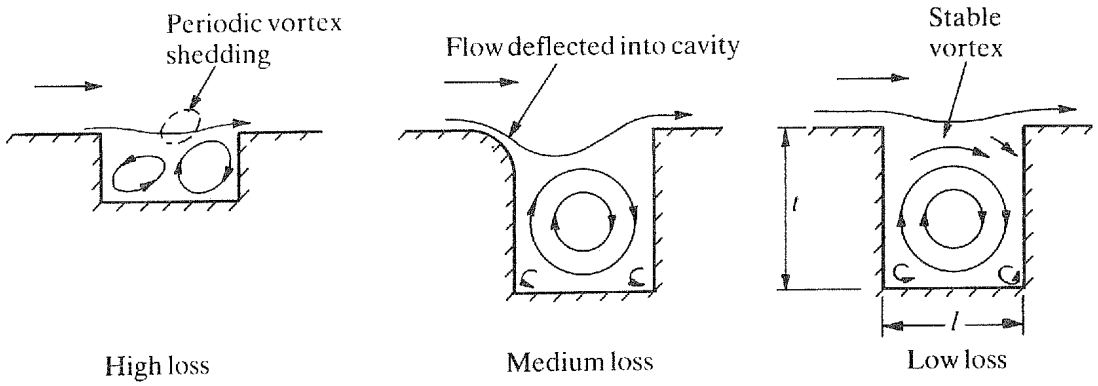

Fig. 5.76. Flow in cavities

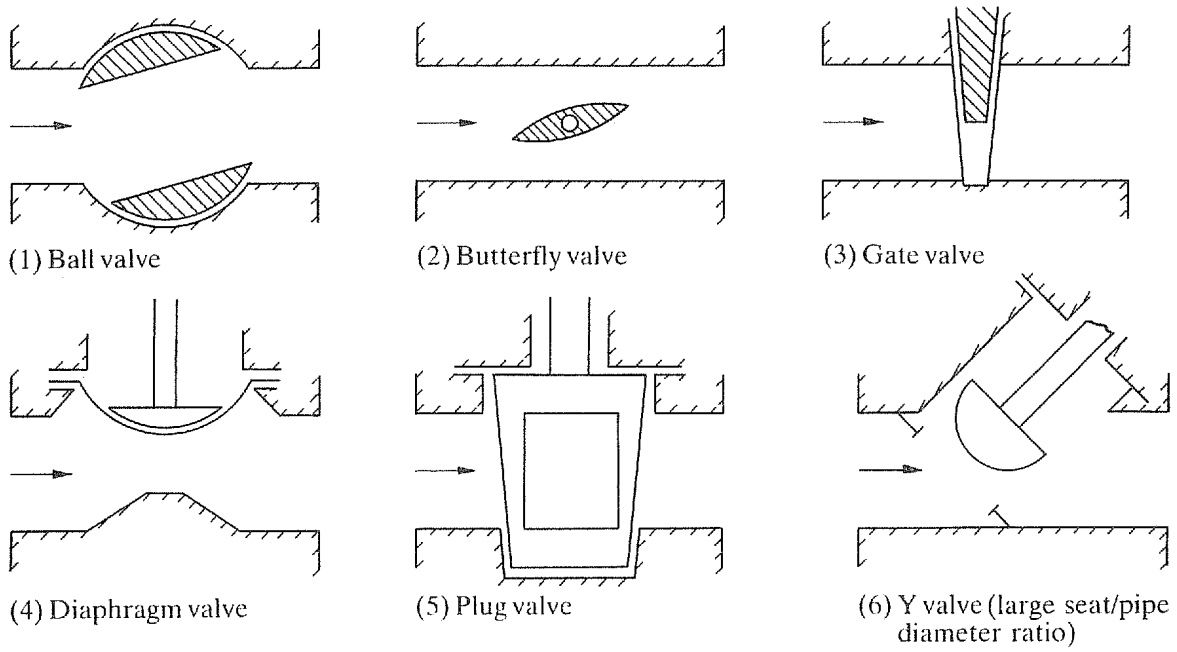

Fig. 5.77. Through flow valves

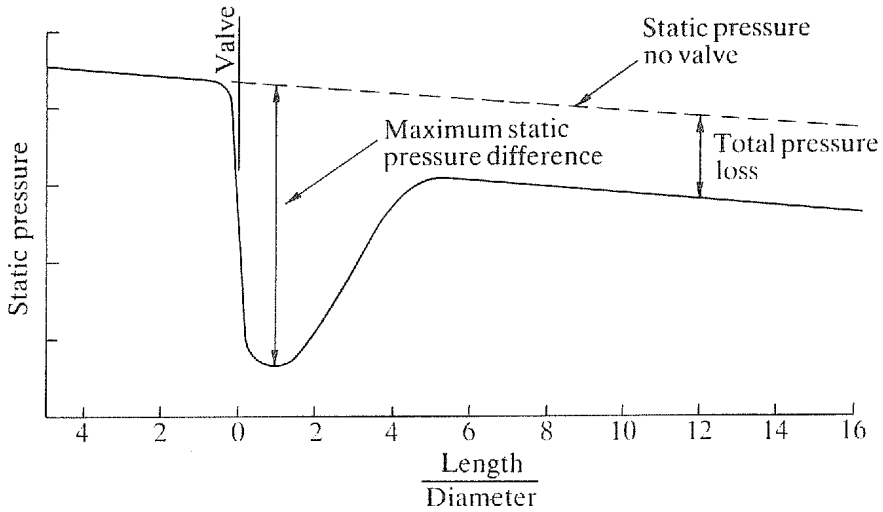

Fig. 5.78. Through flow valve pressure distribution

5.9. LAMINAR FLOW

Laminar flow is associated with very viscous fluids or with low velocities and small dimensions. In pipes, away from disturbances, the flow will be laminar if the Reynolds number is less than 2000. Only viscous forces are important at low Reynolds numbers, making shear and,

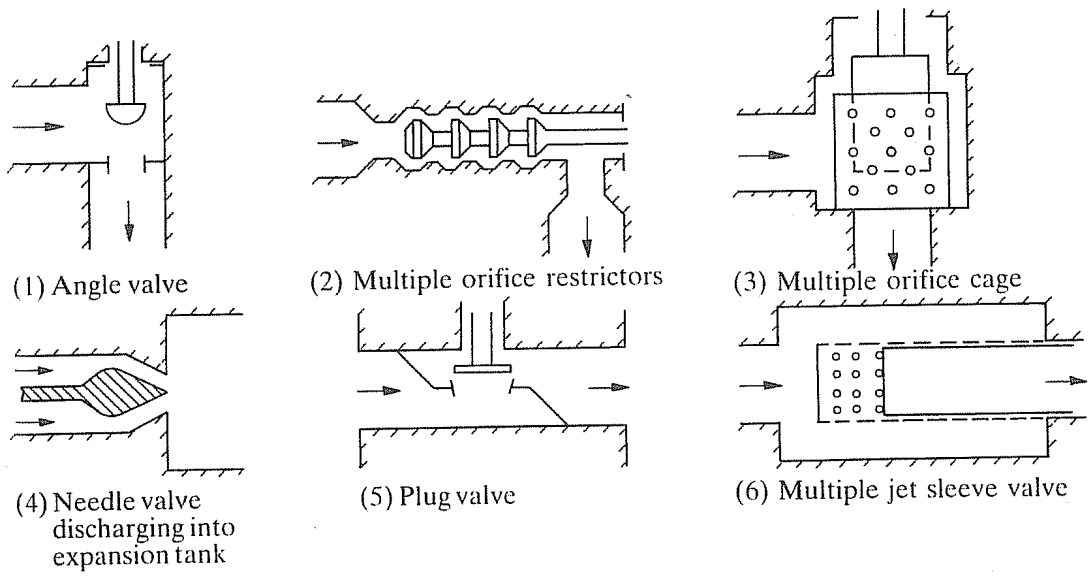

Fig. 5.79. Valves with little downstream static pressure recovery

hence, energy dissipation directly proportional to the velocity. Using the pressure loss equation

$$\Delta P = K\rho U^2/2$$

the loss coefficient K for a particular component is inversely proportional to the Reynolds number. Therefore

$$K = \frac{\text{Constant}}{\text{Reynolds number}}$$

Within components abrupt changes in area and direction induce turbulence at Reynolds numbers much less than 2000. Once turbulence is induced, the loss coefficient of a component is no longer inversely proportional to the Reynolds number.

Flow patterns can also vary and affect loss coefficients in the purely laminar region. Up to Reynolds numbers of about 10, based on the maximum velocity within a component, "creeping" flow without separation is possible at abrupt changes in area. At slightly higher Reynolds numbers inertia forces become important, causing laminar separation followed by laminar re-attachment. A further increase in the Reynolds number results in the separated flow becoming turbulent.

Referring to Fig. 5.80, developed laminar flow is characterised by a kinetic energy coefficient and a peak to mean velocity ratio of 2, compared with a developed turbulent profile, which has a kinetic energy coefficient of just over unity and a peak/mean velocity ratio of about 1.2. If, due to turbulence within a component, an initially laminar flow leaves a component with a nearly uniform velocity, energy has to be taken from the mean flow in order to re-establish developed laminar flow. Following a smooth contraction, the extra pressure drop, above the friction drop calculated using developed flow friction coefficients, is 1.3 times the

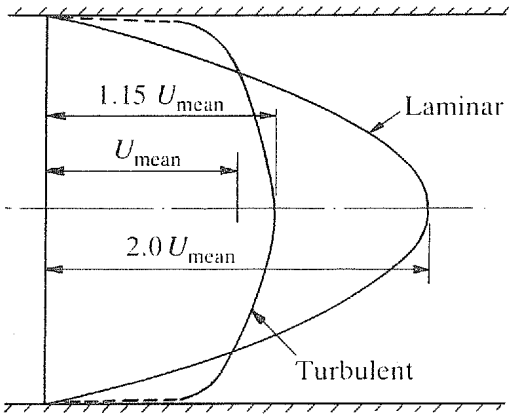

Fig. 5.80. Laminar and turbulent velocity profiles

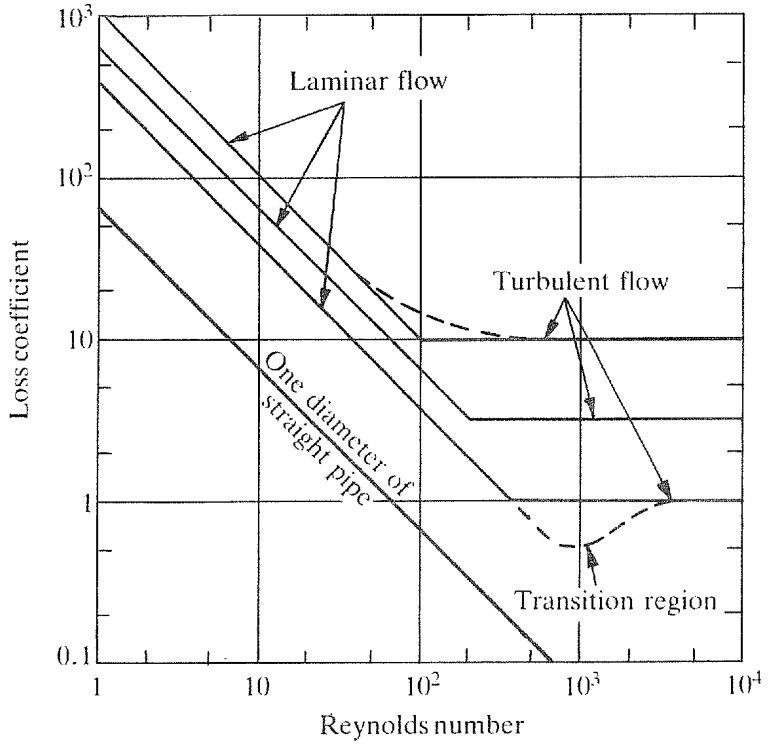

Fig. 5.81. Trends in loss coefficients in the laminar to turbulent transition region

mean velocity pressure. Velocity reduction in laminar flow is accompanied by a greater energy dissipation than the theoretically recoverable velocity pressure, so diffusers as pressure recovery devices have no place when flows are laminar.

The general shape of loss coefficient–Reynolds number curves, in the laminar to turbulent transition region, is shown in Fig. 5.81.

From the foregoing comments it is evident that the laminar to turbulent transition region is the most complex flow region of internal flow. An example of how complex flows become is provided by flow through 90° bends. Above Reynolds numbers of 100, inertia forces become important. Centrifugal and static pressure forces acting on the highly peaked laminar velocity profile at inlet to a bend deflect the core region outwards. Secondary flows are set up in a similar manner to those with turbulent flow (see Section 5.4.2), but with laminar flow they are stronger and stable. The interaction between the secondary flows and the core region, and the effects of flow stability on curvature, tend to delay the onset of turbulence to well above Reynolds numbers at which straight pipe flow would become turbulent. At the same time as the onset of turbulence is being suppressed, the secondary flows grow in strength, increasing viscous energy dissipation within the bend and in the outlet pipe.

PART 2

FRICTION AND LOSS COEFFICIENTS DATA

CLASSIFICATION OF LOSS COEFFICIENTS IN PART 2

Sufficient experimental data are available on particular system components to classify the adequacy or otherwise of the data for design. Where appropriate, data or a suggested design approach have been put into one of three classes. In broad terms, class 1 are definitive loss coefficients; class 2 loss coefficients are adequate for normal design purposes; class 3 are suggested values for situations where experimental data are not available or the data are of doubtful origin.

Class 1. Loss coefficients in this class are based on experimental data usually from two or more sources or from research programmes which have been cross-checked against other work. The loss coefficients are considered definitive. In practice, because of the severe restraints imposed on inlet and outlet conditions and geometrical accuracy, the loss coefficients in class 1 are usually not directly applicable. Correcting the coefficients to apply to situations different from those under which they were established puts them into class 2 or 3.

Class 2. Loss coefficients in class 2 are the following.

1. Experimentally derived loss coefficients from isolated research programmes where no detailed cross-checking is possible against other sources.
2. Estimated loss coefficients from two or more research programmes whose results do not agree with what could be expected to be the experimental accuracy.
3. Loss coefficients from class 1 converted to apply outside the strict limitations imposed for class 1 coefficients and about which experimental information is available to predict the effects of departing from class 1 conditions.

Class 3. Loss coefficients in class 3 are the following.

1. Experimentally derived values from less reliable sources.
2. Loss coefficients from classes 1 and 2 converted to apply outside their range of application and about which there is little or no information to predict the effects of departing from the conditions under which they were derived.

REVISIONS FROM THE FIRST EDITION

The major revisions from the first edition are listed in Appendix 1. Some loss coefficients have changed significantly from the first edition. As far as practical, figure numbers are as in the first edition. Figures followed by † have loss coefficients differing substantially from the first edition. Figure numbers with a suffix number (marked (1), (2) etc). are new figures.

8. FRICTION IN PIPES AND PASSAGES

8.1. INTRODUCTION

In this chapter the procedures for determining friction losses in straight pipes and passages are outlined. Except for Section 8.5 on laminar flow, Reynolds numbers are assumed to be greater than 5×10^3, which normally guarantees turbulent flow in engineering systems. If the Reynolds number is less than 2×10^3 the flow will be laminar and, if disturbed, will return to the laminar condition. Between Reynolds numbers of 2×10^3 and 5×10^3 is an area of uncertainty. If the Reynolds number exceeds 2.5×10^3 and the flow at inlet to the pipe is disturbed by a sharp-edged inlet, partially open valve or other high loss component, then the turbulence generated is likely to persist.

Due to the development of the velocity profile in the initial section of a pipe or passage, higher losses occur than with developed flow. Losses in the initial section of a pipe, above developed flow friction losses, are accounted for in the losses attributed to the upstream component.

The pressure loss in a length of pipe is given by

$$\Delta H = f \frac{L}{D} \frac{U^2}{2g} \quad \text{(m of fluid)} \tag{8.1a}$$

$$\Delta P = f \frac{L}{D} \rho \frac{U^2}{2} \quad (\text{N/m}^2) \tag{8.1b}$$

where f is the friction coefficient, L is the pipe or passage length (m), D is the pipe diameter or the hydraulic diameter (m), given by

$$D = \frac{4 \times \text{Cross-sectional area}}{\text{Wetted perimeter}} \tag{8.2}$$

and U is the mean velocity.

In calculating system losses it is desirable to treat pipes in the same manner as components and to use a pipe loss coefficient given by

$$K_f = f L/D \tag{8.3}$$

Friction coefficients depend on the Reynolds number, on the relative roughness and on the cross-sectional shape. Friction coefficients for circular cross-sections are presented in terms of the Reynolds number, Re, and relative roughness, k/D. Friction coefficients for non-circular cross-sections are obtained by applying a correction factor to the circular cross-section values.

Warning: Two definitions for friction coefficients are in widespread use which differ by a

factor of 4. The definition adopted here is the most appropriate for use in a consistent method for calculating system head losses.

8.1.1. ROUGHNESS VALUES

The main difficulty in calculating friction losses is the uncertainty in selecting a value for the pipe roughness. Suggested roughness values are given in Table 8.1. An allowance must be added to new pipe values to account for deterioration in service brought about by surface deposits, erosion, corrosion, bacterial slimes and growths, and marine- and fresh-water fouling.

Table 8.1. Roughness values, k (mm)

1. Smooth pipes*		
	Drawn brass, copper, aluminium, etc.	0.0025
	Glass, plastic, Perspex, fibreglass, etc.	0.0025
2. Steel pipes		
	New smooth pipes	0.025
	Centrifugally applied enamels	0.025
	Mortar lined, good finish	0.05
	Mortar lined, average finish	0.10
	Light rust	0.25
	Heavy brush asphalts, enamels and tars	0.5
	Heavy rust	1.0
	Water mains with general tuberculations	1.2
3. Concrete pipes		
	New, unusually smooth concrete with smooth joints	0.025
	Steel forms, first class workmanship with smooth joints	0.025
	New, or fairly new, smooth concrete and joints	0.1
	Steel forms, average workmanship, smooth joints	0.1
	Wood floated or brushed surface in good condition with good joints	0.25
	Eroded by sharp material in transit, marks visible from wooden forms	0.5
	Precast pipes, good surface finish, average joints	0.25
	Segmentally lined conduits in good ground conditions with expanded wedge block linings	1.0
	Segmentally lined conduits in other conditions	2.0
4. Other pipes		
	Sheet metal ducts with smooth joints	0.0025
	Galvanised metals, normal finish	0.15
	Galvanised metals, smooth finish	0.025
	Cast iron, uncoated and coated	0.15
	Asbestos cement	0.025
	Flexible straight rubber pipe with a smooth bore	0.025
	Mature foul sewers	3.0

*Extruded, cast and pipes formed on mandrels may have imperfections that can increase the roughness by a factor of 10.

Experience of similar systems is the best guide to selecting roughness values and deterioration allowances. Pipes conveying water pose particular problems because of wide variation of pH, dissolved gases and chemical content. If the water is not aggressive, scale forming, treated or chlorinated a roughness value of 1 mm is appropriate after several years of service, otherwise a roughness of 2 mm is suggested. For chlorinated, untreated, clear, filtered water, that is not scale-forming or aggressive, a roughness value of 0.5 mm is suggested after several years of service.

Precautions against deterioration in service are the following.

1. Good initial surface finish to minimise areas of low velocity where deposits can begin to form in the wakes caused by roughness.
2. Adequate initial protection to prevent corrosion and erosion.
3. Chlorination of water to prevent slimes and the growth of both fresh- and salt-water mussels and other fouling. Continuous water velocities in excess of 2 m/s are usually required in order that the wall shear stress is sufficiently high to discourage settlement and to hinder the feeding of barnacles and other marine organisms.
4. When corrosion is a severe problem in pipes carrying untreated water it may be necessary to deoxygenate the water. Similarly, if hydrogen sulphide is present it may be necessary to remove it.

8.1.2. ACCURACY OF FRICTION CALCULATIONS

Friction calculations involve an element of judgement in selecting roughness values. At high Reynolds numbers an error of 100 per cent in a roughness value causes about a 10 per cent error in the friction coefficient. Since head losses vary inversely with at least the fourth power of the diameter, actual not nominal pipe diameters must be used.

For new pipes with estimated friction coefficients less than 1.2 times the smooth pipe friction coefficient, in which there is no fouling or deterioration of the walls, the head loss can be predicted with an accuracy of 5 per cent, provided the pipe diameter is known to within 0.5 per cent. Friction coefficients for similar pipes, but with estimated friction coefficients less than 1.5 times the smooth pipe values, can be predicted with an accuracy of about 10 per cent.

Typical allowances, where deterioration in service is expected, are 25–50 per cent of new pipe values, but much higher allowances may be necessary where growths, deposits or slimes are expected.

8.2. PIPES OF CIRCULAR CROSS-SECTION (CLASS 1 SUBJECT TO THE RESTRICTIONS OF SECTION 8.1.2)

The accepted presentation of friction coefficients is the Moody chart (Fig. 8.1), which is a plot of the Colebrook–White equation. The Colebrook–White equation requires an iterative solution and is not recommended for computer or calculator calculations. An equation of similar accuracy to the Colebrook–White equation which allows the friction coefficient to be obtained directly is

$$f = 0.25 \Big/ \left[\log\left(\frac{k}{3.7D} + \frac{5.74}{\mathrm{Re}^{0.9}} \right) \right]^2 \qquad (8.4)$$

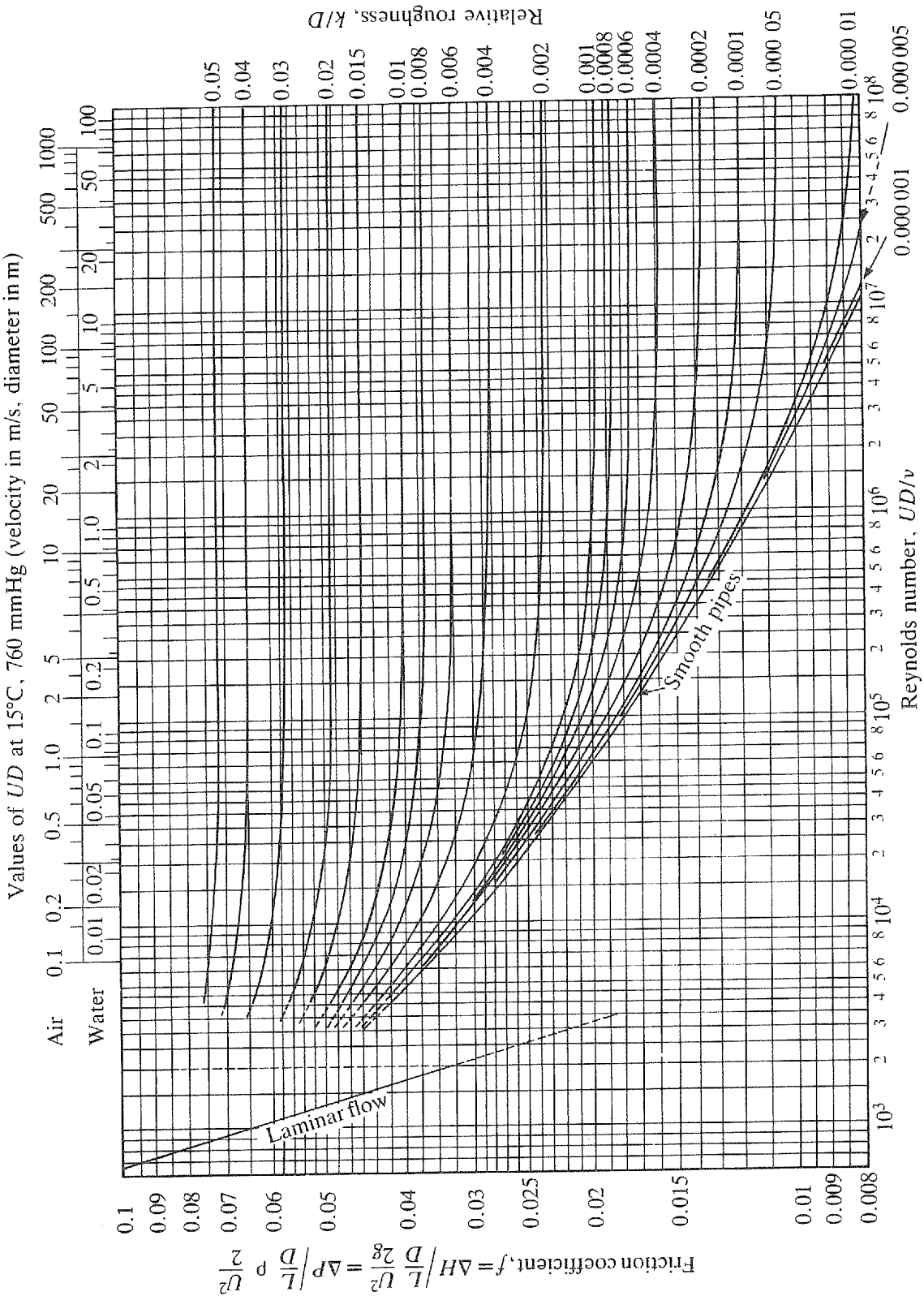

Fig. 8.1. Moody chart — friction coefficient/Reynolds number

8.3. NON-CIRCULAR CROSS-SECTIONS

8.3.1. RECTANGULAR CROSS-SECTIONS

Using the hydraulic diameter in equations (8.1) and (8.3) allows friction coefficients from Fig. 8.1 and equation (8.4) to be used for rectangular passages of aspect ratio less than 10 (class 1 subject to the restrictions of Section 8.1.2). At higher aspect ratios there are indications that the hydraulic diameter concept may result in underestimation of friction losses. For aspect ratios greater than 10 the hydraulic diameter used in the Reynolds number equation should correspond to a passage of aspect ratio 10 (from equation (8.3) the hydraulic diameter for a passage of aspect ratio 10 is 1.82 times the passage height), but the true hydraulic diameter should be used in calculating the head loss (class 2).

8.3.2. CONCENTRIC ANNULI (CLASS 2)

Using the hydraulic diameter concept, friction coefficients for concentric annuli lie within a factor of about 1.05 of those given by equation (8.4) and Fig. 8.1, so

$$f_{\text{annular}} = 1.05 f_{\text{circular}} \tag{8.5}$$

The hydraulic diameter is given by $(d_2 - d_1)$, where d_1 and d_2 are the inner and outer annulus diameters, respectively.

8.3.3. ECCENTRIC ANNULI (CLASS 2)

Correction factors to apply to equation (8.5) to account for eccentricity are given in Fig. 8.2.

8.3.4. PASSAGES OF OTHER CROSS-SECTIONAL SHAPES (CLASS 3)

Replacing U in equation (8.1a) by Q/A and D by $4A/P_r$, where Q is the total flow, A is the cross-sectional area and P_r is the perimeter, gives

$$\Delta H = \frac{f L Q^2}{8g} \frac{P_r}{A^3} \tag{8.6}$$

Within passages having shapes that depart significantly from circular or rectangular, it is possible to fit another cross-sectional shape with a ratio of P_r/A^3 smaller than for the full cross-section. In the areas not encompassed by the minimum P_r/A^3 shape there is little flow, and these areas can be neglected in calculating head losses. Example 4 of Section 8.6 demonstrates the method of calculation.

8.3.5. CORRUGATED PIPE (CLASS 3)

Friction coefficients for corrugated pipe depend on the corrugation shape, the ratio of

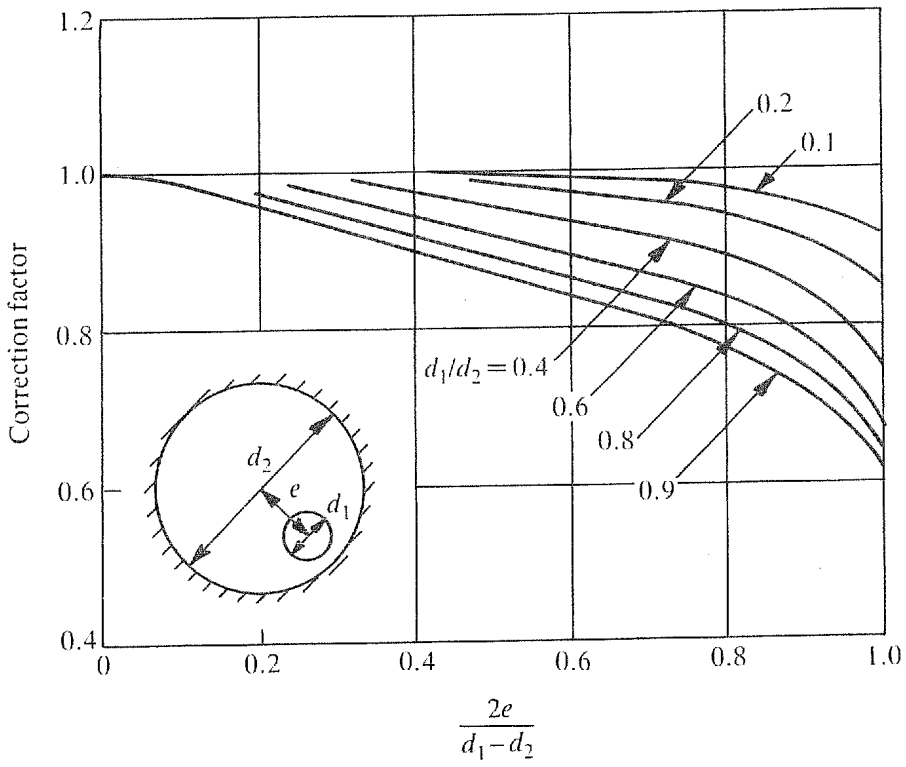

Fig. 8.2. Eccentric annuli

corrugation depth/pipe diameter, the ratio of axial pitch of the corrugations/corrugation depth, the helix angle and the Reynolds number of the flow. For a given corrugation depth/pipe diameter ratio, friction coefficient values are a maximum for axial pitch/depth ratios, t/e, between 5 and 12. The variation in friction coefficients with Reynolds number is usually complex, with no evidence of friction coefficients being independent of Reynolds number above 10^6 as occurs with random pipe wall roughness.

Suggested friction coefficients, for the range of t/e ratios normally encountered with corrugated steel-lined conduits and plastic drainage pipes, can be found from Fig. 8.3(1). The curve for $t/e = 2$ is appropriate for corrugated plastic pipe, and the $t/e = 3$ and 5 curves for steel pipe. Experimental measurements indicate lower friction coefficients for helical corrugated pipe than for standard pipe, but there is insufficient information to quantify the reduction.

8.3.6. UNLINED ROCK TUNNELS (CLASS 3)

In situations where rock of good quality, without excessive jointing or fractures, exists, the economic tunnel construction for flood flow diversion and power generation can be an unlined or an invert lined rock tunnel. Many factors affect the roughness of tunnels driven through hard rock by conventional drill, blast and muck techniques. For this reason the friction

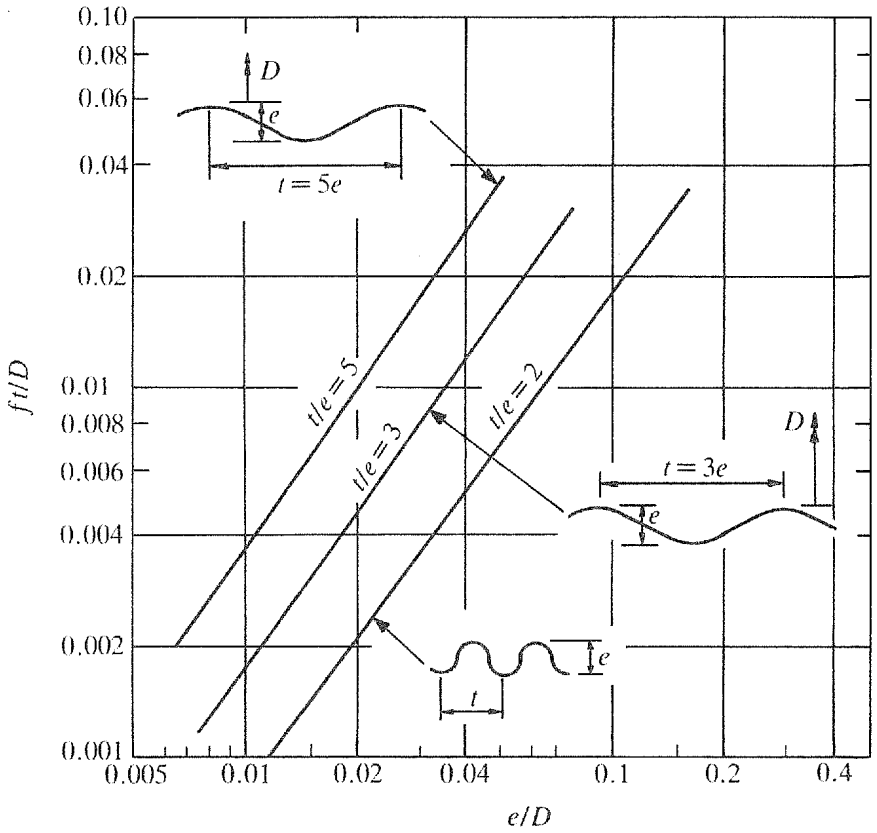

Fig. 8.3(1). Friction coefficients for corrugated pipe

coefficient prediction method given here should be confined to initial estimates. Detailed prediction should be carried out using data from tunnels in similar rock conditions, and once construction is under way, estimates of friction losses should again be made based on the measured tunnel geometry.

Estimation of friction coefficient for unlined and invert lined tunnels

1. Based on an assumed or measured cross-sectional area, calculate the hydraulic diameter, D:

$$D = 4A/P$$

   where A is the average area with a deduction for any area occupied by spoil in the invert, and P is the perimeter associated with the average area, taking into account any spoil left in the invert.
2. From Fig. 8.4(1) obtain an estimate for the normal overbreak, t_n.
3. Calculate the relative roughness t_n/D and find the friction coefficient from Fig. 8.5(1). If the invert is filled with muck that will not be displaced, and levelled, use the lined invert friction coefficient plus one-half of the difference between the lined and unlined friction coefficient.

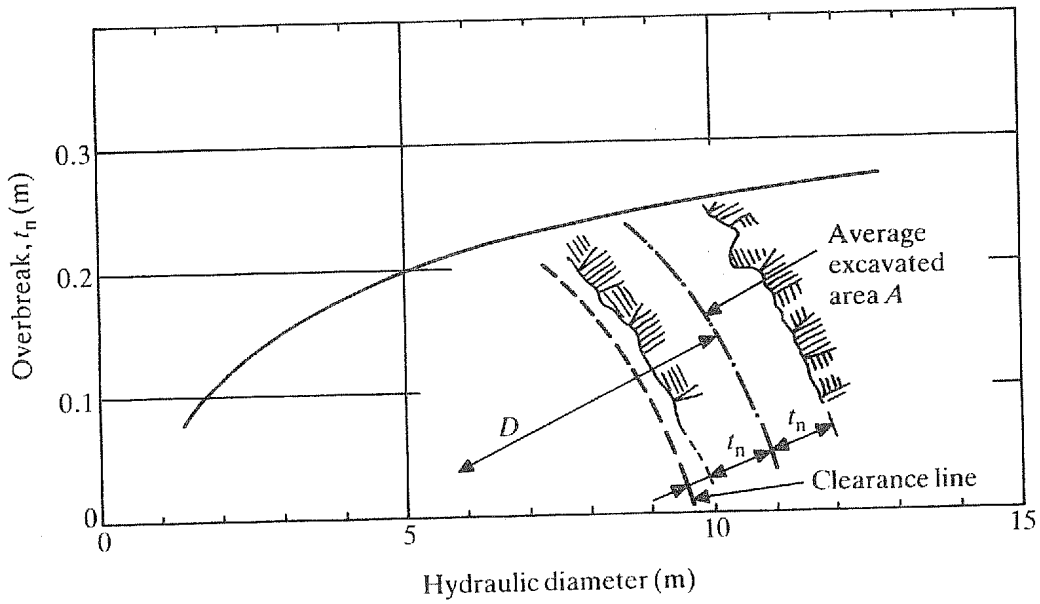

Fig. 8.4(1). Overbreak, t_n, for rock tunnels

8.4. CALCULATION OF HEAD, FLOW OR PIPE SIZE

When the pipe size, flow rate and roughness are known, the Reynolds number and the roughness ratio can be calculated and a friction coefficient found from equation (8.4) or Fig. 8.1, Example 1 of Section 8.6. A direct solution for flow rate or pipe diameter is possible if only pipe friction is involved, but the calculations are much more involved and prone to error than a simple trial and successive approximation approach. The head losses in pipes and components vary approximately with the square of the flow rate and inversely as the fourth to fifth power of the diameter. Small changes in flow or pipe size have, therefore, a large effect on head losses, leading to rapid convergence in a trial and a successive approximation solution; Examples 2 and 3 of Section 8.6 demonstrate the procedure. Estimates of the head loss, or flow or pipe size obtained from pipe manufacturers' catalogues and from direct solution charts should always be checked by solving equations (8.1).

Example calculations are given in Examples 1–4 of Section 8.6.

8.5. LAMINAR FLOW

Developed laminar flow loss coefficients can be expressed as

$$f = C_f/\mathrm{Re} \tag{8.7}$$

where C_f is 64 for circular cross-sections, 56 for square cross-sections and 96 for an infinitely wide two-dimensional passage. C_f values for a number of cross-sectional shapes are given in Figs 8.6–8.8.

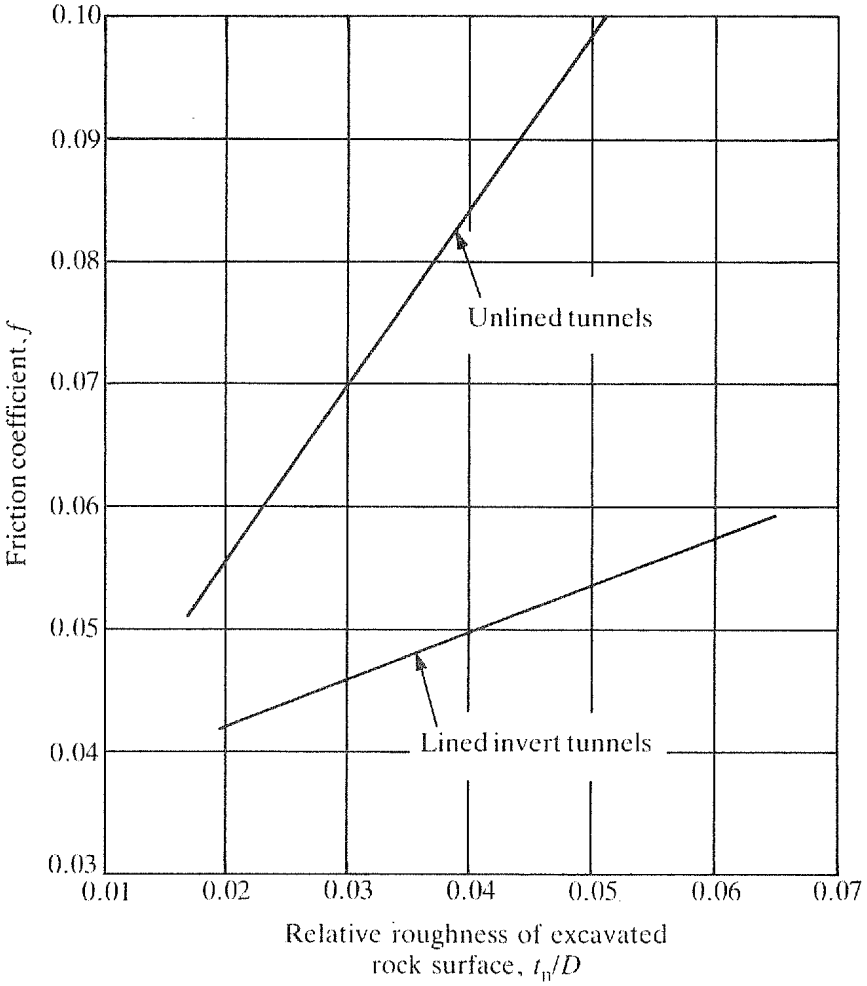

Fig. 8.5(1). Friction coefficients for rock tunnels

8.6. EXAMPLES

EXAMPLE 1: GIVEN Q, L, D, v AND k, FIND THE HEAD LOSS

Calculate the head loss for air flowing in a 0.2 m square cross-section passage 25 m long, given:

$Q = 0.8\ \text{m}^3/\text{s}$ Air density $= 1.23\ \text{kg/m}^3$

Kinematic viscosity $= 1.45 \times 10^{-5}\ \text{m}^2/\text{s}$ Surface roughness, $k = 0.025$ mm

From equation (8.2)

$$D = 4A/P_r = 4 \times 0.2^2/4 \times 0.2 = 0.2\ \text{m}$$

Relative roughness

$$k/D = 0.025 \times 10^{-3}/0.2 = 1.2 \times 10^{-4}$$

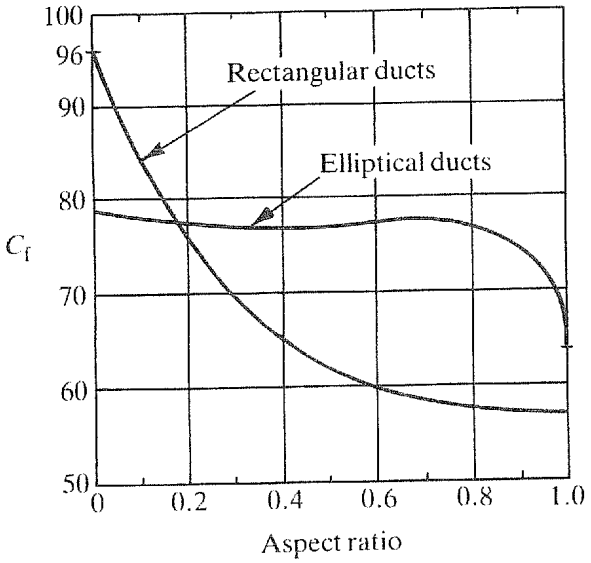

Fig. 8.6. Laminar flow coefficients — rectangular and elliptical cross-sections

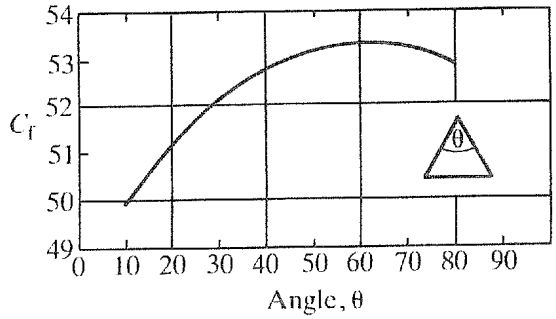

Fig. 8.7. Laminar flow coefficients — isosceles triangle

Mean velocity

$$U = Q/A = 0.8/0.2 \times 0.2 = 20 \text{ m/s}$$

Reynolds number

$$\text{Re} = DU/\nu = 0.2 \times 20/1.45 \times 10^{-5} = 2.8 \times 10^5$$

From equation (8.6)

$$f = 0.25 \Big/ \left[\log\left(\frac{k}{3.7D} + \frac{5.74}{\text{Re}^{0.9}} \right) \right]^2 = 0.25 \Big/ \left[\log\left(\frac{1.2 \times 10^{-4}}{3.7} + \frac{5.74}{(2.8 \times 10^5)^{0.9}} \right) \right]^2 = 0.0158$$

For a Reynolds number of 2.8×10^5 and a relative roughness of 1.2×10^{-4} the friction coefficient from Fig. 8.1 is also 0.0158.

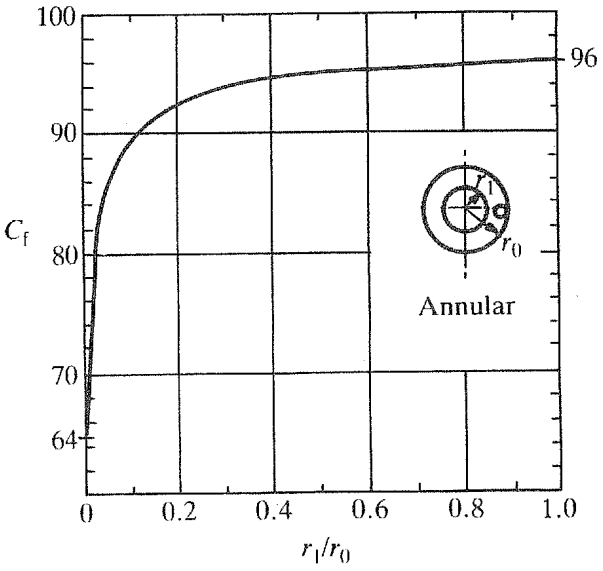

Fig. 8.8. Laminar flow coefficients — annular cross-sections

From equation (8.3)

$$K_f = fL/D = 0.0158 \times 25/0.2 = 1.975$$

Head loss

$$\Delta H = K_f U^2/2g = 1.975 \times 20^2/(2 \times 9.81)$$
$$= 40.3 \text{ m of air} = 49.6 \text{ mm of water}$$

EXAMPLE 2: GIVEN ΔH, L, D, ν AND k, FIND THE FLOW RATE Q

Water at 15°C flows by gravity between two tanks in a system consisting of 50 mm diameter pipes and components. The combined loss coefficient for the components is $K_t = 6.5$ for Reynolds numbers greater than 10^5. If the total length of the straight pipes is 40 m, determine the flow for a head differential between the tanks of 6 m. Assume that the pipe is smooth. Kinematic viscosity = 1.14×10^{-6} m^2/s.

First trial

Assume $f = 0.015$, which lies in the middle of the smooth curve in Fig. 8.1.
Pipe loss coefficient

$$K_f = fL/D = 0.015 \times 40/50 \times 10^{-3} = 12$$

Head loss

$$\Delta H = 6 \text{ m} = (K_f + K_t)U^2/2g$$

Mean velocity

$$U = \sqrt{\frac{6 \times 2 \times 9.81}{(12 + 6.5)}} = 2.52 \text{ m/s}$$

Reynolds number

$$\text{Re} = \frac{UD}{\nu} = \frac{2.52 \times 50 \times 10^{-3}}{1.14 \times 10^{-6}} = 0.111 \times 10^6$$

From Fig. 8.1

$$f = 0.0178$$

Second trial

Assume $f = 0.0178$

$$K_f = 12 \times 0.0178/0.015 = 14.2$$

$$U = 2.52\sqrt{\frac{12 + 6.5}{14.2 + 6.5}} = 2.38 \text{ m/s}$$

$$\text{Re} = 0.111 \times 10^6 \times 2.38/2.52 = 0.105 \times 10^6$$

from Fig. 8.1, $f = 0.0179$, which agrees with the assumed value to within the accuracy of Fig. 8.1.

Flow

$$Q = UA = 2.38 \times 0.785 \times 50^2 \times 10^{-6}$$
$$= 4.68 \times 10^{-3} \text{ m}^3/\text{s}$$

EXAMPLE 3: GIVEN ΔH, Q, L, ν AND k, FIND THE DIAMETER

0.58 m^3 of water at 15°C has to flow through a constant diameter system with a head loss of not more than 3 m of water-gauge. The system consists of a number of sections of straight new steel pipe with a total length of 145 m, and a number of components. The estimated total loss coefficient for the components is $K_t = 2.9$ at Reynolds numbers greater than 10^6. Determine the minimum pipe and component diameter required. Kinetic viscosity $= 1.14 \times 10^{-6}$ m^2/s. From Table 8.1, hydraulic roughness, $k = 0.025$ mm.

First trial

Assume diameter $D = 0.6$ m.
Mean velocity

$$U = Q/A = 0.58/(0.785 \times 0.6^2) = 2.052 \text{ m/s}$$

Reynolds number

$$\mathrm{Re} = UD/v = 2.052 \times 0.6/(1.14 \times 10^{-6}) = 1.08 \times 10^{6}$$

Relative roughness

$$k/D = 0.025/600 = 0.000\,042$$

From Fig. 8.1, the friction coefficient $f = 0.0123$.
Pipe loss coefficient

$$K_f = fL/D = 0.0123 \times 145/0.6 = 2.973$$

Head loss

$$\Delta H = (K_t + K_f)U^2/2g$$

$$= \frac{(2.973 + 2.9)}{2 \times 9.81} \times 2.052^2$$

$$= 1.260 \text{ m of water gauge}$$

SECOND TRIAL

Assume diameter $D = 0.5$ m.
Mean velocity

$$U = 2.052 \times (0.6/0.5)^2 = 2.955 \text{ m/s}$$

Reynolds number

$$\mathrm{Re} = 1.08 \times 10^{6} \times 0.6/0.5 = 1.3 \times 10^{6}$$

Relative roughness

$$k/D = 0.000\,05$$

From Fig. 8.1, the friction coefficient $f = 0.0123$.
Pipe loss coefficient

$$K_f = fL/D = 0.0123 \times 145/0.5 = 3.567$$

Head loss

$$\Delta H = 6.467 \times 2.955^2/2 \times 9.81 = 2.878 \text{ m of water gauge}$$

The minimum pipe and component size is 0.5 m.

EXAMPLE 4

Determine the approximate head loss per metre for a flow of 10^{-3} m^3/s of water in the triangular cross-section shown in Fig. 8.9. Assume that the walls are smooth and the water temperature is 15°C with a kinetic viscosity of 1.14×10^{-6} m^2/s.

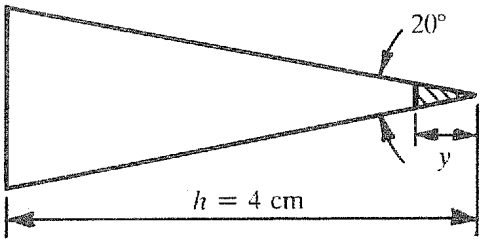

Fig. 8.9. Cross-section for Example 4

Cross-sections similar to that shown in Fig. 8.9 have a long perimeter for their area compared with a circular cross-section, and have very non-uniform velocities around the perimeter. Parts of the passage with a long perimeter surrounding a small part of the cross-section, such as the shaded area, are filled with slowly moving fluid and can be neglected in calculating the head loss.

Equation (8.6) shows that if within the cross-section a shape can be drawn that has a smaller geometrical ratio P_r/A^3 it will have a lower friction loss. By filling in the shaded area of Fig. 8.9 in steps of $y=0.05h$, and plotting the ratio of P_r/A^3 filled in to P_r/A^3 for the complete section against y, it is found that the ratio is a minimum at about $y=0.15h$.

Area

$$A=40\times 40\times \tan 10^\circ\times(1-0.15^2)=275.8\ \text{mm}^2$$

Perimeter

$$P_r=\left(\frac{40\times 2}{\cos 10^\circ}\times 0.85\right)+(40\times 2\times\tan 10^\circ\times 1.15)=85.27\ \text{mm}$$

Hydraulic diameter

$$D=4A/P_r=4\times(275.8/85.27)=12.94\ \text{mm}$$

Mean velocity

$$U=Q/A=10^{-3}/(275.8\times 10^{-6})=3.626\ \text{m/s}$$

Reynolds number

$$\text{Re}=UD/\nu=3.626\times 0.01294/(1.14\times 10^{-6})=4.12\times 10^4$$

From Fig. 8.1 or equation (8.4), the friction coefficient, $f=0.0218$.
Head loss per metre

$$\Delta H=f\frac{L}{D}\frac{U^2}{2g}$$

$$=0.0218\times\frac{1}{0.0129}\times\frac{3.626^2}{2\times 9.81}=1.13\ \text{m of water gauge}$$

Note: In practice the ratio P_r/A^3 would be a minimum if the corners were filled in using circular arcs, the minimum value of P_r/A^3 being found by calculation. However, for the present illustrative purposes the small error is not important.

NOTES AND REFERENCES ON CHAPTER 8

Equation (8.4) for calculating friction coefficients is due to:

1. Swamee, P. K. and Jain, A. K., Explicit equations for pipe-flow problems. *Proc. ASCE, J. Hydraul. Div.*, **102** (HY5), 657–664 (May 1976).

This equation is one of a number of explicit and exponential equations proposed for calculating friction coefficients instead of the implicit Colebrook–White equation. Although historically the Colebrook–White equation was the first equation to provide friction coefficients that are reasonable approximations to experimental sand roughness and commercial pipe data, it is extremely unfortunate that it was not shortly followed by the adoption of an explicit formula. The continued use of Colebrook–White equation by the fluid mechanics community has undoubtably resulted in a number of easier to use, but dimensionally incorrect, equations, remaining in widespread engineering use. The challenge provided by the implicit form of the Colebrook–White equation has involved much academic ingenuity in devising methods of direct solution for pipe size or flow rate. It is to be hoped that the fluid mechanics community will standardise on equation (8.4) or a similar equation, and halt the proliferation of explicit equations.

Much of the literature of flow in non-circular pipes is contained in:

2. Zanker, K. J. and Barratt, G. M., Data on the correlation of pressure losses in straight non-circular pipes flowing full. BHRA Report TN 909 (January 1968), 33 pp.

More recent work on rectangular passages can be found in:

3. Jones, O. C., An improvement in the calculation of turbulent friction in rectangular ducts. *Trans. ASME, J. Fluid Eng., Series I*, **98** (2), 173–181 (June 1976).

The eccentric annuli correction factors are based on:

4. Jonsson, V. L. and Sparrow, E. M., Experiments on turbulent-flow phenomena in eccentric annular ducts. *J. Fluid. Mech.*, **25** (1), 65–86 (May 1966).

The calculation method for passages with a large perimeter compared with a circular cross-section of equal area is taken from:

5. Miller, D. S., *Internal Flow: A Guide to Losses in Pipe and Ducts Systems*. Cranfield, Bedford: BHRA (1971), 329 pp.

Experimental data and recommendations on the calculation of head losses in segmentally lined tunnels is given in:

6. Pitt, J. D. and Ackers, P., Hyrdaulic roughness of segmentally lined tunnels. CIRIA Report 96.

Information on a range of rock tunnels and design recommendations is given in:

7. Wright, D. E., The hydraulic design of unlined and lined-invert rock tunnels. CIRIA Report 29 (March 1971).
8. Brett, M. T., Head loss measurements of hydroelectric conduits. *ASME J. Hydraul. Div.*, **106** (HY1) (January 1980).

9. TURNING FLOW — BENDS

9.1. INTRODUCTION

The presentation of loss coefficient data is made using circular cross-section bends of constant area. Data for other cross-sections and bend geometries are referred back to circular cross-section bends where this is appropriate. It is recommended that the text of Section 9.2, and the example of Section 9.12 be worked through before using other sections.

Bend loss coefficients, K_b, vary markedly with Reynolds number and, usually to a lesser extent, with inlet and outlet pipe arrangements and with surface roughness.

Basic loss coefficients, K_b^*, are defined at a Reynolds number of 10^6 for bends with long and hydraulically smooth inlet and outlet pipes or passages. Correction factors are given to correct the loss coefficients to any other Reynolds number and outlet pipe or passage length. Allowance is made for roughness for multiplying the smooth pipe loss coefficient by the ratio of the rough to smooth friction coefficients as found from the data in Chapter 8. When the roughness correction exceeds 1.4 the validity of the correction is questionable, but so will be the accuracy to which the friction coefficient is known.

When a bend is located in close proximity to other components corrections for interaction effects are necessary. For bend–bend and bend–diffuser interactions, see Chapters 10 and 12, respectively.

Except for data on commercial bends in Section 9.10, the loss coefficients given are for accurately manufactured bends matched to their inlet and outlet pipes or passages.

9.2. CIRCULAR CROSS-SECTION BENDS OF CONSTANT AREA

Geometrical parameters for circular arc bends are shown in Fig. 9.1. The important bend parameters are the radius ratio, r/d, and the bend deflection angle, θ_b.

Head losses due to a bend are made up of losses within the bend and losses associated with flow redevelopment after the bend. The head loss equation is

$$\Delta H = K_b U^2/2g \tag{9.1}$$

where U is the mean inlet velocity.

9.2.1. BASIC COEFFICIENTS K_b^* (CLASS 1)

Basic loss coefficients at a Reynolds number of 10^6 are given in Fig. 9.2.

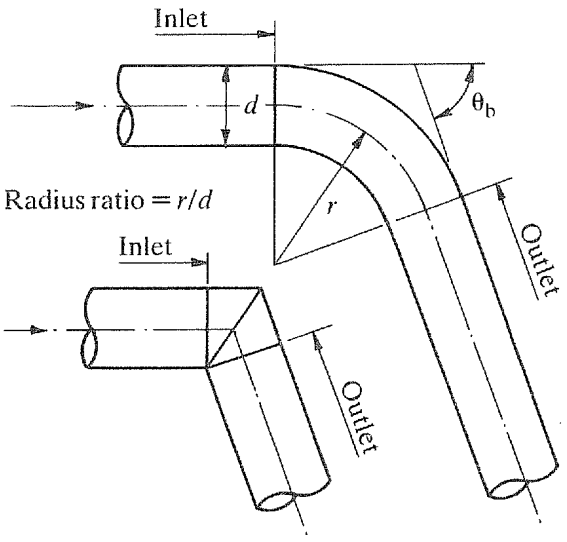

Fig. 9.1. Circular cross-section bend geometries

9.2.2. REYNOLDS NUMBER CORRECTION C_{Re} (CLASS 2 FOR $Re > 10^6$, CLASS 1 FOR $Re < 10^6$)

The Reynolds number correction C_{Re} to be applied to the basic coefficients K_b^* are given in Fig. 9.3. Only part of the loss due to bends of $r/d < 1$ is strongly dependent on the Reynolds number. For $r/d > 0.7$ or $K_b^* < 0.4$, use the correction factors for $r/d = 1$ bends (class 2), otherwise for $r/d < 1$ the correction factor is given by (class 3)

$$C_{Re} = \frac{K_b^*}{K_b^* - 0.2\,(C_{Re} \text{ from Fig. 9.3 for } r/d = 1) + 0.2} \tag{9.2}$$

9.2.3. OUTLET PIPE LENGTH CORRECTION C_o (CLASS 3)

Outlet pipe length correction factors to be used with the basic coefficients are given in Fig. 9.4. Using the basic coefficient K_b^* from Fig. 9.2 along with the outlet tangent length, obtain the outlet correction from Fig. 9.4. If $r/d > 3$ and/or $\theta_b > 100°$, outlet tangent correction factors are closer to unity.

Note: If the bend or pipe discharges to a large space there is a loss of one velocity head from the system, so the loss coefficient must be increased by 1.0.

Tabulated in Table 9.1 are loss coefficients for bends of 90° $r/d = 1$ and 2 and short outlet pipes. Values are given for thick and thin inlet boundary layers. Separation is responsible for the high coefficient of the $r/d = 2$ bend with no outlet pipe and a thin boundary layer. The same bend with a thick inlet boundary layer has strong secondary flows which prevent separation.

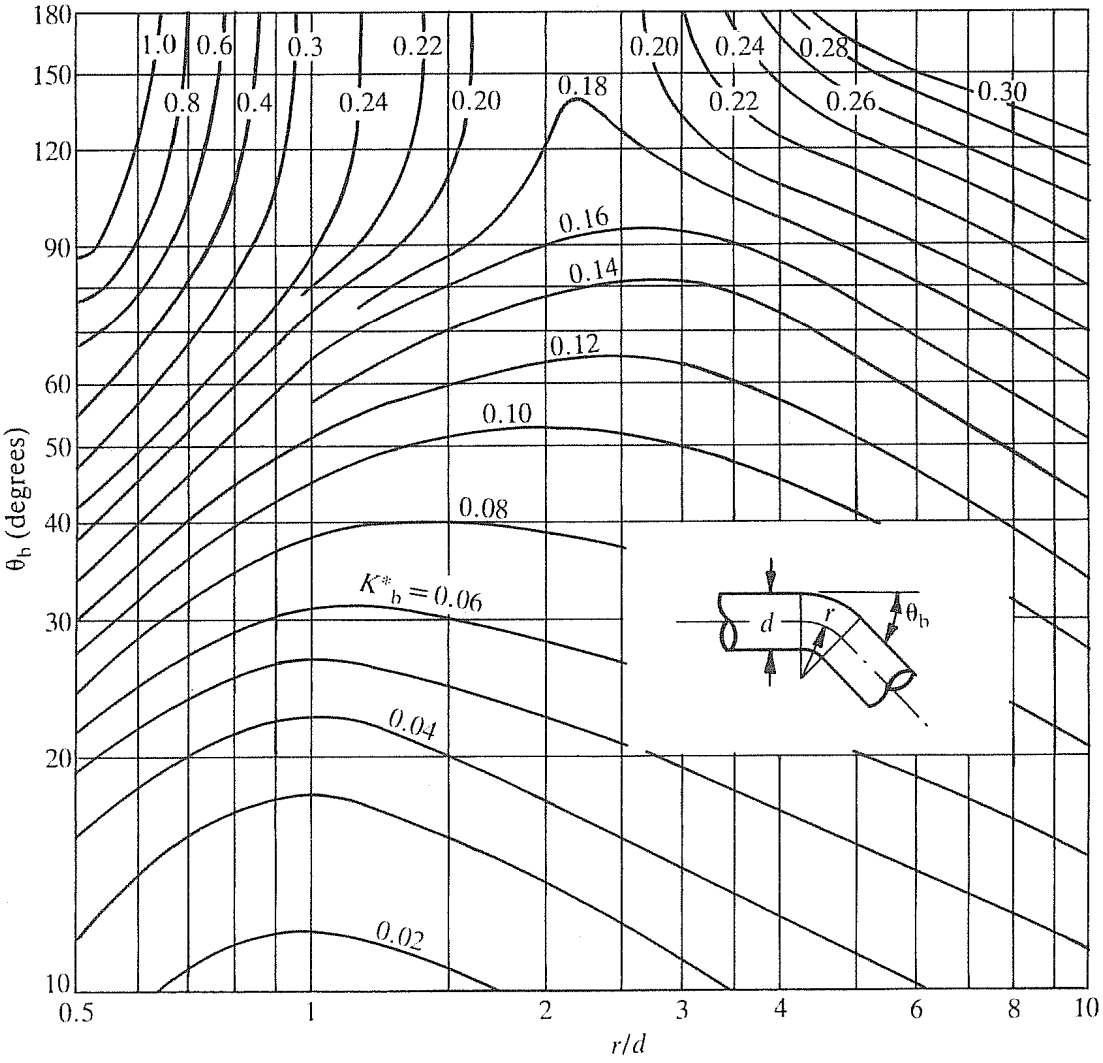

Fig. 9.2. Loss coefficients, K'_b, for circular cross-section bends (Re = 10^6)

9.2.4. ROUGHNESS CORRECTION C_f (CLASS 3)

The roughness correction factor, C_f, for bends of $r/d \geqslant 1$ and $Re \leqslant 10^6$ is given by

$$C_f = f_{rough}/f_{smooth} \tag{9.3}$$

where f_{smooth} is the friction coefficient for a hydraulically smooth pipe and f_{rough} is the friction coefficient found using the assumed pipe and bend roughness.

Friction coefficients are found from Chapter 8, using the bend inlet Reynolds number and the assumed roughness for the pipe and bend.

For $r/d \geqslant 1$ and $Re > 10^6$, use the value of C_f found from equation (9.3) for $Re = 10^6$.

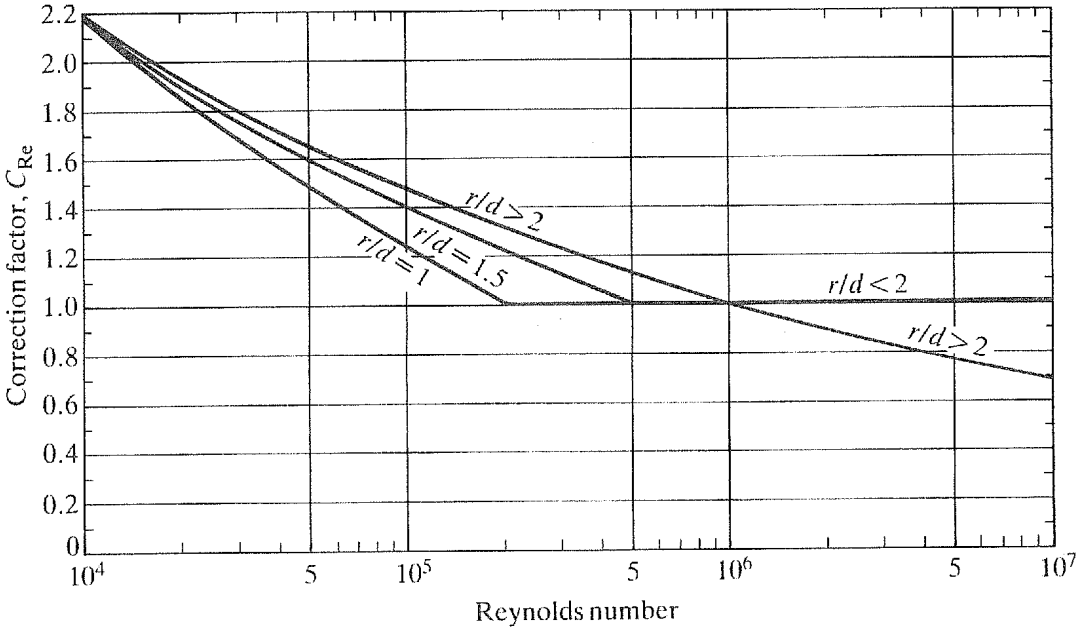

Fig. 9.3. Reynolds number correction factors

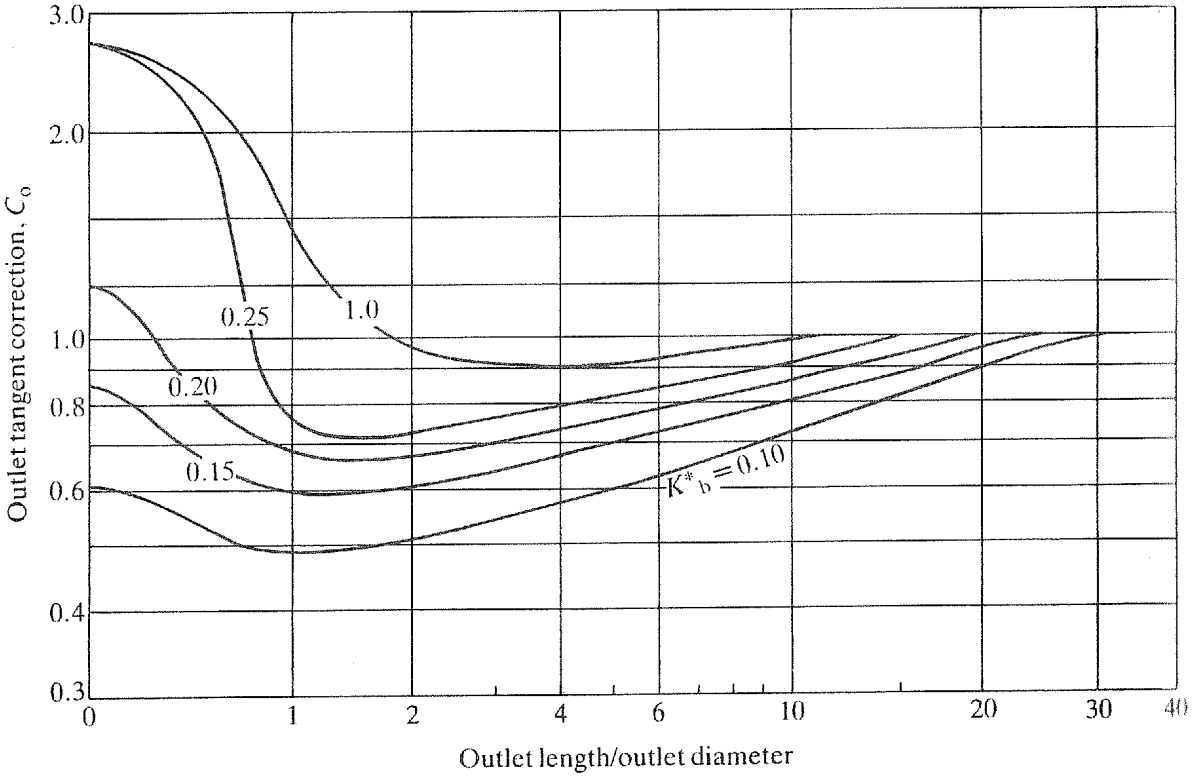

Fig. 9.4. Outlet tangent correction

Table 9.1. Loss coefficients for 90° bends with short outlet pipes at Reynolds number of 10^6 (class 1)

		Loss coefficients*	
r/d	Outlet length (pipe diameters)	Thin boundary layer	Thick boundary layer
1	0	0.64	0.70
1	1	—	0.22
1	4	—	0.18
2	0	0.31	0.19
2	1	0.12	0.11

*Excludes loss in pipe and one velocity head loss if pipe discharges to a large space.

9.2.5. CORRECTED LOSS COEFFICIENT K_b

The corrected bend loss coefficient is given by

$$K_b = K_b^* \times C_{Re} \times C_o \times C_f \tag{9.4}$$

and the head loss by

$$\Delta H = K_b U^2/2g$$

9.2.6. EFFECT OF INLET PIPE LENGTH (CLASS 2)

Provided inlet pipe lengths comply with the following requirements, the loss coefficients in Section 9.2.5 will not normally underestimate head losses.

1. More than two inlet pipe diameters when the bend follows another component which has a loss coefficient of less than 0.25 at $Re = 10^6$.
2. More than four pipe diameters when the bend follows another component which has a loss coefficient greater than 0.5 at $Re = 10^6$.

9.3. RECTANGULAR CROSS-SECTION BENDS OF CONSTANT AREA

Geometrical parameters for circular arc bends of rectangular cross-section are shown in Fig. 9.5. The important geometrical parameters are the radius ratio r/W, the bend deflection angle θ_b and the aspect ratio b/W. The length of the inlet and outlet passage is always referred to in terms of hydraulic diameters D, where

$$D = \frac{4 \times \text{Cross-sectional area}}{\text{Perimeter}} = \frac{4 \times b \times W}{2(b + W)} \tag{9.5}$$

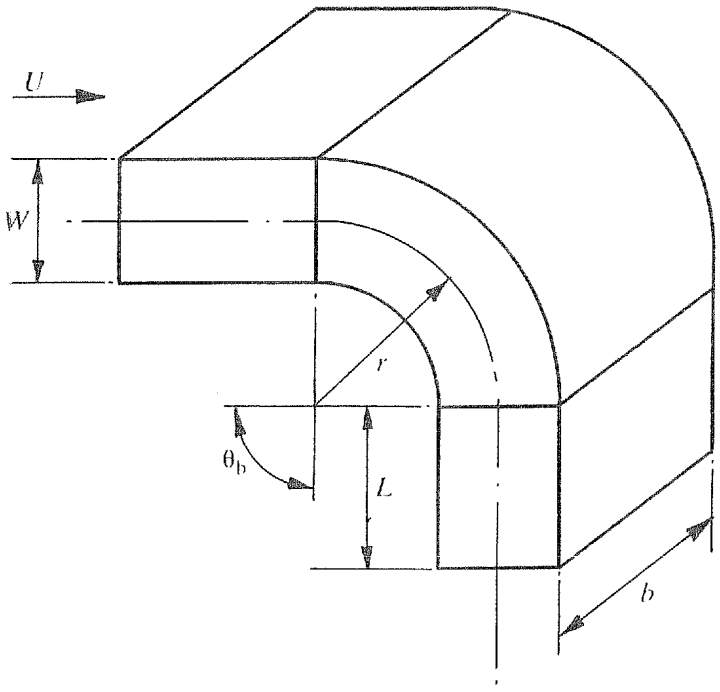

Fig. 9.5. Rectangular cross-section bend geometries

The Reynolds number is given by

$$\mathrm{Re} = UD/\nu \tag{9.6}$$

9.3.1. BASIC COEFFICIENTS K_b^* (CLASS 1)

Basic loss coefficients at a Reynolds number of 10^6 are plotted in Fig. 9.6 for rectangular bends of aspect ratio 0.5, in Fig. 9.7 for rectangular bends of aspect ratio 1.0, and in Fig. 9.8 for bends of aspect ratio 2.0.

9.3.2. REYNOLDS NUMBER CORRECTION C_{Re} (CLASS 2)

Use the circular cross-section Reynolds number correction from section 9.2.2, replacing r/d by r/W.

9.3.3. OUTLET DUCT LENGTH CORRECTION C_o (CLASS 2)

Use the circular cross-section outlet duct correction from Fig. 9.4, but modified as follows.

1. Aspect ratios $b/W < 0.7$ and $L/D > 1$, use $C_{o\,\mathrm{rectangular}} = 1 - (1 - C_{o\,\mathrm{circular}})/2$.

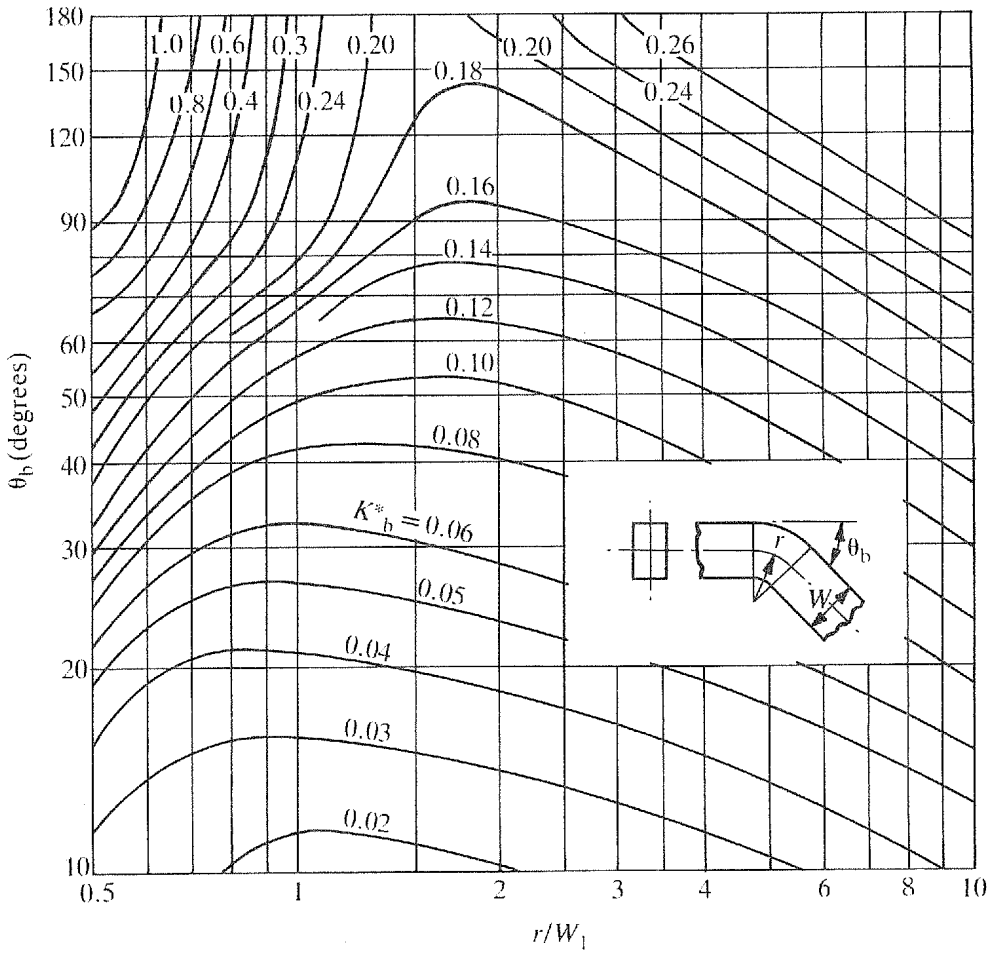

Fig. 9.6. Loss coefficients, K^*_b, for aspect ratio 0.5 rectangular bends ($Re = 10^5$)

2. Aspect ratios $b/W < 0.7$ and $L/D < 1$, use $C_{o\ rectangular} = C_{o\ circular}$.
3. Aspect ratios $b/W > 1.0$ and $L/D > 1$, use $C_{o\ rectangular} = C_{o\ circular}$.
4. Aspect ratios $b/W > 1.0$ and $L/D < 1$, use values of C_o for circular cross-sections except for bends of r/W between 1.5 and 3, when the basic coefficient K^*_b should be multiplied by 2.

A number of loss coefficients for rectangular bends with short outlet tangents are given in Tables 9.2 and 9.3. The loss coefficients do not include the friction loss in the outlet pipe or the loss of one velocity head if the outlet pipe discharges to a large space.

9.3.4. ROUGHNESS CORRECTION C_f (CLASS 3)

Use the same correction as for circular cross-sections (see Section 9.2.4).

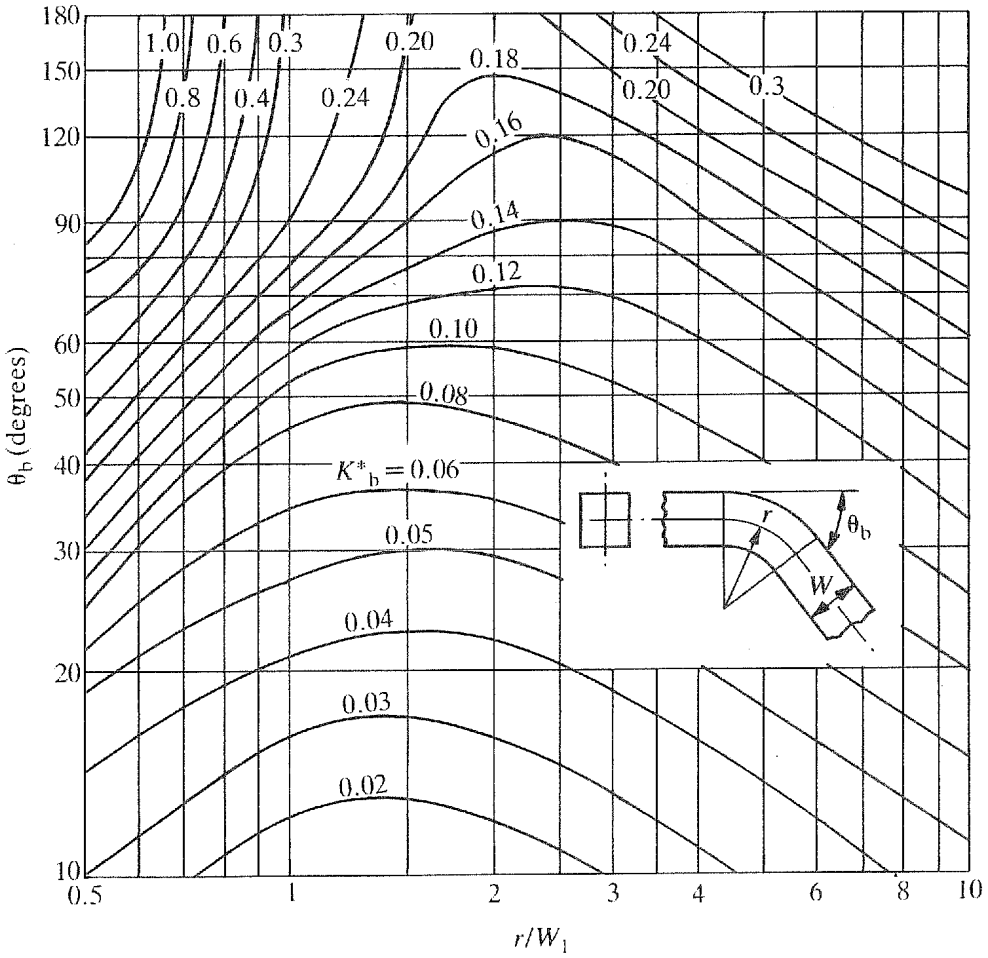

Fig. 9.7. Loss coefficients, K^*_b, for square cross-section bends ($Re = 10^6$)

Table 9.2. 90° bend loss coefficients with short outlet pipes at a Reynolds number of 10^6

r/W	Outlet passage length (passage widths)	Aspect ratio	
		0.5	2.0
1	0	0.75	0.74
1	0.5	0.59	0.73
1	1.0	0.34	0.36
1	2.0	0.20	0.22
2	0	0.17	0.25
2	0.5	—	0.20
2	1.0	0.14	0.11

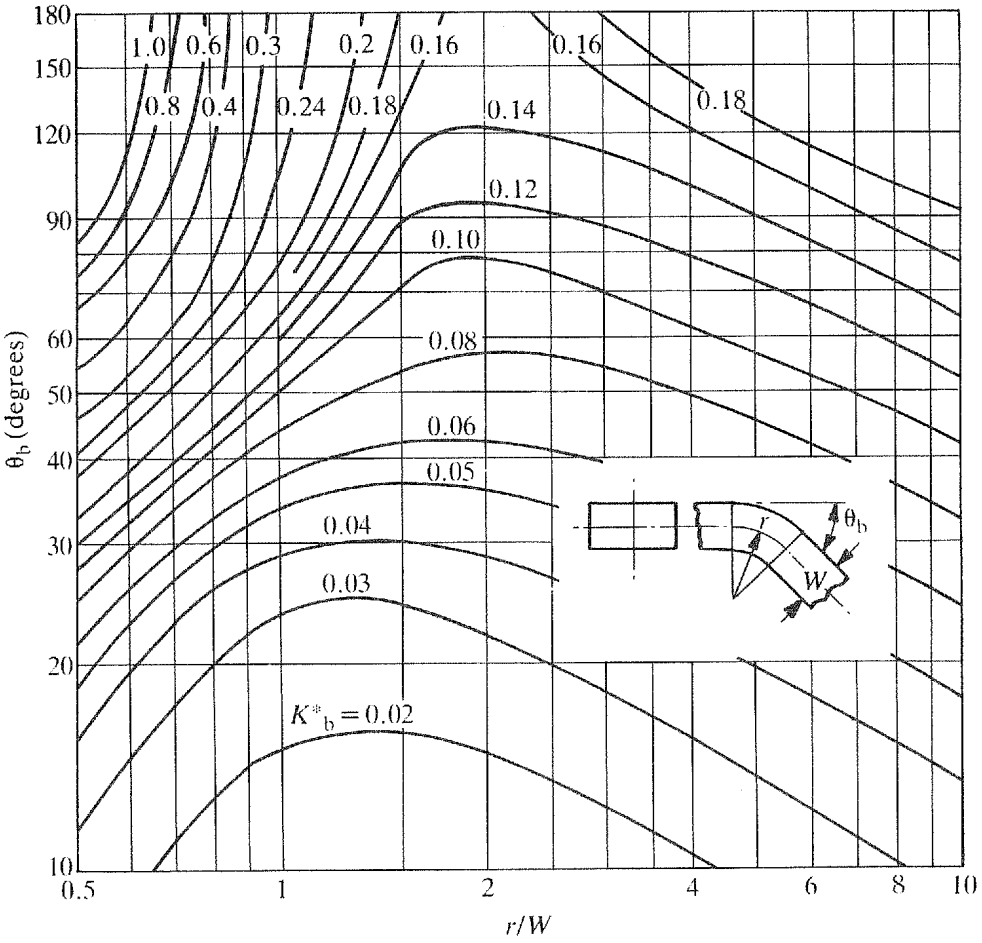

Fig. 9.8. Loss coefficients, K^*_b, for aspect ratio 2 rectangular bends ($Re = 10^6$)

Table 9.3. 45° bend loss coefficients, aspect ratio = 2 at a Reynolds number of 10^6

r/W	Outlet passage length (passage widths)	Loss coefficient
1	0	0.28
1	0.5	0.18
1	1.0	0.07
2	0	0.11
2	0.5	0.07
2	1.0	0.06

9.3.5. CORRECTED LOSS COEFFICIENTS K_b

Corrected loss coefficients are given by

$$K_b = K_b^* \times C_{Re} \times C_o \times C_t$$

9.3.6. EFFECT OF INLET PASSAGE LENGTH (CLASS 2)

Using the loss coefficient found in Section 9.3.5, it is unlikely that head losses will be underestimated provided the inlet passage length exceeds $4D$.

9.4. SINGLE MITRE BENDS (CIRCULAR CROSS-SECTION CLASS 1, RECTANGULAR CROSS-SECTION CLASS 2)

9.4.1. BASIC COEFFICIENT K_b^*

Basic loss coefficients, K_b^*, are plotted against angle in Fig. 9.9 for mitre bends of circular and rectangular cross-section.

9.4.2. CORRECTION TO BASIC COEFFICIENTS (CLASS 3)

Use the Reynolds number correction from Section 9.2.2 for $r/d < 0.7$, the outlet pipe length corrections of Fig. 9.4 and the inlet pipe limitations as in Section 9.2.6. For $\theta_b \leqslant 45^\circ$ use the roughness corrections from Section 9.2.4. For angles $>45^\circ$ roughness corrections are likely to be small and can normally be neglected.

9.5. 90° COMPOSITE MITRE BENDS

9.5.1. BASIC COEFFICIENTS K_b^* (CIRCULAR CROSS-SECTION CLASS 1, RECTANGULAR CROSS-SECTION CLASS 2)

Basic loss coefficients K_b^* are plotted against r/d (or r/W) in Fig. 9.10.

9.5.2. CORRECTIONS TO BASIC COEFFICIENTS (CLASS 3)

Use the Reynolds number corrections from Fig. 9.3 and the outlet pipe corrections from Fig. 9.4. Roughness corrections should be made using Section 9.2.4 and the inlet pipe limitations as in Section 9.2.6.

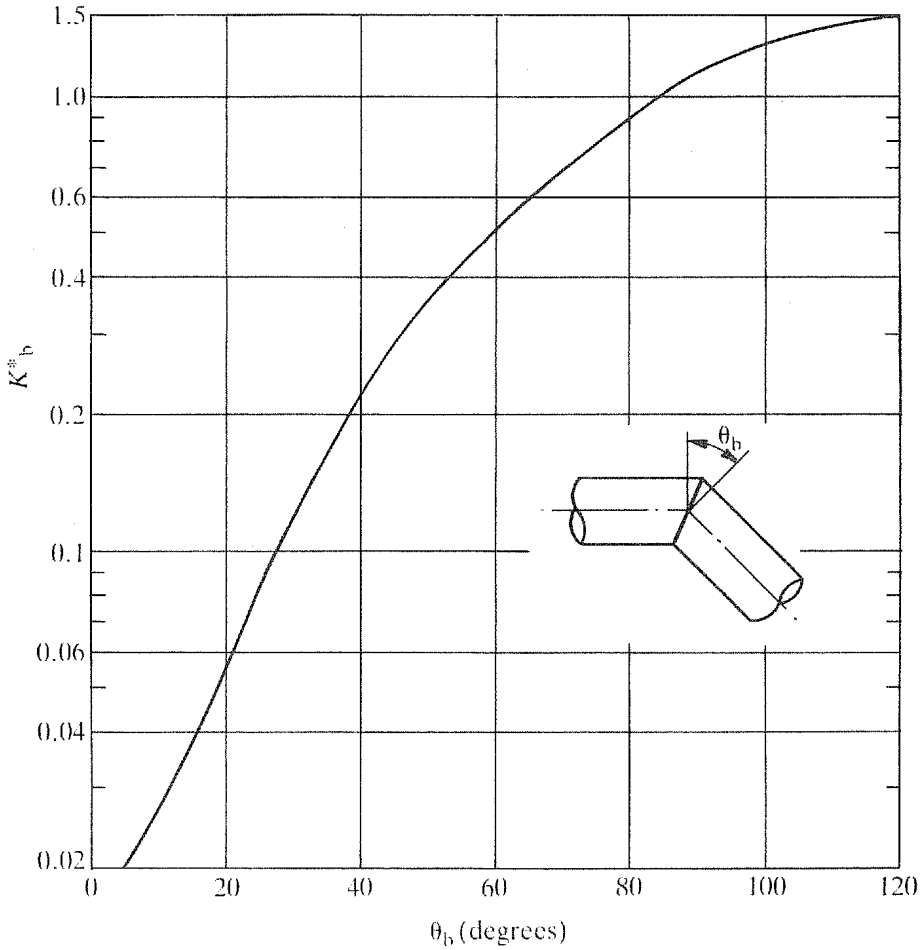

Fig. 9.9. Mitre bend loss coefficients ($Re = 10^6$)

9.6. VARIABLE AREA AND VARIABLE RADIUS RATIO BENDS BETWEEN PIPES OR PASSAGES OF EQUAL AREA

9.6.1. BENDS OF VARIABLE AREA (CLASS 2)

When it is necessary to use a bend having a variable area, minimum losses will be achieved if the inner radius is made as large as possible and the area through the bend is never less than the area of the pipe or passage. Typical examples of loss coefficients for variable area bends are shown in Fig. 9.11 for a Reynolds number of 10^6. To correct for Reynolds number, use the $r/d < 1$ curve of Fig. 9.2.3 (class 3). These values can be used for rectangular and circular bends.

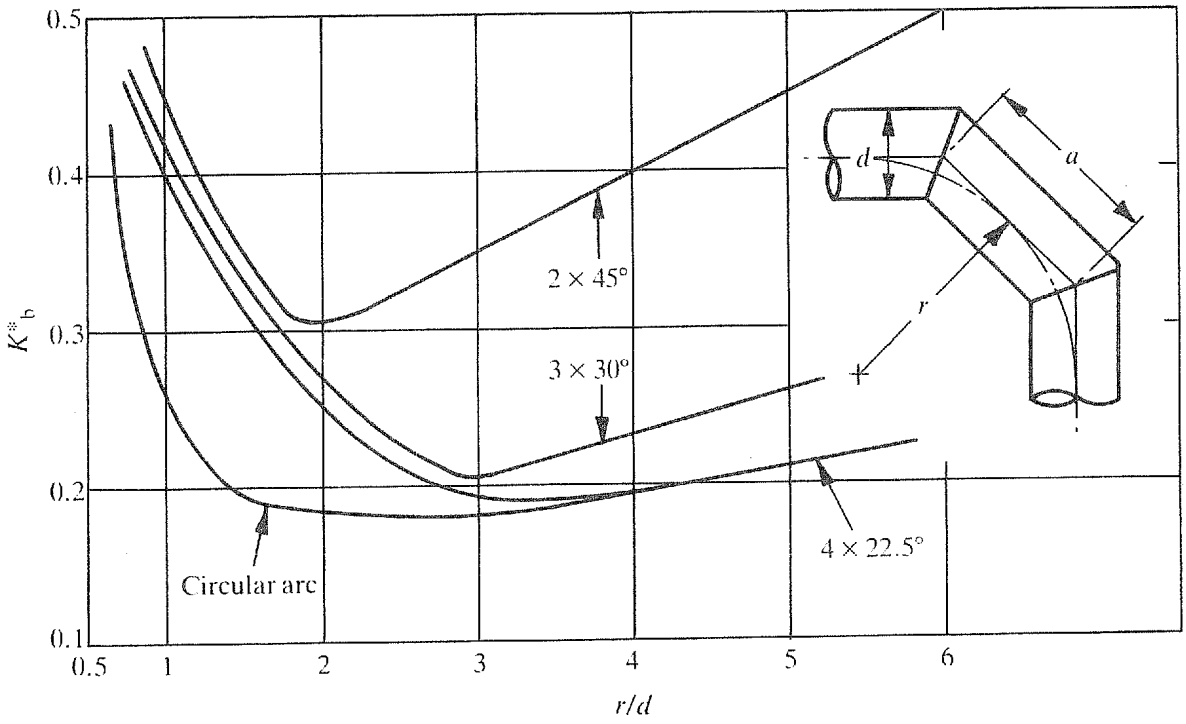

Fig. 9.10. Composite mitre bends — calculations are made using the equivalent circular arc r/d values, where $r = (a/2)\cot(90/2n)$ and n = the number of individual bends

9.6.2 BENDS OF VARYING RADIUS RATIO

Loss coefficients are least if the rate of turning is reduced towards the outlet of a bend, as in the arrangement shown in Fig. 9.12. Two examples of 90° bends made up of two 45° bends of different radius ratios are compared in Table 9.4 with a 90° bend of $r/d = 1.5$. The values given can be corrected for Reynolds number, outlet tangent and roughness, using Section 9.2.

Table 9.4. 90° composite bend loss coefficients for bends of circular cross-section

Bend configuration	K^*_b
$(45° \; r/d = 1) + (45° \; r/d = 2)$	0.16
$(45° \; r/d = 2) + (45° \; r/d = 1)$	0.20
$90° \; r/d = 1.5$	0.18

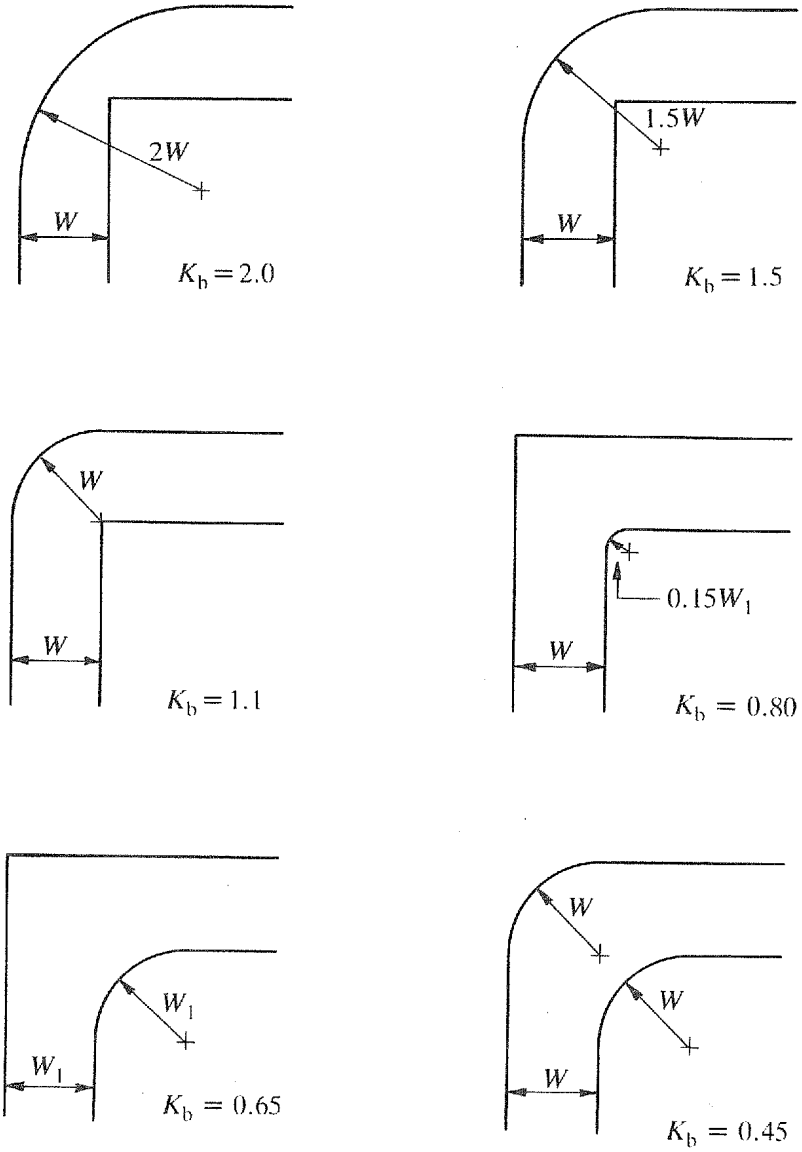

Fig. 9.11. Variable area bend loss coefficients, K_b^*

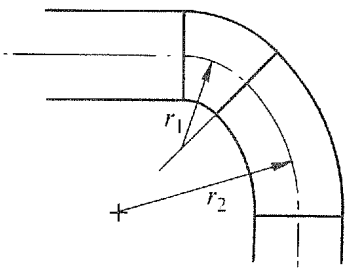

Fig. 9.12. Variable radius ratio bends

9.7. 180° ANNULAR BENDS (CLASS 2)

The geometrical arrangement of the annular bends considered is shown in Fig. 9.13.

The loss coefficients for flow from the pipe to the annulus and flow from the annulus to the pipe are based on the pipe velocity. The head loss is given by

$$\Delta H = K_b U^2/2g$$

where U is the mean pipe velocity.

Figure 9.14 is a plot of the loss coefficient against h/d ratio for the two flow directions with equal pipe and annulus areas. The shape of the curves in Fig. 9.14 shows the following.

1. If h/d is small, losses are high due to contraction of the flow.
2. There is an optimum range of h/d for minimum losses.
3. Losses rise rapidly as h/d is increased above the optimum. This is due to flow remaining attached to the end wall and not turning immediately into the pipe or annulus. The flow in this region is extremely unstable and loss coefficients may vary by a factor of 2.
4. In the case of flow from the annulus to the pipe, when h/d is sufficiently large for the end wall no longer to influence the main flow, coefficients fall to values close to those at optimum h/d.

9.7.1. PIPE TO ANNULUS

Basic loss coefficients, K_b^*, are tabulated in Table 9.5 for flow from the pipe to the annulus with the optimum h/d. The loss coefficients are weakly dependent on the t/d ratio and on the R/D ratio. Loss coefficients are about 0.05 higher for $R/D=0$ than for $R/D=0.3$, which is the optimum R/D ratio.

9.7.2. ANNULUS TO PIPE

Basic loss coefficients, K_b^*, are tabulated in Table 9.6 for flow from the annulus to the pipe with the optimum h/d. The values also apply to h/d values greater than 1.5.

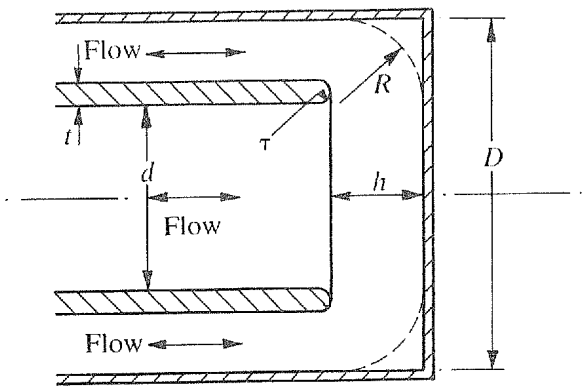

Fig. 9.13. Annular bend geometries

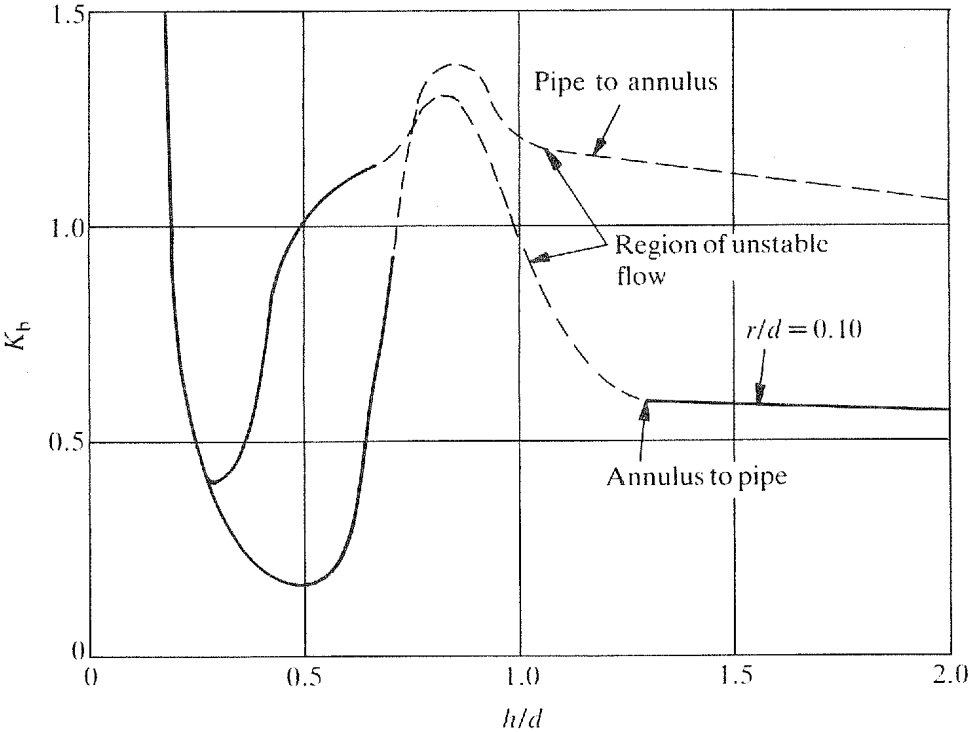

Fig. 9.14. Annular bend loss coefficient variation with h/d for equal areas

Table 9.5. Pipe to annulus loss coefficients

Area ratio annulus/pipe	Optimum h/d range	r/d	t/d	Loss coefficient, K_b^*
0.75	0.4–0.8	0.05	0.1	0.19
1.08	0.5–0.8	0.05	0.1	0.43
2.05	0.6–0.9	0.05	0.1	0.34
0.75	0.4–0.6	0	0.1	0.24
1.08	0.5–0.6	0	0.1	0.40
2.05	0.8–1.0	0	0.1	0.34
0.76	0.3–0.5	0.1	0.2	0.16
1.06	0.3–0.5	0.1	0.2	0.23
2.07	0.6–1.0	0.1	0.2	0.32
0.76	0.4–0.5	0	0.2	0.22
1.06	0.4–0.5	0	0.2	0.26
2.07	0.7–0.9	0	0.2	0.40
0.8	0.2–0.5	0.2	0.4	0.30
1.07	0.3–0.5	0.2	0.4	0.20
2.10	0.2–1.0	0.2	0.4	0.40
0.8	0.3–0.5	0	0.4	0.36
1.07	0.3–0.4	0	0.4	0.26
2.10	0.5–0.9	0	0.4	0.30

Table 9.6. Annulus to pipe loss coefficients

Area ratio annulus/pipe	Optimum h/d range	r/d	t/d	Loss coefficient, K_b^*
0.75	0.18–0.22	0.5	0.10	1.90
1.08	0.24–0.33	0.5	0.10	1.04
2.05	0.33–0.66	0.5	0.10	0.50
0.75	0.23–0.27	0	0.10	1.70
1.08	0.27–0.34	0	0.10	1.0
2.05	0.35–0.45	0	0.10	0.44
0.76	0.18–0.23	0.10	0.20	0.96
1.06	0.20–0.29	0.10	0.20	0.40
2.07	0.28–0.40	0.10	0.20	0.20
0.76	0.22–0.28	0	0.20	1.10
1.06	0.23–0.33	0	0.20	0.45
2.07	0.22–0.48	0	0.20	0.50
0.80	0.22–0.30	0.20	0.40	0.70
1.07	0.18–0.28	0.20	0.40	0.32
2.10	0.17–0.50	0.20	0.40	0.16
0.8	0.30–0.38	0	0.40	0.72
1.07	0.26–0.36	0	0.40	0.40
2.1	0.20–0.40	0	0.40	0.40

Loss coefficients vary markedly with t/d. For t/d less than 0.1, the minimum value for which loss coefficients are given in Table 9.6, the coefficients may be twice the $t/d = 0.1$ value. Local thickening and rounding of the pipe can halve the loss coefficient.

Loss coefficients are only weakly dependent on r/d for values less than about 0.4, with an optimum at 0.3.

9.8. VANED BENDS

By using vanes, the loss coefficient of a mitre bend can be reduced to that of the circular arc bend with lowest loss. The general arrangement of a vaned bend and details of the vanes are shown in Fig. 9.15.

The number of vanes, N, is given by

$$N = (1.8W/R) - 1 \quad \text{to the nearest whole number}$$

where W is the duct height (mm) shown in Fig. 9.15 and R is the vane radius given in Table 9.7.

The vanes can usually be cut from standard tube. Ideally vanes should be closer together on the inside of the bend, but because of strength requirements the vane thickness may be such as to cause excessive blockage on the inside of the bend. Fluctuating forces occur in vaned bends, which may exceed the calculated steady dynamic loads. Allowance should be made for fluctuating forces in strength calculations.

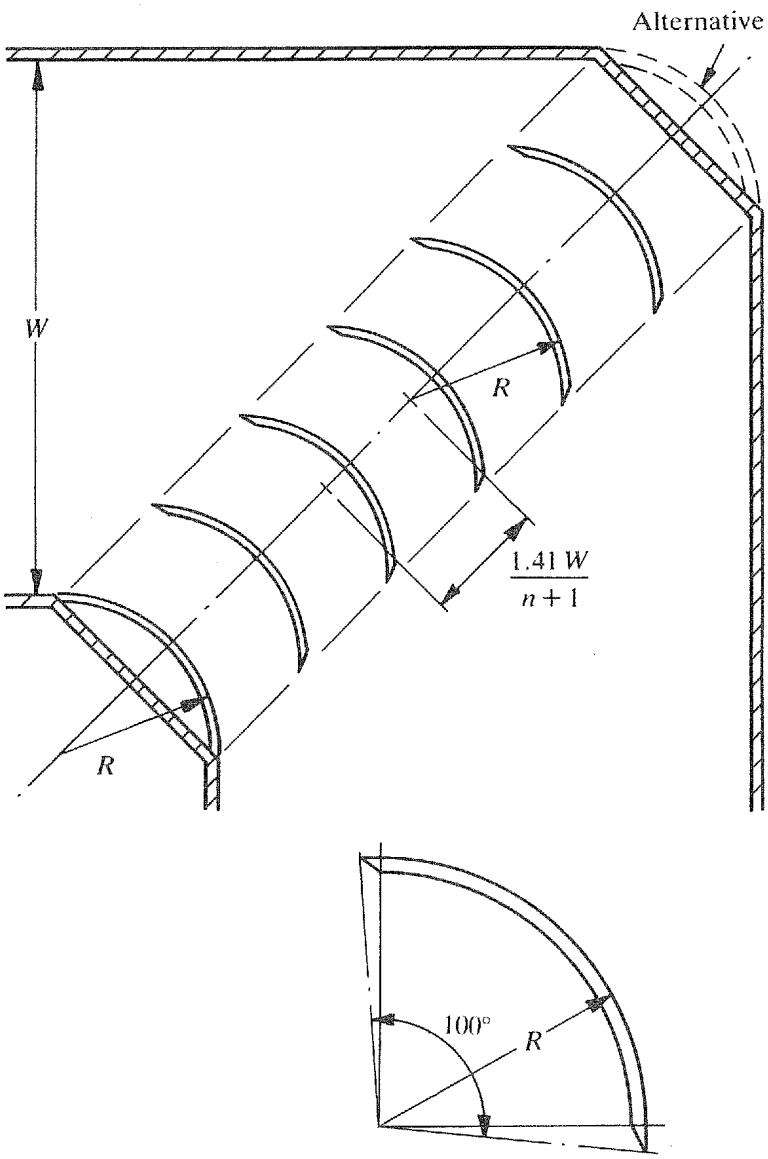

Fig. 9.15. Vaned bend geometry

Table 9.7.

Pipe diameter or passage width (mm)	Vane radius (mm)
100–200	20–30
200–400	30–50
500–800	60–80

Vanes within bends of circular arc are only justified if the bend radius ratio, r/d, is less than unity and the vanes are thin and occupy less than 5 per cent of the cross-sectional area. For radius ratios greater than 0.7 a single vane located at $R=\sqrt{r_i r_o}$ should be used, r_i and r_o being the inner and outer bend radii, respectively. A vane at this location reduces the loss coefficient of an $r/d=0.7$ bend by half and an $r/d=1$ bend by 20 per cent.

9.9. COILS (CLASS 2)

The geometrical parameters of the coils considered are shown in Fig. 9.16. The coil is assumed to be hydraulically smooth.

The length of the coil, excluding the inlet and outlet pipe, is given by

$$L=\pi Dn(1+P^2/4D^2)^{0.5} \tag{9.7}$$

where D is the coil diameter, P is the mean pitch and n is the number of turns.

For a Reynolds number range of 1.5×10^4 to 10^5, the loss coefficient K_b is given by

$$K_b=[0.32\mathrm{Re}^{-0.25}+0.048\ (d_i/D)^{0.5}]\times L/d_i \tag{9.8}$$

where $\mathrm{Re}=d_iU/\nu$ and d_i is the inside diameter.

9.10. COMMERCIAL BENDS — SCREWED, FLANGED, COMPRESSION AND CAPILLARY (CLASS 3)

Approximate loss coefficients are given in Fig. 9.17 for single bends with angles of $\geqslant 90°$. For bends of $<90°$, use a percentage of the 90° loss coefficient; e.g. for a 60° bend use two-thirds of the 90° loss coefficient.

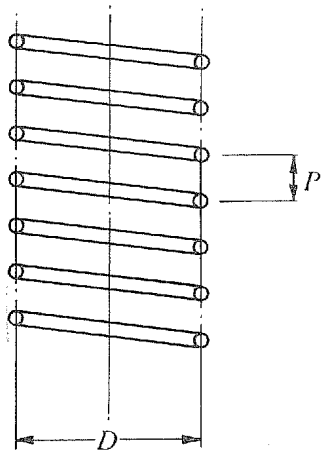

Fig. 9.16. Coil geometry

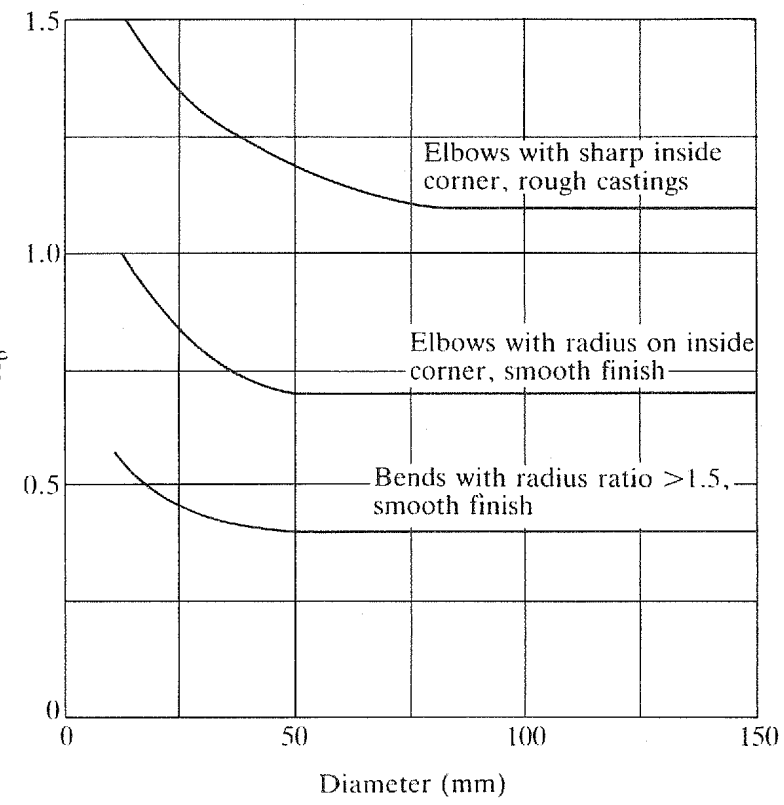

ig. 9.17. Commercial pipe bend loss coefficients

.11. LAMINAR FLOW IN BENDS (CLASS 3)

Approximate loss coefficients for laminar flow through smooth 90° bends with radius ratio between 1.5 and 2 are shown in Fig. 9.18.

.12. EXAMPLE

Estimate the system loss between the inlet to a 90° bend of $r/d = 2$ and the end of the outlet pipe for the following outlet conditions:

a) an outlet pipe of 30 diameters;
b) with the bend directly discharging into an infinite expansion chamber; and
c) with a two diameter outlet pipe connected to another component.

The pipe diameter is 0.6 m, and the mean velocity 4 m/s, the kinematic viscosity is 1.14×10^{-6} m^2/s and the pipe and bend roughness is 0.02 mm.

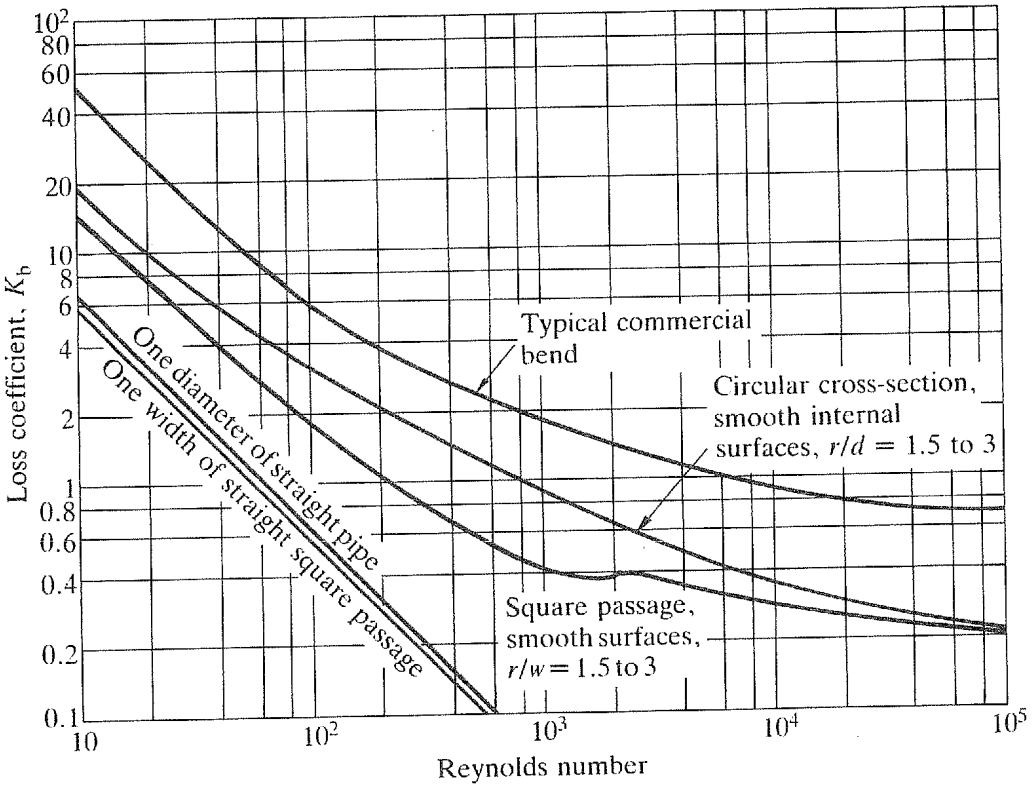

Fig. 9.18†. Approximate loss coefficients for 90° circular and square bends of r/d between 1.5 and 2.0 at low Reynolds numbers

Reynolds number

$$\mathrm{Re} = Ud/\nu = 4 \times 0.6/(1.14 \times 10^{-6}) = 2.1 \times 10^6$$

Basic coefficient from Fig. 9.2

$$K_b^* = 0.16$$

Reynolds number correction from Fig. 9.3

$$C_{\mathrm{Re}} = 0.89$$

Outlet tangent correction from Fig. 9.4 for $K_b^* = 0.16$

(a) $L/d = 30$, $C_o = 1.0$

(b) $L/d = 0$, $C_o = 0.9$

(c) $L/d = 2$, $C_o = 0.62$

Roughness correction from Section 9.2.4:

Since $Re > 10^6$, C_f based on the friction coefficients at $Re = 10^6$ is

$$C_f = f_{rough}/f_{smooth} = 0.0123/0.0117 = 1.05$$

Corrected loss coefficient from Section 9.2.5:

(a) $K_b = 0.16 \times 0.89 \times 1.0 \times 1.05 = 0.150$

(b) $K_b = 0.16 \times 0.89 \times 0.9 \times 1.05 = 0.135$

(c) $K_b = 0.16 \times 0.89 \times 0.62 \times 1.05 = 0.093$

Total head loss = bend loss + friction loss

(a) $\Delta H = [0.15 + (30 \times 0.0114)]\dfrac{4^2}{2 \times 9.81} = 0.40$ m

(b) $\Delta H^* = (0.135 + 1)\dfrac{4^2}{2 \times 9.81} = 0.93$ m

(c) $\Delta H = [0.093 + (2 \times 0.0114)]\dfrac{4^2}{2 \times 9.81} = 0.09$ m

*Included in the head loss is the one velocity head associated with a discharge into an infinite space.

NOTES AND REFERENCES ON CHAPTER 9

The loss coefficients for circular arc bends are taken from:

1. Miller, D. S., *Internal Flow: A Guide to Losses in Pipe and Duct Systems.* Cranfield, Bedford: BHRA (1971), 329 pp.
2. Ito, H., Pressure losses in smooth pipe bends. *Rep. Inst. High Speed Mech., Tohoku Univ.*, **12** (99), 41–62 (1960–61).

Variable area bend data are based on:

3. Sprenger, H., Pressure head losses in 90° bends for tubes or ducting of rectangular cross-section. BHRA Report T1027, 17 pp. (October 1969). (Translated from *Schweiz. Bauzeit.*, **87** (13), 223–231 (27 March 1969).

The information on 180° annular bends is due to:

4. Idelchik, I. E. and Ginzburg, Ya, L., The hydraulic resistance of 180° annular bends. *Thermal Eng.*, **15** (4), 109–114 (1968).

References and formulae for flow in coils are given in:

5. Srinvasan, P. S., Nandapukar, S. S. and Holland, F. A., Friction factors for coils. *Trans. Inst. Chem. Engrs*, **48** (4–6), T156–T161 (July–August 1970).

Laminar loss coefficients given in Fig. 9.18 for circular cross-section bends are based on a wide variety of sources, none of which agree. (Experimenters continue to test "commercial" fittings rather than components of defined geometry.) The square cross-section loss coefficients are based on:

6. Shiragami, N. and Inoue, I., Pressure losses in square section bends. *J. Chem. Eng. Jpn*, **14** (3) 173–177 (1981).

10. CORRECTING FOR BEND–BEND INTERACTIONS

10.1. INTRODUCTION

This chapter is concerned with correcting the bend loss coefficients of Chapter 9 to account for interaction between bends. If the bends are separated by a spacer of more than 30 diameters, interaction effects are not important. Neglecting interaction effects will usually result in an overestimate of head losses, except for mitre bends of radius ratio less than unity, which require a four diameter spacer to guarantee a correction factor of less than unity.

The procedure is to multiply the combined less coefficients for two bends by an interaction correction factor $C_{b\text{-}b}$:

$$K_{b\text{-}b} = (K_{b_1} + K_{b_2})C_{b\text{-}b} \tag{10.1}$$

where K_{b_1} and K_{b_2} are bend loss coefficients from Chapter 9.

Friction losses within spacers are calculated as for pipes or passages.

The correction factors apply to bend–spacer–bend combinations with a long pipe after the second bend. When the outlet pipe is less than 30 diameters long an estimate of the effect of the short outlet pipe can be made using an outlet pipe correction from Section 9.2.

10.1.1. REYNOLDS NUMBER (CLASS 2)

Interaction correction factors for bends of circular cross-section apply to Reynolds numbers greater than 10^4.

10.1.2. CROSS-SECTIONAL SHAPE

The interaction correction factors given are for circular cross-section bends. Limitations on applying the loss coefficients to other cross-sections are outlined.

10.2. COMBINATIONS OF 90° BENDS (CLASS 1)

The notation used for combinations of 90° bends is shown in Fig. 10.1.

Table 10.1 contains interaction correction factors for bend–spacer–bend combinations with spacer lengths of 0, 1, 4 and 8 diameters and bend radius ratios of 1, 2 and 3. Interaction correction factors for combinations of two bends of the same radius ratio are plotted in Figs 10.2–10.4.

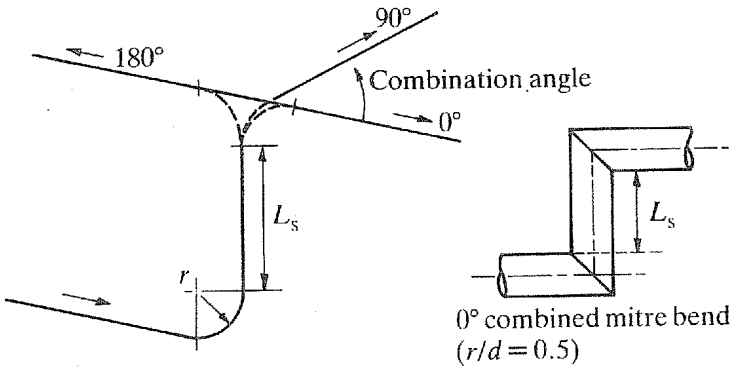

Fig. 10.1. Notation for combinations of two 90° bends

Table 10.1. Interaction correction factors for combinations of two 90° bends

	Spacer length (pipe diameters)											
	0	1	4	8	0	1	4	8	0	1	4	8
θ_c^*	$(r/d=1)$ + spacer + $(r/d=1)$				$(r/d=1)$ + spacer + $(r/d=2)$				$(r/d=1)$ + spacer + $(r/d=3)$			
0	1.00	0.86	0.71	0.81	1.06	0.91	0.74	0.83	1.02	0.93	0.78	0.87
30	1.16	1.04	0.94	0.83	1.15	1.05	0.85	0.84	1.06	1.05	0.83	0.83
60	1.04	0.93	0.76	0.82	1.01	0.96	0.82	0.84	0.97	0.92	0.83	0.83
90	0.81	0.79	0.74	0.82	0.81	0.86	0.80	0.82	0.86	0.90	0.82	0.83
120	0.69	0.69	0.72	0.81	0.71	0.78	0.79	0.81	0.78	0.82	0.82	0.83
150	0.60	0.63	0.73	0.81	0.64	0.71	0.78	0.81	0.72	0.78	0.81	0.84
180	0.53	0.58	0.71	0.80	0.60	0.64	0.77	0.81	0.67	0.72	0.81	0.85
	$(r/d=2)$ + spacer + $(r/d=1)$				$(r/d=2)$ + spacer + $(r/d=2)$				$(r/d=2)$ + spacer + $(r/d=3)$			
0	0.76	0.74	0.69	0.74	0.86	0.83	0.72	0.77	0.88	0.85	0.74	0.83
30	0.73	0.72	0.73	0.79	0.79	0.79	0.71	0.81	0.84	0.83	0.77	0.82
60	0.71	0.70	0.74	0.80	0.77	0.74	0.70	0.81	0.81	0.81	0.79	0.83
90	0.67	0.68	0.74	0.80	0.73	0.71	0.70	0.80	0.78	0.79	0.81	0.84
120	0.64	0.66	0.75	0.81	0.68	0.68	0.69	0.80	0.76	0.77	0.82	0.85
150	0.60	0.64	0.75	0.81	0.63	0.65	0.69	0.80	0.72	0.75	0.82	0.86
180	0.57	0.62	0.75	0.81	0.58	0.62	0.72	0.80	0.69	0.73	0.83	0.87
	$(r/d=3)$ + spacer + $(r/d=1)$				$(r/d=3)$ + spacer + $(r/d=2)$				$(r/d=3)$ + spacer + $(r/d=3)$			
0	0.79	0.76	0.70	0.76	0.85	0.83	0.72	0.77	0.86	0.87	0.82	0.85
30	0.76	0.75	0.73	0.81	0.83	0.81	0.74	0.81	0.83	0.85	0.81	0.85
60	0.73	0.73	0.75	0.81	0.80	0.79	0.75	0.80	0.81	0.83	0.81	0.85
90	0.70	0.72	0.77	0.81	0.76	0.76	0.76	0.80	0.78	0.79	0.80	0.85
120	0.68	0.70	0.78	0.82	0.73	0.74	0.77	0.80	0.76	0.77	0.80	0.85
150	0.65	0.69	0.78	0.82	0.69	0.71	0.77	0.80	0.74	0.75	0.79	0.85
180	0.64	0.68	0.79	0.82	0.65	0.68	0.77	0.80	0.71	0.73	0.79	0.85

*θ_c combination angle (degrees), see Fig. 10.1.

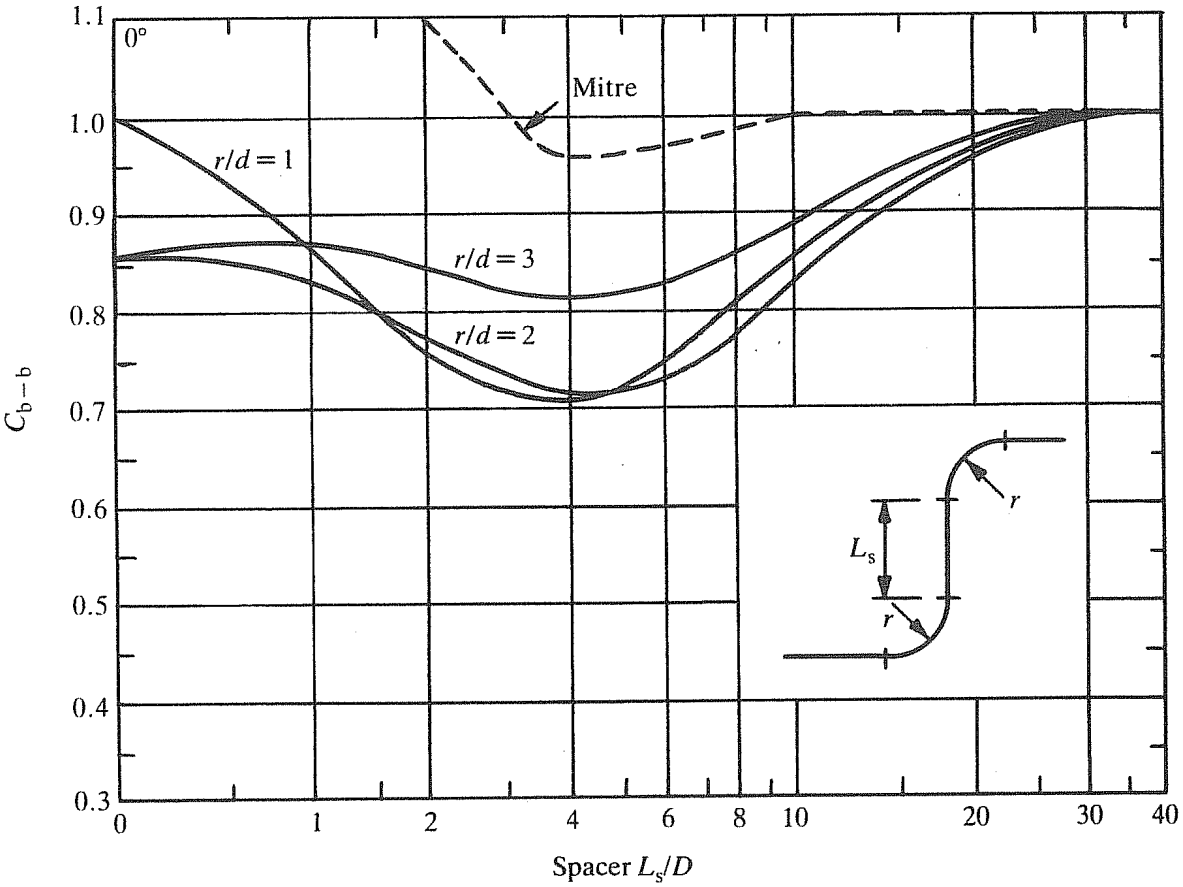

Fig. 10.2. Correction factors for 0° combined bends

Mitre bend interaction correction factors for 0° combined bends exceed 3 at zero spacer length.

Bend interaction correction factors are at a maximum at a combination angle of about 30°. This arrangement gives rise to a strong secondary rotation that can be detected 100 diameters or more after the second bend.

An example is given in Section 10.6.

10.3. COMBINATIONS OF TWO SIMILAR BENDS OF LESS THAN 90° (CLASS 3)

Combinations of two similar bends with individual angles greater than 70° have similar correction factors to bends of 90°, so the data in Section 10.2 can be used.

For combinations of two similar bends, each with an angle of less than 45° in 90° or 180° combined configurations, use correction factors from Fig. 10.3.

A situation not uncommon is two 30° or 45° bends in a 180° combination — see Fig. 10.5(1).

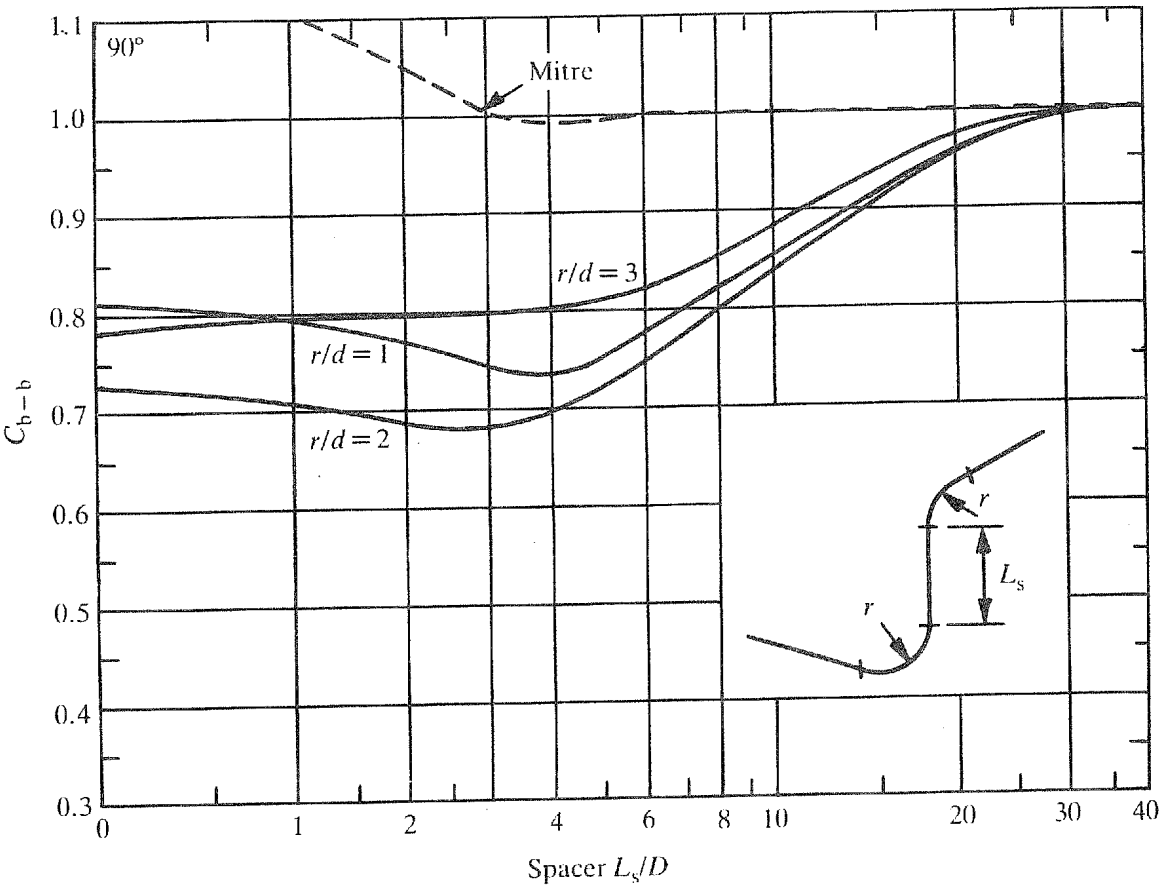

Fig. 10.3. Correction factors for 90° combined bends

For 180° combinations of bends with angles of 40° or less and spacers $Ls/d < 4$ use $C_{b\text{-}b} = 0.64$, and for $Ls/d > 4$ use Fig. 10.2.

For combinations of two similar bends with angles between 45° and 70° use Fig. 10.3.

The variation in correction factors for combinations of similar mitre bends with spacers of less than four diameters is complex. If the individual mitre bend angles are less than 45° and the spacer is more than one diameter, then use the curve for $r/d = 1$ bends in Fig. 10.3 for all combination angles.

10.4. COMBINATIONS OF NON-CIRCULAR CROSS-SECTION BENDS (CLASS 3)

For rectangular bends of aspect ratio less than 0.7, use correction factors from Fig. 10.4 for all combination angles, but reduce their difference from unity by half. That is,

$$\text{Correction factor} = 1 - (1 - C_{b\text{-}b})/2$$

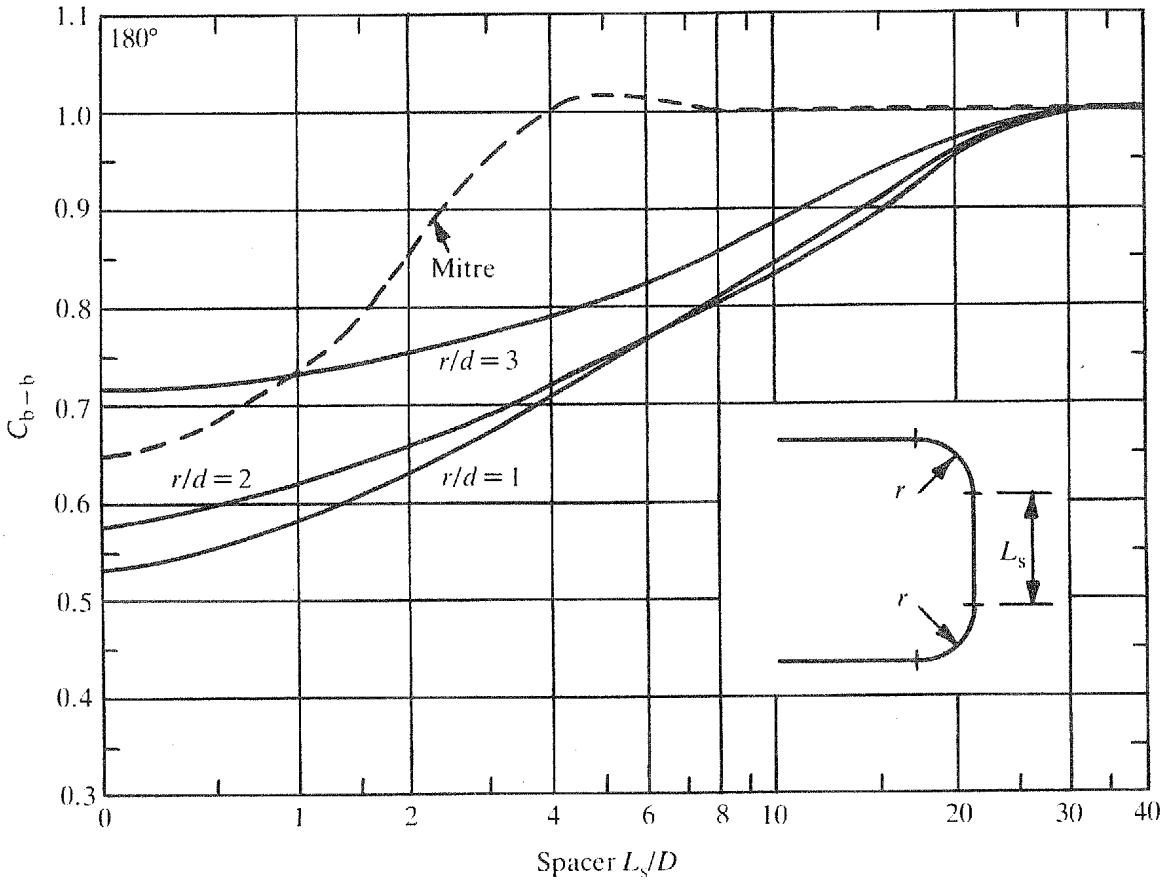

Fig. 10.4. Correction factors for 180° combined bends

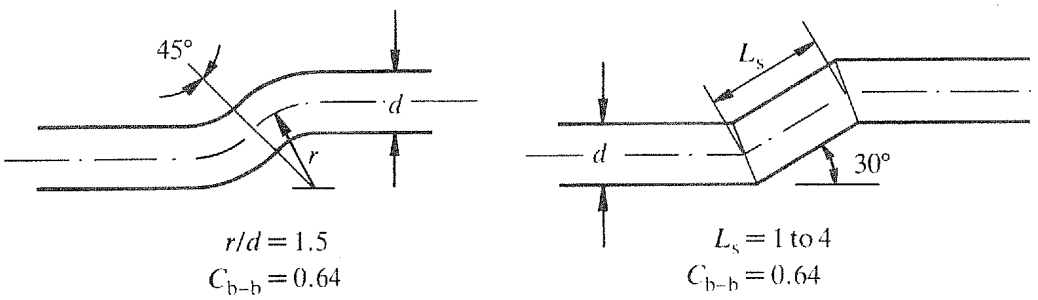

$r/d = 1.5$
$C_{b-b} = 0.64$

$L_s = 1$ to 4
$C_{b-b} = 0.64$

Fig. 10.5(1). 180° combined bends

For rectangular bends of aspect ratios greater than 1.5, use correction factors from Fig. 10.2 for all combination angles.

Between aspect ratios of 0.7 and 1.5, use circular cross-section data.

When bends of different aspect ratios are connected together, such as a bend of aspect ratio 2 to one with an aspect ratio 0.5, use correction factors from Fig. 10.2.

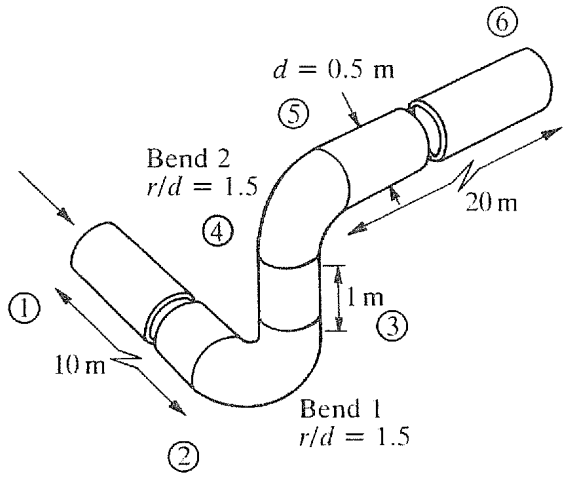

Fig. 10.6. 90° combined bend

10.5. COMBINATION OF 90° VANED BENDS (CLASS 2)

An interaction correction factor of unity applies to two well designed (Fig. 9.15) 90° bends arranged to form a 0° or an 180° bend.

10.6. EXAMPLE

Determine the head loss between stations 1 and 6 in Fig. 10.6 for water flowing at 2 m/s. The 0.5 m diameter pipe can be taken as hydraulically smooth and the kinematic viscosity is 1.14×10^{-6} m^2/s.

1. Reynolds number

$$\mathrm{Re} = UD/\nu = 2 \times 0.5/(1.14 \times 10^{-6}) = 0.88 \times 10^6$$

2. From Fig. 8.1 the friction coefficient for an hydraulically smooth pipe with a Reynolds number of 0.88×10^6 is

$$f = 0.0118$$

3. From Fig. 9.2 the basic loss coefficient for an $r/d = 1.5$ bend is

$$K_b^* = 0.185$$

The Reynolds number correction factor for an $r/d = 1.5$ bend at $\mathrm{Re} = 0.88 \times 10^6$ from Fig. 9.3 is 1.0.

4. Interpolating between the $r/d = 1$ and 2 curves of Fig. 10.2, the interaction factor for the two $r/d = 1.5$ bends with a two diameter spacer is 0.74.

5. From equation (10.1)

$$K_{b\,b} = (0.185 + 0.185) \times 0.74$$
$$= 0.274$$

6. The loss coefficient for the three sections of pipe between stations 1 and 6 is

$$K_f = fL/D = 0.0118(10+1+20)/0.5 = 0.732$$

7. The total head loss between stations 1 and 6 is

$$\Delta H = K_{total} \times U^2/2g = (0.274+0.732) \times 2^2/(2 \times 9.81)$$
$$= 0.21 \text{ m}$$

NOTES AND REFERENCES ON CHAPTER 10

The bend interaction correction factors are based on experimental work and correlations in:

1. Ito, H., Experimental and theoretical studies on the flow in curved pipes. *Mem. Inst. High Speed Mech., Tohoku Univ.*, **15**, Paper 142 (1959). (In Japanese.)
2. Miller, D. S., *Internal Flow: A Guide to Losses in Pipe and Duct Systems.* Cranfield, Bedford: BHRA (1971), 329 pp.

13. DIVIDING AND COMBINING FLOW

13.1. INTRODUCTION

In this chapter loss coefficients are given for dividing and combining junctions. The junction geometries considered are shown in Fig. 13.1. Important geometrical parameters are the area ratio, the angle between the legs and the chamfers or radii at the junction of the legs.

The notation used for the junction legs is shown in Fig. 13.1. A loss coefficient K_{ij} is defined as the ratio of the total head loss between legs i and j to the mean velocity head in the leg carrying the total flow. The leg carrying the total flow is always referred to as leg 3. In the case of T junctions leg 1 is the branch and leg 2 is the leg carrying the through flow. Symmetrical Y configurations have only one coefficient, since leg 2 can be substituted for leg 1 or vice versa. Loss coefficients are:

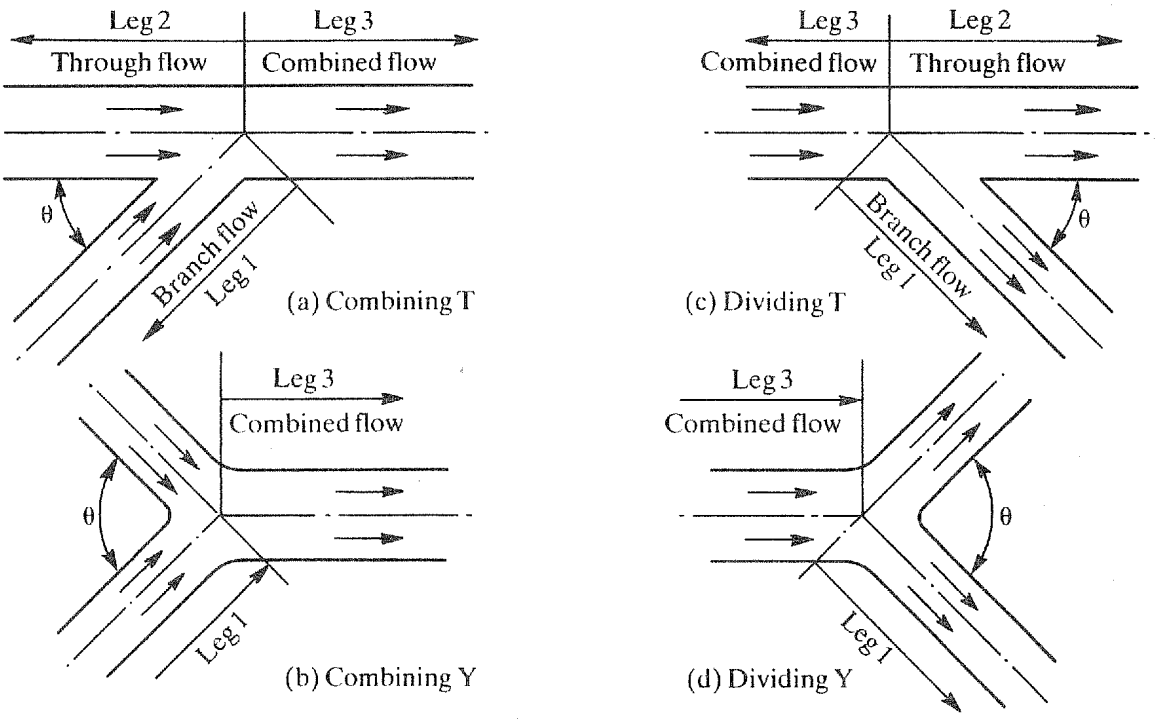

Fig. 13.1. Geometrical parameters for combining and dividing junctions

Combining flow

$$K_{13}=\left[\left(\frac{U_1^2}{2g}+h_1\right)-\left(\frac{U_3^2}{2g}+h_3\right)\right]\Big/\frac{U_3^2}{2g} \tag{13.1}$$

$$K_{23}=\left[\left(\frac{U_2^2}{2g}+h_2\right)-\left(\frac{U_3^2}{2g}+h_3\right)\right]\Big/\frac{U_3^2}{2g} \tag{13.2}$$

Dividing flow

$$K_{31}=\left[\left(\frac{U_3^2}{2g}+h_3\right)-\left(\frac{U_1^2}{2g}+h_1\right)\right]\Big/\frac{U_3^2}{2g} \tag{13.3}$$

$$K_{32}=\left[\left(\frac{U_3^2}{2g}+h_3\right)-\left(\frac{U_2^2}{2g}+h_2\right)\right]\Big/\frac{U_3^2}{2g} \tag{13.4}$$

The loss coefficients apply to junctions with inlet and outlet legs 30 or more diameters long. Conditions are given under which the loss coefficients can be applied to junctions with short inlet and outlet legs.

Chamfers or radii at junctions can reduce one or both of the junction loss coefficients. Guidance is given on where radii are useful in reducing losses. Because of the marked effect of edge sharpness on T junctions and additional inaccuracies introduced in having to measure flow rates in two legs, scatter in experimental results is often quite high compared with other components.

Loss coefficients of most practical "sharp-edged" T junctions, with smooth flow passages without discontinuities, are unlikely to exceed the loss coefficients for sharp-edged T junctions in this chapter. Screwed T junctions and other junctions with discontinuities can have significantly higher loss coefficients — double that of junctions with smooth passages.

13.1.1. REYNOLDS NUMBER EFFECTS (CLASS 3)

There are no reliable data from experiments on T junctions over a wide range of Reynolds numbers. However, the limited data that exists indicate that the effects of Reynolds number on T junction loss coefficients follows the established trends for other components.

Additional complications arise with T junctions because they have three Reynolds numbers. For instance, when the ratio of flow from the branch into the main leg of a combining T is close to zero, flow in the branch can be laminar with turbulent flow in the other two legs. In practice, provided the Reynolds number of the flow in the leg carrying the combined flow is greater than 10^4, it is of little consequence that the Reynolds number may be in the laminar region in one of the other legs. This is because the contribution from flow in the leg with laminar flow to the total junction energy loss is small.

In the absence of reliable data on Reynolds number effects it is suggested that the loss coefficients given be taken as basic coefficients at a Reynolds number of 10^6 in the leg carrying the combined flow, and that these coefficients be converted to apply to other combined flow

leg Reynolds numbers as follows.

1. For Reynolds numbers greater than 10^6, no correction.
2. For Reynolds numbers between 2×10^5 and 10^6, no correction.
3. For Reynolds numbers between 10^4 and 2×10^5 and loss coefficients with values between 0 and 0.2 at a Reynolds number of 10^6, use the Reynolds number correction factors for $r/d=1$ bends from Fig. 9.3.
4. For Reynolds numbers between 10^4 and 2×10^5 and loss coefficients greater than 0.2 at a Reynolds number of 10^6, the loss coefficient K_{ij} is given by

$$K_{ij}=(\text{loss coefficient at } 10^6-0.2)+(0.2\times\text{the correction factor for } r/d=1 \text{ bends from Fig. 9.3})$$

5. For loss coefficients that are negative at $\mathrm{Re}=10^6$, assume that the coefficients remain constant down to a combined flow Reynolds number of 10^5 and then change linearly to zero by a Reynolds number of 10^4. This is not likely to be the case for K_{13} for very low Q_1/Q_3 or for K_{23} with angled junctions with a high Q_1/Q_3 but, since in both cases only a small quantity of the total flow is involved, errors in the prediction of energy requirements will not be significant.

13.1.2. CROSS-SECTIONAL SHAPE (CLASS 2)

The cross-sectional shape is usually not an important parameter, as regards pressure losses, provided the relevant non-dimensional geometrical parameters are used when comparing the performance of junctions with different cross-sections. Except for Section 13.9 and 13.10, loss coefficients are from experiments on junctions with legs of circular cross-section. These loss coefficients can be applied, usually without significant errors, to junctions with legs of rectangular cross-section and to junctions having a branch leg of a cross-sectional shape different from that of the other legs.

Loss coefficients vary markedly with changes in the junction edge geometry, small radii or chamfers often markedly reducing the junction losses. If the geometry of a junction, with legs of different cross-sectional shapes, provides a more streamlined arrangement, then significantly lower losses may be obtained than for a junction with three circular cross-sectional legs and sharp junction edges.

13.1.3. FLOW STABILITY

Combining flow is a relatively stable process. Velocities increase through the junction in many combining junctions. This aids flow stability by reducing the tendency for transient movement, growth and decay of flow separation regions.

Dividing flows can lead to large flow instabilities that have caused structural failures of large symmetrical dividing T junctions. There are probably numerous situations in industry where systems and processes are adversely affected by dividing junction instabilities. These instabilities are associated with changes in flow patterns within junctions with the size and

location of flow separation regions changing as the incoming flow is biased first towards one outlet leg and then the other. Instabilities can be at a maximum at or close to the typical design operating conditions, such as a 50/50 split in a symmetrical dividing T junction. Under conditions of violently unsteady flow, head losses across a junction may be several times the predicted values. Chamfering a junction can reduce unstable flow, but in other cases it may induce unstable flow.

It is recommended that when the head losses after a symmetrical T junction do not exceed the junction loss by a factor of 10 and flow distribution is important, a symmetrical 180° T junction should not be used. Symmetrical T junctions are best avoided in large systems, systems with high velocities and systems with flexible pipework.

13.2. SHARP-EDGED COMBINING Ts (CLASS 1)

Performance charts showing contours of constant loss coefficients for sharp-edged combining Ts with legs 2 and 3 of the same area are given for:

1. 15° branch angle, K_{13} in Fig. 13.2, K_{23} in Fig. 13.3;

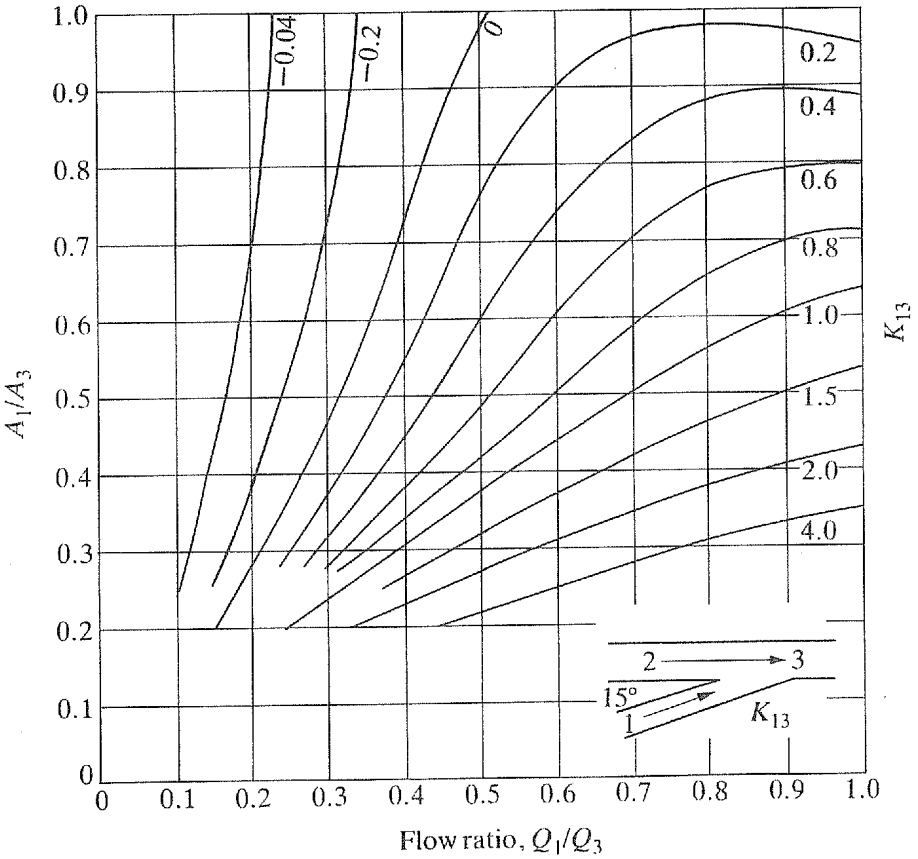

Fig. 13.2. Combining flow: branch angle 15°, loss coefficient K_{13}

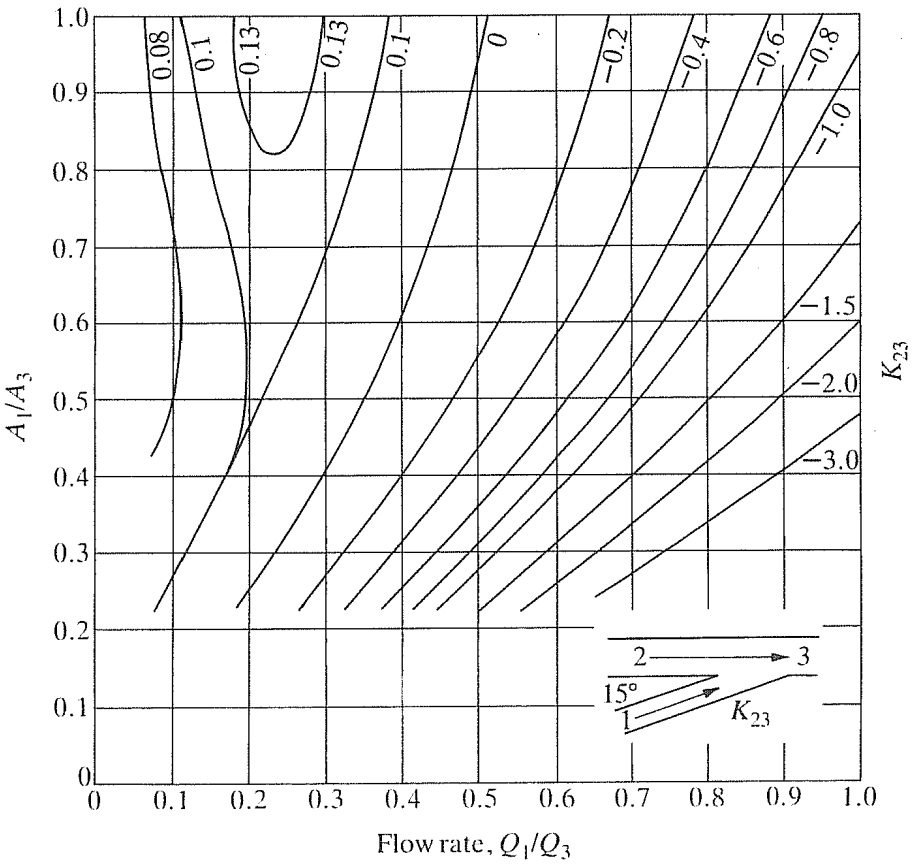

Fig. 13.3. Combining flow: branch angle 15°, loss coefficient K_{23}

2. 30° branch angle, K_{13} in Fig. 13.4†, K_{23} in Fig. 13.5;
3. 45° branch angle, K_{13} in Fig. 13.6, K_{23} in Fig. 13.7;
4. 60° branch angle, K_{13} in Fig. 13.8, K_{23} in Fig. 13.9;
5. 90° branch angle, K_{13} in Fig. 13.10†, K_{23} in Fig. 13.11;
6. 120° branch angle, K_{13} in Fig. 13.12, K_{23} in Fig. 13.13.

13.2.1. INLET AND OUTLET CONDITIONS (CLASS 2)

Provided the outlet leg 3 is three or more diameters long, system losses will usually not be underestimated provided the inlet legs 1 and 2 are:

1. more than one diameter long if the upstream component is a bend of $r/d > 1.5$ or any component with a loss coefficient less than 0.2 at a Reynolds number of 10^6; or
2. more than three diameters long.

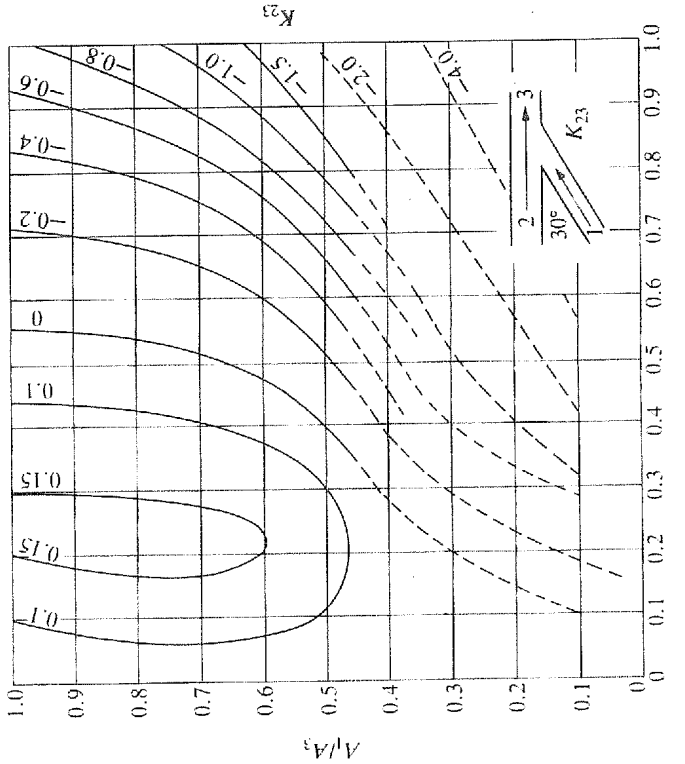

Fig. 13.5. Combining flow: branch angle 30°, loss coefficient K_{23}

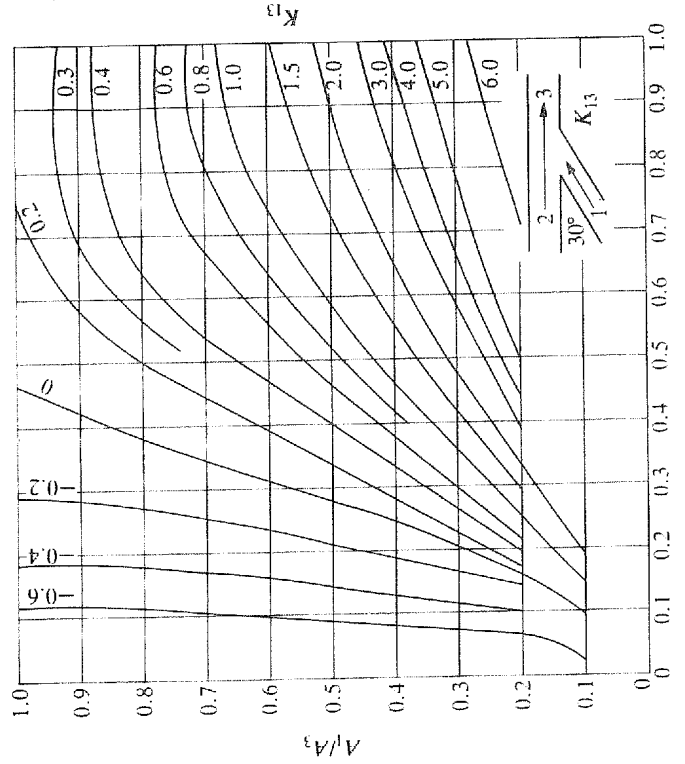

Fig. 13.4†. Combining flow: branch angle 30°, loss coefficient K_{13}

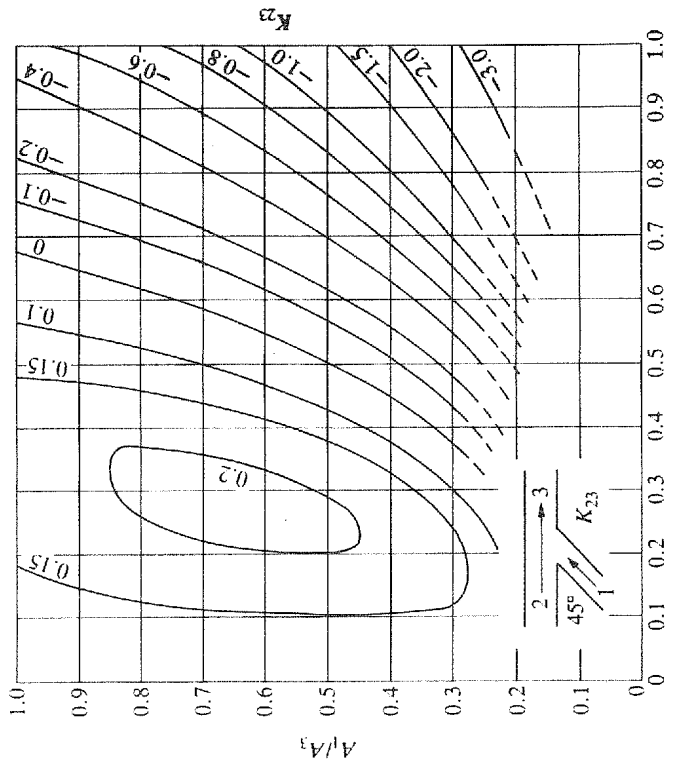

Fig. 13.7†. Combining flow: branch angle 45°, loss coefficient K_{23}

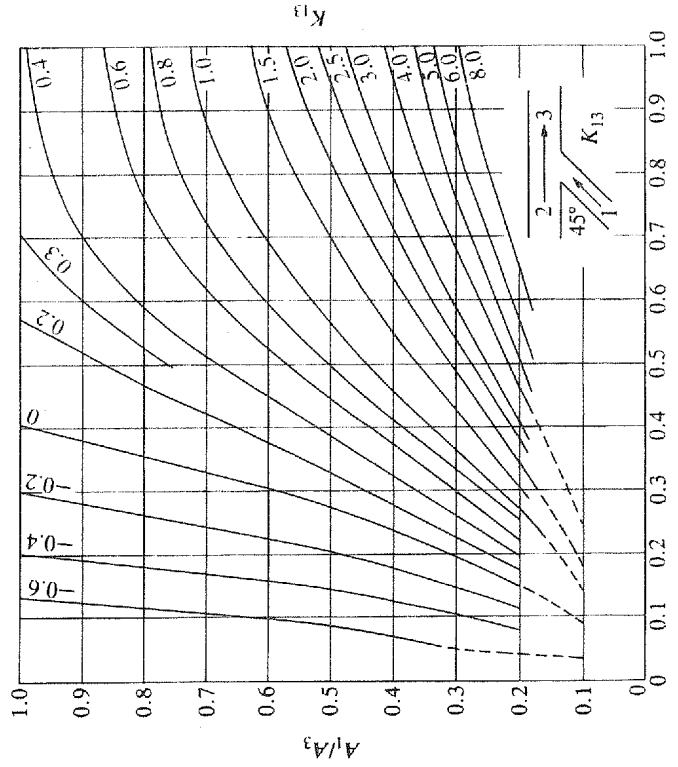

Fig. 13.6. Combining flow: branch angle 45°, loss coefficient K_{13}

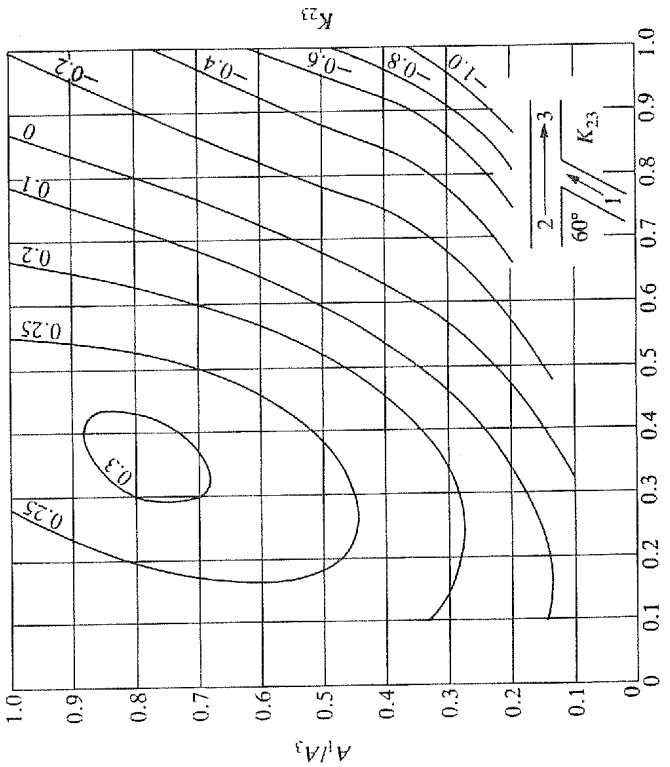

Fig. 13.9. Combining flow: branch angle 60°, loss coefficient K_{23}

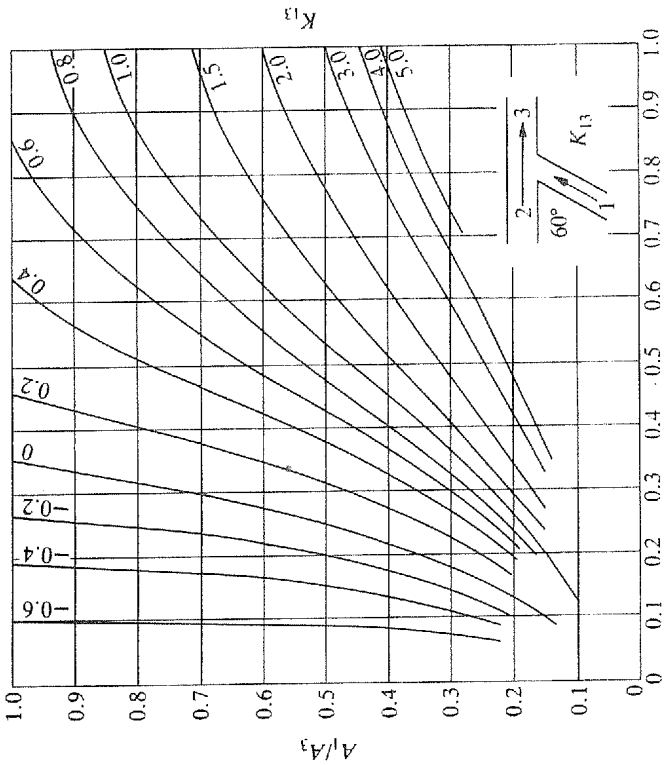

Fig. 13.8. Combining flow: branch angle 60°, loss coefficient K_{13}

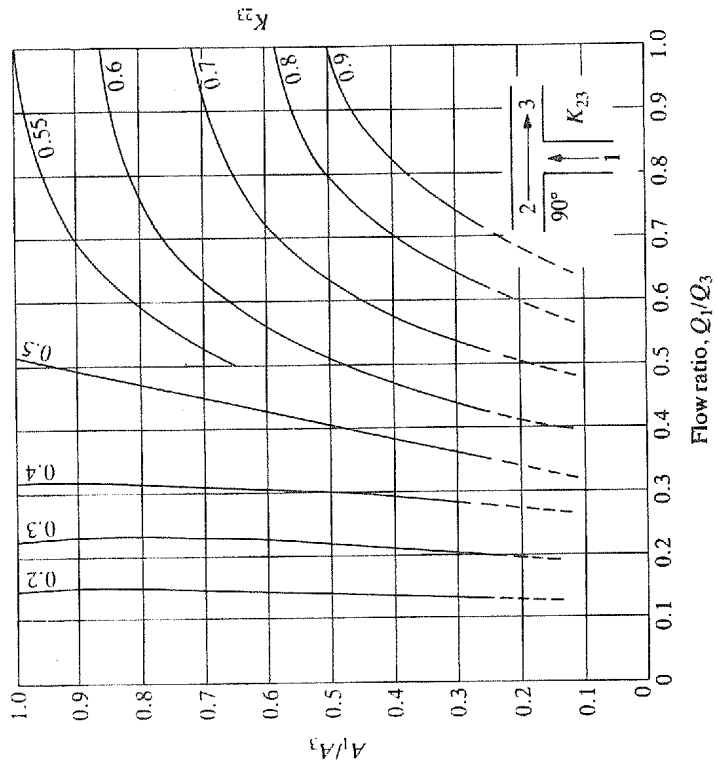

Fig. 13.11. Combining flow: branch angle 90°, loss coefficient K_{23}

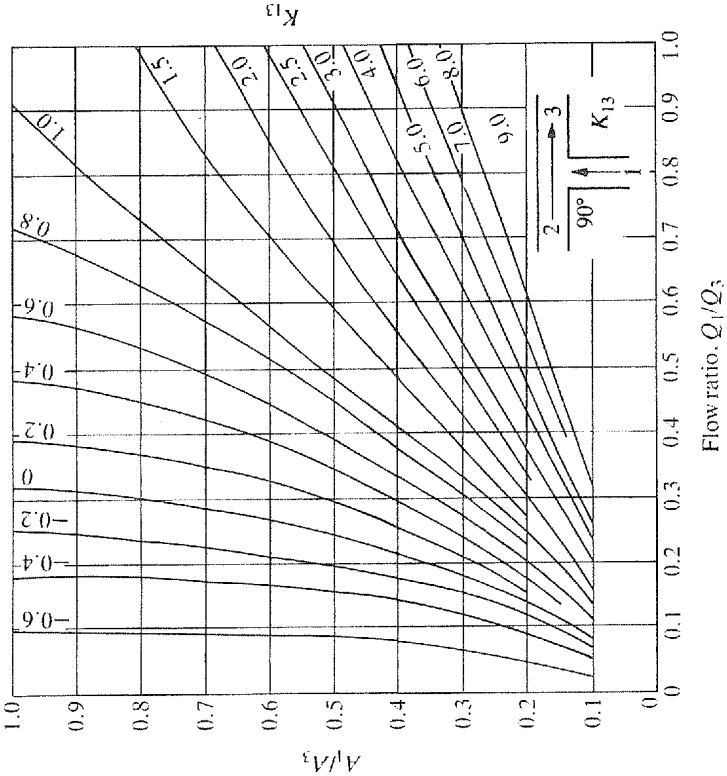

Fig. 13.10†. Combining flow: branch angle 90°, loss coefficient K_{13}

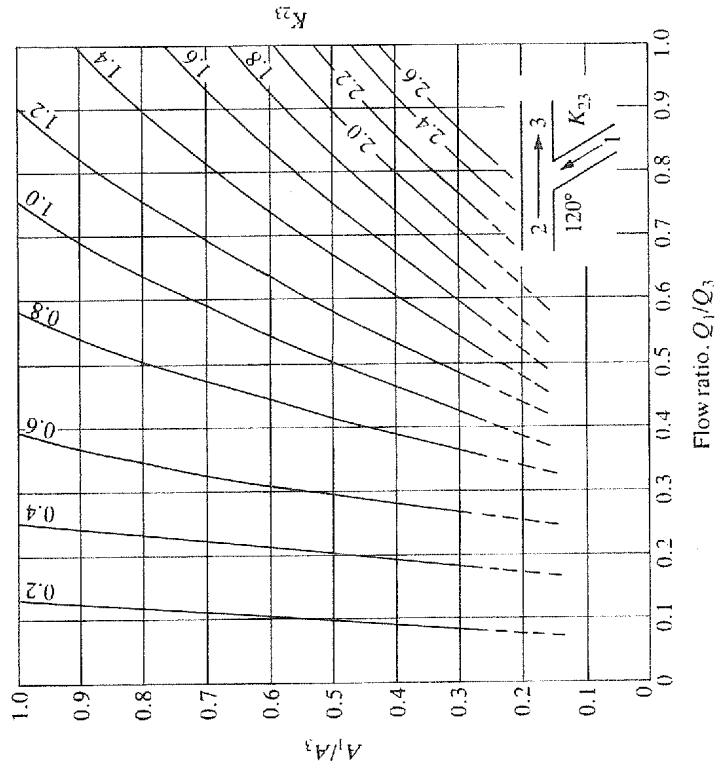

Fig. 13.13. Combining flow: branch angle 120°, loss coefficient K_{23}

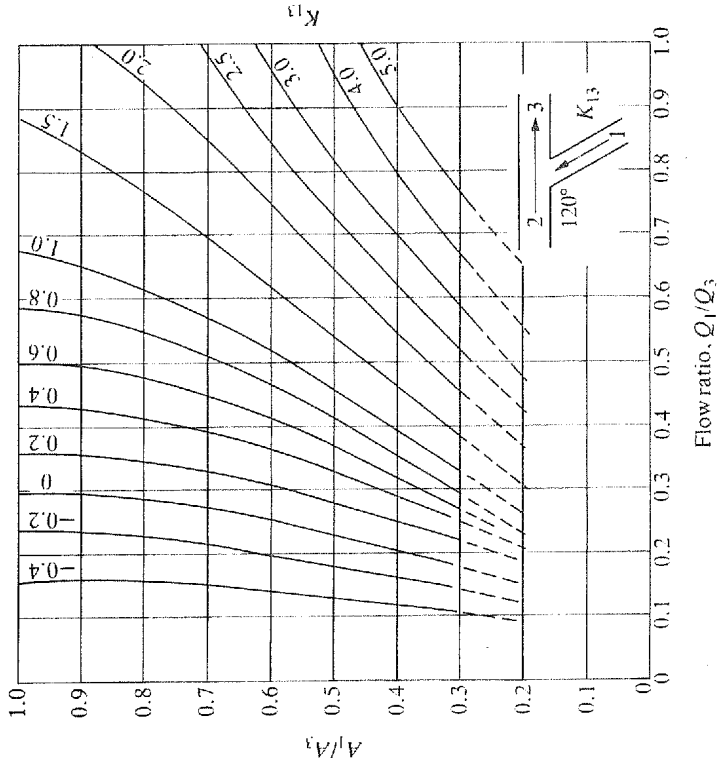

Fig. 13.12. Combining flow: branch angle 120°, loss coefficient K_{13}

13.3. EFFECT OF RADII ON COEFFICIENTS OF COMBINING Ts (CLASS 2)

A radius or chamfer between legs 1 and 3 has an effect on both K_{13} and K_{23}. About 70 per cent of the possible reduction is obtained with a radii or chamfer of 0.1 of the branch diameter. Loss coefficients for 90° junctions with radii between legs 1 and 3 of $0.1D_1$ are given in Figs 13.14† and 13.15†.

In cases where the flow out of leg 1 is small, a chamfer or radii between legs 2 and 1 will cause the through flow to expand into leg 1 with an increased loss.

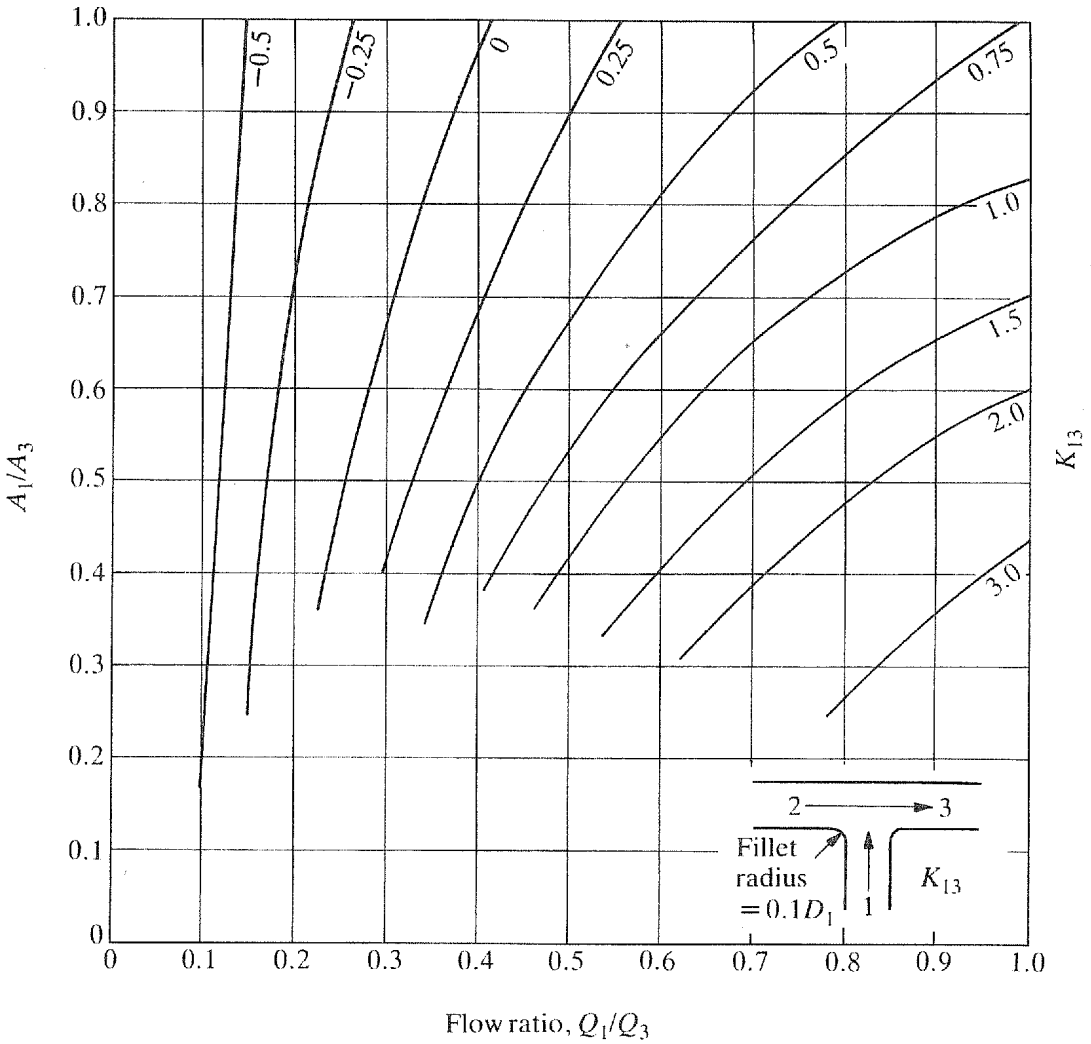

Fig. 13.14†. Combining flow: branch angle 90°, loss coefficient K_{13} for a radius of $0.1D_1$

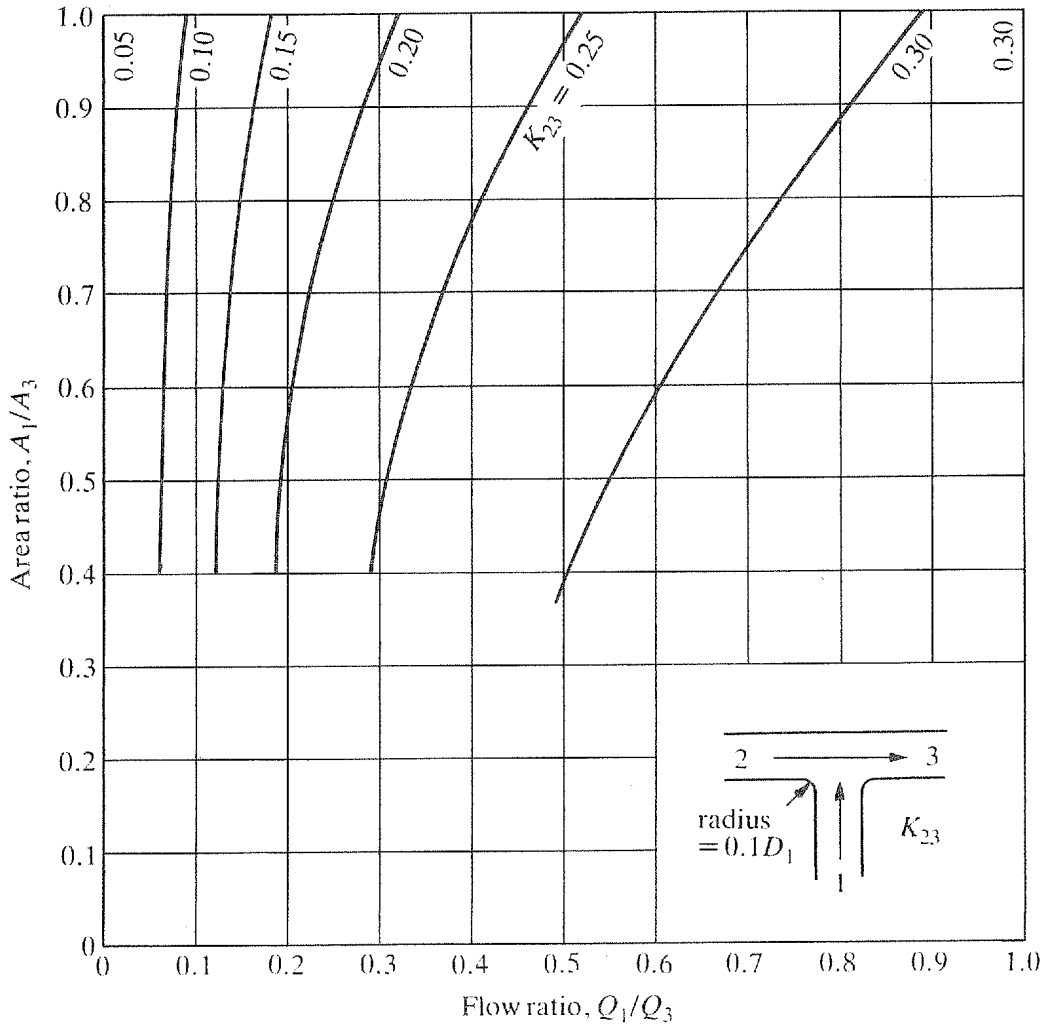

Fig. 13.15†. Combining flow: branch angle 90°, losscoefficient K_{23} for a radius of $0.1D_1$

13.4. SYMMETRICAL COMBINING JUNCTIONS

Loss coefficients, K_{13}, for symmetrical combining T junctions with three legs of equal area are given in Fig. 13.16 for four junction radii (class 1).

Loss coefficients K_{13} and K_{23} for symmetrical 90° combining Y junctions with three legs of equal area are given in Fig. 13.16 (class 2).

A performance chart showing contours of constant loss coefficients is given in Fig. 13.17 for combining Y junctions with areas $A_1 = A_2$ and $A_1 + A_2 = A_3$ (class 2). Figure 13.18 is a performance chart for combining Y junctions with $A_1 = A_2 = A_3$ (class 3).

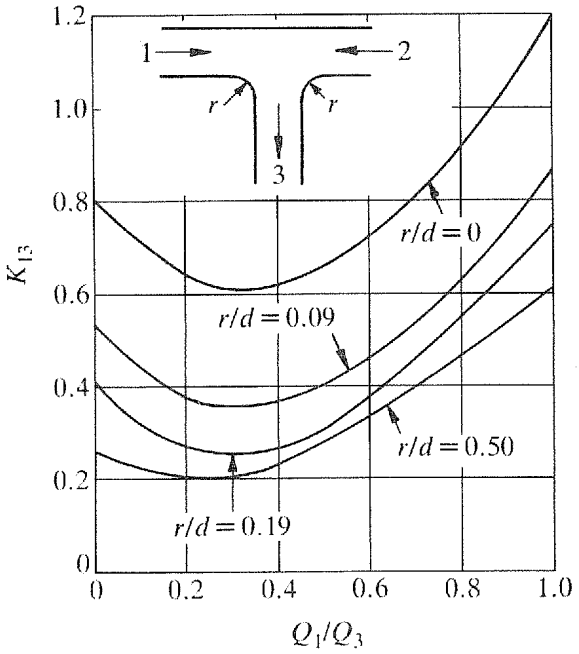

Fig. 13.16. Symmetrical combining T junction with legs of equal area

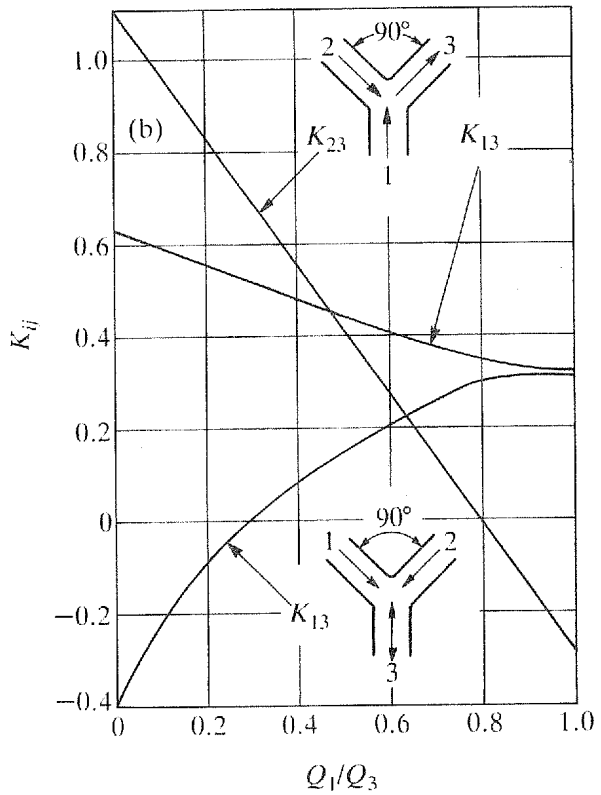

Fig. 13.16(1). Symmetrical 90° combining Y junctions with legs of equal area

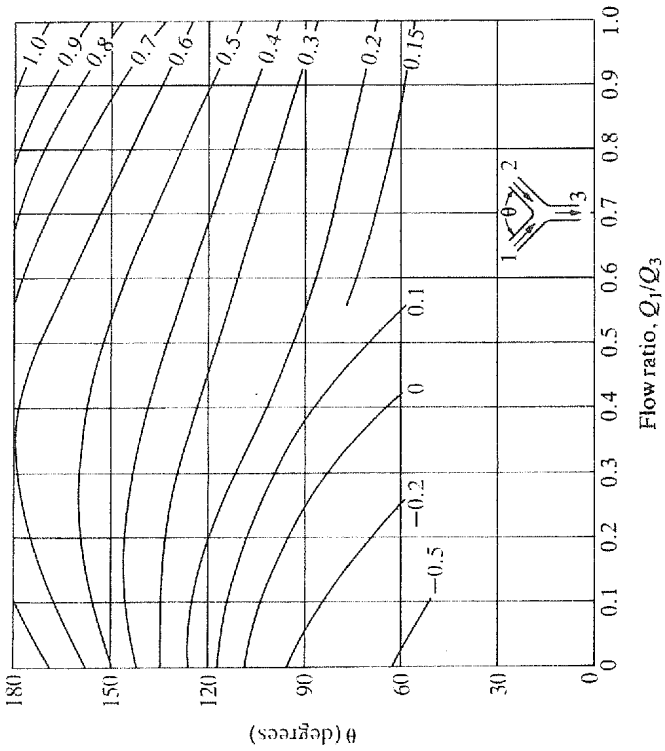

Fig. 13.18. Combining flow: symmetrical Y junction with $A_1 + A_2 = A_3$, loss coefficient K_{23}

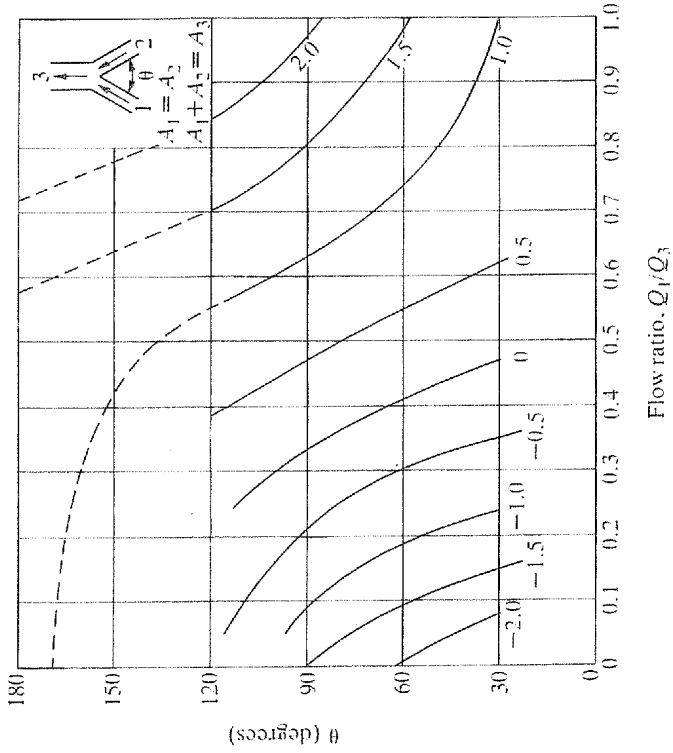

Fig. 13.17. Combining flow: symmetrical Y junction with $A_1 + A_2 = A_3$, loss coefficient K_{13}

13.5. SHARP-EDGED DIVIDING Ts (CLASS 2)

Performance charts showing contours of constant loss coefficients, K_{31}, for flow from the main, leg 3, to the branch, leg 1, are given for:

1. 45° branch, Fig. 13.19†;
2. 60° branch, Fig. 13.20†;
3. 90° branch, Fig. 13.21†;
4. 120° branch, Fig. 13.22.

The through flow loss coefficient, K_{32}, is virtually independent of the branch angle, the junction radii and the area ratio. K_{32} is plotted in Fig. 13.23 against the flow ratio Q_1/Q_3.

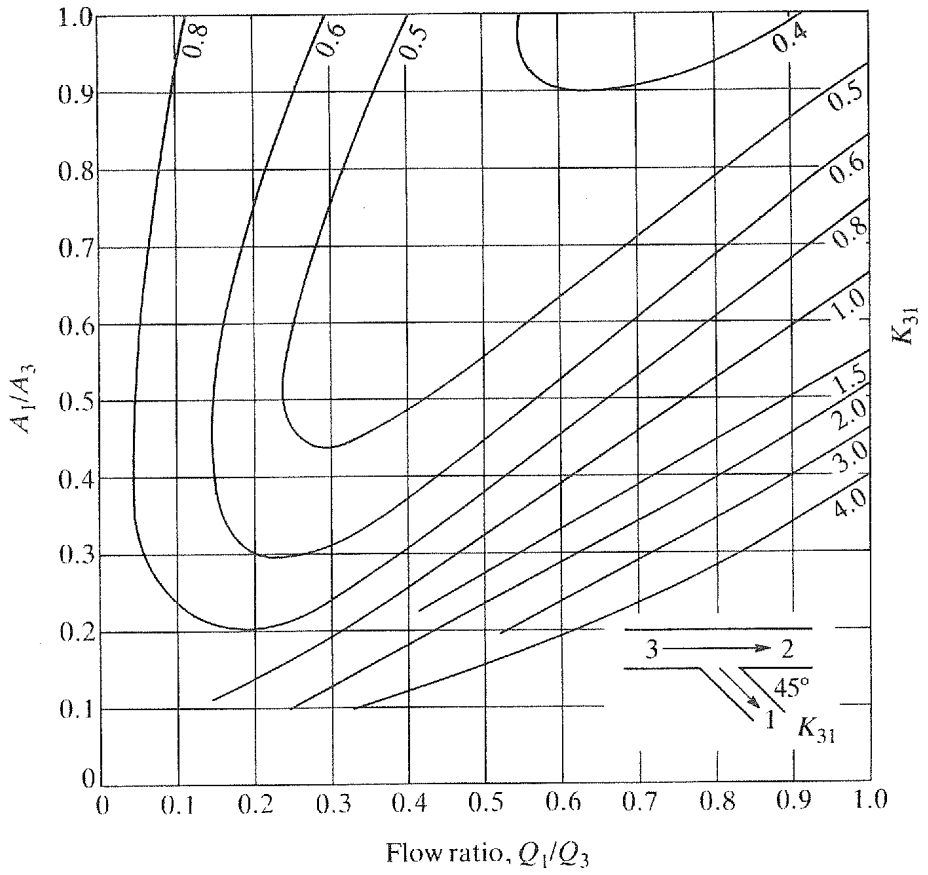

Fig. 13.19†. Dividing flow: branch angle 45°, loss coefficient K_{31}

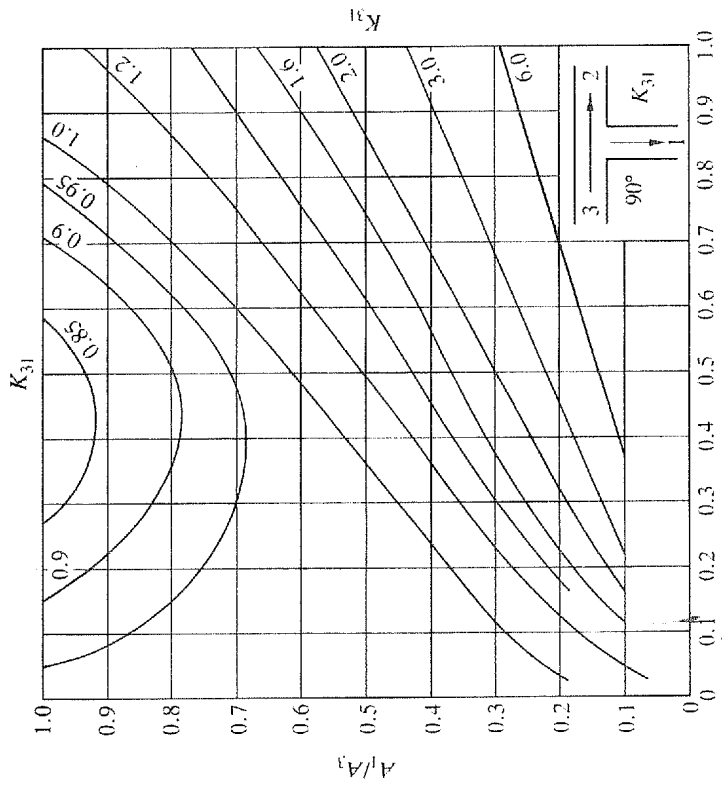

Fig. 13.21†. Dividing flow: branch angle 90°, loss coefficient K_{31}

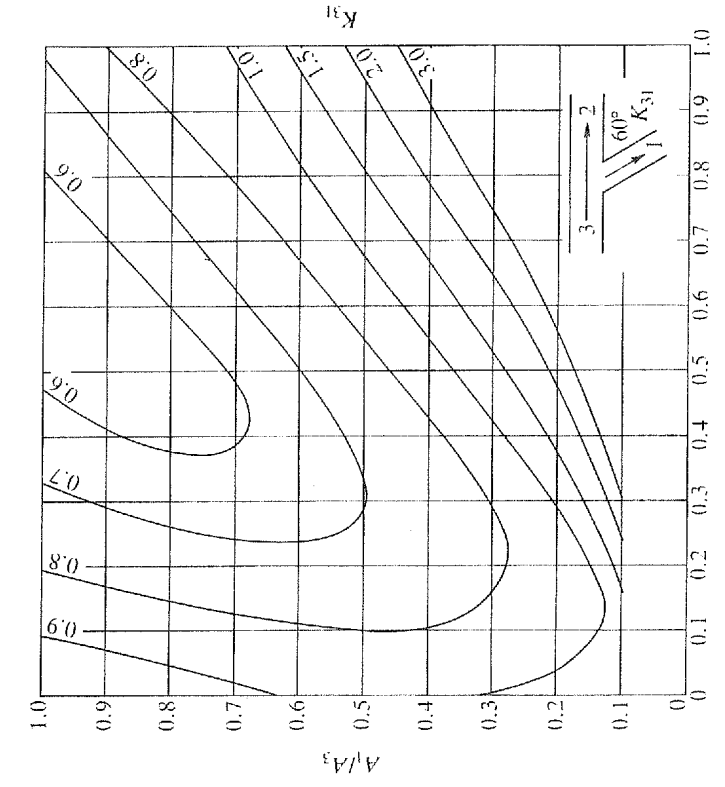

Fig. 13.20†. Dividing flow: branch angle 60°, loss coefficient K_{31}

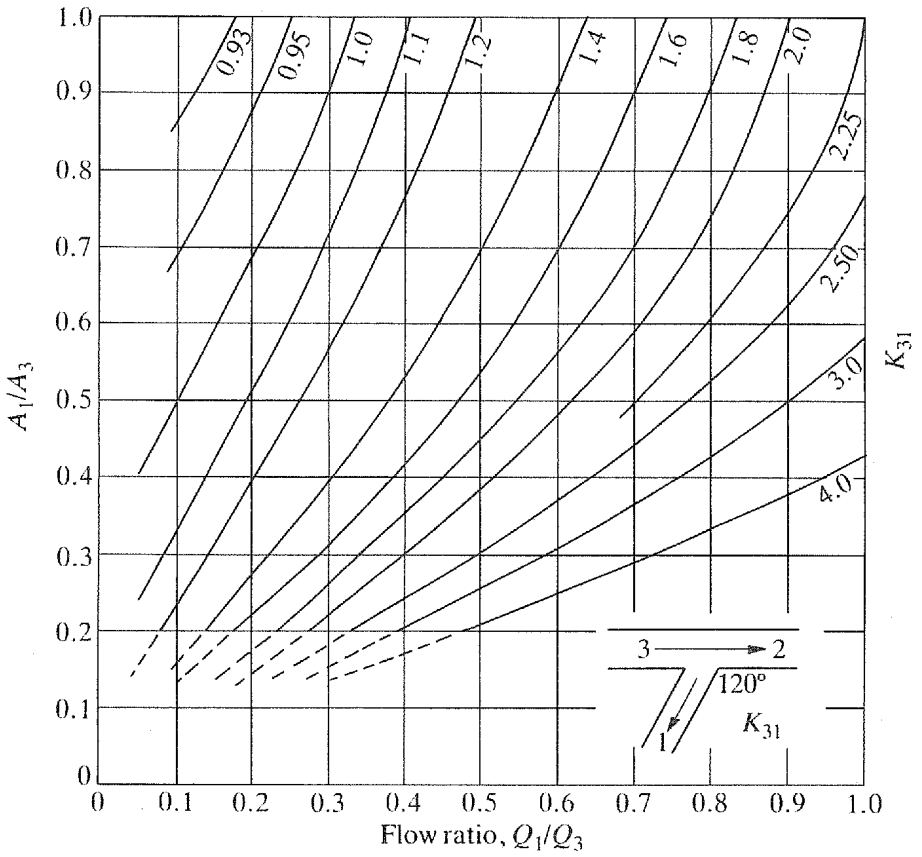

Fig. 13.22. Dividing flow: branch angle 120°, loss coefficient K_{31}

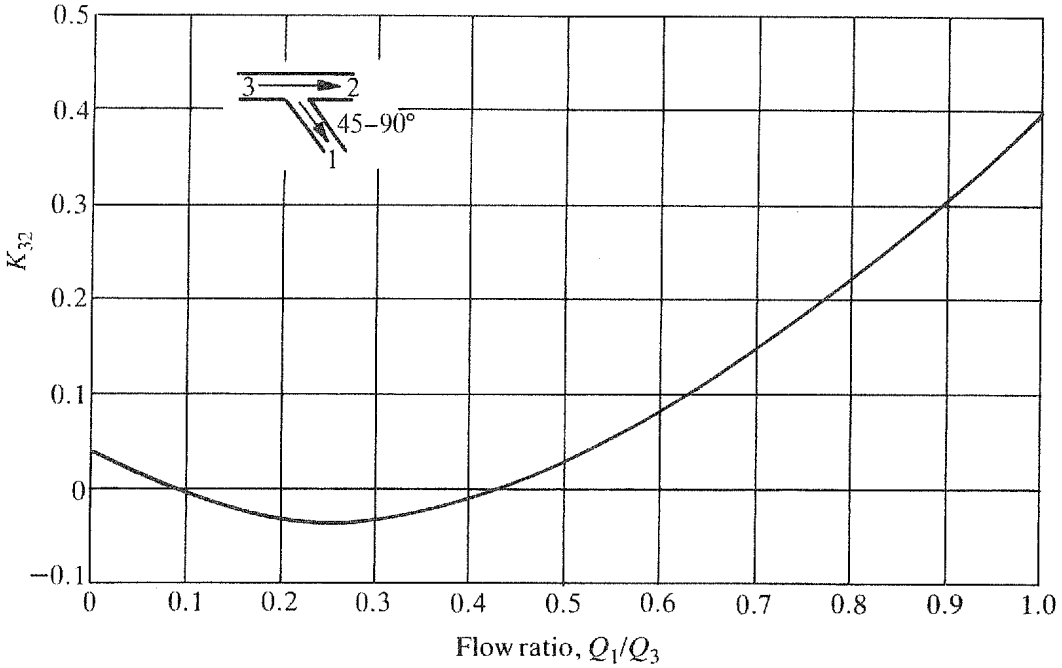

Fig. 13.23. Dividing flow: branch angles of 45–90°, loss coefficient K_{32}

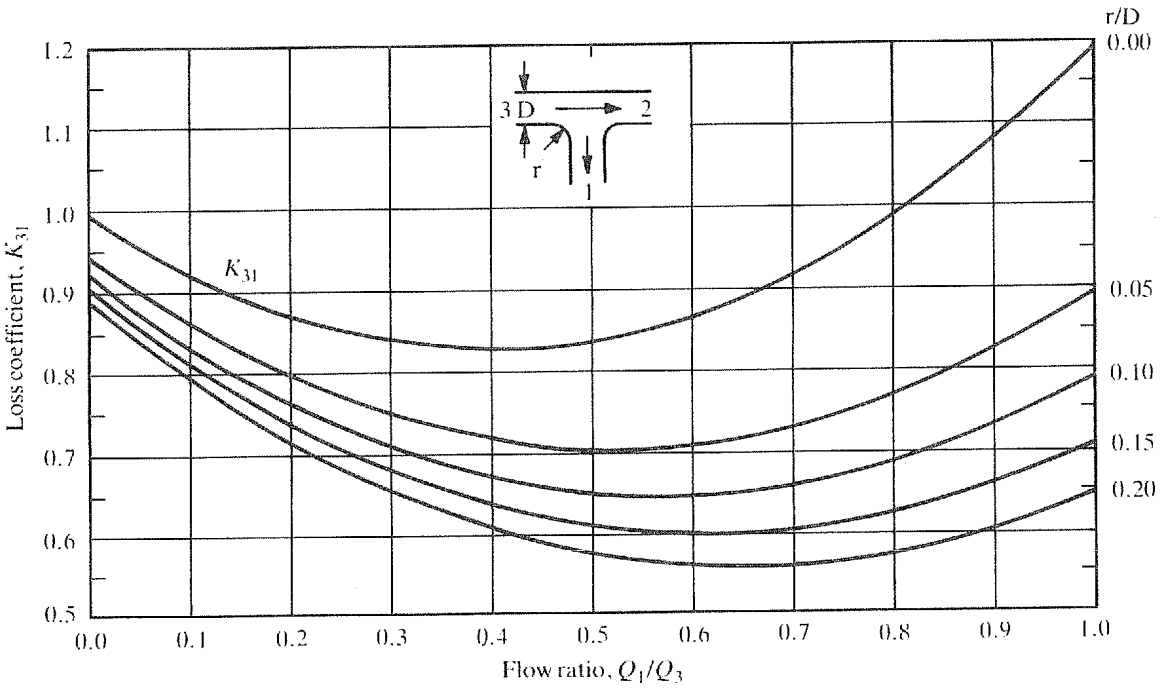

Fig. 13.24(1). Dividing flow: branch angles 90°, $A_1 = A_3$ loss coefficient

13.5.1. INLET AND OUTLET CONDITIONS (CLASS 2)

Provided the outlet legs 1 and 2 are three or more diameters long, then the loss in leg 2 is unlikely to be underestimated if:

1. leg 3 is two or more diameters long if the upstream component is a bend of $r/d > 1$; or
2. leg 3 is four or more diameters long.

When leg 3 is less than 10 diameters long the negative values of K_{32} predicted in Fig. 13.23 are unlikely to occur. If leg 3 is less than 10 diameters long and Q_1/Q_3 is less than 0.4, a loss of $0.10(U_3^2 - U_2^2)/2g$ can be assumed for K_{32} (class 3). If legs 2 and 3 are of rectangular cross-section, obtain K_{32} from Fig. 13.41.

13.6. EFFECT OF RADII ON COEFFICIENTS OF DIVIDING Ts

The through flow coefficients K_{32} are virtually unaffected by radii at the junction. Loss coefficients K_{31} continue to fall as a radius or chamfer is varied from zero up to the equivalent of the branch diameter.

Figure 13.24(1) gives loss coefficients K_{31} for 90° T-junctions with $A_1 = A_3$ and radii between legs 1 and 3.

Loss coefficients for 90° junctions with radii between legs 1 and 3 of $0.1D$ are given in Fig. 13.25† for K_{31}.

13.7. IMPROVED PERFORMANCE OF DIVIDING Ts (CLASS 2)

Compared with many loss coefficients, the coefficients K_{31} for flow from the main to the branch are excessive. In large or high velocity systems special measures to reduce head losses are often justified. The basic approach is to diffuse the flow before the junction. Figure 13.26 is a performance chart for a well designed 45° junction. If the branch is followed within five diameters by a 45° bend of $r/d > 2$, to give a total angle of 90°, the bend loss coefficient will be about half the isolated bend value found from Chapter 9.

13.8. SYMMETRICAL DIVIDING JUNCTIONS

Loss coefficients K_{31} for symmetrically dividing T junctions with the legs of equal area are given in Fig. 13.27 for four junction radii (class 1). The increased head losses with a small flow into either leg 1 or 2 with small junction radii should be noted as it is probably the result of flow instabilities.

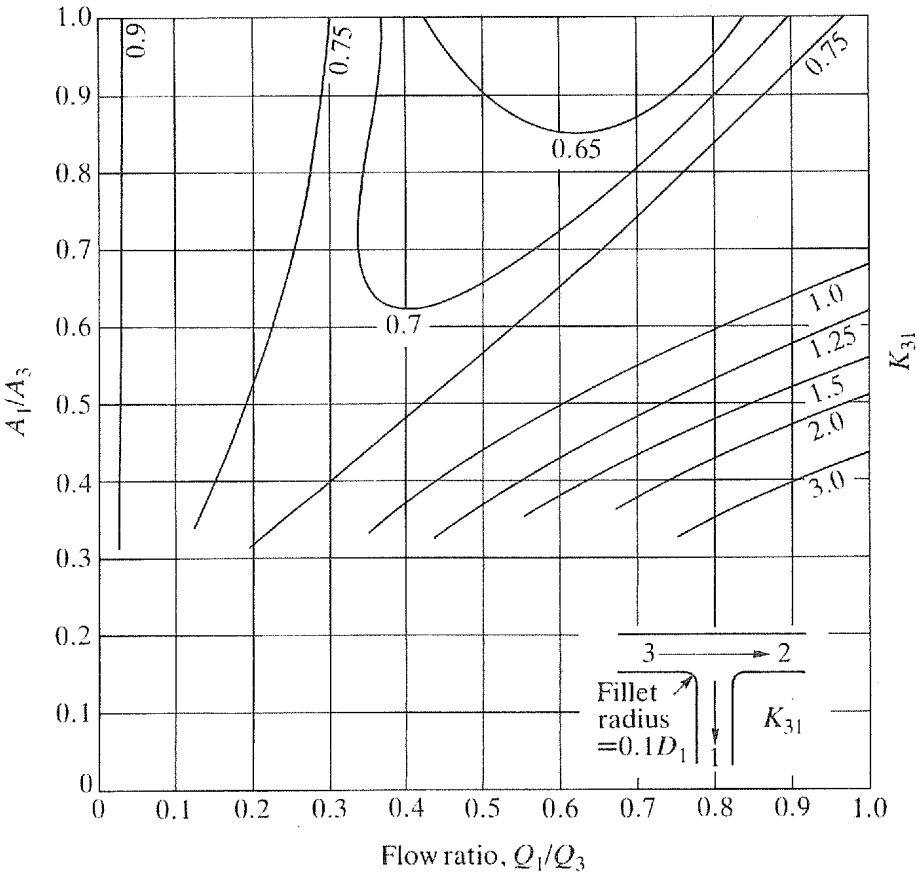

Fig. 13.25†. Dividing flow: branch angle 90°, loss coefficient K_{31} for a radius of $0.1D_1$

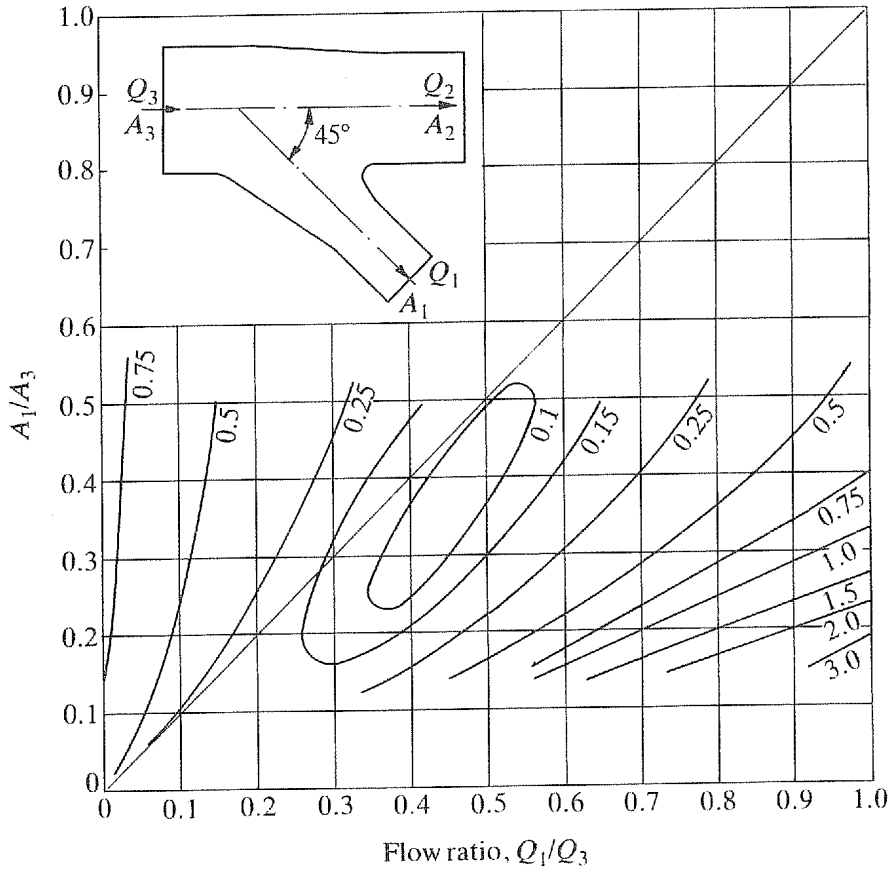

Fig. 13.26. Improved performance 45° dividing junction, $A_2 = A_3 - A_1$, loss coefficient K_{31}

Loss coefficients K_{31} and K_{32} for symmetrical 90° dividing Y junctions with three legs of equal area are given in Fig. 13.27(1) (class 1).

Performance charts showing contours of constant loss coefficients are given in Fig. 13.28 for dividing Y junctions with area $A_1 = A_2$ and $A_1 + A_2 = A_3$ (class 2) and in Fig. 13.29 for dividing Y junctions with $A_1 = A_2 = A_3$ (class 2).

13.9. JUNCTIONS WITH MORE THAN THREE LEGS

Information available for junctions with more than three legs indicates that loss coefficients for combining flow can be predicted reasonably well using information for T junctions for situations of similar flow. In the case of dividing flow, predictions of losses in symmetrical dividing junctions can be unreliable because of the possibility of large scale flow instabilities which give rise to high losses.

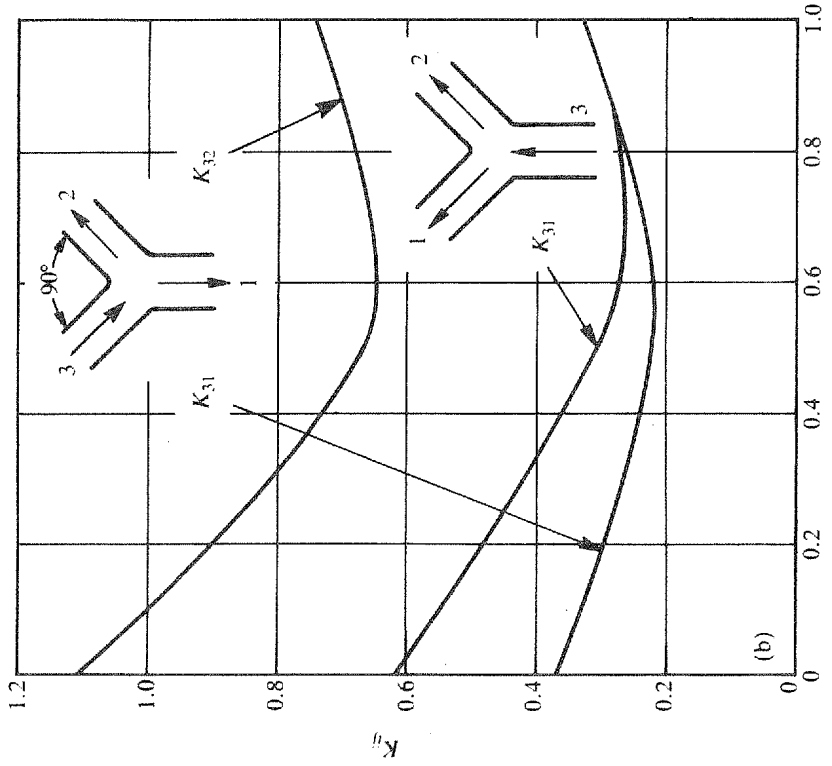

Fig. 13.27(1). Symmetrical 90° dividing Y junction with legs of equal area

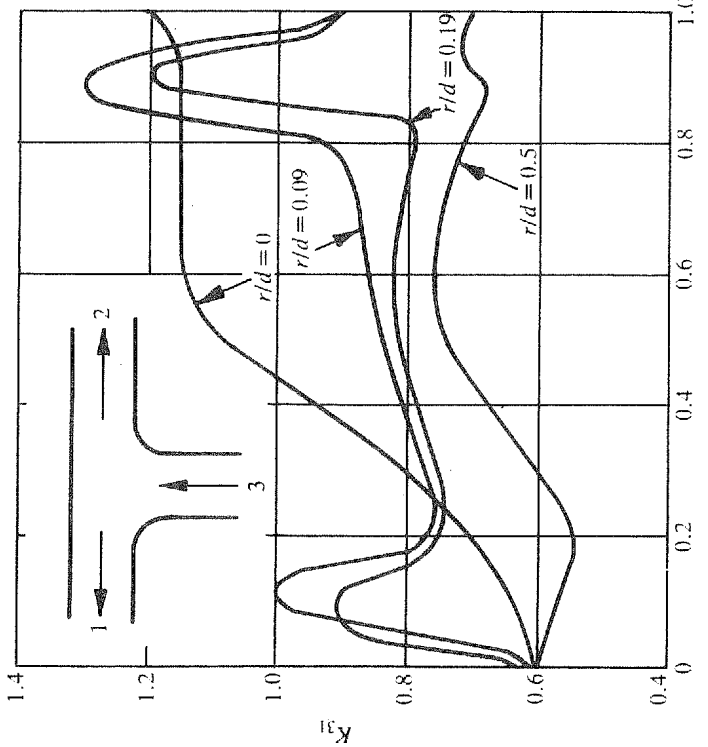

Fig. 13.27. Symmetrical dividing T junction with legs of equal area

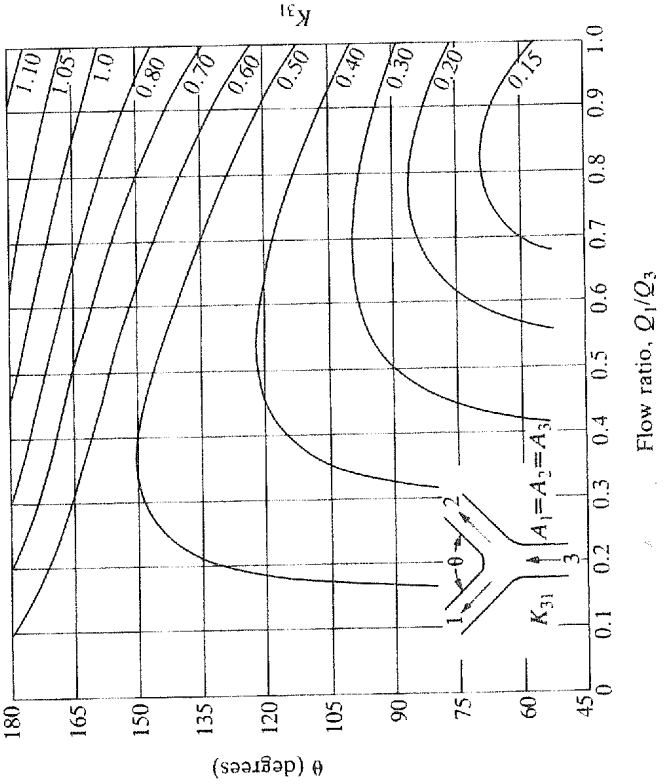

Fig. 13.29. Dividing flow: symmetrical Y junction with $A_1 = A_2 = A_3$, loss coefficient K_{31}

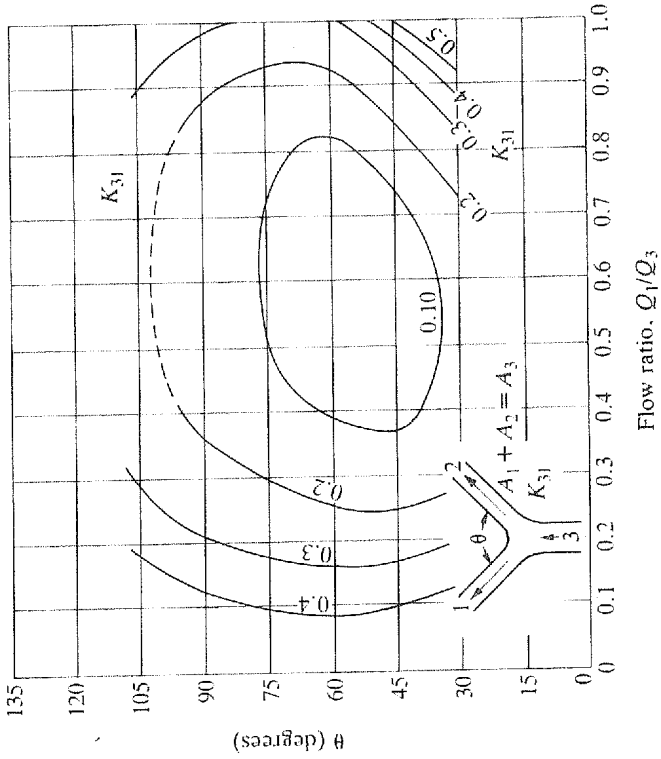

Fig. 13.28. Dividing flow: symmetrical Y junction with $A_1 + A_2 = A_3$, loss coefficient K_{31}

13.9.1. FOUR-, FIVE- AND SIX-LEGGED COMBINING JUNCTIONS (CLASS 2)

Loss coefficients for the six-legged junction in Fig. 13.29(1) are given as follows.

1. In Fig. 13.29(2), with two branches sealed off and equal flow in the remaining branches. Also plotted in this figure are the equivalent T junction loss coefficients from Fig. 13.10. The junction coefficients are slightly higher than, but follow closely the trends of, the T junction coefficients.
2. In Fig. 13.29(3), for leg 6 blanked off and equal flow in the four branch legs. The loss coefficient is higher, but not substantially so, than that for a symmetrical combining 180° T junction.
3. In Fig. 13.29(4), with equal flow in four branch legs. The end points of the K_{13} and K_{36} curves and their general shape agree with those for combining T junctions.

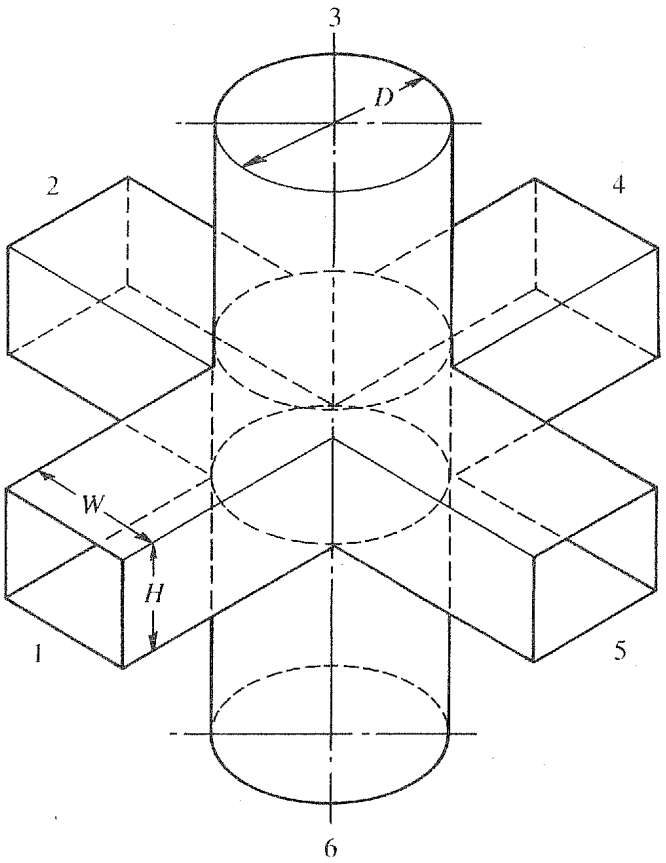

Fig. 13.29(1). Six-legged junction ($W=0.71D$, $H=0.55D$, area of legs $1+2+4+5=2\times$ area of leg 3)

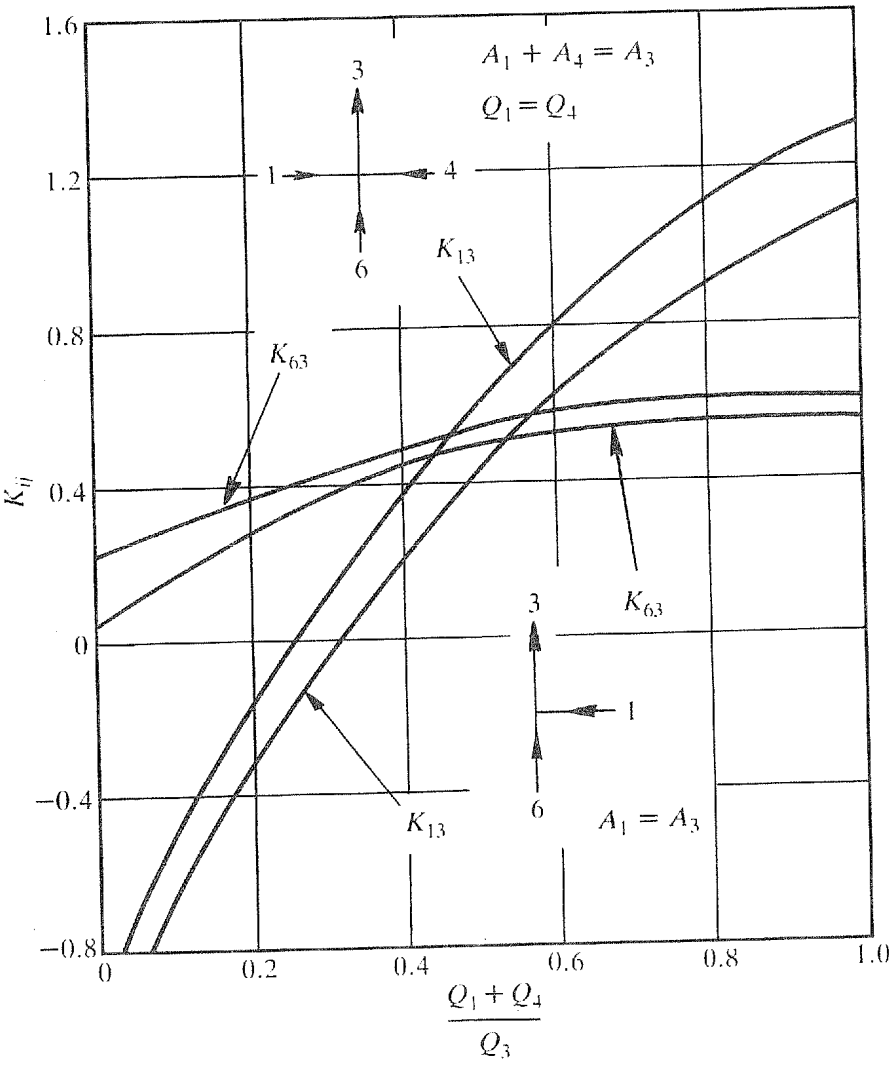

Fig. 13.29(2). Combining flow loss coefficients for the junction in Fig. 13.29(1) with two side branches sealed off

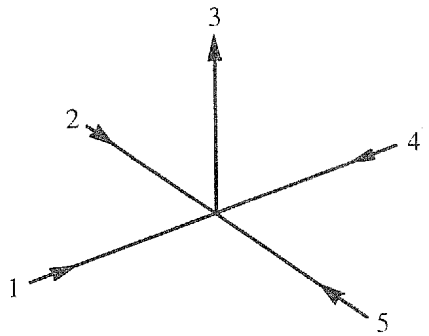

$Q_1 = Q_2 = Q_4 = Q_5$

$K_{13} = 0.78$

From Fig. 13.18 for
$\theta = 180°$ and $Q_1/Q_3 = 0.5$

$K_{13} = 0.66$

Fig. 13.29(3). Combining flow loss coefficients for the junction in Fig. 13.29(1) with leg 6 sealed off

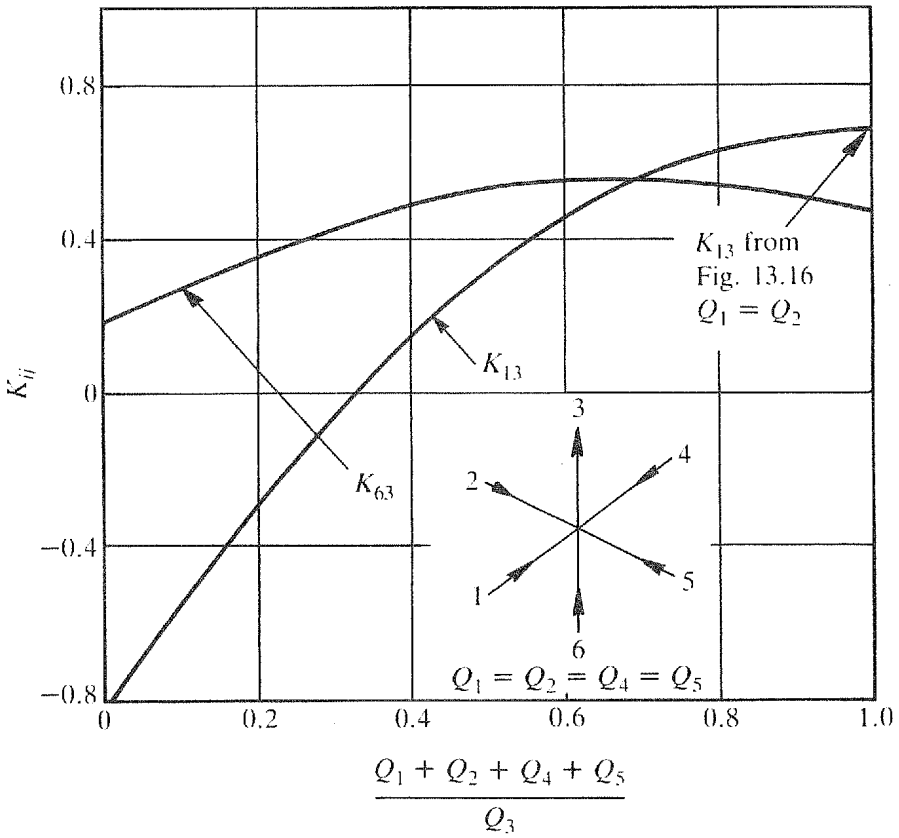

Fig. 13.29(4). Combining flow loss coefficients for the junction in Fig. 13.29(1)

13.9.2. FOUR-LEGGED DIVIDING JUNCTION (CLASS 2)

Loss coefficients for four-way dividing junctions with all legs of equal area are given in Fig. 13.30 for branch flows and in Fig. 13.31 for through flows. The peak in K_{31} at low Q_2/Q_3, and for nearly balanced branch flows, corresponds to an expected unstable flow region. Generally, loss coefficients agree with T junction losses from Figs 13.21 and 13.23 with $A_1/A_3 = 1$.

13.9.3. FOUR-, FIVE- and SIX-LEGGED DIVIDING FLOW (CLASS 3)

Loss coefficients for the six-legged junction in Fig. 13.29(1) are given as follows.

1. In Fig. 13.31(1), for four branches with equal flow and for two branches sealed off and equal flow in the other two branches. Also shown are the T-junction loss coefficients K_{31} from Fig. 13.21† and K_{32} from Fig. 13.23. With high through flow all of the curves are similar, but when most of the flow is into the branches the two-branch configuration has very high losses due to flow instability.

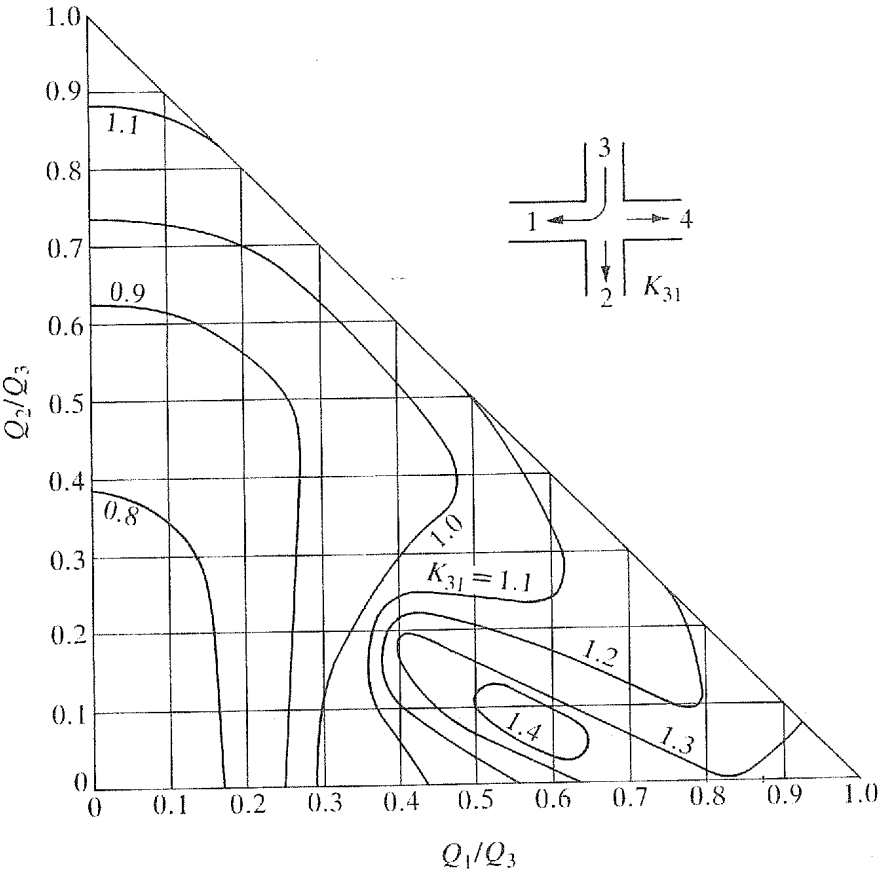

Fig. 13.30. Four-legged dividing junction loss coefficient K_{31}

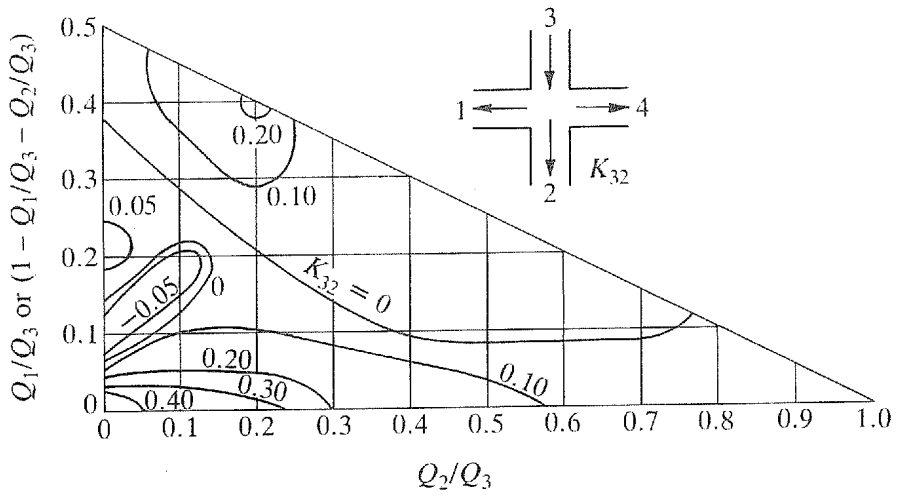

Fig. 13.31. Four-legged dividing junction loss coefficient K_{32}

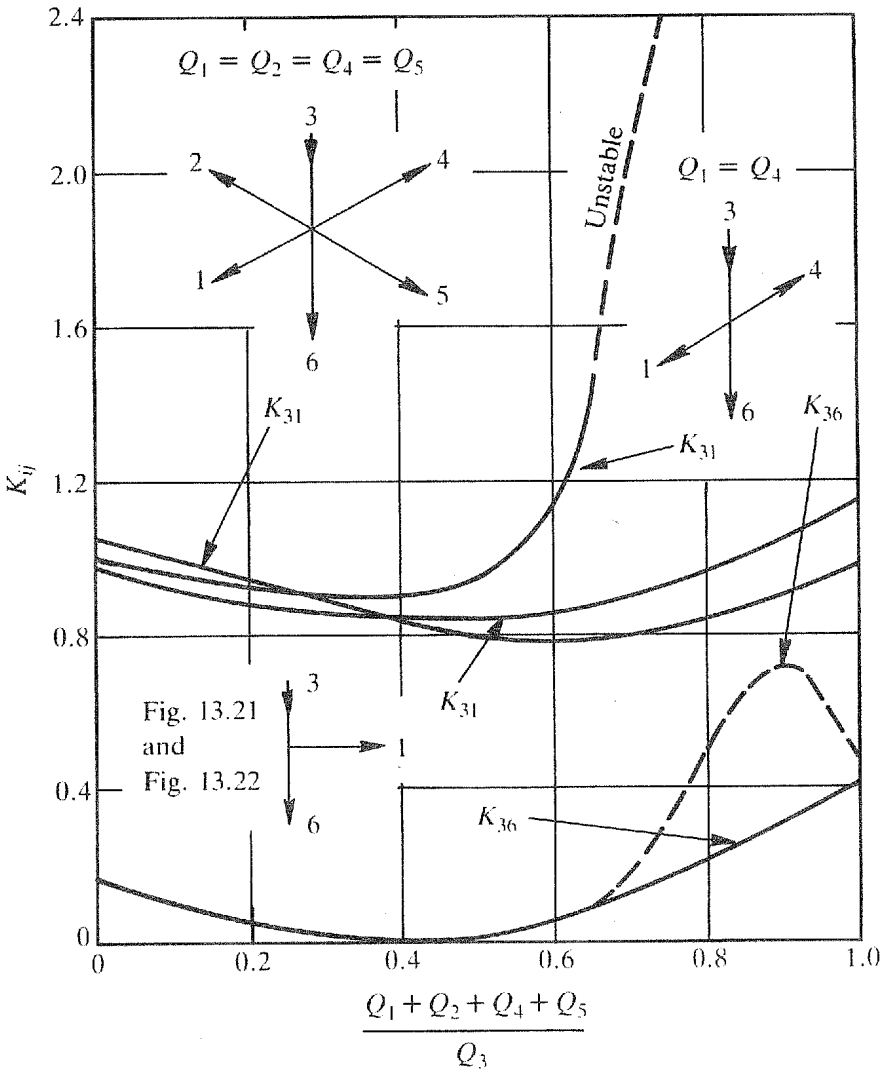

Fig. 13.31(1). Dividing flow loss coefficients for the junction in Fig. 13.29(1)

2. In Fig. 13.31(2), for leg 6 sealed off and various flow distributions. When legs 2 and 5 are sealed off, rather than blanked off, six diameters along the legs the flow is unstable and the loss coefficients are much higher. Cavities at a symmetrical junction may stabilise the flow.

13.10. EFFECTS OF CROSS-SECTIONAL SHAPE (CLASS 2)

When experimental loss coefficients for different cross-sectional shapes are compared, on the basis of area and flow ratios, the trends shown by the coefficients are similar.

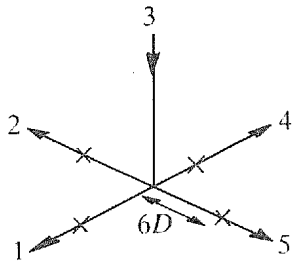

$K_{31} = 0.55$	$Q_1 = Q_2 = Q_4 = Q_5$
$K_{31} = 0.70$	$Q_1 = Q_4 = 0.35$
$K_{32} = 0.48$	$Q_2 = Q_5 = 0.15$
$K_{31} = 0.75$	$Q_1 = Q_2 = Q_4$
$K_{35} = 0.43$	$Q_5 = 0$
$K_{31} = 1.17$	$Q_1 = Q_4$
$K_{32} = 0.52$	$Q_2 = Q_5 = 0$

Fig. 13.31(2). Dividing flow loss coefficients for the junction in Fig. 13.29(1) with no leg 6

Loss coefficients K_{13} and K_{23} for combining flow are given for the following arrangements having legs 2 and 3 of square cross-section:

1. branch leg 1 of square cross-section of the same dimensions as legs 2 and 3 (Figs 13.32 and 13.33);
2. branch leg 1 of circular cross-section having a diameter equal to the through flow width (Figs 13.34 and 13.35); and
3. branch leg 1 of circular cross-section having a diameter 0.67 of the through flow width (Figs 13.36 and 13.37).

Also shown in Figs 13.32–13.37 are loss coefficients for T junctions of circular cross-section. The loss coefficients for the square cross-sections are slightly higher, but this may in part be due to "sharp edges" as the square cross-section values are for much larger and more accurately made Ts. Also chamfers may not be as effective as radii.

Loss coefficients K_{31} for dividing flow are given for the following arrangements having legs 2 and 3 of square cross-section:

1. branch leg 1 of square cross-section of same dimensions as legs 2 and 3 (Fig. 13.38);
2. branch leg 1 of circular cross-section having a diameter equal to the through flow width (Fig. 13.39); and
3. branch leg 1 of circular cross-section having a diameter of 0.67 of the through flow width (Fig. 13.40).

The through flow loss coefficients K_{32} are given in Fig. 13.41.

Also shown in Fig. 13.38 are the loss coefficients for circular cross-section Ts. Loss coefficients for square and circular cross-sections are similar. Available data for the branches of smaller area ratio are not sufficiently accurate to make any useful comparisons. The

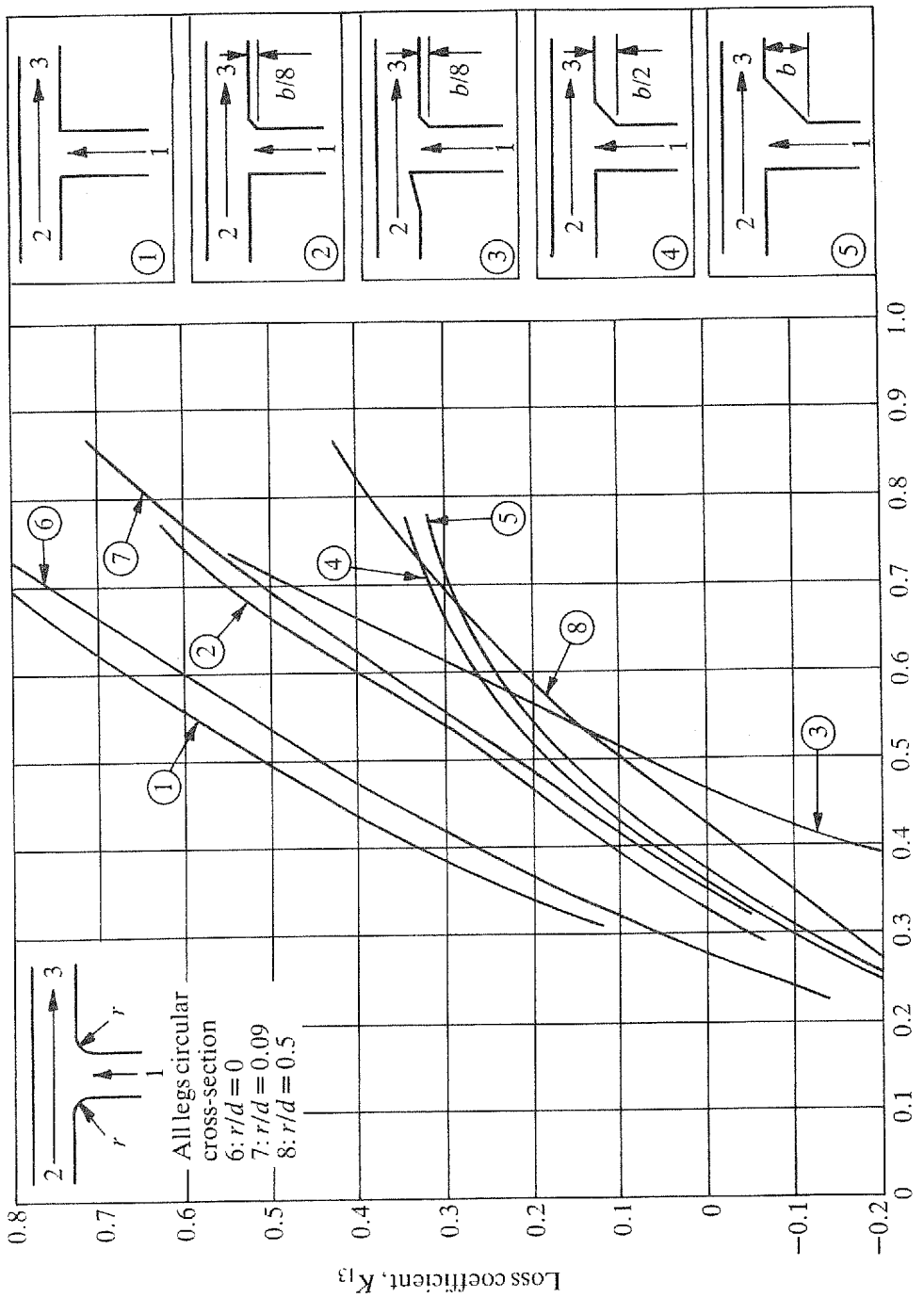

Fig. 13.32. Combining flow: loss coefficients K_{13}. Arrangements 1–5, all legs square cross-section; arrangements 6–8, all legs circular cross-section

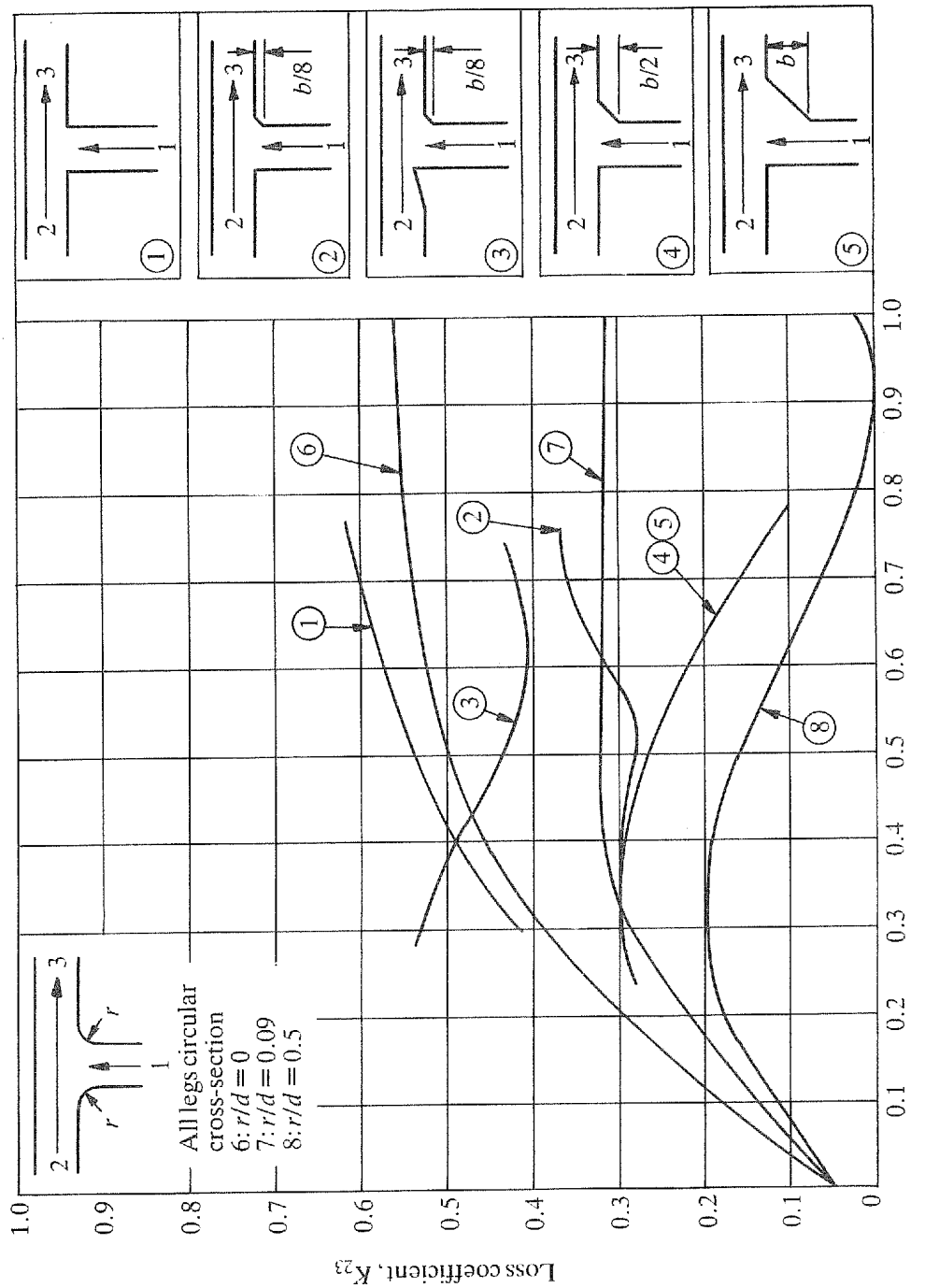

Fig. 13.33. Combining flow: loss coefficient K_{23}. Arrangements 1–5, all legs square cross-section; arrangements 6–8, all legs circular cross-section

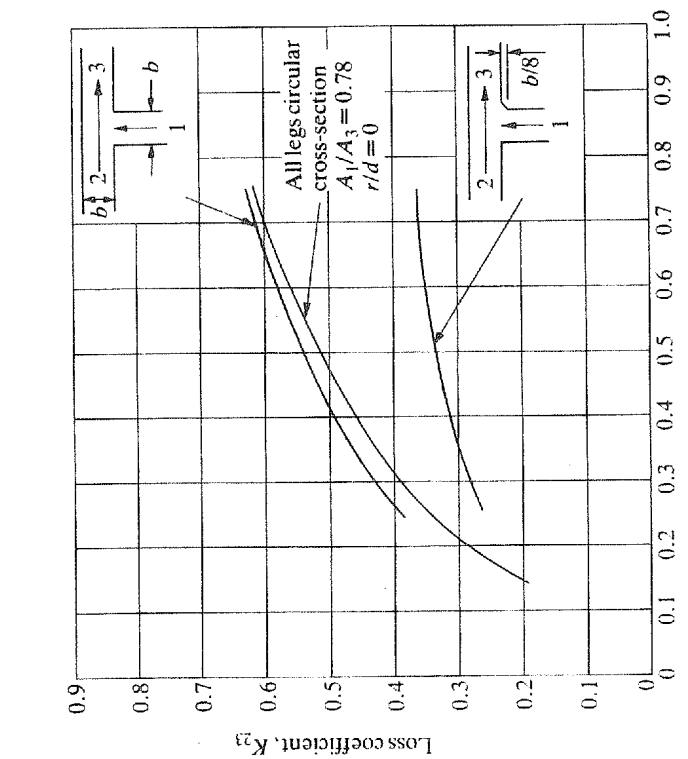

Fig. 13.35. Combining flow: loss coefficient K_{23}, legs 2 and 3 square cross-section

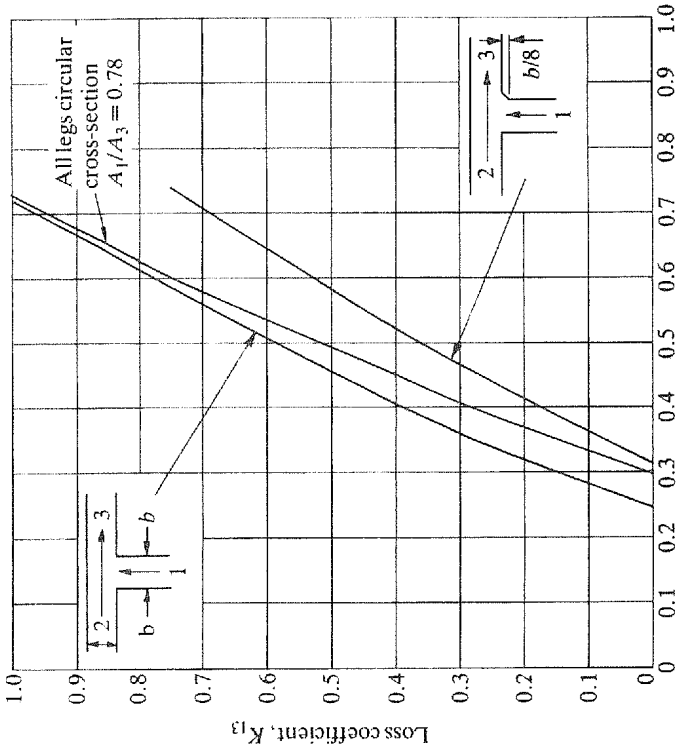

Fig. 13.34. Combining flow: loss coefficient K_{13}, legs 2 and 3 square cross-section

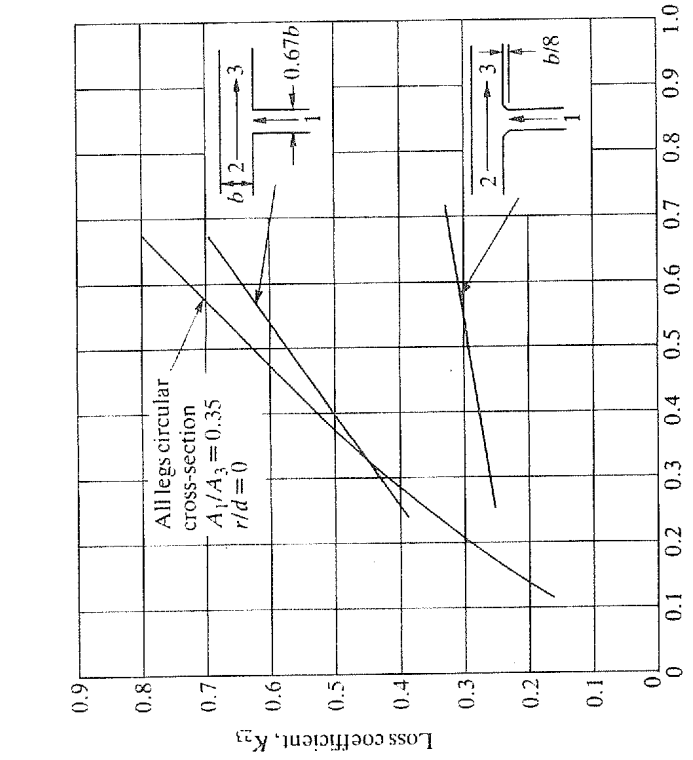

Fig. 13.37. Combining flow: loss coefficient K_{23}, legs 2 and 3 square cross-section

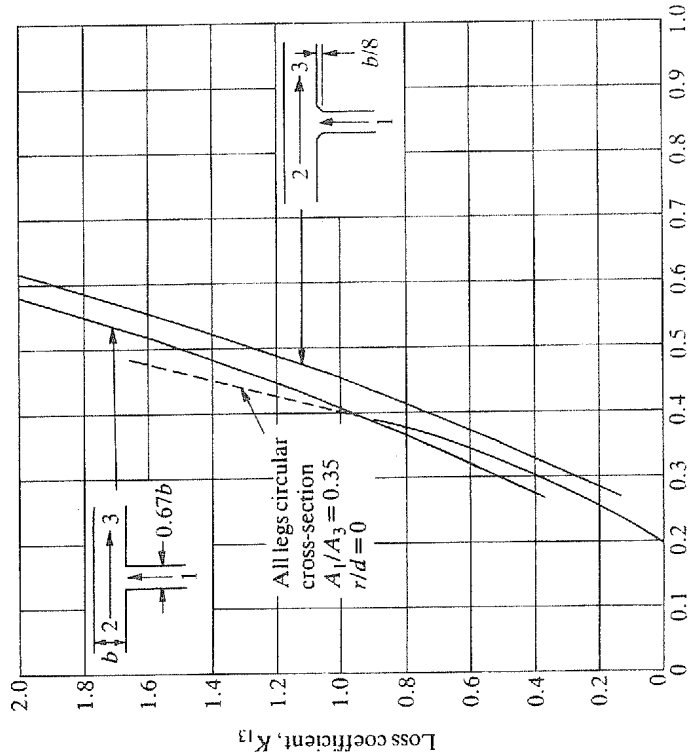

Fig. 13.36. Combining flow: loss coefficient K_{13}, legs 2 and 3 square cross-section

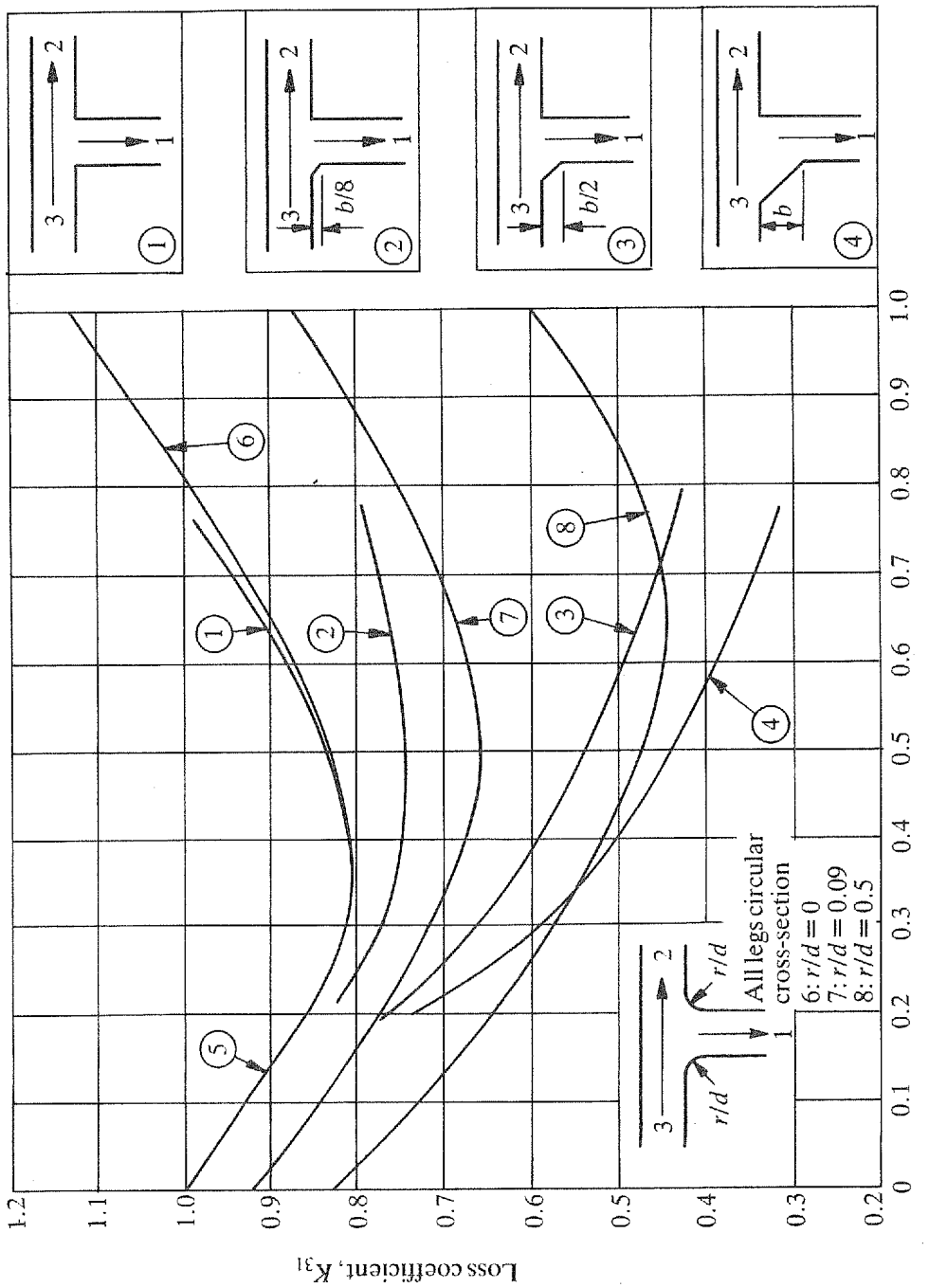

Fig. 13.38. Dividing flow: loss coefficient K_{31}. Arrangements 1–5, all legs square cross-section; arrangements 6–8, all legs circular cross-section

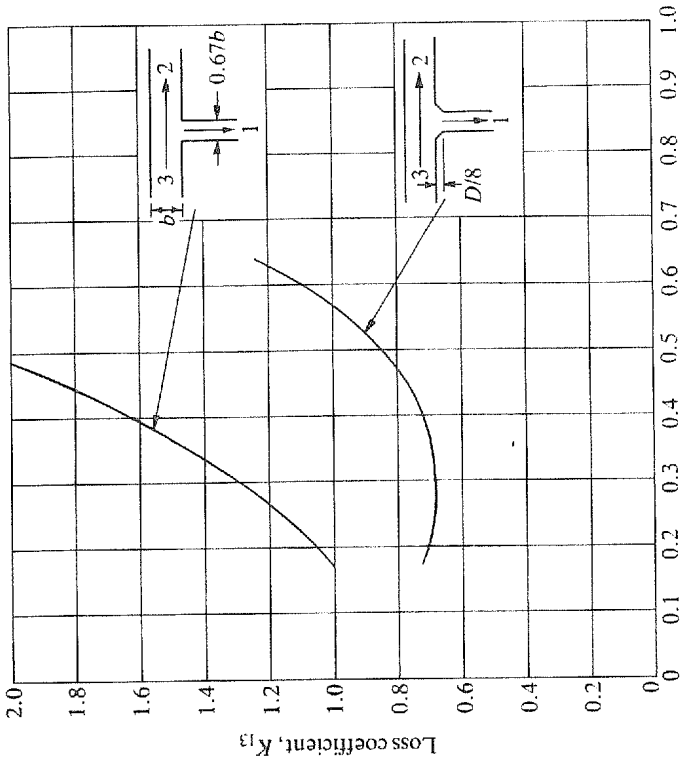

Fig. 13.40. Dividing flow: loss coefficient K_{31}, legs 2 and 3 square cross-section

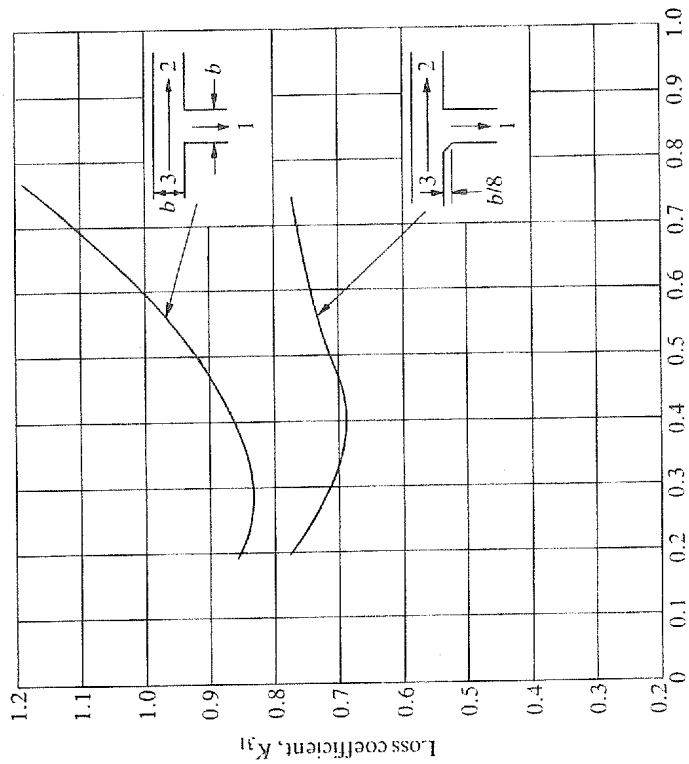

Fig. 13.39. Dividing flow: loss coefficient K_{31}, legs 2 and 3 square cross-section

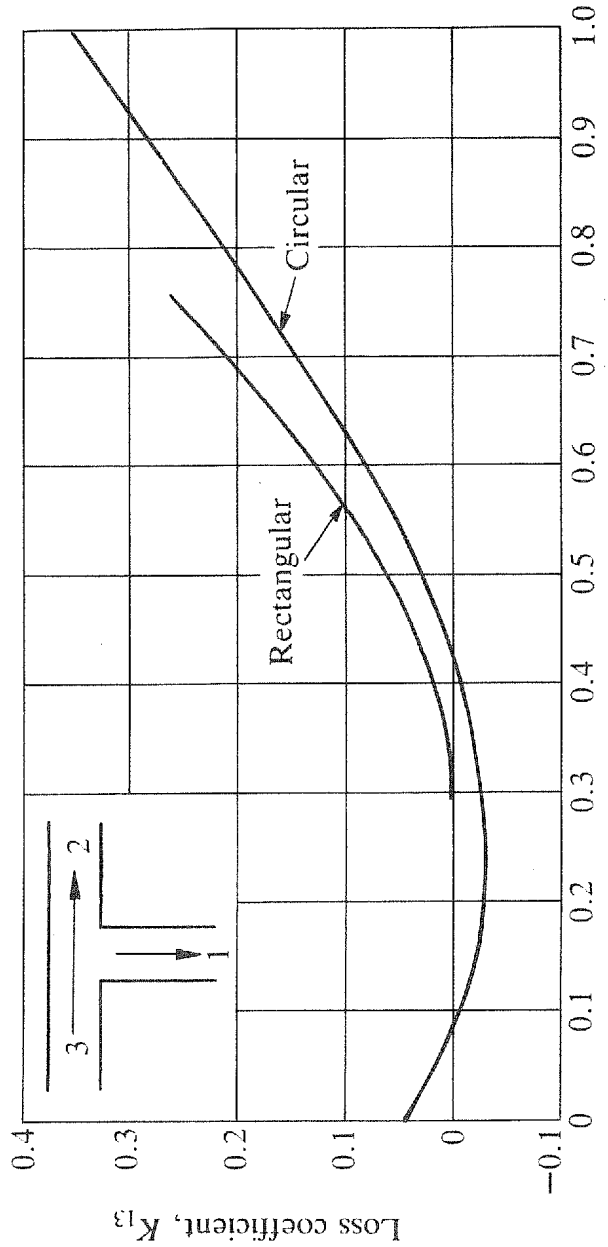

Fig. 13.41. Dividing flow: loss coefficients, arrangements as Fig. 13.40, all edges chamfered

indication from Fig. 13.41 is that through flow loss coefficients K_{32} are higher in square or rectangular sections. This may be due to the modification of the secondary flows which are present in rectangular sections, and to less low energy near-wall flow passing into branch leg 1.

13.11. T JUNCTION INTERACTIONS WITH BENDS (CLASS 2)

13.11.1. INTERACTION COEFFICIENTS

Closely coupled bends and Ts give rise to interactions. The effect on the loss coefficients K_{ij} depends on which leg of the T the bend is connected, the orientation of the bend in relation to the T, the flow ratio Q_1/Q_3 and whether the flow is combining or dividing.

The loss coefficient for a T with a closely coupled bend, K'_{ij}, is obtained by adding an interaction coefficient, K_{BTij}, to the loss coefficient of the T, K_{ij}:

$$K'_{ij} = K_{ij} + K_{BTij}$$

The loss coefficients for the bend and spacer between the bend and T should be added to the other components in the appropriate leg. If the bend is upstream of the T, then no correction for outlet pipe length should be applied to the bend loss coefficient.

Interaction coefficients are presented as a function of flow ratio for two area ratios ($A_1/A_3 = 1.0$; $A_1/A_3 = 0.56$) for T junctions with a radius at the junction of 0.1 times the junction diameter. The data apply for a spacer between bend and T of one pipe diameter. For other area ratios, refer to Section 13.11.4. For other spacer lengths, refer to Section 13.11.5.

Interaction coefficients are for a bend of $r/d = 1.5$ but can be applied for r/d ratios between 1 and 3 (class 3).

13.11.2. COMBINING FLOW K_{BTij} INTERACTIONS

Interaction coefficients for combining flow Ts with a one diameter spacer between bend and T are given for the following:

1. bend on branch leg in Figs. 13.42 and 13.43, for $\theta = 0°$, 90° and 180°;
2. bend on through leg in Figs 13.44 and 13.45, for $\theta = 0°$ and 180°; and
3. bend on combined leg in Figs 13.46 and 13.47, for $\theta = 0°$ and 180°.

θ is defined as the bend–T combination angle, and is given on the configuration sketches on each figure. A linear interpolation can be made to other angles (class 3).

13.11.3. DIVIDING FLOW K_{BTij} INTERACTIONS

Interaction coefficients for combining flow Ts with a one diameter spacer between bend and T are given for:

1. bend on branch leg in Figs 13.48 and 13.49, for $\theta = 0°$, 90° and 180°;

2. bend on through leg in Figs 13.50 and 13.51, for $\theta = 0°$ and 180°; and
3. bend on combined leg in Figs 13.52 and 13.53, for $\theta = 0°$ and 180°.

θ is defined as the bend–T combination angle, and is given on the configuration sketches on each figure. A linear interpolation can be made for other angles (class 3).

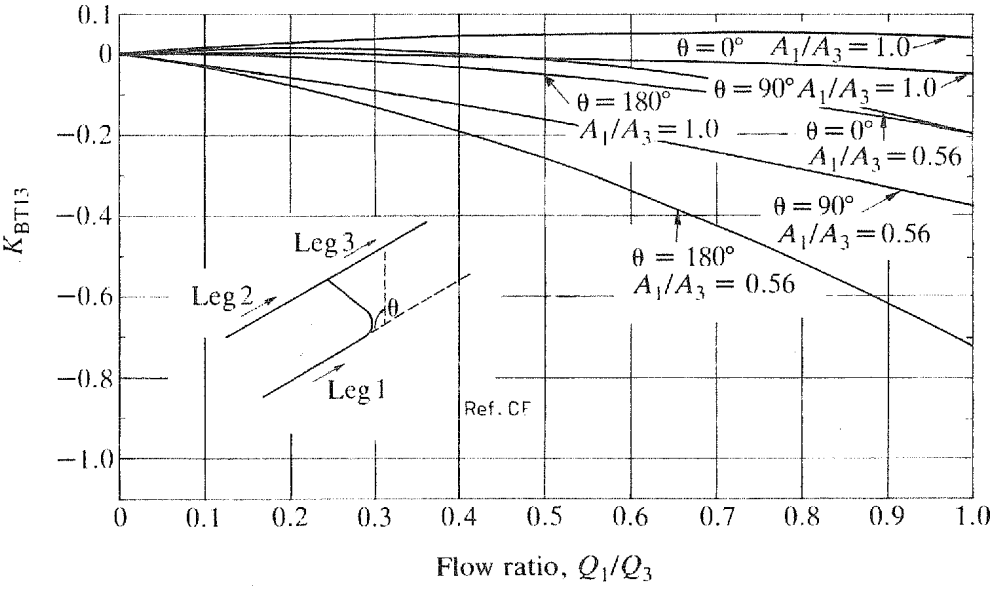

Fig. 13.42. Combining flow, bend on branch leg, correction coefficient K_{BT13}

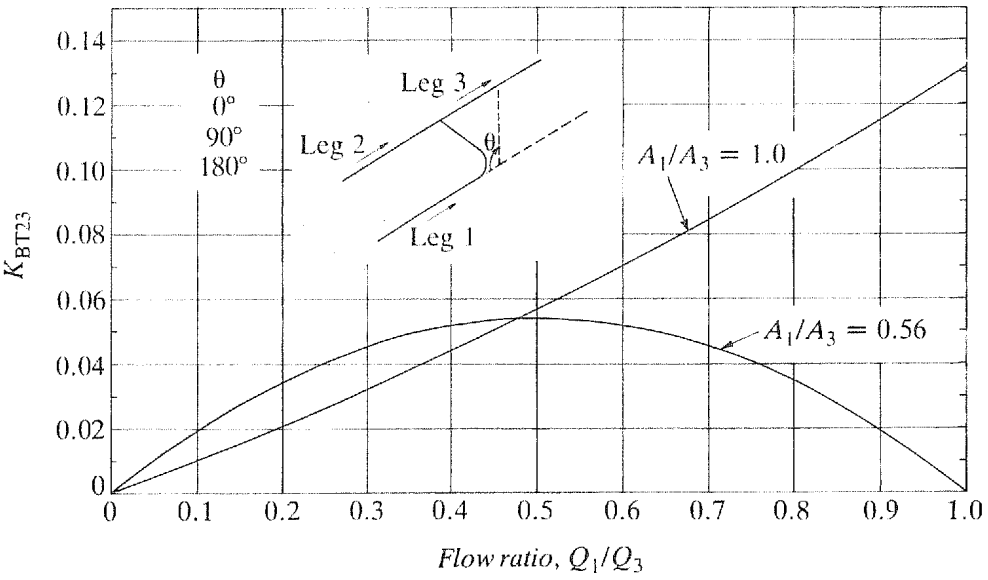

Fig. 13.43. Combining flow, bend on branch leg, correction coefficient K_{BT23}

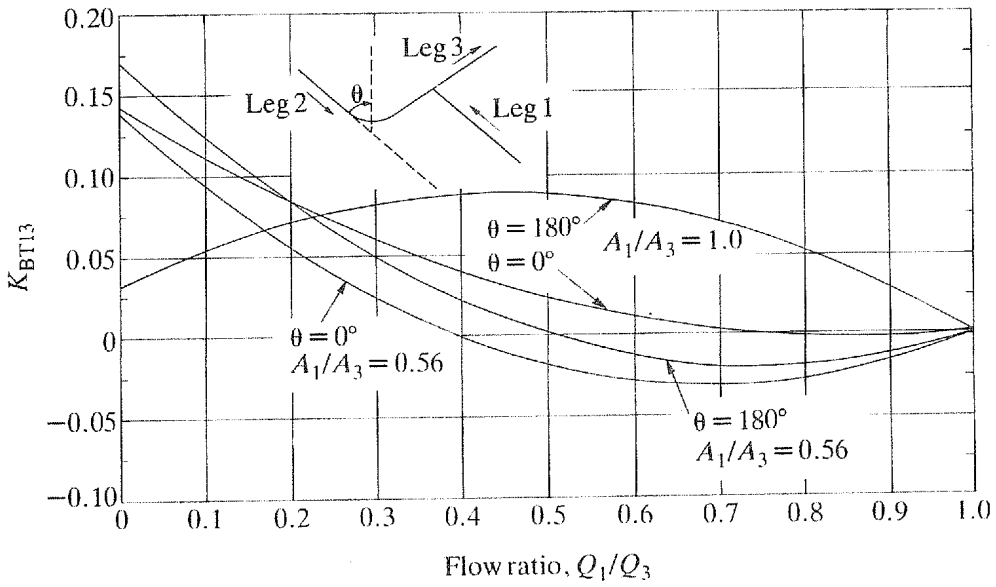

Fig. 13.44. Combining flow, bend on through leg, correction coefficient K_{BT13}

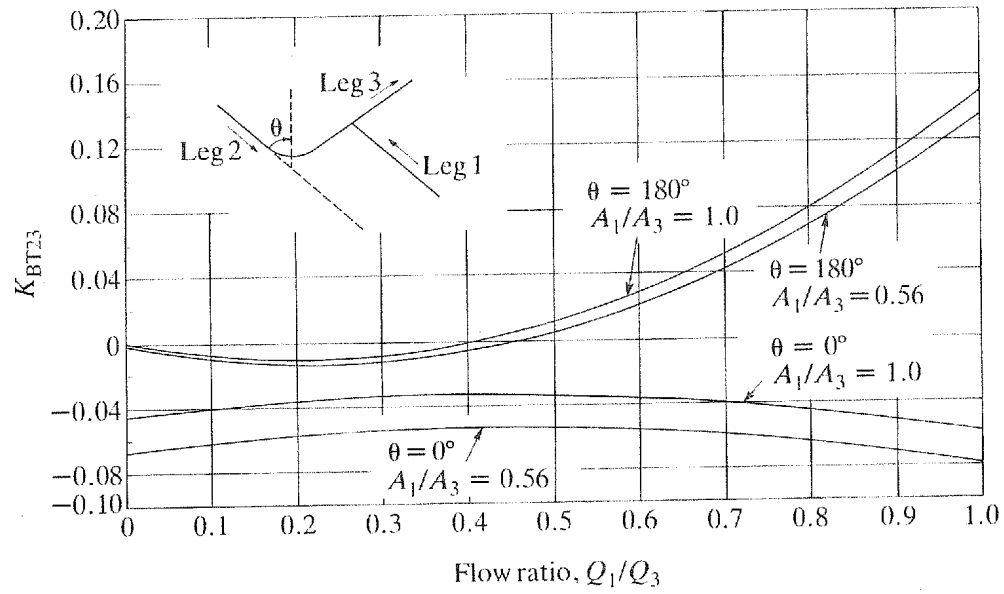

Fig. 13.45. Combining flow, bend on through leg, correction coefficient K_{BT32}

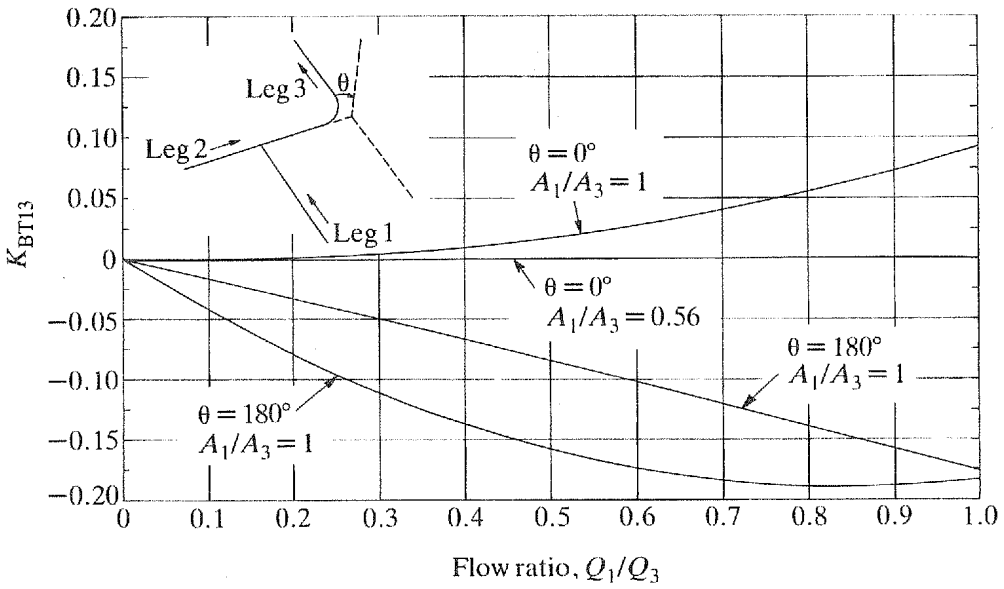

Fig. 13.46. Combining flow, bend on combined leg, correction coefficient K_{BT13}

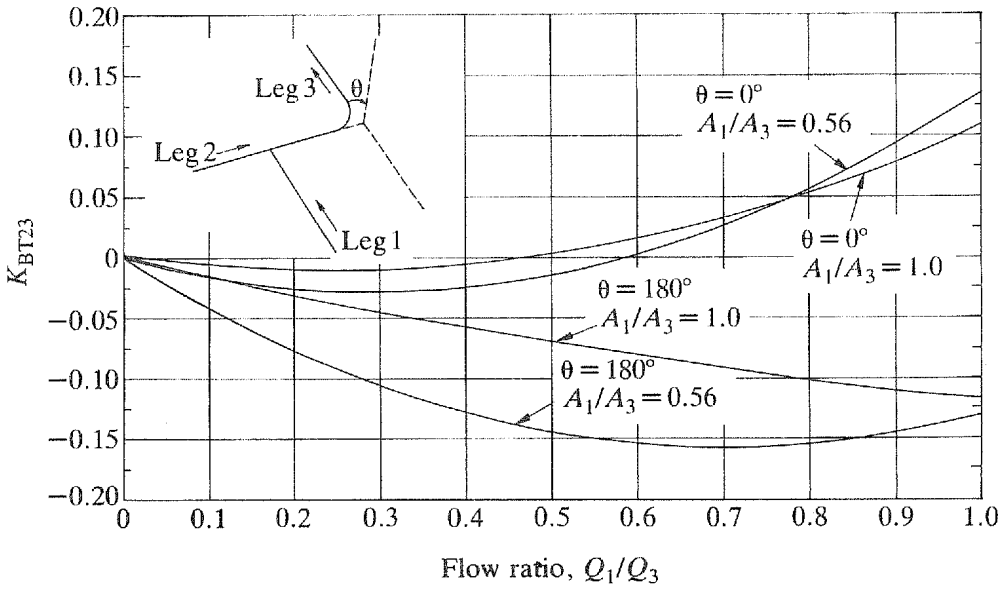

Fig. 13.47. Combining flow, bend on combined leg, correction coefficient K_{BT23}

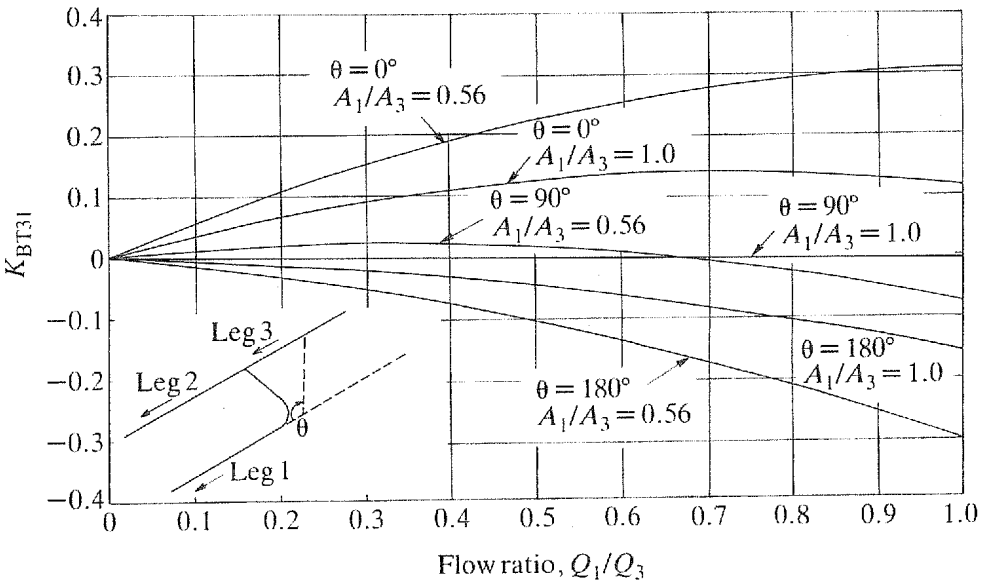

Fig. 13.48. Dividing flow, bend on branch leg, correction coefficient K_{BT31}

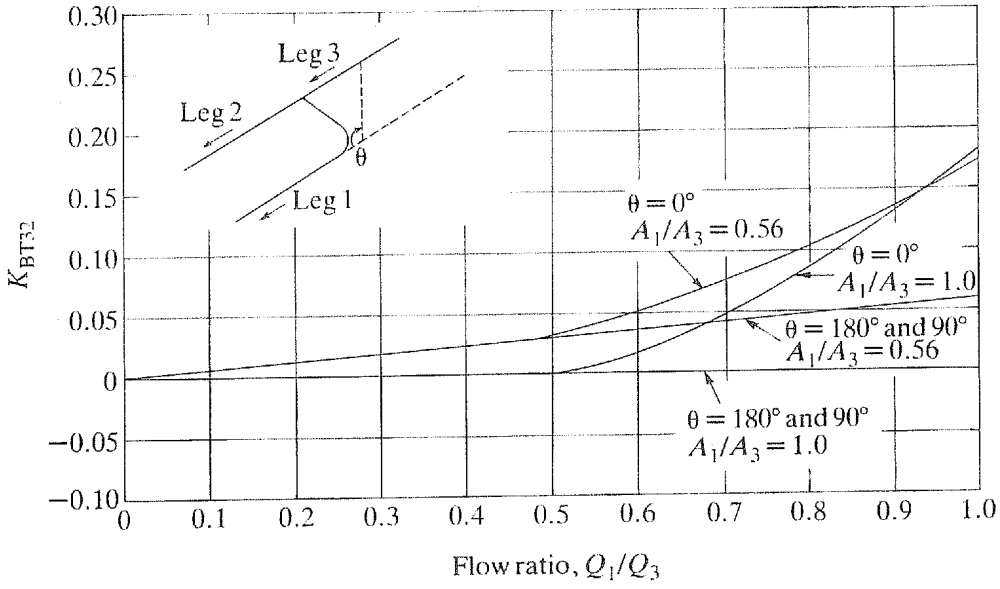

Fig. 13.49. Dividing flow, bend on branch leg, correction coefficient K_{BT32}

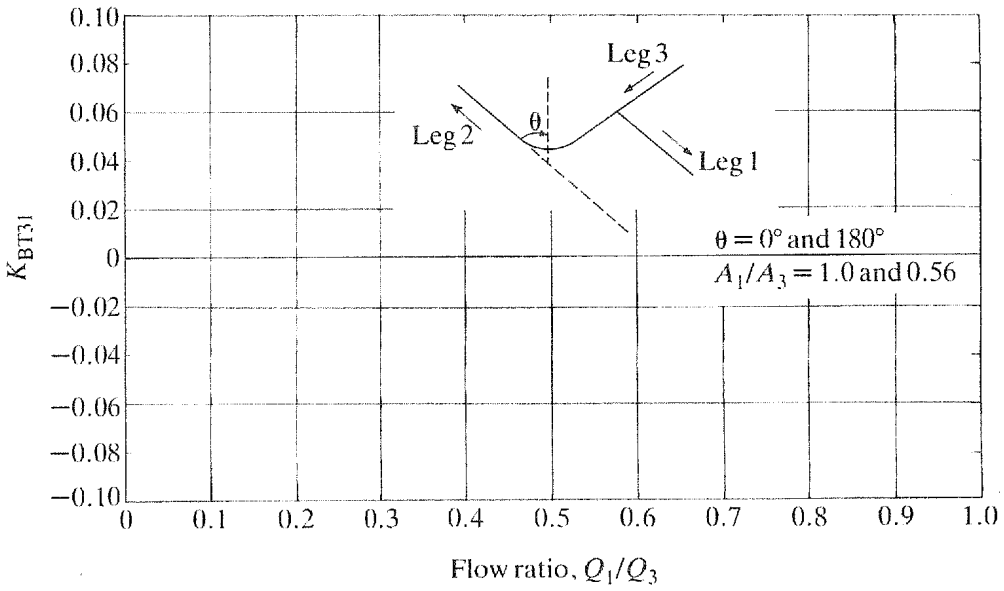

Fig. 13.50. Combining flow, bend on through leg, correction coefficient K_{BT31}

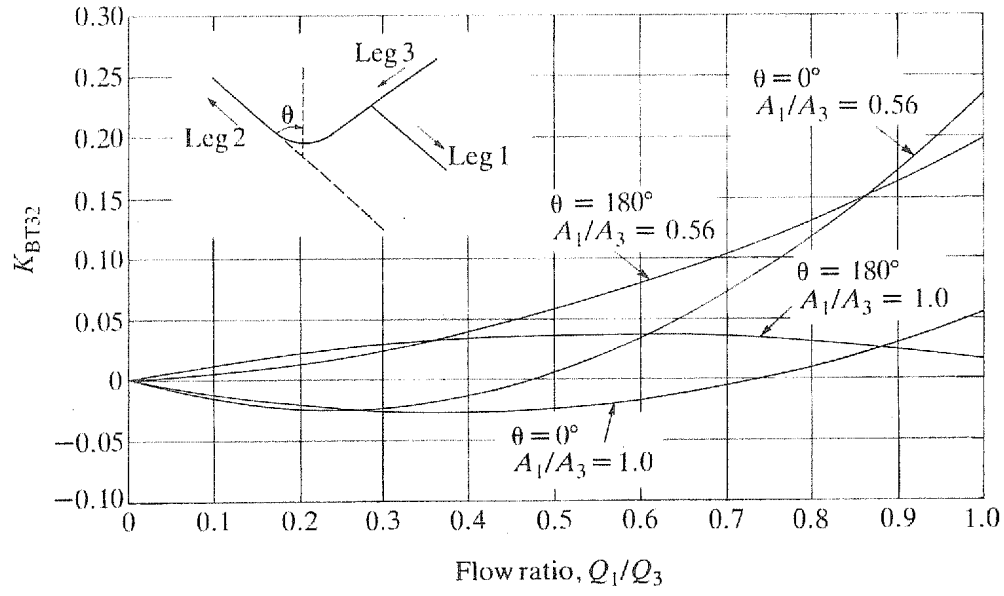

Fig. 13.51. Dividing flow, bend on through leg, correction coefficient K_{BT32}

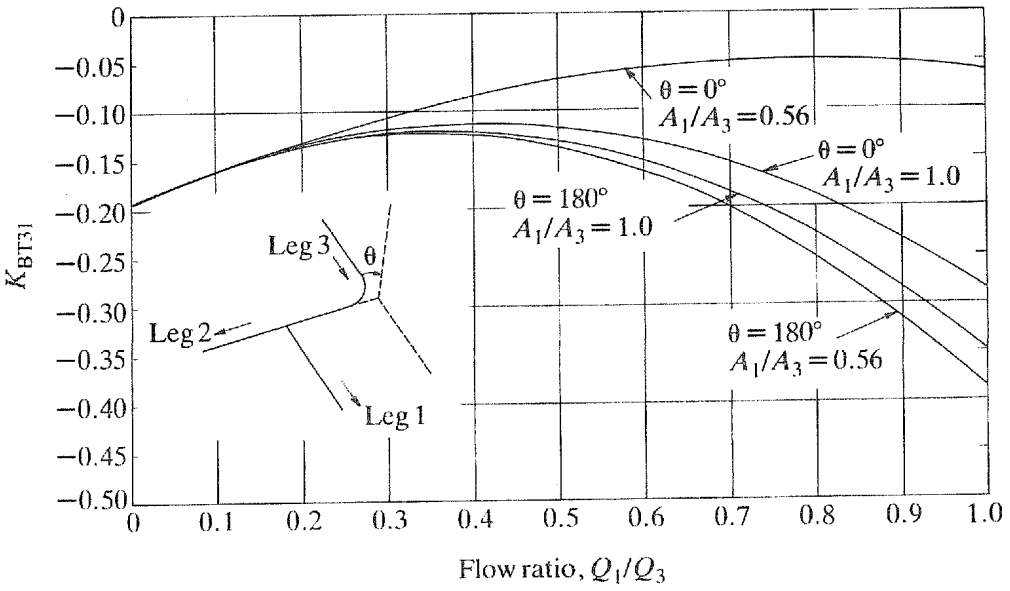

Fig. 13.52. Dividing flow, bend on combined leg, correction coefficient K_{BT31}

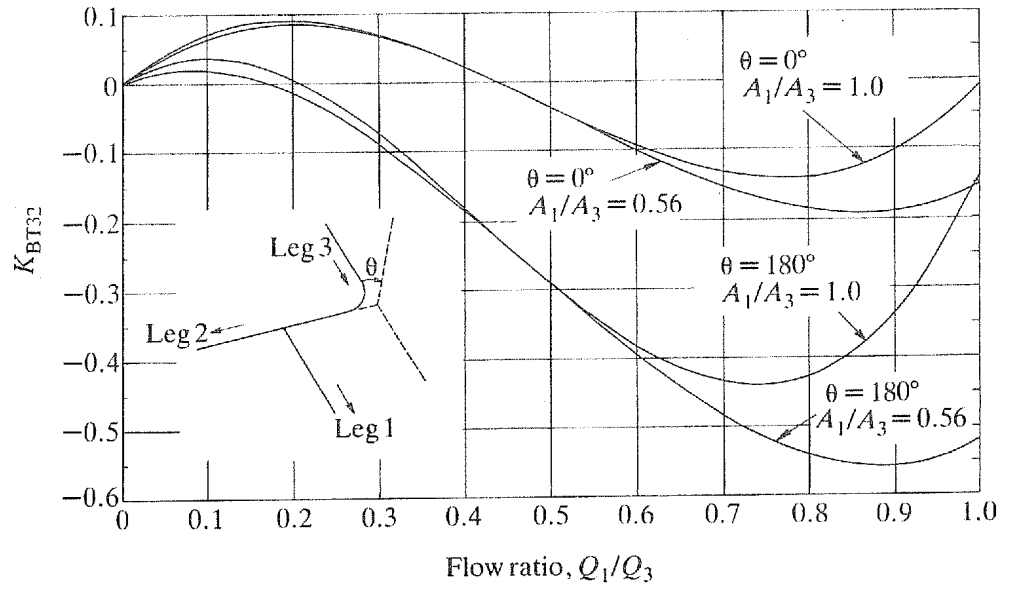

Fig. 13.53. Dividing flow, bend on combined leg, correction coefficient K_{BT32}

13.11.4. CORRECTING FOR AREA RATIO (CLASS 3)

For area ratios other than those given ($A_1/A_3 = 1.0$ and 0.56) it is suggested that linear interpolation and extrapolation be used. For an area ratio $A_1/A_3 = A'$ the interaction coefficient is given by

$$K_{BTij}(A') = K_{BTij}(1.0) + \left(\frac{K_{BTij}(0.56) - K_{BTij}(1.0)}{0.44}\right)(1.0 - A')$$

where $K_{BTij}(1.0)$ and $K_{BTij}(0.56)$ are the interaction coefficients for area ratios 1.0 and 0.56 at the appropriate flow ratio.

13.11.5. CORRECTING FOR SPACER LENGTH (CLASS 3)

For fabrication reasons, particularly on high pressure piping, T junctions have leg lengths of one or more diameter. The correction coefficients given are for a spacer of $L_s/D = 1$. For other spacer lengths, L_s, the following interaction coefficients are recommended.

1. $1 < L_s/D < 5$:

$$K_{BTij}(L_s) = K_{BTij} \times \tfrac{1}{4}(5 - L_s/D)$$

   where K_{BTij} is the interaction coefficient at $L_s/D = 1$.

2. $L_s/S \geqslant 5$

$$K_{BTij}(L_s) = 0$$

An example is given in Example 2 of Section 13.14.

13.12. LOSS COEFFICIENTS FOR HOLES IN PIPE WALLS (CLASS 2)

13.12.1. SUCTION FLOW INTO PIPE

Entrainment coefficients, C_e, for flow through rounded-edge and sharp-edged holes of diameter less than 0.25 of the pipe diameter are shown in Fig. 13.54. The flow into the pipe is given by

$$Q = C_e \frac{\pi d^2}{4}\sqrt{2g\Delta h}$$

where d is the hole diameter and Δh is the head difference between ambient and just upstream of the hole. The head loss coefficient K_{23} for the pipe flow can be taken from Fig. 13.11.

If the hole is one of a series along the pipe, a calculation of the hole flow rates should commence at the end of the pipe and work upstream, as in Example 3(a) of Section 13.14.

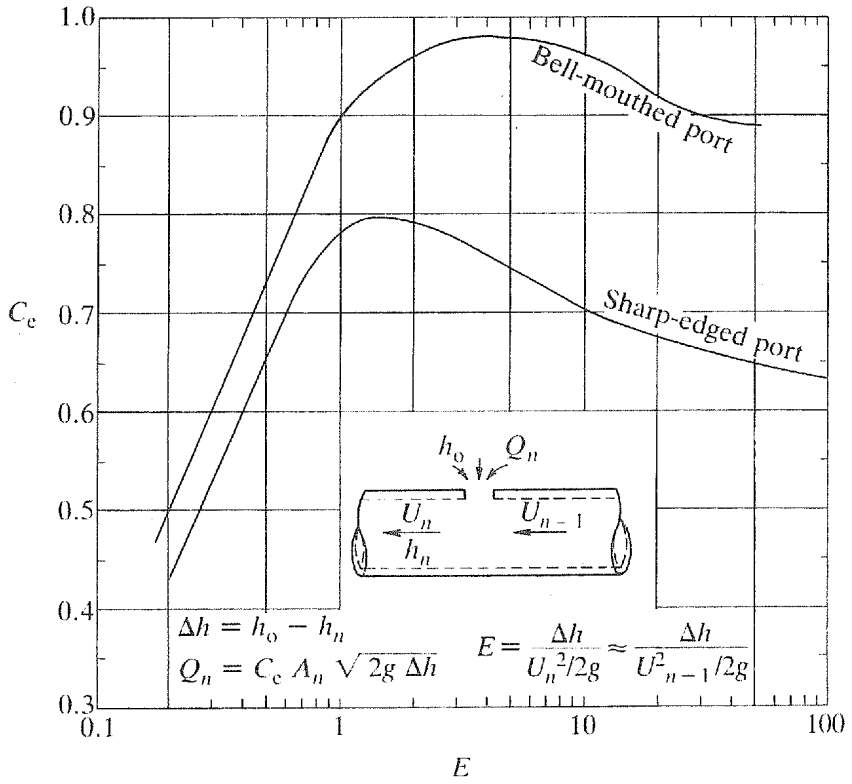

Fig. 13.54. Discharge coefficients for suction ports of less than 0.25 × pipe diameter

13.12.2. DISCHARGE FROM A PIPE

Discharge coefficients, C_d, for flow through rounded-edge and sharp-edged holes of diameter less than 0.25 of the pipe diameter are shown in Fig. 13.55. The flow out of the pipe is given by

$$Q_n = C_d(\pi d_n^2/4)\sqrt{2gE_n}$$

where $E_n = h_n + U_n^2/2g$.

The loss coefficient K_{32} for the pipe can be found from Section 13.5.

If the hole is one of a series along the pipe, the calculation commences at the end hole and proceeds as in Example 3(b) in Section 13.14.

13.13. MANIFOLDS

Although it is possible to derive expressions for the flow distribution out of or into ideal manifolds, it is more practical to carry out a step-by-step solution. Many variations in manifold layout are possible, but the basic concepts for calculating pressure and flow distributions apply to all manifolds.

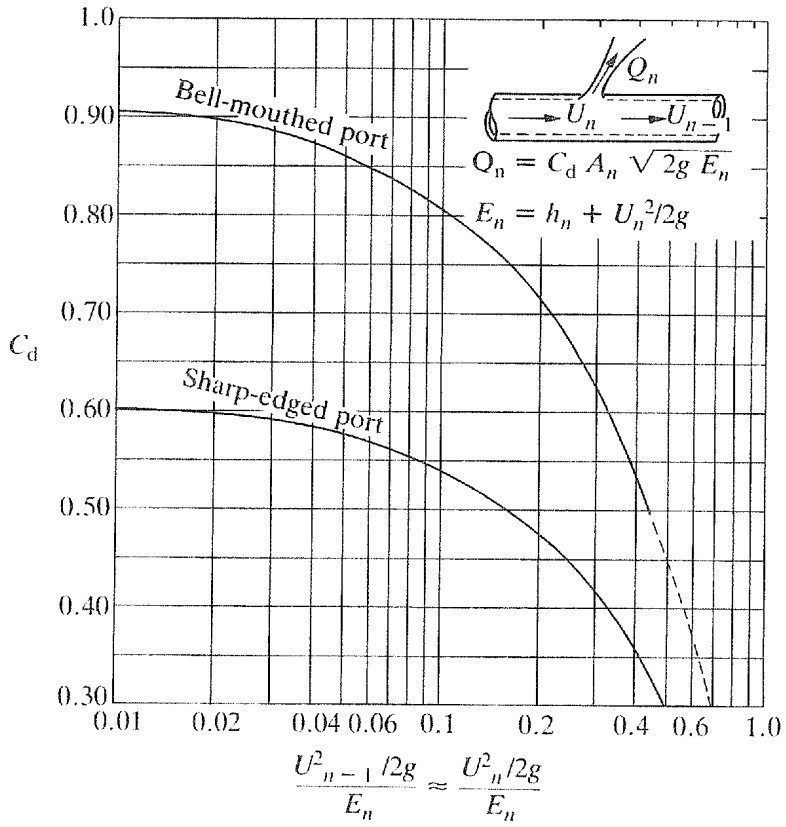

Fig. 13.55. Discharge coefficients for ports of less than 0.25 × pipe diameter (sharp-edged port values only apply if the wall thickness is less than 0.5 × hole diameter. If the wall thickness exceeds the hole diameter, multiply the sharp-edges coefficients by 1.2)

The numbering system for branches and reference stations along a manifold is shown in Fig. 13.56. Between station j and the ambient fluid the head loss is the same regardless of the flow path taken from the ambient fluid to station j in the case of a suction manifold or from station j to the ambient fluid in the case of an exhaust manifold. Determining the head loss is, therefore, a question of finding the flow distribution between branches, such that the head loss between station j and the ambient fluid is the same for all outlets 1 to j.

In most cases loss coefficients, including those accounting for friction, are only weakly dependent on the Reynolds number. This allows a calculation of the head loss at one flow rate to be scaled to any other flow rate, provided in the case of an exhaust manifold that the ambient fluid is of the same density as the fluid being discharged. Exhaust manifolds discharging a fluid of density different from that of the ambient fluid (for example, sewage into the sea) are affected by changes in manifold levels. In the case of sewage discharging into the sea from a manifold that slopes offshore, the effect of the density difference is to increase the flow from the inshore branches. When density differences are important, direct scaling from one flow to another is not possible as the effect of density on the static

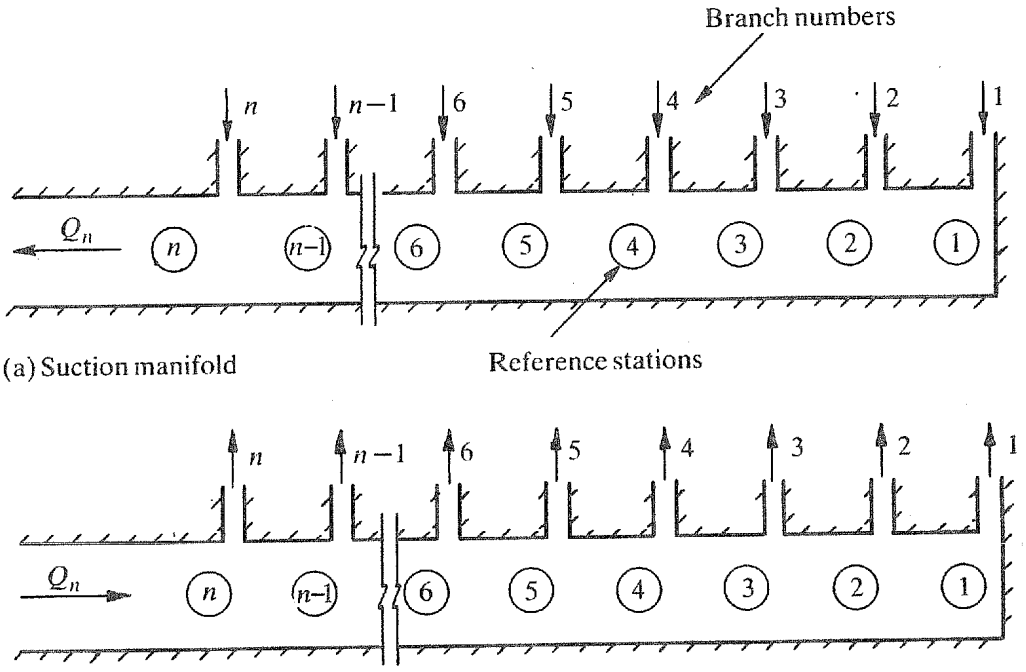

(a) Suction manifold

(b) Exhaust manifold

Fig. 13.56. Manifold notation

pressure along the manifold must be taken into account. This necessitates a lot of tedious calculations. Computer solution of manifold problems may be justified for optimisation studies involving changes in geometrical parameters or when differences in density are involved. When the manifold consists of a pipe with holes, the information contained in Section 13.12 can be used to find flow distributions and head losses.

13.13.1. SOLUTION METHOD

It is convenient, but not essential, to work in terms of modified loss coefficients, K', based on a flow at the highest number station and to assume that this flow, Q_n, is unity. In parts of the manifold where the area, A, differs from that of the highest number station, A_n, the coefficients are multiplied by $(A_n/A)^2$ to bring all modified loss coefficients to a common base.

Suction manifold (Fig. 13.57)

Step 1. Assume flows Q'_1 and Q'_2 in paths 1 and 2 to station 2 and calculate the loss coefficients K' of paths 1 and 2 up to station 2. Use Fig. 5.62 as a guide in selecting flows.

Step 2. If the modified loss coefficients along paths 1 and 2 to station 2 do not agree within about 2 per cent, repeat step 1 with revised estimates of flow.

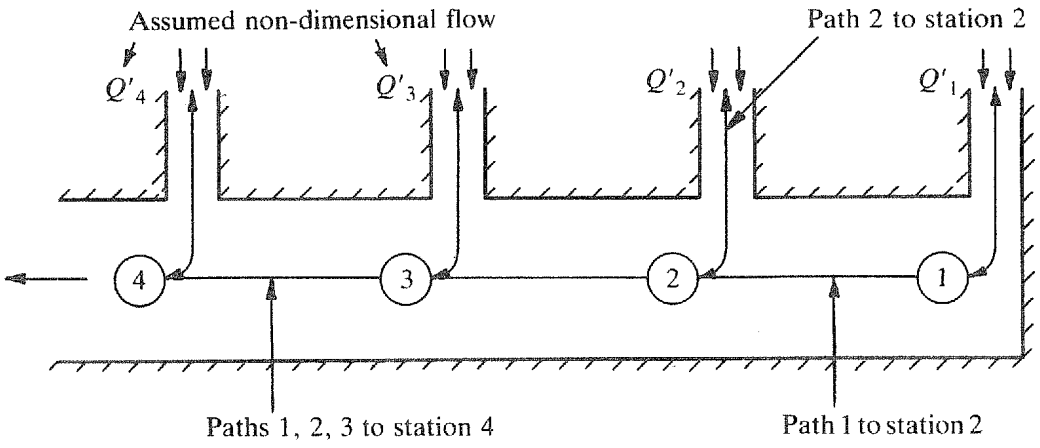

Fig. 13.57. Suction manifold

Step 3. Assume a flow Q'_3 along path 3 to station 3 and calculate the loss coefficients K' for flow in paths 1 and 2 to station 3 and in path 3 to station 3.

Step 4. If the modified loss coefficients in step 3 do not agree within 2 per cent or other appropriate tolerance, repeat step 3 with a revised estimate of flow along path 3.

Step 5. Proceed along the manifold, each time using the calculated loss coefficient up to station $j-1$ to find the flow and loss coefficient at station j by estimating a flow Q_j along path j and refining the estimate.

Step 6. On reaching the final station the overall manifold loss coefficient is given by

$$K = \frac{\text{Calculated total modified loss coefficient, } K'}{(\text{Calculated total } Q')^2}$$

Step 7. The head loss is given by

$$\Delta H = KU^2/2g$$

where U is the velocity at the final station.

Exhaust manifold (Fig. 13.58)

When flow is out of the manifold the same procedure as for the suction manifold is used, except the calculation is from a station within the manifold via a particular path to ambient. The calculation is again started at the end of the manifold, using assumed flows in paths 1 and 2.

13.14. EXAMPLES

EXAMPLE 1

Forty per cent of the water flowing in a 1.2 m pipe is withdrawn through a sharp-edged 90° T with a branch diameter of 0.8 m (Fig. 13.59). For a combined velocity of 3.5 m/s calculate

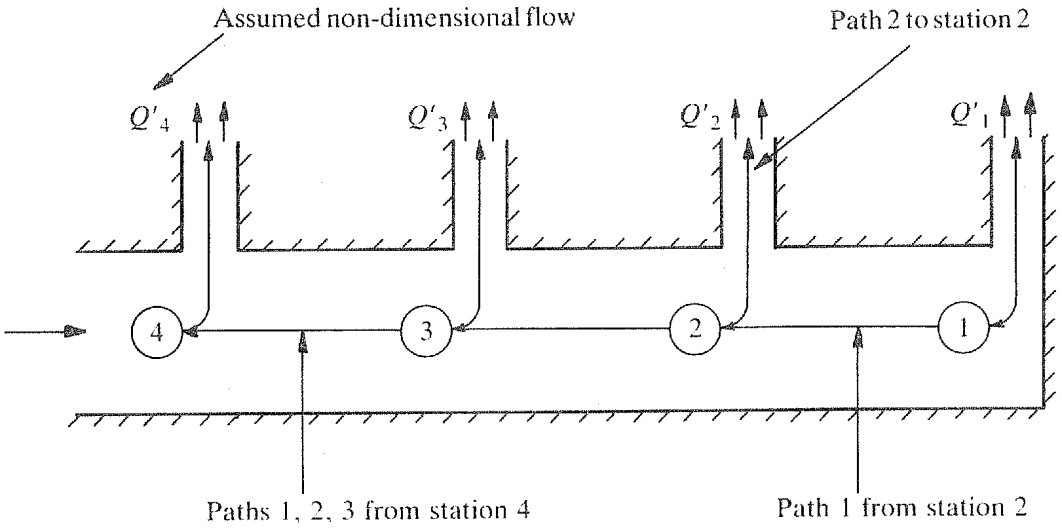

Fig. 13.58. Exhaust manifold

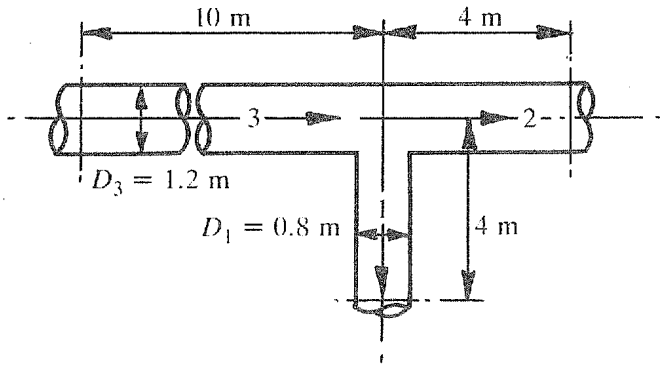

Fig. 13.59. Example T junction

the head loss between points 10 m before the T and 4 m after the T for both main and branch. What is the effect of a 0.08 m radius between main and branch? The pipes are new smooth steel and the water kinematic viscosity is 1.14×10^{-6} m/s.

1. Velocity
   (a) Leg 1:

$$U_1 = 0.4 \times 3.5 \times (1.2/0.8)^2 = 3.15 \text{ m/s}$$

   (b) Leg 2:

$$U_2 = 0.6 \times 3.5 = 2.1 \text{ m/s}$$

2. Reynolds number: $\mathrm{Re} = UD/v$
   (a) Leg 1:

$$\mathrm{Re}_1 = \frac{3.15 \times 0.8}{1.14 \times 10^{-6}} = 2.2 \times 10^6$$

   (b) Leg 2:

$$\mathrm{Re}_2 = \frac{2.1 \times 1.2}{1.14 \times 10^{-6}} = 2.2 \times 10^6$$

   (c) Leg 3:

$$\mathrm{Re}_3 = \frac{3.5 \times 1.2}{1.14 \times 10^{-6}} = 3.68 \times 10^6$$

3. From Section 8.1, roughness = 0.025 mm.

4. Relative roughness:
   (a) Leg 1:

$$\frac{k}{D} = \frac{0.025}{0.8 \times 10^3} = 3 \times 10^{-5}$$

   (b) Legs 2 and 3:

$$\frac{k}{D} = \frac{0.025}{1.2 \times 10^3} = 2 \times 10^{-5}$$

5. From Fig. 8.1, friction coefficient:
   (a) Leg 1: $f = 0.011$.
   (b) Leg 2: $f = 0.011$.
   (c) Leg 3: $f = 0.0105$.

6. Area ratio:

$$A_1/A_3 = (0.8/1.2)^2 = 0.444$$

7. From Fig. 13.21†, $K_{31} = 1.18$.

8. From Fig. 13.23, $K_{32} = -0.01$.

9. Total head loss, legs 3–1:

$$\Delta H = f_3 \frac{L_3}{D_3} \frac{U_3^2}{2g} + K_{31} \frac{U_3^2}{2g} + \frac{L_1}{D_1} \frac{U_1^2}{2g}$$

$$= \frac{0.0105 \times 10 \times 3.5^2}{1.2 \times 2 \times 9.81} + \frac{1.18 \times 3.5^2}{2 \times 9.81} + \frac{0.011 \times 4 \times 3.15^2}{0.8 \times 2 \times 9.81}$$

$$= 0.82 \text{ m of water gauge}$$

10. Total head loss, legs 3–2:

$$\Delta H = f_3 \frac{L_3}{D_3}\frac{U_3^2}{2g} + K_{32}\frac{U_3^2}{2g} + f_2\frac{L_2}{D_2}\frac{U_2^2}{2g}$$

$$= \frac{0.0105 \times 10 \times 3.5^2}{1.2 \times 2 \times 9.81} - \frac{0.01 \times 3.5^2}{2 \times 9.81} + \frac{0.011 \times 4 \times 2.1^2}{1.2 \times 2 \times 9.81}$$

$$= 0.06 \text{ m of water gauge}$$

11. A radius between the main branch affects only the branch loss for dividing flow:

$$r/D = 0.08/0.8 = 0.1$$

From Fig. 13.25†, for an area ratio of 0.445 and a flow ratio of 0.4, $K_{31} = 0.82$. The reduction in the head loss with a radius is

$$\Delta H = \frac{(1.18 - 0.82) \times 3.5^2}{2 \times 9.81} = 0.22 \text{ m of water gauge}$$

EXAMPLE OF T-JUNCTION BEND INTEGRATION

For the T–bend arrangement in Fig. 13.60, find the head loss between points A and B for water flow and the following conditions.

1. T to ANSI B16.9 ($r/D_1 = 0.1$ at junction).
2. Pipe friction coefficient, $f = 0.01$.
3. Kinematic viscosity $\gamma = 1.14 \times 10^{-6}$ m^2/s.

$$\text{Reynolds number leg } 3 = \frac{4.0 \times 0.584}{1.14 \times 10^{-6}}$$

$$= 2 \times 10^6$$

$$\text{Reynolds number leg } 1 = 10^6$$

No Reynolds number corrections will be necessary.

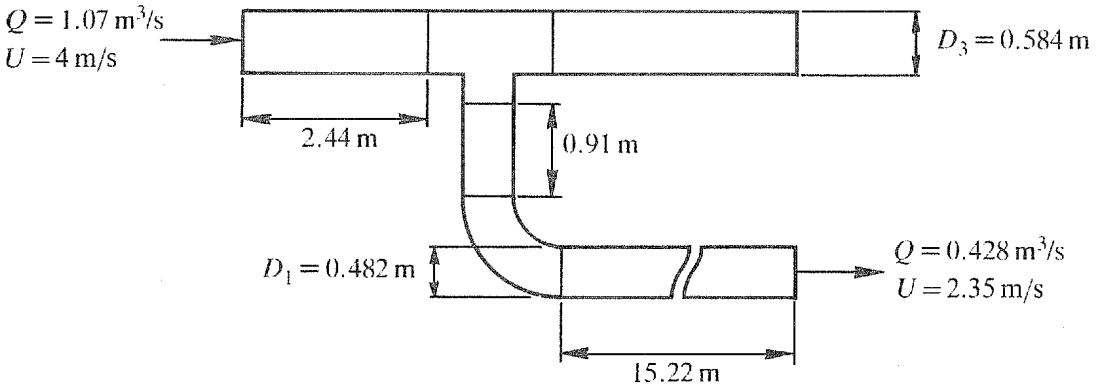

Fig. 13.60. Example dividing T–bend combination with bend on the branch in a $\theta = 0°$ arrangement

Inlet pipe loss:

$$K_f = fL/D = 0.01 \times 2.44/0.584 = 0.042$$

Total pressure loss:

$$\Delta h = K_f U^2/2g = 0.042 \times 4^2/(2 \times 9.81) = 0.034 \text{ m}$$

T loss:

$$\text{Area ratio} = (0.482/0.584)^2 = 0.68$$

$$\text{Flow ratio} = (0.428/1.07) = 0.4$$

From Fig. 13.24(1), $K_{31} = 0.69$.

There is a bend in the branch leg in a combination angle $\theta = 0$ configuration. From Fig. 13.48, at a flow ratio of 0.4

$$A_1/A_3 = 1.0,\ K_{BT31}(1.0) = 0.11$$

$$A_1/A_3 = 0.56,\ K_{BT31}(0.56) = 0.2$$

From Section 13.11.4, for $A_1/A_3 = 0.68$

$$K_{BT31}(0.68) = 0.11 + \left[\left(\frac{0.2 - 0.11}{0.44}\right) \times 0.32\right]$$

$$= 0.176$$

There is a spacer between the T and bend:

$$L_s/D = 0.91/0.482 = 1.9$$

From Section 13.11.5, the correction for the spacer is

$$K_{BT31}(L_s) = K_{BT31} \times (5 - L_s/D)/4$$

$$= 0.176 \times (5 - 1.9)/4$$

$$= 0.14$$

Corrected loss coefficient for the T is, from Section 13.11.1

$$K'_{31} = K_{31} + K_{BT31}$$

$$= 0.69 + 0.14 = 0.83$$

The loss in total head across the T referred to the leg 3 velocity head is

$$\Delta h = K' U^2/2g$$

$$= 0.83 \times 4^2/19.6 = 0.68 \text{ m}$$

For the pipe downstream of the T:

$$\text{Total length} = 0.91 + 15.22 = 16.13 \text{ m}$$

$$\text{Friction loss coefficient} = 0.01 \times 16.13/0.482 = 0.33$$

The bend loss coefficient from Fig. 9.2 for $r/d=1.5$ is $K_b=0.18$.

The total loss coefficient from the T to point B is

$$K=0.33+0.18=0.51$$

The head loss from the T to point B is

$$\Delta h=0.51\times 2.35^2/(2\times 9.81)=0.14 \text{ m}$$

So the total head loss from A to B is

$$\Delta h=0.68+0.14=0.82 \text{ m}$$

EXAMPLE OF MANIFOLD CALCULATIONS

An inlet and outfall for a cooling water system are to be constructed by tunnelling under the sea and breaking through to the sea bed. The preliminary design is shown in Fig. 13.61. It is required to estimate the flow distribution between the three riser pipes and the overall head loss for both the intake and outfall. The termination structures at the sea bed are assumed to have loss coefficients of 0.25 as inlets and 1.0 as outlets. A friction coefficient of 0.015 can be assumed. (Use the solution method from Section 13.13.1.)

(a) Suction arrangement

In short manifolds, pipe friction is not important and can normally be neglected in a preliminary study, but for completeness it is included in the present analysis. The branches are more than three diameters apart and have outlet lengths of four diameters, so the pipe length criteria of Section 13.2.1 are satisfied.

For path 1 up to station 2 the total loss coefficient, based on the flow area at station 3, is made up of

$$K' = \text{inlet loss coefficient} \times (A_3/A_1 \times Q'_1)^2$$
$$+ \text{vertical leg friction loss coefficient} \times A/A_3 \times Q'^2_1$$
$$+ \text{junction loss coefficient (taken as a T with zero through flow)} \times Q'^2_1$$
$$+ \text{tunnel friction loss} \times Q'^2_1$$
$$+ \text{through flow junction loss to station } 2 \times (Q'_1+Q'_2)^2$$

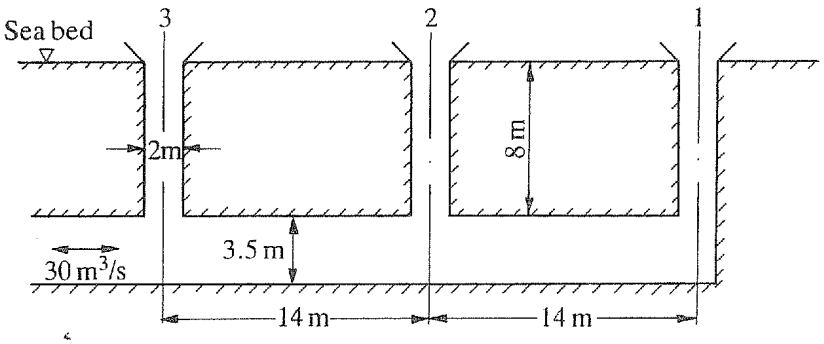

Fig. 13.61. Manifold arrangement for examples

where K' is the loss coefficient based on the velocity at station 3. Referring to Fig. 13.62

$$K' = (K_{1\text{-}1} + K_{1\text{-}2})(A_3/A_1)^2 Q_1'^2 + (K_{1\text{-}3} + K_{1\text{-}4})Q_1'^2 + K_{1\text{-}5}(Q_1' + Q_2')^2$$

From Fig. 5.63 a possible flow distribution is $Q_1' = 0.28$, $Q_2' = 0.32$ and $Q_3' = 0.4$, noting that $A/A_3 = 0.33$.

Step 1 (Fig 13.62)

Loss coefficients to station 2

Path 1 to station 2

$K_{1\text{-}1}$ specified — $K_{1\text{-}1} = 0.25$

$K_{1\text{-}2} = fL/D$ $\quad f = 0.015, \quad L/D = 4$ — $K_{1\text{-}2} = 0.06$

$K_{1\text{-}3}$ from Fig. 13.10† for $A_1/A_3 = 0.33, \quad Q_1/Q_3 = 1$ — $K_{1\text{-}3} = 8.0$

$K_{1\text{-}4} = fL/D$ $\quad f = 0.015, \quad L/D = 4$ — $K_{1\text{-}4} = 0.06$

$K_{1\text{-}5}$ from Fig. 13.11 for $A_1/A_3 = 0.33$ $\quad Q_1/Q_3 = 0.32/0.60 = 0.53$ — $K_{1\text{-}5} = 0.69$

Total loss coefficient for path 1 to station 2

$$K' = (0.25 + 0.06)\left(\frac{0.28}{0.33}\right)^2 + (8 + 0.06)(0.28)^2 + 0.69(0.60)^2 = 1.10$$

Path 2 to station 2

$K_{2\text{-}1}$ specified — $K_{2\text{-}1} = 0.25$

$K_{2\text{-}2} = fL/D$ $\quad f = 0.015, \quad L/D = 4$ — $K_{2\text{-}2} = 0.06$

$K_{2\text{-}3}$ from Fig. 13.10† for $A_1/A_3 = 0.33$ $\quad Q_1/Q_3 = 0.32/0.60 = 0.53$ — $K_{2\text{-}3} = 2.4$

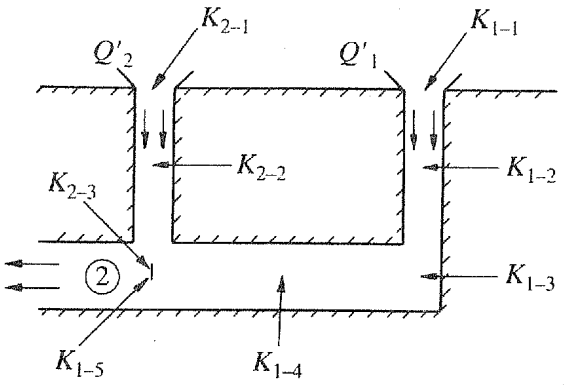

Fig. 13.62. Loss coefficients: path 1 and 2 to station 2

Total loss coefficient for path 2 to station 2

$$K' = (0.25 + 0.06)\left(\frac{0.32}{0.33}\right)^2 + 2.4(0.6)^2 \qquad = 1.16$$

Step 2

Loss coefficients to station 2

Path 1 to station 2

Revised estimates of $Q'_1 = 0.285$, $Q'_2 = 0.315$

$K_{1\text{-}5}$ from Fig. 13.11 for $A_1/A_3 = 0.33$ $\quad Q_1/Q_3 = 0.315/0.60 = 0.525$ $\quad K_{1\text{-}5} = 0.68$

$$K' = (0.25 + 0.06)\left(\frac{0.285}{0.33}\right)^2 + (8 + 0.06)(0.285)^2 + 0.68(0.60)^2 \qquad = 1.13$$

Path 2 to station 2

$K_{2\text{-}3}$ from Fig. 13.10† for $A_1/A_3 = 0.33$ $\quad Q_1/Q_3 = 0.315/0.60 = 0.525$ $\quad K_{2\text{-}3} = 2.4$

$$K' = (0.25 + 0.06)\left(\frac{0.315}{0.33}\right)^2 + 2.4(0.6)^2 \qquad = 1.14$$

Take $Q'_1 = 0.285$, $Q'_2 = 0.315$ and $K' = 1.13$.

Step 3 (Fig. 13.63)

Loss coefficients to station 3

Paths 1 and 2 to station 3

Assume $Q'_3 = 0.40$

$K_{2\text{-}4} = f\,L/D$ $\quad f = 0.015$, $\quad L/D = 4$ $\quad K_{2\text{-}4} = 0.6$

$K_{2\text{-}5}$ from Fig. 13.11 for $A_1/A_3 = 0.33$ $\quad Q_1/Q_3 = 0.4/1.0 = 0.4$ $\quad K_{2\text{-}5} = 0.52$

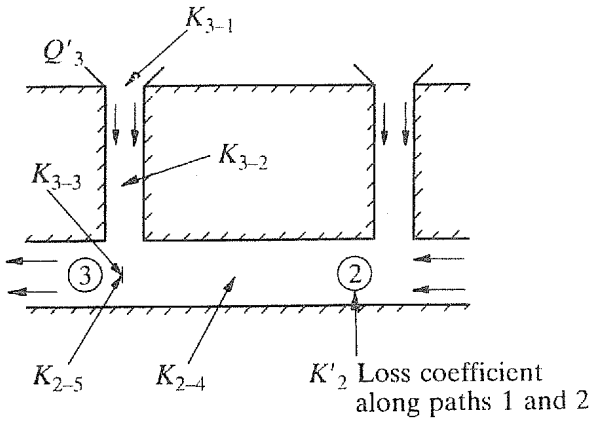

Fig. 13.63. Loss coefficients to station 3

$K' = 1.13 + (0.06)(0.6)^2 + (0.52)(1.0)^2 = 1.67$

Path 3 to station 3

$K_{3\text{-}1}$ specified $K_{3\text{-}1} = 0.25$

$K_{3\text{-}2} = fL/D \quad f = 0.015, \quad L/D = 4$ $K_{3\text{-}2} = 0.6$

$K_{3\text{-}3}$ from Fig. 13.10† for $A_1/A_3 = 0.33 \quad Q_1/Q_3 = 0.4$ $K_{3\text{-}3} = 1.4$

$$K' = (0.25 + 0.06)\left(\frac{0.4}{0.33}\right)^2 + 1.4(1.0)^2 = 1.86$$

The loss coefficient for path 3 is too high. Assume a lower flow ratio of 0.38.

Step 4

Loss coefficients to station 3

Paths 1 and 2 to station 3

$K_{2\text{-}5}$ from Fig. 13.11 for $A_1/A_3 = 0.33 \quad Q_1/Q_3 = 0.38/0.98 = 0.39$ $K_{2\text{-}5} = 0.52$

$K' = 1.14 + (0.06)(0.6)^2 + (0.52)(0.98)^2 = 1.66$

Path 3 to station 3

$K_{3\text{-}3}$ from Fig. 13.10† for $A_1/A_3 = 0.33 \quad Q_1/Q_3 = 0.38/0.98 = 0.39$ $K_{3\text{-}3} = 1.3$

$$K' = (0.23 + 0.06)\left(\frac{0.38}{0.33}\right)^2 + 1.3(0.98)^2 = 1.66$$

Take $Q_3' = 0.38$ and $K' = 1.66$.

Step 5 not applicable

Step 6

$$K = \frac{\text{Calculated } K'}{(\text{calculated } Q')^2} = \frac{1.66}{(0.285 + 0.315 + 0.38)^2} = 1.73$$

Step 7

$$U = Q/A = 30/3.5^2 \times 0.785 = 3.12 \text{ m/s}$$

$$\Delta H = KU^2/2g = 1.73 \times 3.12^2/2 \times 9.81 = 0.85 \text{ m}$$

Flow in branch $1 = 30 \times 0.285/0.98 = 8.72 \text{ m}^3/\text{s}$

Flow in branch $2 = 30 \times 0.315/0.98 = 9.64 \text{ m}^3/\text{s}$

Flow in branch $3 = 30 \times 0.38/0.98 = 11.63 \text{ m}^3/\text{s}$

Total $= 30.0 \text{ m}^3/\text{s}$

(b) Exhaust manifold

From Fig. 5.63 a possible flow distribution is $Q'_1 = 0.38$, $Q'_2 = 0.33$ and $Q'_3 = 0.29$.

Step 1 (Fig. 13.64)

Loss coefficients from station 2

Station 2 via path 1

$K_{1\text{-}1}$ specified $K_{1\text{-}1} = 1.0$

$K_{1\text{-}2} = fL/D \quad f = 0.015, \quad L/D = 4$ $K_{1\text{-}2} = 0.06$

$K_{1\text{-}3}$ from Fig. 13.21† for $A_1/A_3 = 0.33 \quad Q_1/Q_3 = 1$ $K_{1\text{-}3} = 5.0$

$K_{1\text{-}4} = fL/D \quad f = 0.015, \quad L/D = 4$ $K_{1\text{-}4} = 0.06$

$K_{1\text{-}5}$ from Fig. 13.23 for $A_1/A_3 = 0.33 \quad Q_1/Q_3 = 0.33/0.71 = 0.46$ $K_{1\text{-}5} = 0.01$

Total loss coefficient for station 2 via path 1

$$K' = (1.0 + 0.06)\left(\frac{0.38}{0.33}\right)^2 + (5.0 + 0.06)(0.38)^2 + 0.01(0.71)^2 = 2.14$$

Station 2 via path 2

$K_{2\text{-}1}$ specified $K_{2\text{-}1} = 1.0$

$K_{2\text{-}2} = fL/D \quad f = 0.015, \quad L/D = 4$ $K_{2\text{-}2} = 0.06$

$K_{2\text{-}3}$ from Fig. 13.21† for $A_1/A_3 = 0.33 \quad Q_1/Q_3 = 0.33/0.71 = 0.46$ $K_{2\text{-}3} = 1.7$

$$K' = (1 + 0.06)\left(\frac{0.33}{0.33}\right)^2 + 1.7(0.71)^2 = 1.92$$

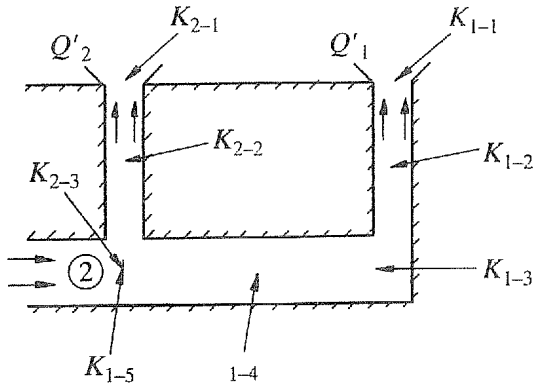

Fig. 13.64. Loss coefficient: paths 1 and 2 from station 2

Step 2

With a dividing manifold, changing the branch flow by a few per cent has only a small effect on the through flow coefficient, so it is usually adequate just to recalculate the branch coefficient.

Station 2 via path 2

Assume $Q'_2 = 0.34$.

$K_{2\text{-}3}$ from Fig. 13.21† for $A_1/A_3 = 0.33$ $\quad Q_1/Q_3 = 0.34/0.72 = 0.47$ $\quad K_{2\text{-}3} = 1.7$

$$K'_2 = (1.0 + 0.06)\left(\frac{0.34}{0.33}\right)^2 + 1.7(0.72)^2 = 2.01$$

Assume $Q'_2 = 0.35$.

Station 2 via path 2

$K_{2\text{-}3}$ from Fig. 13.21† for $A_1/A_3 = 0.33$ $\quad Q_1/Q_3 = 0.35/0.73 = 0.48$ $\quad K_{2\text{-}3} = 1.8$

$$K'_2 = (1.0 + 0.06)\left(\frac{0.35}{0.33}\right)^2 + 1.8(0.73)^2 = 2.15$$

This agrees with the loss coefficient for path 1 found in step 1.

Step 3 (Fig. 13.65)

Loss coefficients from station 3

Station 3 via paths 1 and 2

$K_{2\text{-}4} = fL/D$ $\quad f = 0.015, \quad L/D = 4$ $\quad K_{2\text{-}4} = 0.06$

$K_{2\text{-}5}$ from Fig. 13.23 for $A_1/A_3 = 0.33$ $\quad Q_1/Q_3 = 0.29/1.02 = 0.28$ $\quad K_{2\text{-}5} = -0.03$

$$K' = 2.14 + (0.06)(0.73)^2 - (0.03)(1.02)^2 = 2.14$$

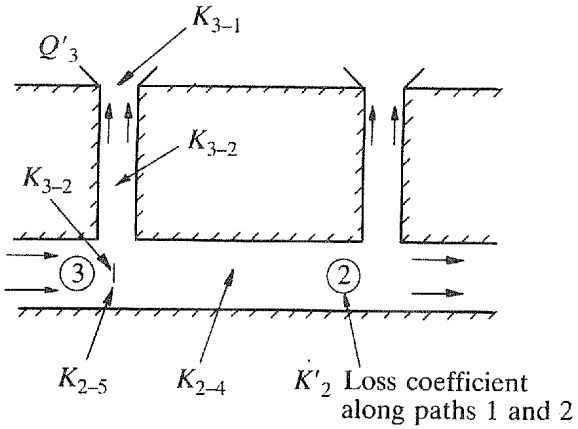

Fig. 13.65. Loss coefficients from station 3

Station 3 via path 3

$K_{3\text{-}1}$ specified $K_{3\text{-}1}=1.0$

$K_{3\text{-}2}=fL/D \quad f=0.015, \quad L/D=4$ $K_{3\text{-}2}=0.6$

$K_{3\text{-}3}$ from Fig. 13.21† for $A_1/A_3=0.33 \quad Q_1/Q_3=0.29/1.02=0.28$ $K_{3\text{-}3}=1.3$

$$K'=(1.0+0.06)\left(\frac{0.29}{0.33}\right)^2+1.3(1.02)^2 \qquad =2.17$$

Take a mean value of 2.16.

Steps 4 and 5 not applicable

Step 6

$$K=\frac{\text{Calculated total } K'}{(\text{Calculated total } Q)^2}=\frac{2.16}{(0.38+0.35+0.29)^2}=2.08$$

Step 7

$$\Delta H=KU^2/2g=2.08\times 3.12^2/(2\times 9.81)=1.03 \text{ m}$$

$$\text{Flow in branch } 1=\frac{30\times 0.38}{1.02}=11.18 \text{ m}^3/\text{s}$$

$$\text{Flow in branch } 2=\frac{30\times 0.35}{1.02}=10.29 \text{ m}^3/\text{s}$$

$$\text{Flow in branch } 3=\frac{30\times 0.29}{1.02}=8.53 \text{ m}^3/\text{s}$$

$$\text{Total}=30\text{m}^3/\text{s}$$

NOTES AND REFERENCES ON CHAPTER 13

A review of the literature on combining and dividing flow is carried out by:

1. Crow, D. A. and Wharton, R., A review of literature on the division and combination of flow in closed conduits. BHRA Report TN 937 (January 1968), 23 pp.

The performance charts for T and Y junctions are mainly taken from:

2. Miller, D. S., *Internal Flow: A Guide to Losses in Pipe and Duct Systems.* Cranfield, Bedford: BHRA (1971), 329 pp.
3. Boldy, A. P., Performance of dividing and combining tees. BHRA Report RR 1061 (December 1970), 62 pp.

The experimental data for the combining flow performance charts originate mainly from:

4. Blaisdell, F. W. and Manson, P. W., Loss of energy at sharp-edged pipe junctions in water conveyance systems. *US Dept. Agric. Res. Serv. Tech. Bull. 1283* (August 1963), 163 pp.

The main source for dividing Ts is data from experiments at Munich 1928–1931. However, the Munich loss coefficients, particularly at lower area ratios, are too large. The trends in the dividing flow loss coefficient curves are well established, so that using results from isolated tests, such as the square to circular data in Section 13.10 and

5. Gardel, A., Pressure drops in flows through T-shaped pipe fittings, Part 1. *Bull. Tech. Suisses Romande*, **85** (9), 123–130 (April 1957). Pressure drops in flows through T-shaped pipe fittings, Part 2. *Bull. Tech. Suisse Romande*, **85** (10), 143–148 (May 1957). (In French. BHRA translation or translation by F. W. Blaisdell, Agric. Res. Service, St Anthony Falls Hydraul. Lab.)

it is possible to prepare accurate performance charts. In Ref. 5 Gardel gives equations which are a reasonable approximation to the experimental data except for some dividing Ts. For Ts of equal area:

6. Ito, H. and Imai, K., Energy losses at 90° pipe junctions. *Proc. ASCE, J. Hydraul. Div.*, **99** (HY9), 1353–1368 (September 1973).
7. Ito, H., Sato, M. and Oka, K., Energy losses due to division and combination of flow in 90° wyes. *Bull. JSME*, **27** (232) (October 1984).

Refs 6 and 7 provide information on symmetrical dividing and combining flow in Y and T junctions with legs of equal area.

8. Muller, W. and Stratmann, H., Pressure losses in branch pipes and distributors. *Sulzer Tech. Rev.*, **53** (4), 280–298 (1971).

gives loss coefficients for a number of low loss dividing junctions, with some information about interaction between closely spaced branches, and about symmetrically dividing flow.

The six-legged junction data are based on:

9. Wilson, P. H., Aerodynamic losses in downcast shaft/airway intersections, TR13, and Aerodynamic losses in upcast shaft/airway intersections, TR14, Division of Mechanical Engineering, CSIRO, Highett, Victoria, Australia (1977).

These reports also contain information on the effect of chamfers and unbalanced flows in the branch legs.

The four-way dividing junction data are based on:

10. Colin, P. E., Méchanique des fluides: les pertes de pression dans les jonctions à 3 et 4 branches. Centre Scientifique et Technique de la Construction Revue, No. 3, pp. 11–22. (May–June 1969).

The data on correction coefficients for T-bend combinations are the result of a programme of work sponsored by the Pipeline Research Supervisory Committee (PRC) of the American Gas Association. The permission of the committee to publish the results is gratefully acknowledged, along with the support of the Compressor Research Supervisory Committee in carrying out the research work.

A summary of the research programme is given in:

11. Armstrong, S. G., Green, A. J., Pressure losses in compressor station yard pipework — Phase II BHRA CR2794 (June 1987) 39 pp.

The discharge coefficients for ports in a pipe wall are based on:

12. Rawn, A. M., Bowerman, F. R. and Brooks, N. H., Diffusers for disposal of sewage in sea water. *Proc. ASCE, J. Sanit. Eng. Div.*, **86** (SA2), 65–105 (March 1960).
13. Nece, R. E., Goldstern, P. P. and Black, J. L., Single port suctions manifolds. *Proc. ASCE, J. Hydraul. Div.*, **92** (HY1), 43–64 (January 1966).

14. MISCELLANEOUS SYSTEM COMPONENTS

14.1. INTRODUCTION

Concentrated energy losses are usually associated with flow separation followed by intense mixing and flow re-attachment. At the point of separation the static pressure varies markedly because the flow is converging (Fig. 14.1). Contraction of the flow persists downstream until a minimum effective flow area, the vena contracta, is reached. At the vena contracta the static pressure is constant across the flow. Following the vena contracta, large scale turbulence spreads throughout the flow, causing it to expand rapidly to fill the full cross-section. Up to

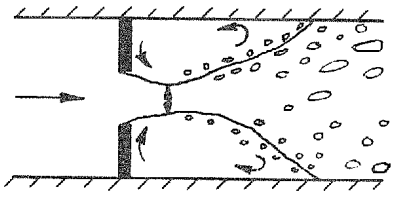

(a) Orifice plate

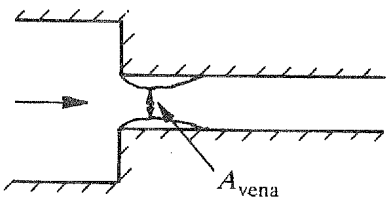

(b) Sudden contraction

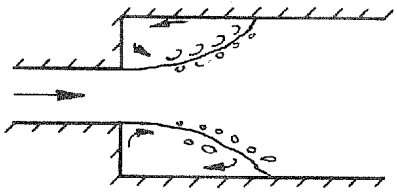

(c) Abrupt expansion

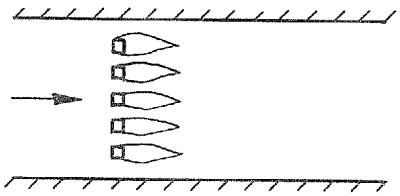

(d) Screen

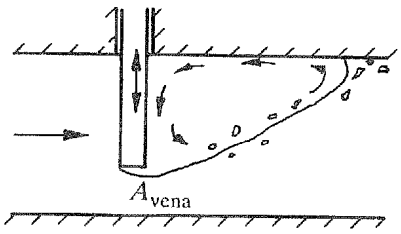

(e) Gate valve

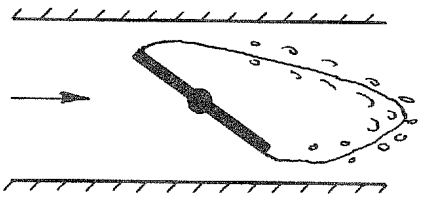

(f) Butterfly valve

Fig. 14.1. Flow separation in components

the vena contracta there is little energy dissipation, but after it considerable dissipation takes place.

Loss coefficients for situations where the vena contracta is well defined, arrangements (a), (b) and (c) in Fig. 14.1, can be predicted with reasonable accuracy using one-dimensional momentum and continuity equations:

$$K_{vena} = \left(1 - \frac{A_{vena}}{A_{pipe}}\right)^2 \tag{14.1}$$

Relating the loss coefficient to velocities in the downstream pipe the system loss coefficient K_o is

$$K_o = \left(1 - \frac{A_{vena}}{A_{pipe}}\right)^2 \left(\frac{A_{pipe}}{A_{vena}}\right)^2 \tag{14.2}$$

Contraction coefficients obtained from theoretical calculations and found to be in good agreement with measured values are shown in Fig. 14.2. To convert the contraction coefficients, C_c, of Fig. 14.2 to head loss coefficients, equation (14.2) becomes, for circular cross-sections

$$K_o = [1 - (d_o/D)^2 C_c]^2 \frac{1}{(d_o/D)^4 C_c^2} \tag{14.3}$$

and for the two-dimensional slots

$$K_o = [1 - (b/B) C_c]^2 \frac{1}{(b/B)^2 C_c^2} \tag{14.4}$$

Equation (14.1) is the base for determining the loss coefficients for a range of components considered in Sections 14.2–14.5. Within valves the vena contracta is often undefined and the contracted flow may be subjected to turning. Valves are considered in Section 14.6. Section 14.7 is concerned with laminar flows.

14.2. ORIFICES, SCREENS AND PERFORATED PLATES

The correlation of loss coefficients in this section is based on the geometrical ratio

$$\frac{A_2}{A_1} = \frac{\text{Free area at plane of orifice or screen}}{\text{Area of pipe or passage}}$$

A solidity parameter is sometimes used in the literature, and is given by

$$S = 1 - \frac{A_2}{A_1} = \frac{\text{Blockage area of screen}}{\text{Area of pipe or passage}}$$

Loss coefficients for components such as screens and orifice plates are based on measurements made just sufficiently far upstream to be unaffected by the component and

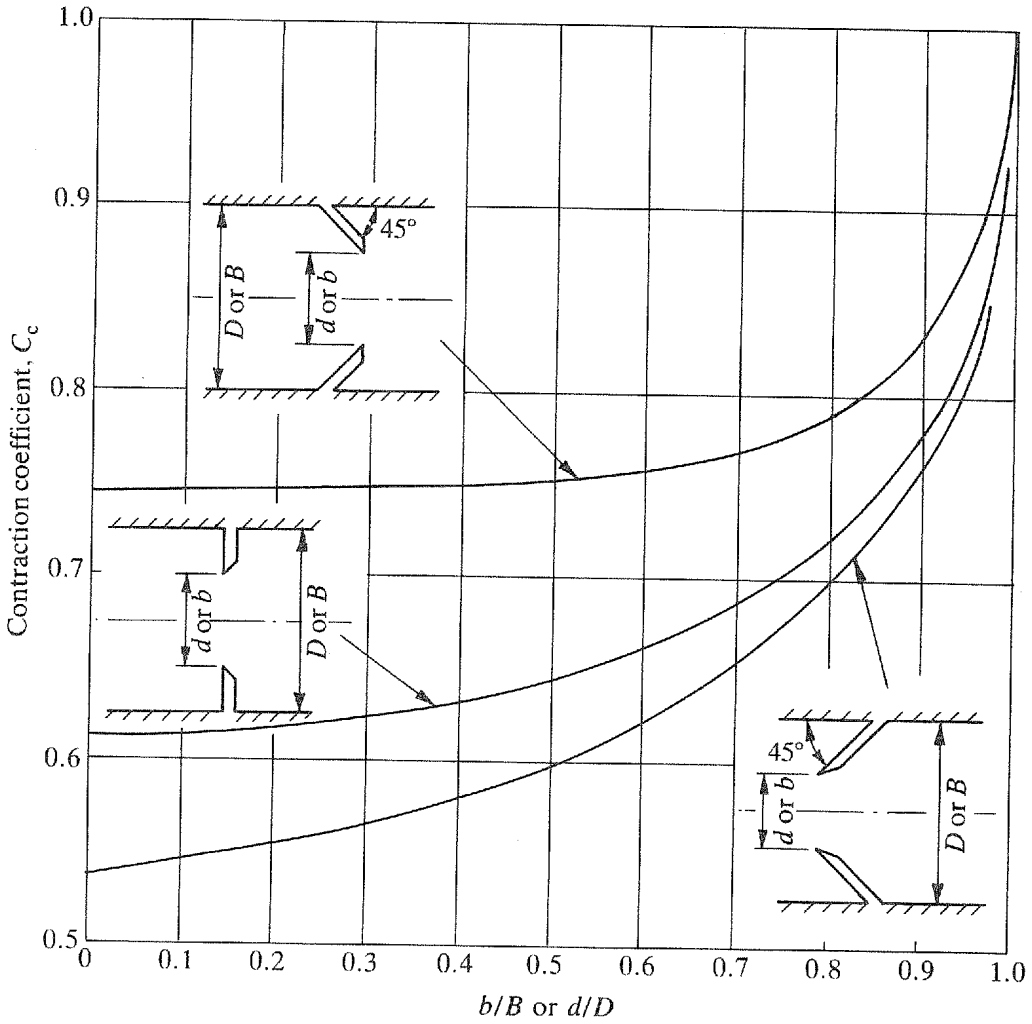

Fig. 14.2. Contraction coefficients (coefficients apply if no downstream pipe or passage; in the case of slot coefficients the coefficients apply if the centreline is replaced by a solid boundary)

just after the component, where the flow has expanded to fill the pipe or passage and any static pressure recovery is complete. If the component is not followed within four diameters by another component, the loss coefficient should be increased by 0.01 for each additional diameter of length, up to 10 diameters, in order to allow for flow redevelopment (class 3). This is in addition to the normal friction loss in the pipe or passage.

If the effective free area of a screen or perforated plate is less than 50 per cent of the pipe or passage area, the flow out of the screen or plate will tend to coalesce into a number of discrete jets, resulting in a very poor downstream velocity distribution. If screens are used to improve the flow distribution, several low loss screens are much more effective than a single high loss screen.

14.2.1. SHARP-EDGED THIN ORIFICES (CLASS 2)

Loss coefficients, K_o, against area ratio for sharp-edged thin orifices are shown in Fig. 14.3. The coefficients are based on the mean velocity in the pipe or passage and apply to Reynolds numbers greater than 10^3. The Reynolds number is based on the orifice diameter and the mean orifice velocity. Correction factors to account for orifice edge radii are given in Fig. 14.4.

14.2.2. SHARP-EDGED LONG ORIFICES (CLASS 3)

Loss coefficients, K_o, against orifice length/diameter for sharp-edged long orifices are shown in Fig. 14.5† for a range of area ratios. The coefficients are based on the mean velocity in the pipe or passage and apply to Reynolds numbers greater than 10^4. The Reynolds number is based on the orifice diameter and the mean orifice velocity.

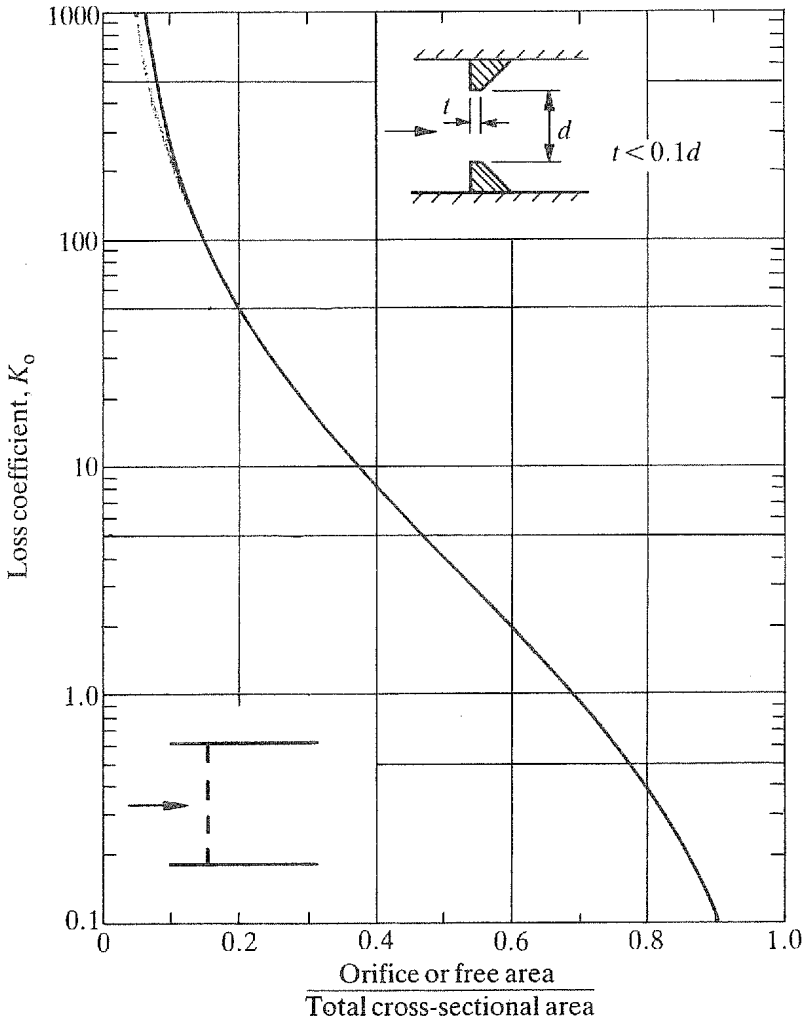

Fig. 14.3. Loss coefficients for sharp-edged thin orifices (also applies to square holes)

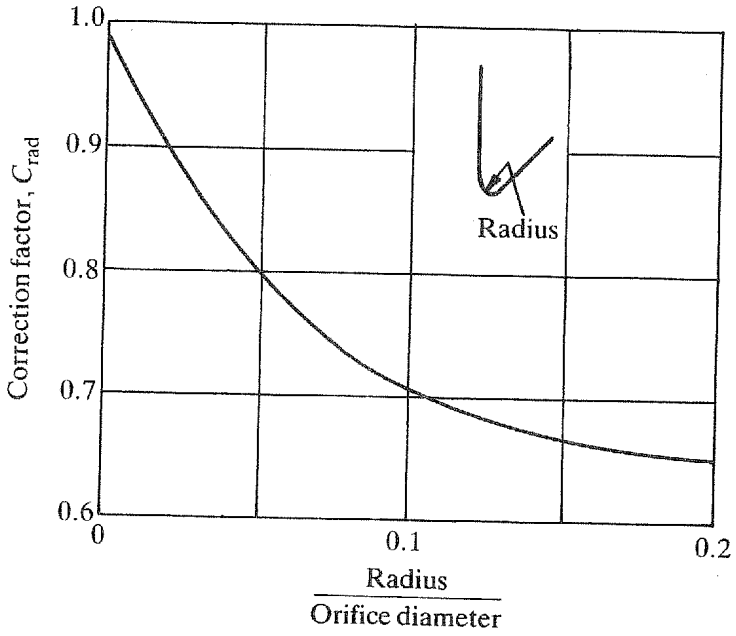

Fig. 14.4. Correction factors for edge radii

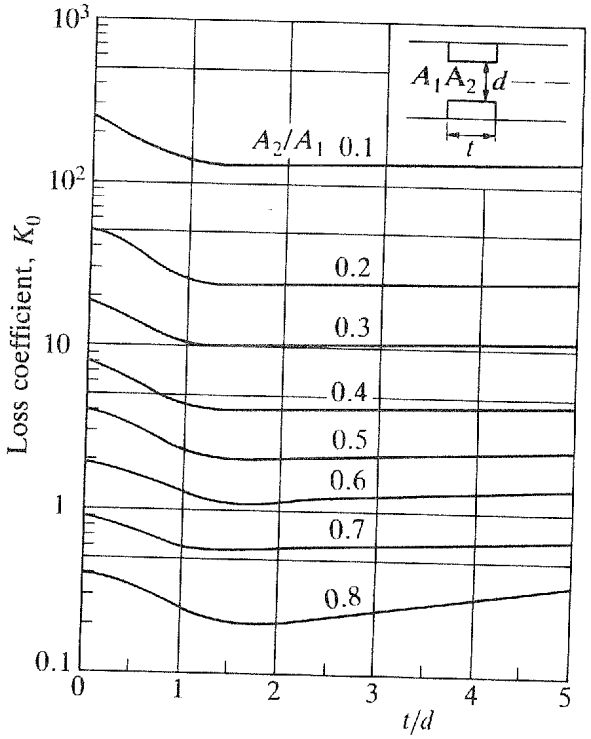

Fig. 14.5†. Loss coefficient for long orifices.

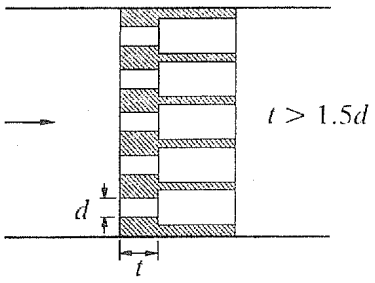

Fig. 14.6(1). Stepped orifices

Over the range of orifice length/diameter ratio of 0.1 to 0.8 flow instabilities may occur because of intermittent flow re-attachment.

If the orifice is longer than 5 diameters, friction losses in the length over 5 diameters must be added.

If the orifice area ratio is less than about 0.4 it is more appropriate to sum the losses for a sudden contraction found from Section 14.4, a friction loss found from Chapter 8 and a sudden expansion loss found from Section 14.5.

Long orifices used for flow normalisation can be stepped (Fig. 14.6(1)) to reduce head loss and to improve velocity and turbulence profiles. Calculations can be made on the basis of a sudden contraction plus orifice friction plus a sudden expansion plus sudden expansion. Figure 5.67 can be used to determine the sudden expansion length to diameter ratio for full pressure recovery.

14.2.3. SHARP-EDGED PERFORATED PLATES (CLASS 2)

If the plate thickness is less than 0.1 of the hole diameter, the loss coefficients for sharp-edged orifices in Section 14.2.1 can be used. Similarly, if the plate thickness exceeds 0.1 hole diameters, use Section 14.2.2. Commercial perforated plate may have burrs and rounded edges which increase or reduce the loss coefficients by 25 per cent or more.

14.2.4. ROUND WIRE SCREENS AND NETTING (CLASS 2)

Loss coefficients are plotted against area ratio in Fig. 14.7 for round wire screens and textile netting. The loss coefficients are based on the mean pipe or passage velocity. The coefficients apply for Reynolds numbers greater than 500, based on the mean velocity through the screen and on the wire diameter.

To correct the loss coefficients of Fig. 14.7 for situations when the flow is not normal to the screen, multiply K_0 from Fig. 14.7 by $\cos^2\theta$. This correction applies only up to angles of 45°.

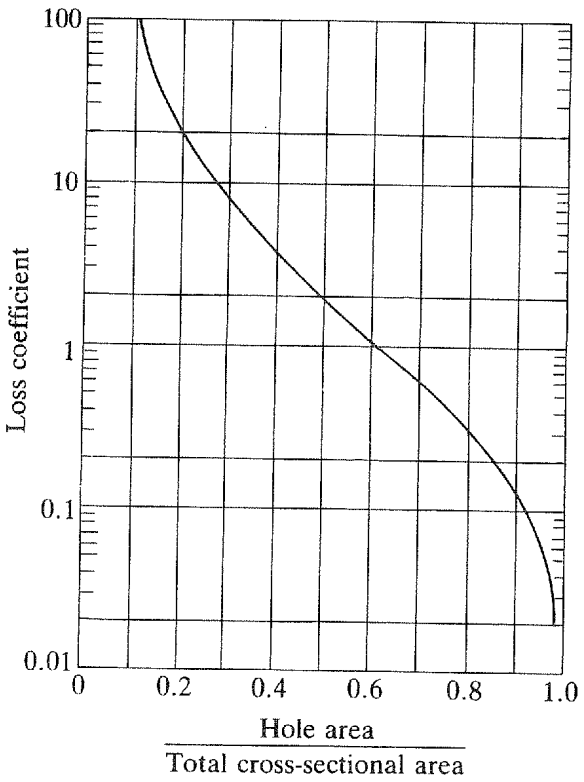

Fig. 14.7. Loss coefficients for round wire screens or netting (Re > 500 based on wire diameter and velocity in holes)

14.2.5. TRASHRACKS (CLASS 2)

Loss coefficients for trashracks with various bar shapes are shown in Fig. 14.8. In calculating the head loss account must always be taken of any bracing members, as these may be a major source of loss.

14.2.6. ISOLATED OBSTRUCTIONS IN PIPES AND PASSAGES (CLASS 3)

Loss coefficients for isolated obstructions across pipes and passages can be calculated in the same manner as for orifices, screens or trashracks. Calculate the ratio of the free area to the area of pipe or passage and obtain a value of K from Figs 14.3–14.8, depending on the shape of the obstruction. Add 0.10 to this value to allow for flow redevelopment which may take 10 to 30 diameters.

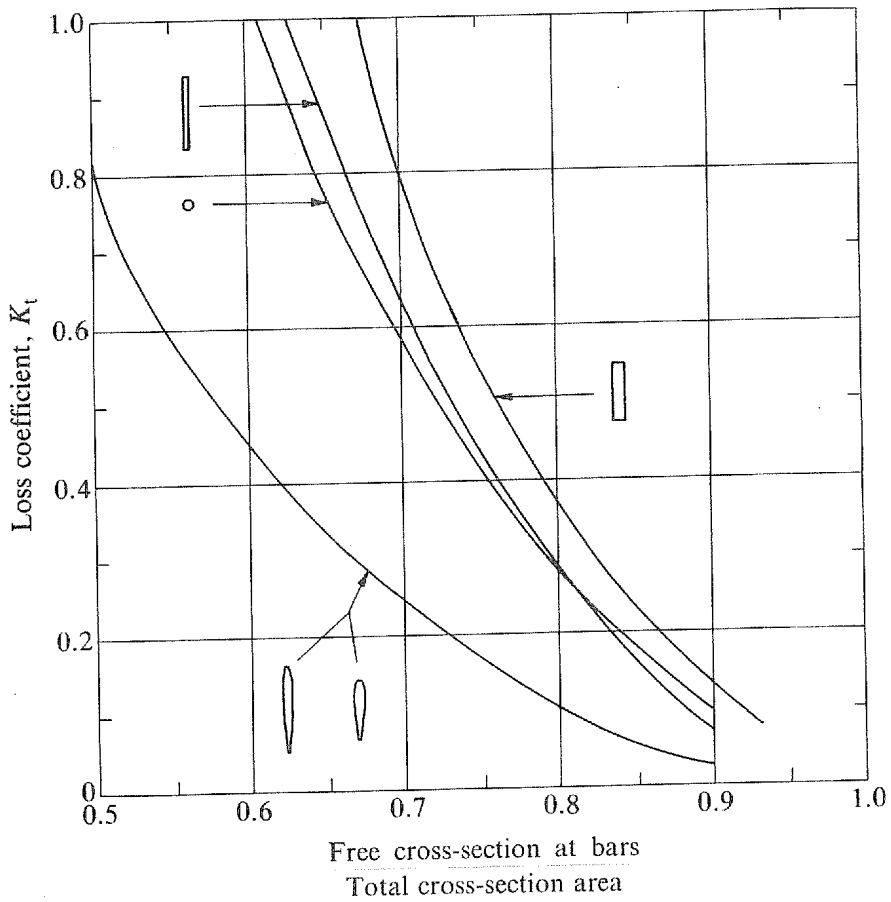

Fig. 14.8. Loss coefficients for trashracks

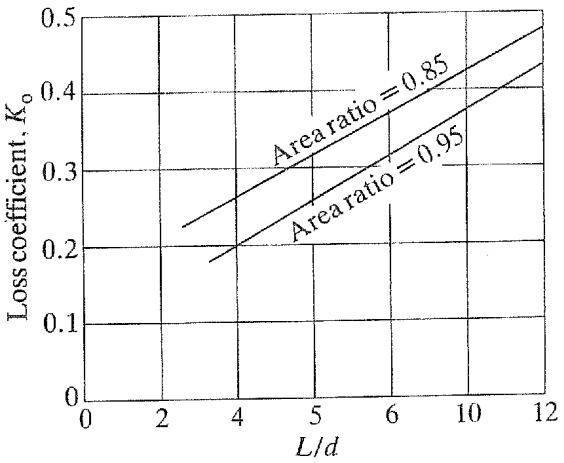

Fig. 14.9. Loss coefficients for honeycombs (L = cell length, d = cell hydraulic diameter)

14.2.7. HONEYCOMBS (CLASS 2)

Loss coefficients K_o for honeycombs are given on Fig. 14.9 for honeycombs with square and hexagonal cell shapes. The coefficients are based on the mean pipe passage velocity, and apply for Reynolds numbers greater than 10^4, based on the cell hydraulics diameter (4 × area of cell/cell perimeter).

14.3. DIFFERENTIAL FLOWMETERS (CLASS 2)

Loss coefficients for orifice plates, nozzles, venturi and Dall tubes are plotted in Fig. 14.10 against the throat/pipe area ratio. The loss coefficients are based on the mean pipe velocity.

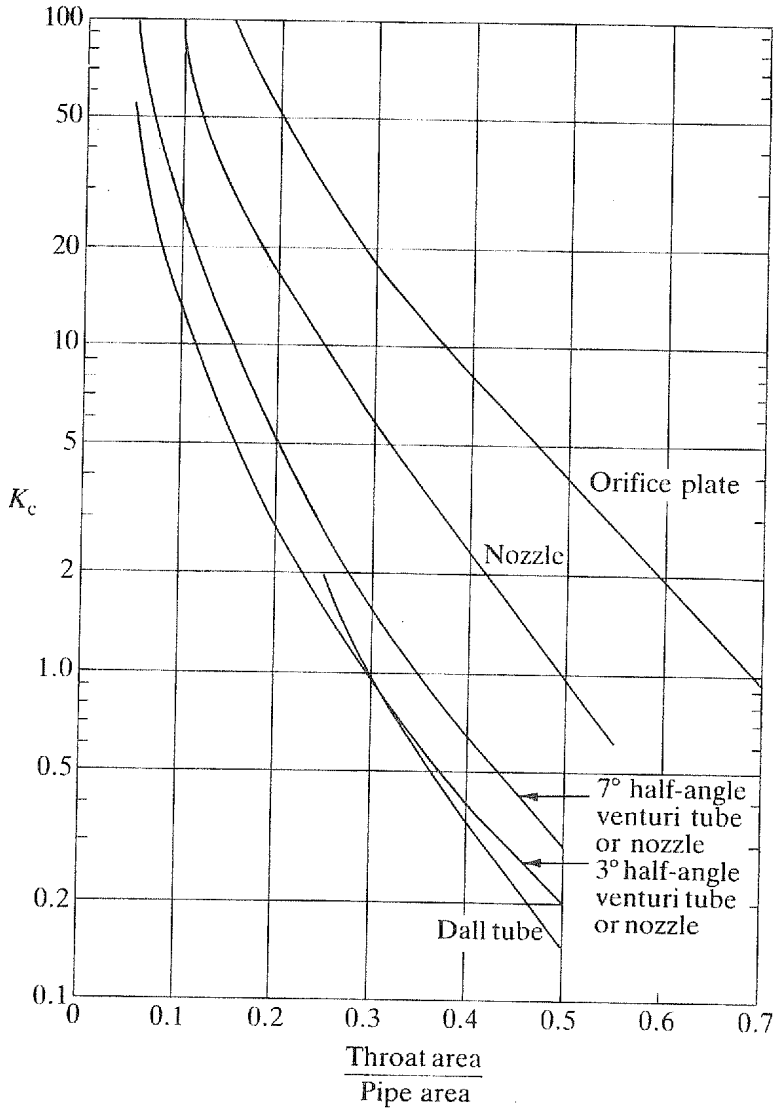

Fig. 14.10. Loss coefficients for differential flowmeters

14.4. INLETS AND CONTRACTIONS

14.4.1. INLETS (CLASS 2)

Figure 14.11 gives loss coefficients for flush inlets with Reynolds numbers greater than 10^5. If a flow metering nozzle with circular or elliptical arcs is used as an inlet, a loss coefficient of $K_i = 0.06$ is appropriate. Figure 14.12 gives loss coefficients for re-entrant inlets at Reynolds numbers greater than 10^5. Loss coefficients and Reynolds numbers are based on velocities in the pipe.

When inlet velocities are high and static pressures are low, liquids may cavitate in a simple inlet nozzle. An appropriate inlet design for high velocity flows is shown in Fig. 14.13 for the case where there is an outlet pipe or passage.

Loss coefficients for rectangular cross-section inlets are typically 0.02–0.05 above the circular cross-section values (class 3).

14.4.2. CONTRACTIONS

Loss coefficients for sudden contractions are given in Fig. 14.14†. The loss coefficients are based on the mean velocity head in the smaller pipe (class 1), and are for Reynolds numbers greater than 10^5.

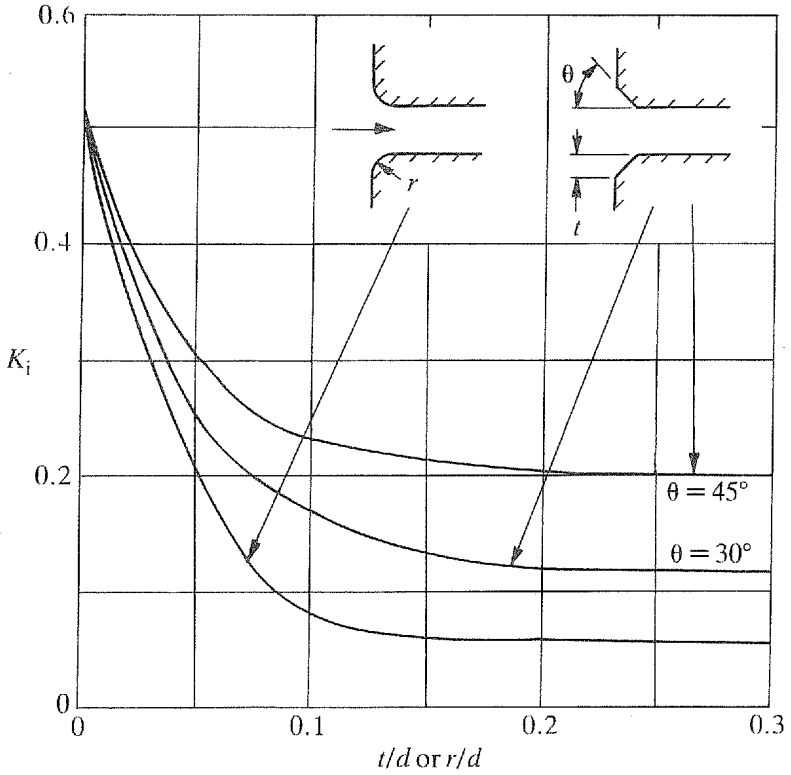

Fig. 14.11. Loss coefficients for flush mounted intakes

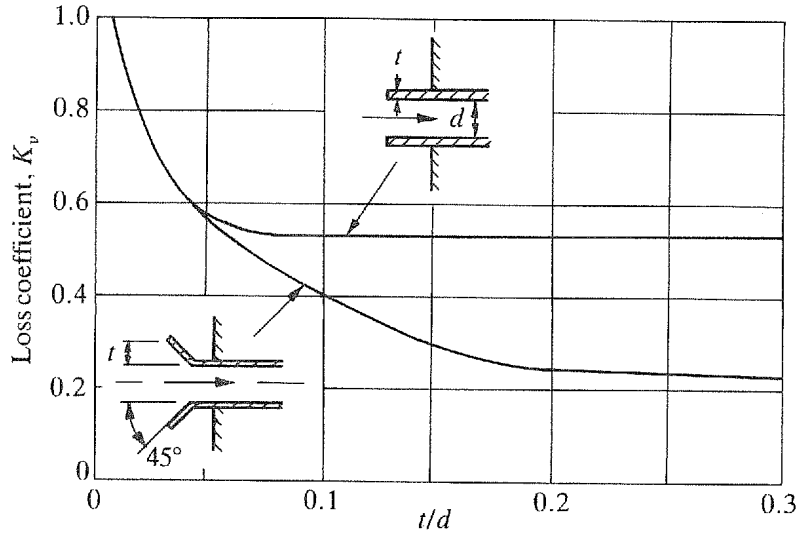

Fig. 14.12. Loss coefficients for re-entrant intakes

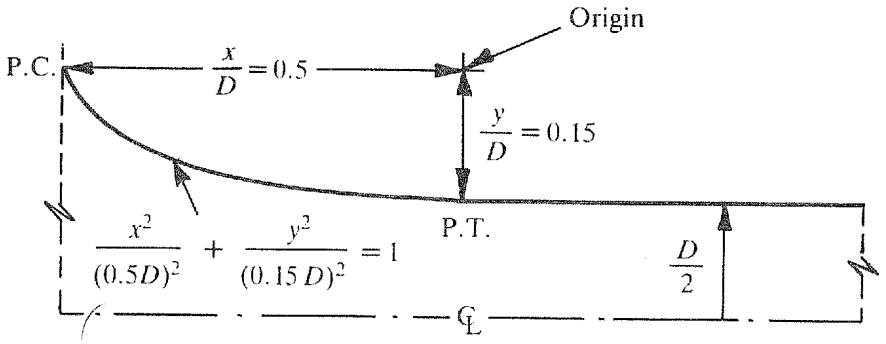

Fig. 14.13. Inlet (D = pipe diameter)

Loss coefficients for gradual contractions are plotted in Fig. 14.14(1) (class 2) based on the velocity in the smaller pipe (class 2). Loss coefficients are for Reynolds numbers greater than 10^5.

14.5. EXPANSIONS AND FREE DISCHARGE NOZZLES

14.5.1. ABRUPT EXPANSIONS (CLASS 1)

Loss coefficients for abrupt expansions in area are shown in Fig. 14.15. Loss coefficients are based on the velocity in the upstream pipe.

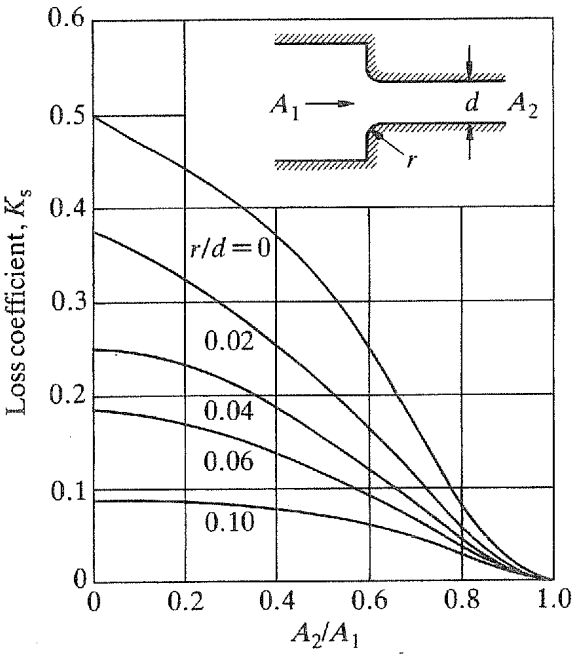

Fig. 14.14†. Abrupt contraction loss coefficients (based on velocity in A_2)

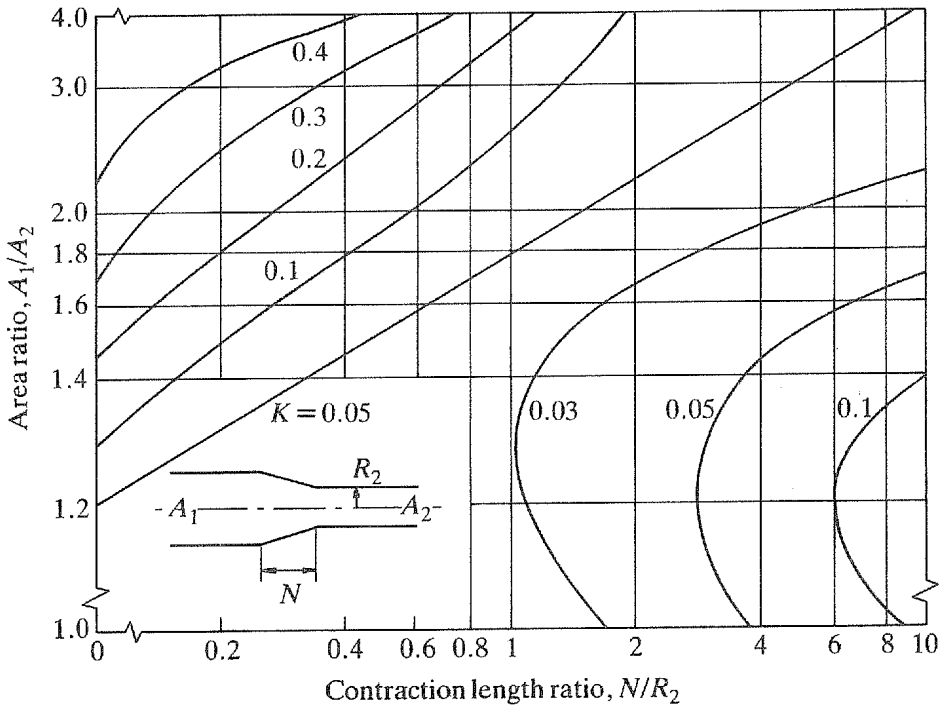

Fig. 14.14(1). Contraction loss coefficients

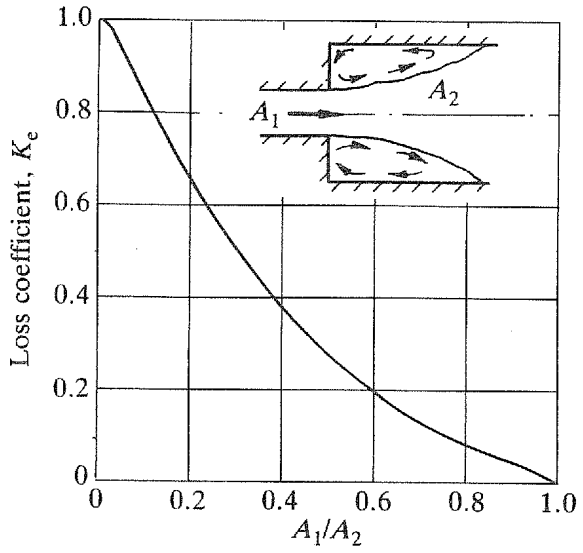

Fig. 14.15. Abrupt expansion loss coefficients (based on velocity in A_1)

14.5.2. FREE DISCHARGE NOZZLES (CLASS 2)

When a liquid is to be discharged into a gas and a coherent jet is required, careful design of the nozzle is essential and the inlet flow should be free from swirl and large scale turbulence. If liquid velocities are high and the static head is low, cavitation may occur in both submerged nozzles and nozzles discharging into air.

Two nozzle shapes of good performance, provided they are made accurately, are shown in Fig. 14.16. The loss coefficient, K_n, accounts for all of the energy lost from the system. The discharge coefficient, C_d, for the 7° nozzle is approximately 0.96, whereas for the 30° nozzle

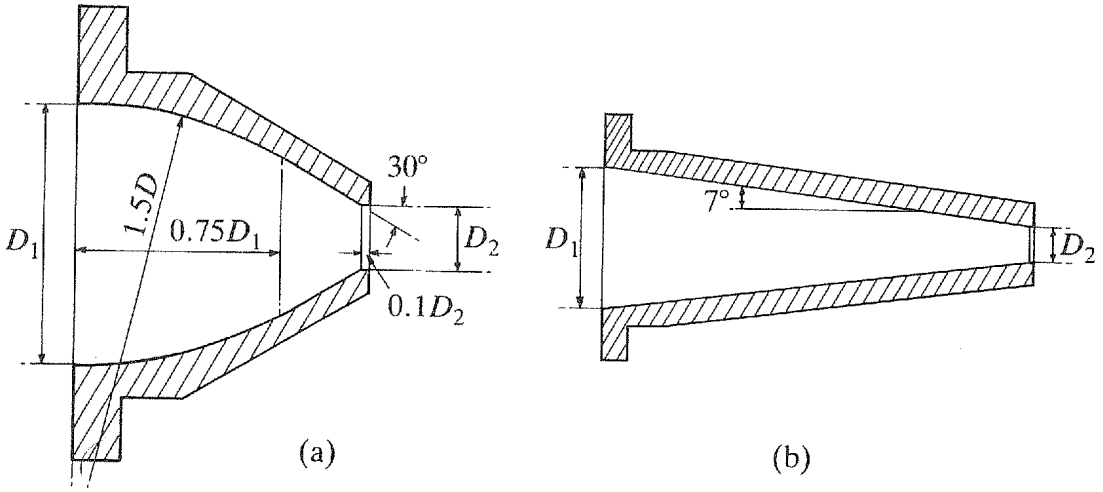

Fig. 14.16. Good performance nozzles

C_d varies linearly from 0.805 to 0.825 as the nozzle area ratio is varied from 0.1 to 0.25. To convert a discharge coefficient to a loss coefficient, based on the inlet velocity to the nozzle, use

$$K_n = (A_1/A_2 C_d)^2$$

14.6. VALVES

Wide variations in valve geometry are possible, to the extent that a manufacturer will not necessarily maintain geometrical similarity between valves of the same type but of different size. In most cases the loss coefficients given are typical values, and more accurate values should be requested from the valve manufacturer. When a valve is required for control purposes, a predetermined partial opening of the valve will be required in order to give good control characteristics.

Loss coefficients are based on the mean pipe or passage velocity head, and apply to Reynolds numbers greater than 5×10^3.

14.6.1. BALL VALVES (CLASS 2)

The loss coefficient for a fully open ball valve with the same area as the pipe is essentially the friction loss of an equivalent length of pipe. A typical value is 0.05. Loss coefficients are plotted against valve angle in Fig. 14.17 for partially open valves.

14.6.2. BUTTERFLY VALVES (CLASS 2)

Typical loss coefficients are plotted against disc thickness in Fig. 14.18. Figure 14.19 gives loss coefficients plotted against valve opening for three types of valve disc.

14.6.3. DIAPHRAGM VALVES (CLASS 3)

Approximate loss coefficients for two types of diaphragm valves are given in Fig. 14.20.

14.6.4. GATE AND SLUICE VALVES (CLASS 2)

Typical loss coefficients for fully open gate valves are plotted against valve seat/pipe diameter in Fig. 14.21. Loss coefficients against valve openings are plotted in Fig. 14.22 for gate and sluice valves.

14.6.5. GLOBE, Y AND ANGLE VALVES (CLASS 3)

Figure 14.23 shows typical loss coefficients for fully open globe valves plotted against the

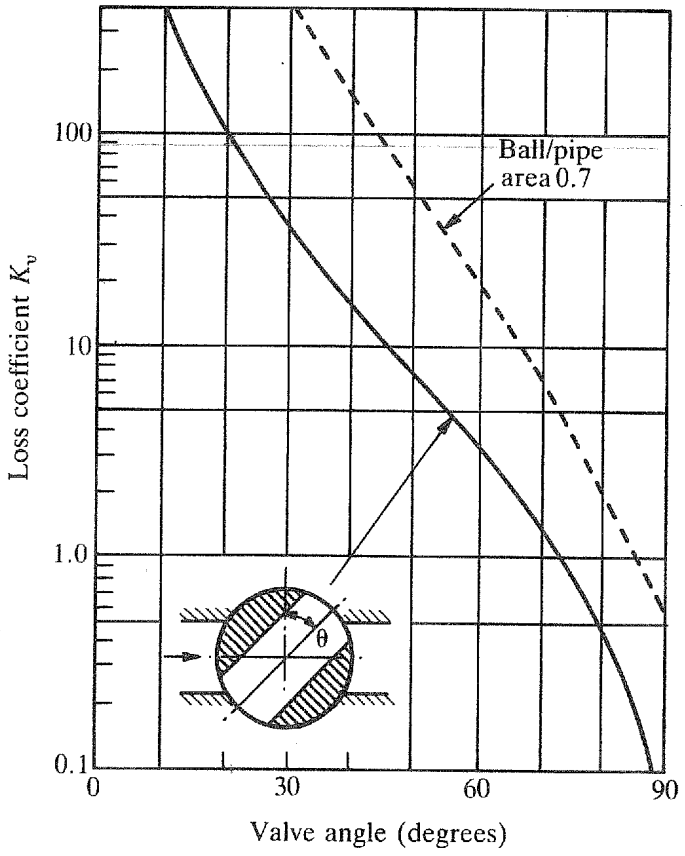

Fig. 14.17. Ball valve loss coefficients

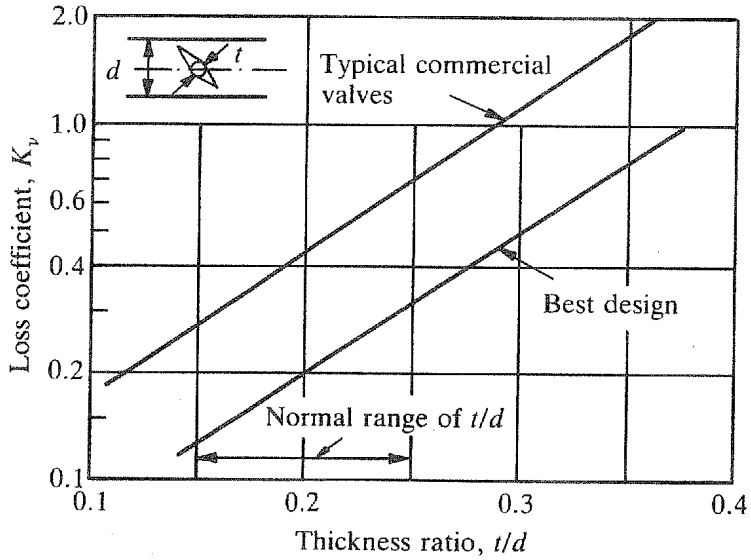

Fig. 14.18. Loss coefficients for fully open butterfly valves

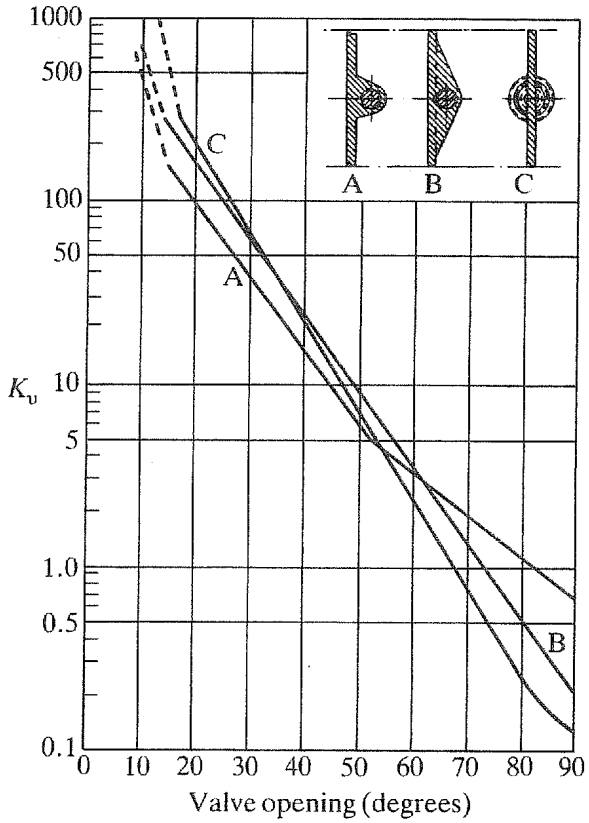

Fig. 14.19. Loss coefficients for butterfly valves

valve seat area/pipe area ratio. A loss coefficient for one-quarter of the equivalent globe valve coefficient may be taken for valves with the spindle at 45° to the pipe centreline. A valve with a 60° spindle angle will have a loss of about half the equivalent globe valve. Free flow valves, which present little obstruction to the flow in the fully open position, may have loss coefficients as low as $K_v = 0.4$. Figure 14.24 gives typical loss coefficients against valve opening for globe, angle and Y valves.

14.6.6. POPPET VALVES (CLASS 3)

Loss coefficients for poppet valves discharging into a large space are plotted in Fig. 14.25 against valve lift. The loss coefficients are based on the velocity in an area defined as πLD and assume no pressure recovery after the valve. Abrupt changes in loss coefficients shown in Fig. 14.25 are due to flow attachment and separation from the valve seat.

Poppet valves, where the flow is from a large space through the valve, have loss coefficients of about 2 over the same opening range as Fig. 14.25, when the seat width ratio is greater than $W/D = 0.05$ and the seat angle is 45°.

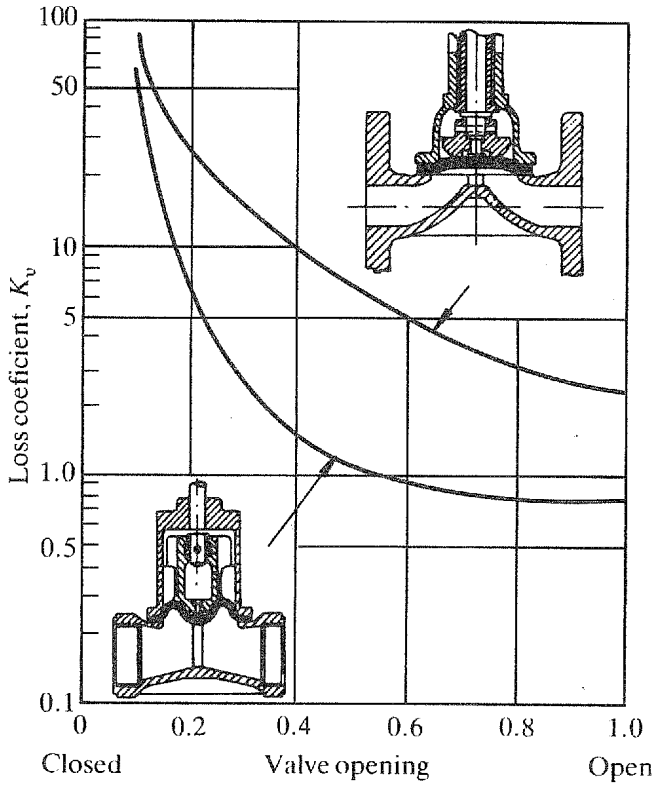

Fig. 14.20. Diaphragm valve loss coefficients

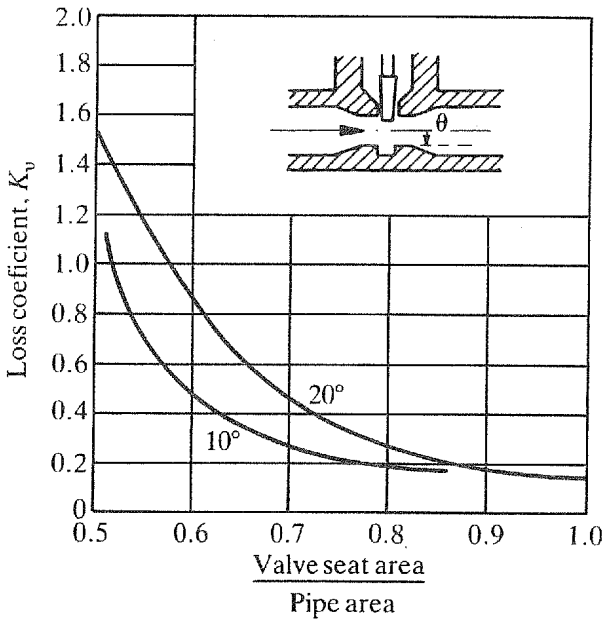

Fig. 14.21. Fully open gate valve loss coefficients

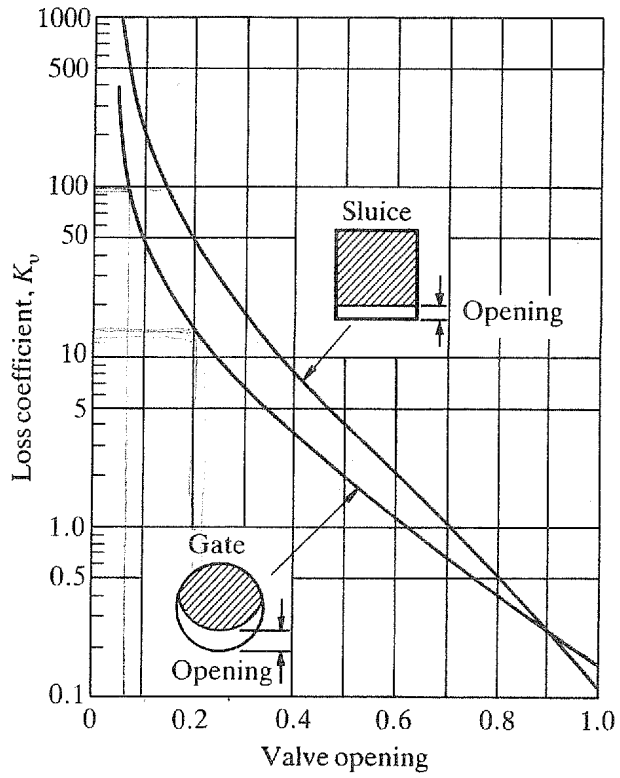

Fig. 14.22. Gate and sluice valve loss coefficients (seat area = pipe area)

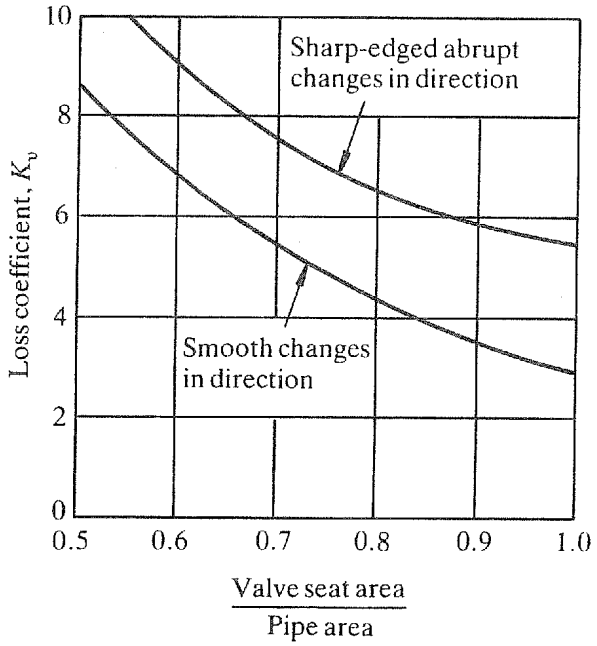

Fig. 14.23. Approximate loss coefficients for fully open globe valves

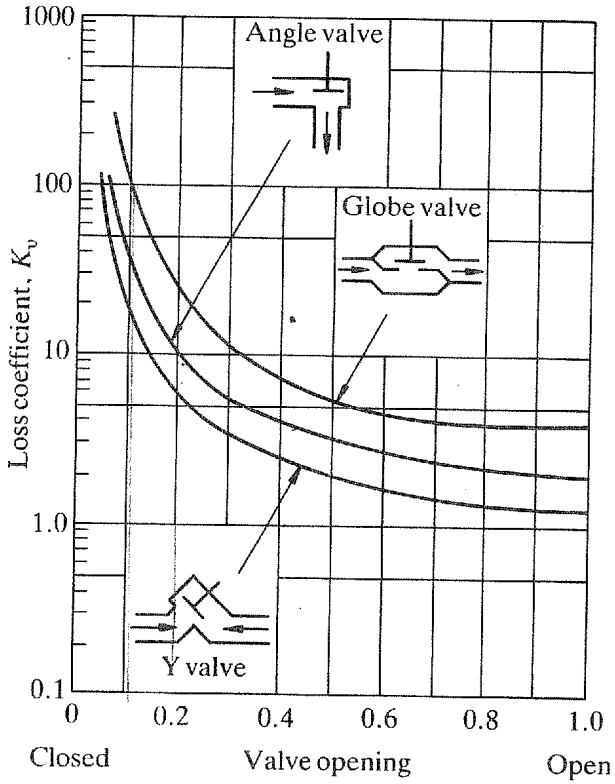

Fig. 14.24. Approximate loss coefficients for globe, Y and angle valves

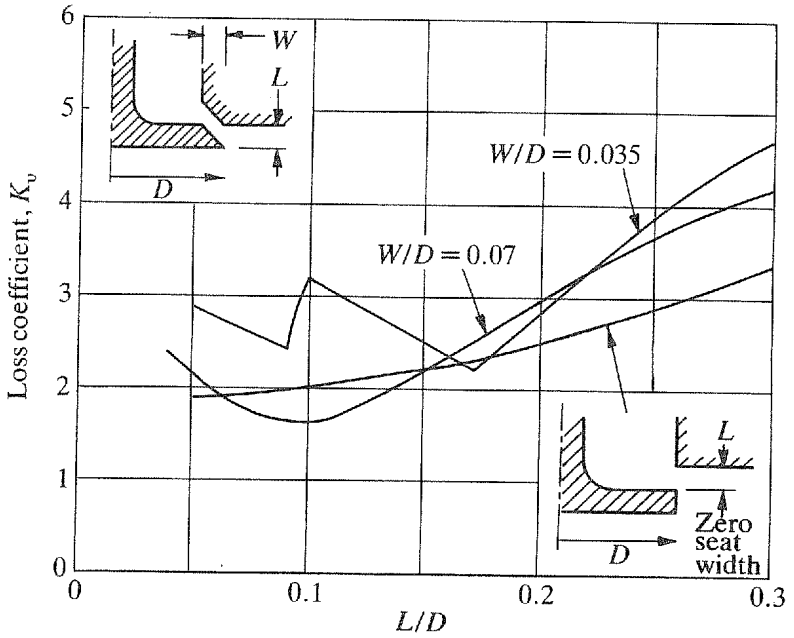

Fig. 14.25. Loss coefficients for poppet valves with 45° seats

14.6.7. PLUG VALVES (CLASS 3)

Loss coefficients for fully open rectangular ported plug valves with diameters greater than 0.2 are given in Table 14.1.

Table 14.1.

Port area/pipe area	1.0	0.8	0.6
Loss coefficient	0.5	0.7	1.5

14.6.8. REFLUX AND CHECK VALVES

Loss coefficients of a reflux valve whose door is raised out of the flow, as in Fig. 14.26, may have a loss coefficient as low as 0.3 at liquid velocities above 2 m/s, which is usually sufficient to hold the door open. When the door protrudes into the flow, loss coefficients may exceed 1.0.

Tilting disc check valves may have loss coefficients as low as 0.5 for specially designed valves, but typical loss coefficient values range from 1.0 to 3.0, depending on the blockage.

Note: Reflux and check valves are often mounted directly after the pump, where velocities are usually higher than in the rest of the system. Head losses due to the valve can form a disproportionate part of the total system head requirements. In assessing the suitability of a valve the energy dissipated by the valve as well as its dynamic characteristics should be considered.

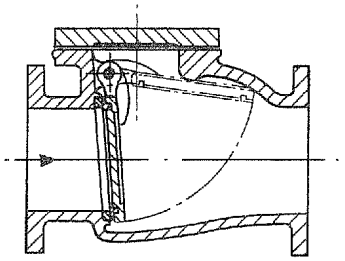

Fig. 14.26. Reflux valve

14.7. LAMINAR FLOW

14.7.1. SMOOTH INLETS (CLASS 2)

The pipe length following a smooth inlet before developed laminar flow is established is shown in Fig. 14.27. As the laminar to transition region is approached, the inlet length required for flow development becomes indeterminate. In reaching developed flow there is

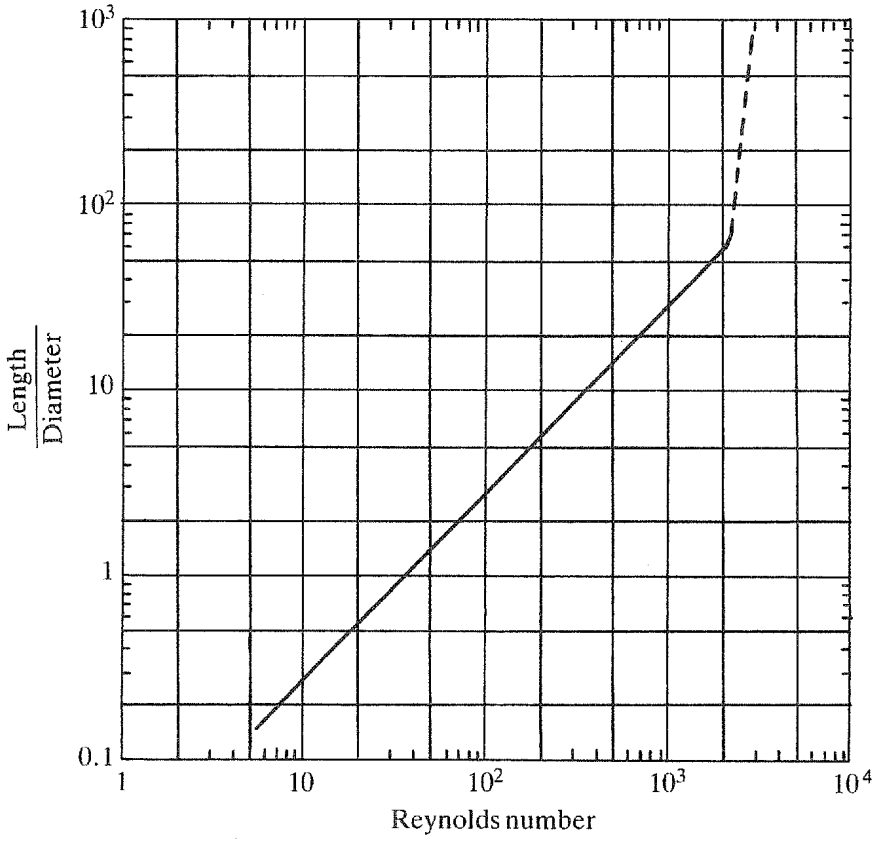

Fig. 14.27. Laminar flow development length

a head loss above that calculated using fully developed laminar flow of

$$\Delta H = 1.3U^2/2g$$

If the inlet pipe is shorter than that required for developed flow, the inlet head loss is given by

$$\Delta H = K_{li}U^2/2g$$

where K_{li} is taken from Fig. 14.28.

An example is given in Example 2 of Section 14.8.

14.7.2. SHARP-EDGED ORIFICES (CLASS 3)

Loss coefficients for sharp-edged orifices are plotted against Reynolds number in Fig. 14.29 for five orifice/pipe diameter ratios. The loss coefficients and Reynolds numbers are based on the mean pipe velocity.

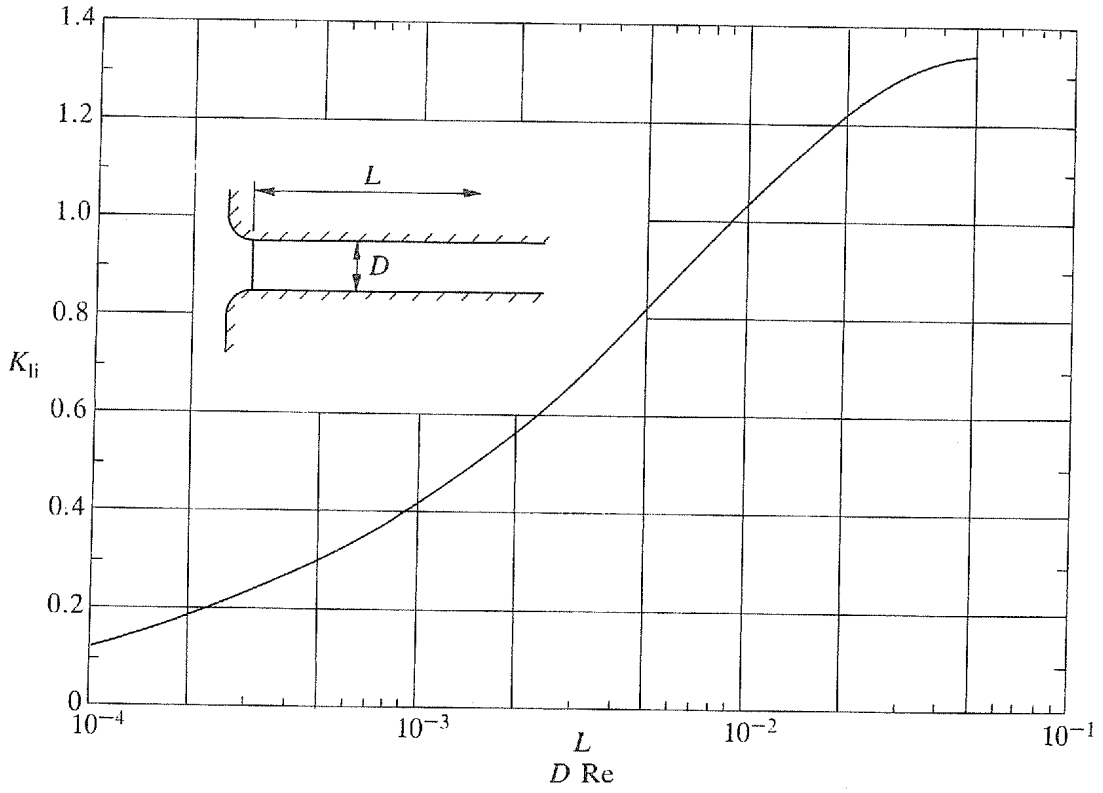

Fig. 14.28. Excess loss coefficient

14.7.3. LONG ORIFICES (CLASS 3)

Loss coefficients for sharp-edged long orifices are plotted against Reynolds number in Fig. 14.30 for five orifice length/diameter ratios. The loss coefficients and Reynolds number are based on the mean velocity in the orifice. The loss coefficients apply only to orifice/pipe diameter ratios of less than 0.3.

14.7.4. ROUND WIRE SCREENS (CLASS 3)

Loss coefficients for round wire screens are plotted against Reynolds number in Fig. 14.31 for four ratios of flow area at the screen to pipe or passage area. The loss coefficients and Reynolds number are based on the mean velocity in the screen and the wire diameter is used in the Reynolds number.

14.7.5. VALVES (CLASS 3)

No reliable experimental data are available for laminar flow through valves. If the loss coefficient, K_{tur}, of a valve is known for turbulent flow, an estimate of the laminar flow loss coefficient can be obtained by using Fig. 14.32.

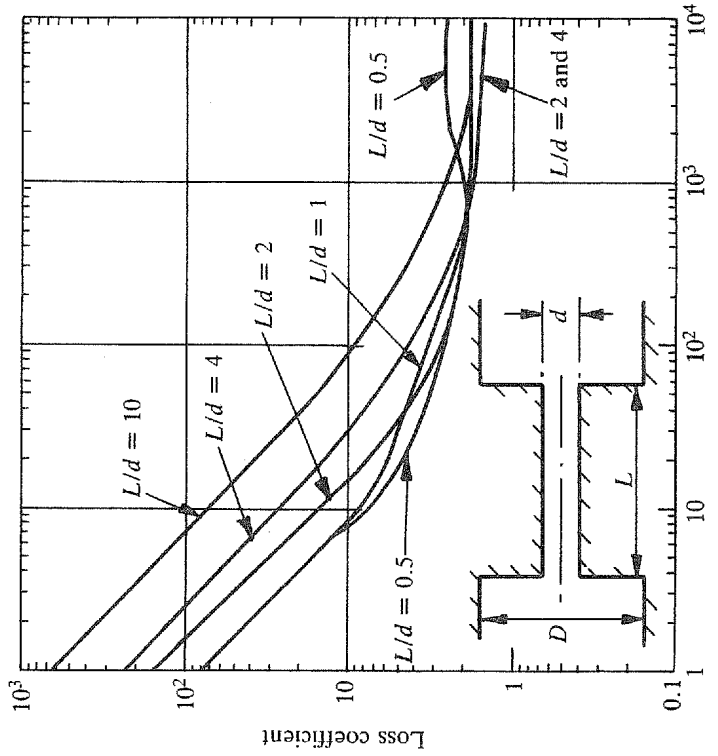

Fig. 14.30. Long orifice loss coefficients (based on orifice mean velocity)

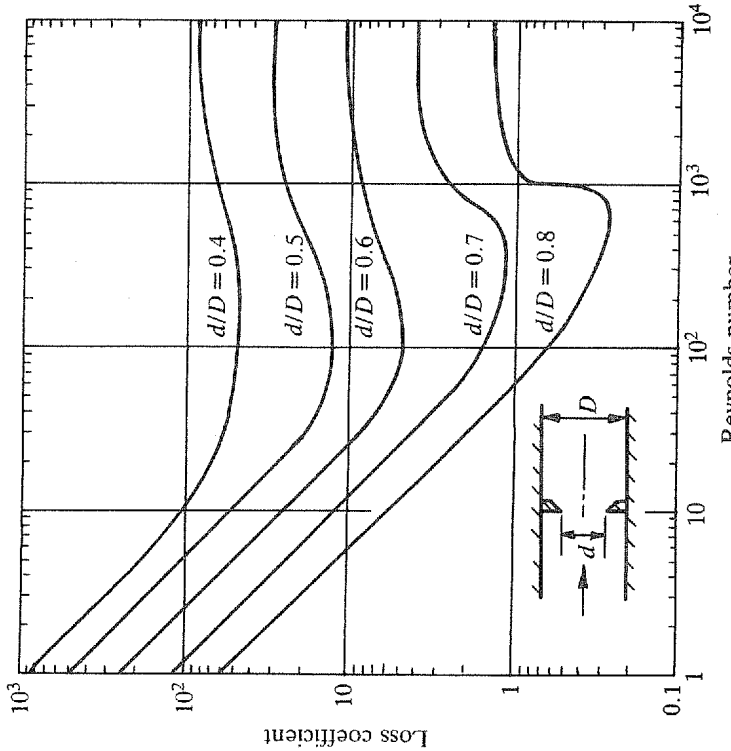

Fig. 14.29. Sharp-edged orifice loss coefficients

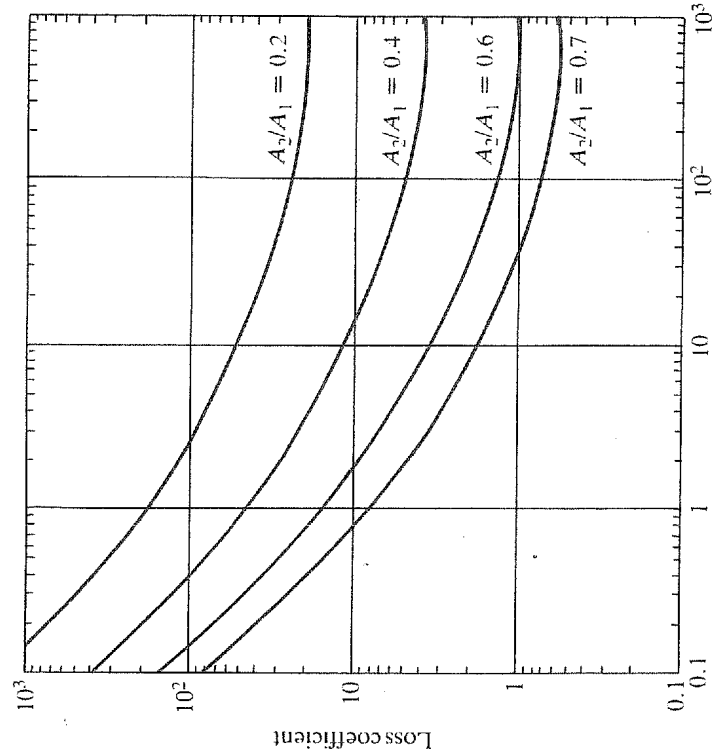

Fig. 14.32. Laminar loss coefficient relationship to turbulent loss coefficient

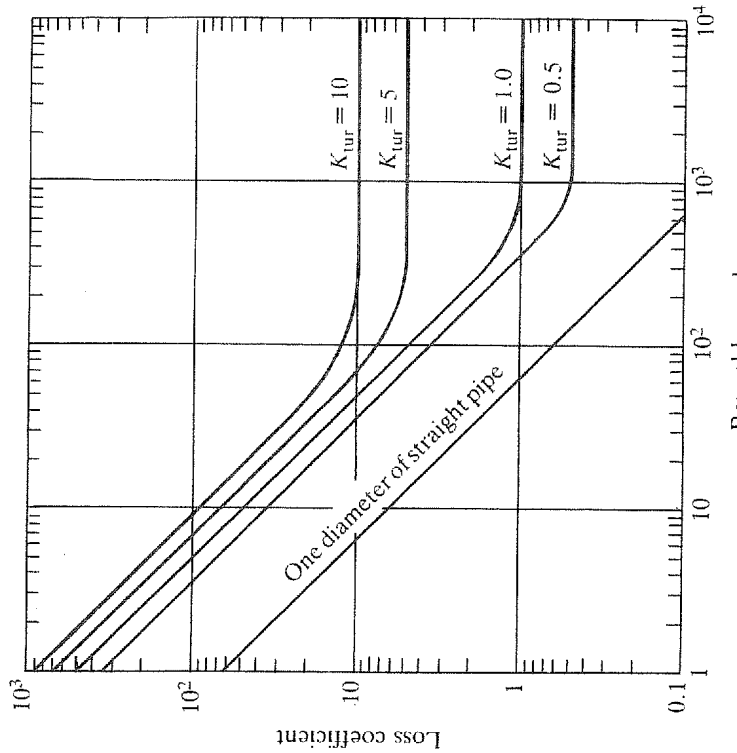

Fig. 14.31. Round wire screen loss coefficient

NOTES AND REFERENCES ON CHAPTER 14

The literature on screens, orifices and grids can be accessed through:

1. Papworth, M., The effects of screens on flow characteristics. BHRA Report TN 1198 (November 1972), 23 pp. A number of the more extensive papers on valves are given in the notes on Chapter 6. Additional information is given in:

2. Gurevich, D. F., *Design and Construction of Pipe Fittings*, 4th edition. Leningrad: Mashinostroenie (1969). (In Russian.)

Data on poppet valves are summarised in:

3. Annand, W. J. D. and Roe, G. E., *Gas Flow in the Internal Combustion Engine*. Yeovil: G. T. Foulis (1974), 218 pp.

The loss coefficients for laminar flow through sharp-edged orifice plates are based on:

4. Rao, N. S. L. and Sridharan, K., Orifice losses for laminar approach flow. *Proc. ASCE, J. Hydraul. Div.*, **98** (HY11), 2015–2034 (November 1972).

and for long orifices:

5. Lichtarowicz, A., Duggins, R. K. and Markland, E., Discharge coefficients for incompressible non-cavitating flow through long orifices. *J. Mech. Eng. Sci.* 7 (2), 210–219 (June 1965).

Reference 4 contains references to many of the papers on laminar flow through components.
The affect of radii on sudden contractions in pipes is based on

6. Bullen, S. R., Cheeseman, D. J., Husain, L. A., Ruffell, A. E., The determination of pipe contraction pressure loss coefficients for incompressible turbulent flow. *Int. J. Heat Fluid Flow* **8** (2) 111–118 (June 1987 — see also **9** (4) 431–432 (December 1988).

The most extensive collection of loss coefficients data is given by

7. Idelchik, I. E., Handbook of Hydraulic Resistance, (2nd edn) Hemisphere Publishing, 640 pp.(1986).

Figure 13.25 changed from correction factor curves to loss coefficient curves.

Figures 13.42 onwards included in the first edition have been re-numbered in this edition.

Chapter 14

Figure 14.5 changed from correction factor curves to loss coefficient curves and the calculation procedure in Section 14.2.2, for correcting, for orifice length to diameter ratio, removed.

Figure 14.11 curves re-instated to original form (errata to first edition altered termination point at $t/d = 0$).

Figure 14.14 curve for $r/d = 0$ revised and curves for a range of edge radii added.